A Study of Evaporation and Friction on Hydrated Forearm Skin

Wing Kei Rebecca Wong

Continence and Skin Technology Group
Department of Medical Physics and Bioengineering
University College London

Supervisors
Dr. Alan M. Cottenden
Dr. Clare E. Elwell

Thesis submitted for the degree of Doctor of Philosophy
(Ph.D) at the University of London

March 2008

UMI Number: U593320

UMI

Dissertation Publishing

ProQuest

I, Wing Kei Rebecca Wong, confirm that the work presented in this thesis is my own. Where information has been derived from other sources, I confirm that this has been indicated in the thesis.

ACKNOWLEDGEMENTS

ABSTRACT

When skin is occluded by continuous wearing of incontinence pads, it becomes over-hydrated, making the skin more susceptible to mechanical damage and bacterial attack than normal skin. This project focused on understanding the impact of skin occlusion on (i) the hydration of the stratum corneum (SC) – the outermost layer of the skin, and (ii) friction between the skin and nonwoven materials.

A methodology for measuring the excess water in over-hydrated skin using evaporimetry was developed, validated and used to compare the performances of five commonly used evaporimetry devices, and to investigate their strengths and limitations. All measurements were made on the volar forearm skin of one young female subject. Good reproducibility was found for each of the five devices, but some significant differences were found between measurements made with different devices. Some possible causes for these discrepancies were investigated with partial success: correction factors obtained from various calibration procedures were applied and reduced differences to some extent, but significant difference still remained. It was concluded that the methodology developed could be used with confidence to compare readings made with the same device, but it would be unwise to trust the absolute values obtained until the reasons for differences between devices have been more fully explained.

A new approach for measuring the water distribution within the SC - Opto-Thermal Transient Emission Radiometry (OTTER) - was adopted in this work and a methodology was developed for measuring the saturation profile within over-hydrated

SC. The relationship between the SC saturation at the surface (measured using OTTER) and the water vapour flux from over-hydrated SC (measured using evaporimetry) was investigated using the volar forearms of three young female subjects. As expected, strong correlation was found during desorption, with a dog-leg in the plot at about 36% saturation from two subjects, which was consistent with the transition between loosely and tightly bound water reported by Berardesca (1997).

Two methods for measuring friction between nonwoven materials and the over-hydrated or normal skin were developed and validated, on the volar forearms of five young female subjects. Coefficients of friction were measured with the two methods and compared. Good reproducibility and remarkably good agreement was found between the two methods, even though one of the methods (*curved friction*) assumed the arm to be a rigid cylinder and the nonwoven material to be inextensible. Additional theoretical work (by Cottenden (2007)) and experimental work (by Karavokiros (2007)) was conducted to explain and extend the findings. The theoretical analysis showed that the equation describing friction around a cylinder is valid for any convex prism, and the experimental work supported the solution very well. It was concluded that the *curved* method developed was simple to run and produced results with good reproducibility.

TABLE OF CONTENTS

LIST OF TABLES

LIST OF FIGURES

GLOSSARY

This glossary provides definitions of various important terms used in the thesis.

Urinary incontinence: Involuntary escape of urine to a degree that imposes a socially or hygienically unacceptable situation on the individual.

Stratum corneum (SC): the outermost layer of the skin that acts as a water barrier to prevent excessive water loss from the body.

Corneocyte: is a keratinocyte that had lost its nucleus and organelles during its maturation from the base of the epidermis to the surface of the skin.

Superabsorbent polymers (SAP): polymers that can absorb and retain extremely large amounts of a liquid relative to their own mass, commonly used in the core of absorbent products.

Normal skin: used in this thesis to refer to skin that is untreated.

Over-hydrated skin: used in this thesis to refer to skin that has been fully hydrated by occlusion with wet material.

Occlusion: covering the skin with material such as to impede or prevent water vapour loss from it.

In vivo: the technique of performing a given experiment in or on the living tissue of a whole, living organism.

In vitro: the technique of performing a given experiment in a controlled environment outside a living organism.

Diaper dermatitis: irritant contact dermatitis on the skin that is induced by wearing of diapers.

Transepidermal Water Loss (TEWL): the flux density of liquid water diffusing across the epidermis, from inside the body to its surface.

Water vapour flux density: the flux density of liquid water in grams per meter square per hour ($g \cdot m^{-2} h^{-1}$) measured on the skin surface that is not only contributed by TEWL.

Background TEWL: the water vapour flux density in $g \cdot m^{-2} h^{-1}$ evaporating from the skin, measured on the untreated, normal skin surface.

Desorption curve: A water vapour flux density versus time graph which indicates the recovery of an over-hydrated skin. Recovery is considered to be complete when flux density has decreased to the background TEWL value.

Skin Surface Water Loss (SSWL): Total amount of excess water in an over-hydrated skin in grams per meter square ($g \cdot m^{-2}$) measured from the area under a water vapour flux density versus time graph, having subtracted the background TEWL value.

Opto-Thermal Transient Emission Radiometry (OTTER): an instrument that emits radiation source and detect the sample's blackbody radiation due to the temperature increase. The water concentration and saturation gradient within the SC can then be measured from the signal.

Coefficient of static friction (μ_s): the ratio of the initial friction force that get an object moving along the surface to the normal force.

Coefficient of dynamic friction (μ_k): the ratio of the friction force that is required to sustain the constant motion of one object past another to the normal force.

NOTATION

Z	Impedance
R	resistance
f	frequency of alternating current
C	capacitance
A	absorbance
ε	specific extinction coefficient
c_a	concentration of absorber
d	distance of light travelled
J	water vapour flux density
D_w	diffusion coefficient of water vapour in air
c	water vapour concentration
z	distance from the skin
$\dfrac{\partial c}{\partial z}$	water vapour concentration gradient
$H(z)$	SC water concentration
H_0	water content at skin surface
H_1	water content at the base of SC
W	water concentration gradient
L	thickness of the SC
D	thermal diffusivity
β_0	emission absorption coefficient of the skin surface
τ	surface lifetime of OTTER signal
$erfc$	complementary error function
β_H	emission absorption coefficient of skin of fractional volume hydration H
β_W	emission absorption coefficient of water

β_d	emission absorption coefficient of dry skin
F	friction force
N	normal force
μ	coefficient of friction
μ_s	coefficient of static friction
μ_k	coefficient of dynamic friction
s	shear stress at the contacting surface
A_R	real contact area
F_{total}	total frictional force
$F_{deformation}$	force used in deformation
$F_{adhesion}$	force used in adhesion
t_0	foam thickness under zero load
t	average thickness of the four corners of the foam
β	angle of contact between belt and capstan
F_1	leaving tension in the fabric strip at point of slippage
F_2	incoming tension in the fabric strip at point of slippage
P	pressure under the fabric strip
F_{max}	maximum value of friction force
w	width of fabric strip
r	radius of a 'cylinder' used in the curved friction configuration
θ	Angle measured about the origin from the point of first contact in a curved friction configuration
$\mu_{s(f)}$	coefficient of static friction calculated from flat configuration
$\mu_{s(c)}$	coefficient of static friction calculated from curved configuration
$m_1 g$	weight applied to the flat friction configuration
$m_2 g$	weight applied to the curved friction configuration

Chapter 1

INTRODUCTION

Three million people in the UK are incontinent of urine and the prevalence is set to increase as the population ages (DOH, 2000). Most sufferers who cannot be fully cured by medical, surgical or physiotherapy treatments, use absorbent pads to manage their incontinence. These wearers of incontinence pads often report discomfort, soreness and skin damage associated with their use of pads (Zimmerer, 1986). When skin is exposed to prolonged contact with pad materials, especially when they are wet, the outer-most layer of the skin (the stratum corneum (SC)) becomes over-hydrated, which leads to obstruction of the normal ventilation of the skin, increasing the permeability and penetration of other substances, and making the skin more susceptible to mechanical damage and bacterial attack than normal skin (discussed in Section 2.2).

Many studies have attempted to understand the interaction between skin and pads by measuring the wetness and the friction between skin and pad materials. However, it is difficult to interpret the results by combining them into a coherent scheme of understanding because of the variety of experimental conditions, measurement instruments and methodologies used. Also, no method has been validated by conducting repeat measurements under controlled conditions to establish that the degree of repeatability is adequate.

Furthermore, while the hydration level of the test skin site is crucial for investigating the effects of water on skin, there is a lack of a standard method for uniformly hydrating the

skin in hydration-related measurements (discussed in Section 2.4.3.5). Therefore a standard method for uniformly hydrating the skin is needed before the effect of water on skin can be properly investigated.

A variety of instruments have been used to characterise skin that has become over-hydrated, but evaporimetry devices for measuring transepidermal water loss (TEWL) have been particularly widely used to evaluate the barrier function of the skin. A number of evaporimetry devices have come on to the market recently but there has been little work to measure the repeatability of their measurements and to compare and contrast their strengths and limitations when used for work on over-hydrated skin (discussed in Section 2.4). A newly developed technique, the Opto-Thermal Transient Emission Radiometry (OTTER), has the aim of complementing evaporimetry data by measuring the water distribution within the SC that, similarly has not been used much to study over-hydrated skin.

A number of studies of the influence of hydration on skin friction have been reported during the past forty years, but relatively few studies have focused on the friction between skin and fabric materials (see Section 2.5). Incontinence pad manufacturers are keen to develop pads which cause less abrasion damage to skin but lack a robust method for measuring the coefficient of friction between skin and pad materials – particularly the coverstock, the water-permeable nonwoven material that lays against the skin.

The work described in this thesis aims to pave the way for improved incontinence pads, by increasing understanding of the interaction between pad materials and skin.

Chapter 2

LITERATURE REVIEW

2.1 Urinary incontinence

Urinary incontinence is defined as the inability to control the release of urine from the

bladder (Newman, 2002). Worldwide there are over 200 million people who have

significant urinary incontinence and many more with mild bladder problems (Abrams et

al., 2002). Table 2.1 provides a summary of UK prevalence data from the Department of

Health (2000), which shows a particularly high prevalence of incontinence in people

living in institutional settings.

Table 2.1. Prevalence of urinary incontinence (reproduced from DOH, 2000)

For people living at home

Between 1 in 20 and 1 in 14 women aged 15-44

Between 1 in 13 and 1 in 7 women aged 45-64

Between 1 in 10 and 1 in 5 women aged 65 and over

Over 1 in 33 men aged 15-64

Between 1 in 14 and 1 in 10 men aged 65 and over

For people (both sexes) living in institutions

1 in 3 in residential homes

Nearly 2 in every 3 in nursing homes

1 in 2 to 2 in 3 in wards for elderly and elderly mentally infirm

Stress and urge incontinence are the most common types of urinary incontinence. Stress

incontinence is the involuntary leakage of small amounts of urine in response to

increased intra-abdominal pressure caused by such activities as sneezing, coughing,

laughing, or lifting heavy objects (Newman, 2002). This type of incontinence can be

caused by weakened support for the pelvic muscles, and weakness in the sphincter (the muscles that contract to seal the bladder and relax to release urine through the urethra). Urge incontinence is the leakage of urine that occurs when a person is not able to reach the toilet in time after the urge to void is perceived (Newman, 2002). The sufferer may also experience discomfort and an urgency to urinate with only a small amount of urine in the bladder. This type of incontinence can be caused by urinary tract infections, changes in the bladder's ability to contract and neurological disorders such as stroke, Parkinson's disease, brain tumours, multiple sclerosis, and spinal cord injury. The degeneration of the nervous system with age is the most common cause of urge incontinence for older adults.

There are several treatments available for incontinence sufferers by drug therapy surgery and behavioural treatments, such as bladder training/retraining, pelvic muscle exercises and biofeedback may cure incontinence or reduce its severity (Abrams et al., 2005). However, in many cases these treatments do not completely cure the incontinence problem. Sufferers will then need to manage their incontinence by using products that will contain the urinary leakage, of which absorbent products are the most commonly used.

Absorbent pads and pants come in many types and absorbency levels, from thin panty liners or sanitary pads to adult diapers or briefs (Fig 2.1). Bed and chair pads for furniture protection are also available. Pads may be disposable (single use) or reusable / washable (for multiple uses). Fig 2.2 shows the generic structure of a pad. The absorbent core may be made from fluff pulp, superabsorbent polymers (SAP), tissue paper, cotton gauze or nonwoven felt and is faced with a water permeable coverstock (next to the skin) of knitted, woven or nonwoven fabric made from viscose, polyester,

olefin or cotton, and backed with a waterproof layer (Verdell and Bouda, 1990).

Light to Moderate Urine Loss

Pantiliners
Very thin, discreet, for light urine loss.

Pads
Contains super absorbent materials. Available in serveral absorbency level.

Guards for Men
Contoured design to fit a man's anatomy. Can be worn inside close-fitting underwear.

Moderate to Heavy Urine Loss

Undergarment
Open-sided design and stretchy straps for comfort. Leg gathers designed to help prevent leakage.

Protective Underwear
Slim-fitting, comfortable and discreet. Designed to slip on like regular underwear

Refastenable Underwear
Slip on like regular underwear or open the perforations on the sides and attach the fasteners.

Fitted Briefs
Elastic at the waist and legs for a close fit. Adhesive tapes for fastening.

Fig 2.1 Different types of absorbent pads for different levels of incontinence

(adapted from Newman, 2002)

Permeable coverstock

Middle absorbent layer

Waterproof backsheet
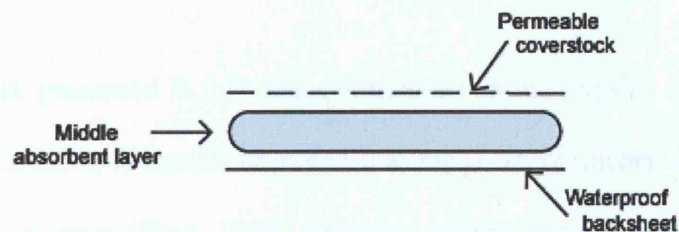
Fig 2.2 General composition of an absorbent pad.

Manufacturers aim to arrange these components into a product that absorbs urine quickly, is comfortable to wear, does not leak, retains odour, and is affordable (Perlman, 1991). A major challenge for manufacturers is to produce pads that can minimise skin problems for wearers.

2.2 Skin health and incontinence

Despite advances in continence management, many residents in nursing homes have intractable incontinence. A study from the Medical Devices Agency (2003) established that about 8% of incontinent residents in UK nursing homes have incontinence-related skin problems at any one time. A survey of nursing home residents by Fader (2005) reported that 62% of the 104 subjects studied had had their current incontinence-related skin problem for five days or more. An estimated 46% of these subjects had had the problem for a month or more, and for 16% of them the skin problem was permanent.

Recently, Ersser et al. (2005) reviewed the literature relevant to skin vulnerability and incontinence. The authors showed that insufficient attention has been given to the effect of incontinence on the skin, and they also highlighted elements of the research agenda required to improve skin care practices for those with or at risk of urinary incontinence.

Although the work presented in this thesis is focused on the physics of wet skin caused by urinary incontinence, it should be noted that faecal incontinence may present even more risk to skin integrity (Berg, 1988). Its prevalence is more difficult to estimate than urinary incontinence because it is seen by professionals and the public to be more embarrassing, resulting in reluctance to ask questions and to seek help (Johanson and Lafferty, 1996).

Wearers of incontinence pads may be exposed to prolonged contact with urine, sweat and faeces. Their skin will therefore become over-hydrated which increases the permeability of the stratum corneum of the skin, allowing greater penetration of chemical agents and bacteria in urine and faeces (Berg, 1988). Most of these substances

can act as skin irritants if applied for sufficient time and in sufficient concentration (du

Vivier, 1992). The effect of such agents on skin is known as irritant contact dermatitis

and is characterized by skin inflammation; this irritant contact dermatitis induced by

wearing of diapers or nappies is usually referred to as diaper dermatitis.

Berg (1988) hypothesized that skin occluded by diapers forms the basis for a chain of

actions which result in diaper dermatitis. Fig 2.3 shows Berg's model of diaper

dermatitis development and resolution. The cycle begins when healthy skin becomes

weakened or compromised by an increase in skin wetness and the interaction of urine

and faeces with skin within the diaper environment. The barrier of the skin is then

disrupted, allowing friction, chemical irritation and microbial infection to cause diaper

dermatitis. Caretaker intervention contributes to the restoration of normal skin from

diaper dermatitis by changing habits and practices.

Diaper environment:
- Increased skin wetness
- Increased skin permeability
- Higher skin friction coefficient
- Lower skin abrasion resistance
- Greater microbial load
- Increased pH

Caretaker intervention:
- Increased diaper changing freq.
- Increased bathing freq.
- Medication
- Improved diapers

Healthy skin

Compromised skin

Diaper dermatitis

Etiology Factors:
- Faecal enzymes
- Chemical irritation
- Mechanical irritation

Fig 2.3 Berg's model of the cycle of diaper dermatitis.

(reproduced from Berg ,1988)

Prolonged exposure of skin to water has been shown to cause hydration dermatitis (Tsai

and Maibach, 1999) and prolonged occlusion of the skin (as within an absorbent pad)

has been demonstrated to reduce the barrier function of the skin (Fluhr et al., 1999). Aly and colleagues (1978) also studied the effect of prolonged occlusion and found a significant rise in microbial counts.

Berg et al. (1986) used a hairless mouse model to examine the role of urine in the etiology of diaper dermatitis. After exposure to infants' urine for 48 hours, the skin did not suffer irritation but after continuous exposure for 10 days, skin damage became apparent. The authors also measured skin permeability and found that continuous exposure to urine greatly increased the permeability of the skin. Furthermore, Buckingham and colleagues (1986) found that the addition of faeces increased the production of ammonia from urine causing an increase in pH, which increased the irritation of skin.

The influence of hydration on friction between fabrics and skin was investigated by Kenins (1994), who observed an increase in frictional force between fabric and over-hydrated skin. In a more recent study, Hong and colleagues (2005) investigated the friction between skin and the wet top surface of disposable diapers; it was found that the friction coefficients (defined as the ratio of the friction force to the normal force) of all the tested top layers were higher when wet than when dry (by factor of between two (for polypropylene through-air bonded fabric) and 10 (for a cotton spunlace fabric)). This increase in friction coefficient makes the skin more vulnerable to abrasion damage due to the friction forces (Zimmerer, 1986). It can also disrupt skin barrier function by removing skin lipids leading to an acceleration of water loss from skin (Montiero-Rriviere et al., 2001).

In summary, the effects of prolonged contact of urine on skin are as follow:

- Skin occlusion increases skin hydration which leads to an increase in the permeability of the skin.

- The presence of urine leads to a greater microbial load on the skin.

- The combination of urine and faeces results in an increase in pH which causes greater faecal enzyme activity and irritate the skin

- Over-hydrated skin has an increased coefficient of friction against fabric which increases the skin's vulnerability to abrasion damage.

2.3 Structure of the skin

Skin is one of the largest organs in the body. It is an ever-changing organ that contains many specialized cells and structures (Fig 2.4). The skin is made up of three distinct layers: epidermis, dermis and subcutaneous layer. The subcutaneous layer is a layer of fat that lies on the muscles and bones. Dermis lies above the subcutaneous layer, regulates body temperature and provides oxygen and nutrients to the skin via blood vessels. The epidermis is the outermost layer of the skin, it protects the body from the environment, and prevents excessive water loss from the body. The epidermis continually rebuilds the surface of the skin from within, maintaining the skin's strength and preventing wear and tear. The visible, outermost layer of the epidermis is called the stratum corneum.

2.3.1 Stratum Corneum as a barrier

The stratum corneum (SC) is formed and continuously replenished about every two weeks in mature adults (Montagna, 1961) by the slow upward migration of cells from the basal layer of the epidermis. It is a horny cell layer that is made up of layers of protein-rich dead cells, arranged in a 'brick and mortar' structure (Fig 2.5) in which

protein-rich dead cell "bricks" (corneocytes) are held together by lipid-rich "mortar", which helps to conserve moisture since water cannot pass through it easily (Montagna and Parakkal, 1974).
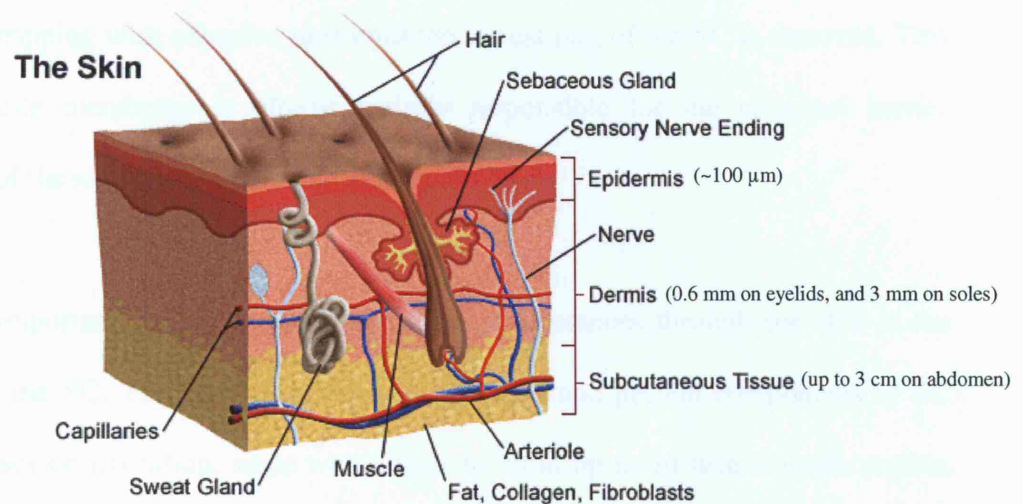
Fig 2.4 Structure of the skin

(adapted from www.lpch.org/photos/greystone/ei_0390.gif)
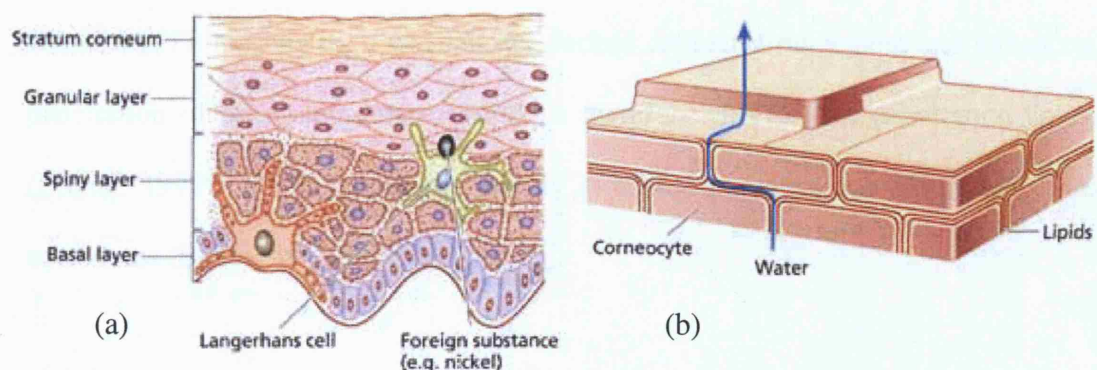
Fig 2.5 (a) Structure of the epidermis layer.

(b) A 'bricks and mortar' model of structure of the stratum corneum

(adapted from Gray, 2000)

Since the SC comprises dead cells and lipids, it does not depend upon the activities of living cells. Swarbrick et al. (1982) showed that the SC lasts long after skin is removed from the body, and has the ability to lose and gain water in a reversible and consistent manner. The permeability of the SC is not determined by the number of cell layers or its thickness, but the lipid concentration of the intercellular material (Elias et al. 1981).

Removing the SC causes as much as a 50-fold increase in the rate of water loss from the skin surface (Montagna and Parakkal, 1974). In early work, Blank (1953) showed that the water permeability of excised full-thickness skin remains almost normal after successive stripping with adhesive tape until the lowest part of the SC is removed. This semi-permeable membrane is almost entirely responsible for the principal barrier mechanism of the skin (Scheuplein and Blank, 1971).

One of the important factors in the penetration of substances through the skin is the hydration of the SC. The separation between the lipid and protein components of SC tissue increases on hydration, since water tends to build up multi-layers on the protein and helps protect it from the lipids (Scheuplein and Blank, 1971).

Hydration increases the thickness of the stratum corneum several-fold (Scheuplein and Blank, 1971), loosens its tight, densely packed cellular arrangement and enhances the penetration of other substances. Water is therefore an effective penetration enhancer (Ebling, 1992), which allows the greatly increased percutaneous absorption of some substances (Behl et al., 1980).

To investigate the hydration of the SC, Lévêque (2004) described the sorption and desorption isotherms of excised SC (Fig 2.6), which reflects the quantity of water that can bind at a given temperature and relative humidity. Fig 2.6 shows that the equilibrium hydration is rather low at 23°C, ~10% or less for RH values up to ~60%, but rises rapidly at RH values >80%.
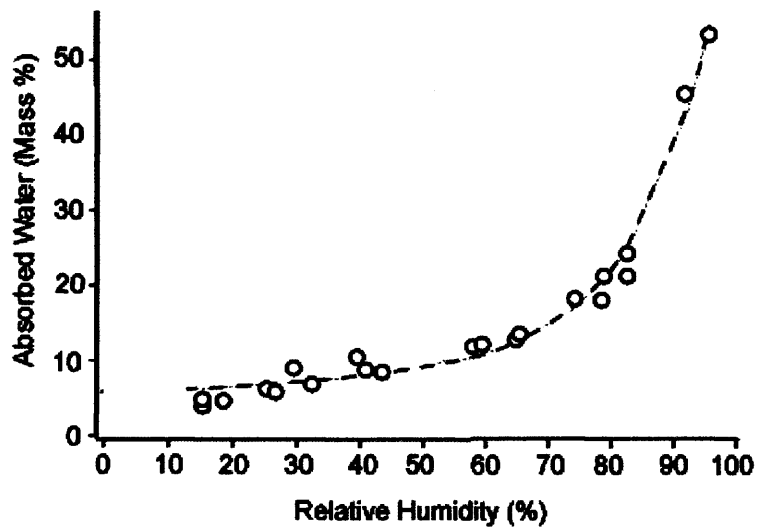
Fig 2.6 Sorption isotherm at 23°C for excised SC.

(reproduced from Lévêque, 2004)

When skin is hydrated by continuous wearing of incontinence absorbent pads, it becomes over-hydrated, leading to obstruction of the normal ventilation of the skin, increasing the permeability and penetration of other substances, and making the skin more susceptible to mechanical damage and bacterial attack than normal skin. This thesis focuses on understanding the effects of water on the wetness of the SC and the friction between skin and materials.

2.4 Characterising skin wetness

Measurements of skin water content are commonly used in many areas of research and they are important for studying the barrier function of the skin. Various techniques have been used for these measurements – electrical measurements (Leveque and de Rigal, 1983), Near Infrared Spectroscopy (NIRS) (Martin, 1993), evaporimetry (Zimmerer, 1986) and Opto-Thermal Transient Emission Radiometry (OTTER) (Xiao and Imhof, 1996).

Electrical measurements aim to estimate the total water content of the superficial layers

of the skin by passing an electric current through them and measuring the impedance, the frequency dependent ratio of voltage to current. Near infrared spectroscopy measures the amount of water in the skin on the basis of the absorption of infrared radiation by the water molecules. Evaporimetry has mostly been used to investigate the barrier function of the SC by estimating the evaporation rate of water from the skin surface. Since the barrier function is affected by the SC water content, many have used spot evaporimetry measurements as a measure of skin wetness (Dallas and Wilson, 1992). A minority have used evaporimetry to log drying curves of wet skin to estimate the excess water in the skin caused by, for example, wearing diapers (Zimmerer, 1986). Finally, OTTER is a newly developed technique that aims to measure the water saturation profile within the SC, by applying laser pulses to the skin and measuring the heat radiation change at the skin surface. Each of these methods for measuring skin wetness is reviewed in more detail below.

2.4.1 Electrical measurements

It has been known for a long time that the electrical properties (impedance, comprising resistance and capacitance) of the skin are related to the water content of the stratum corneum (Leveque and de Rigal, 1983). The dry SC acts like a dielectric medium, a medium of weak electrical conduction. Addition of water makes the SC responsive to an electrical field, because water is strongly dipolar, the water molecules combine easily with the structural components of the SC, making it more sensitive to an electrical field. At least three types of structural components are involved here (Tagami, 1995):

(1) keratin chains and the embedding protein, which have a dipolar moment and are made more mobile by the plasticizing effect of water

(2) ions in the inter- and intracellular spaces, which can react to the applied electrical field and move with it

(3) water molecules, which form a continuous network of hydrogen bonds, allowing the

exchange of a proton between two radicals of the types OH_3^+ and OH^-.

However, agents other than water – such as urea and salts – can undergo changes in

dipole orientation and ion mobility and they can cause dramatic change in SC

impedance due to their intrinsic ion mobilities (Potts, 1986).

When skin is submitted to an applied alternating current of frequency f, the total

impedance of the skin Z depends on the resistance R and capacitance C, with the

following relationship (Barel and Clarys, 1995a):

$$Z = [R^2 + (\frac{1}{2\pi f C})^2]^{\frac{1}{2}}$$ .... Equation 2.1

The relationship between conductance and water content is not linear, but depends on

the binding state of water molecules to the keratin chains. Three types of water binding

are identified in the literature according to their strength of binding to the keratin:

'tightly bound water' for water contents between 0 - 7%; 'bound water' between about

7 - 35 %; and 'free water' above 35 % (Berardesca, 1997). Due to this variation in

water binding strength, there is no direct proportionality between total water content and

electrical conductance.

The electrical characteristics of human skin are known to vary with the frequency of the

measuring current (Tagami, 1995). Three dispersion zones are recognised for

determining the impedance of the skin: α dispersion (0.1 - 1000 Hz) appears to be

entirely located in the SC (it disappears when the SC is stripped); β dispersion (100

kHz – 400 MHz) is due to the bound water and is characteristic of most biological

macromolecules; and γ dispersion (5 – 15 GHz) is due to the dipolar relaxation of free

water. The literature describes four different methods for measuring the impedance of

the SC, and they can be categorised by the frequency of the measuring current used.
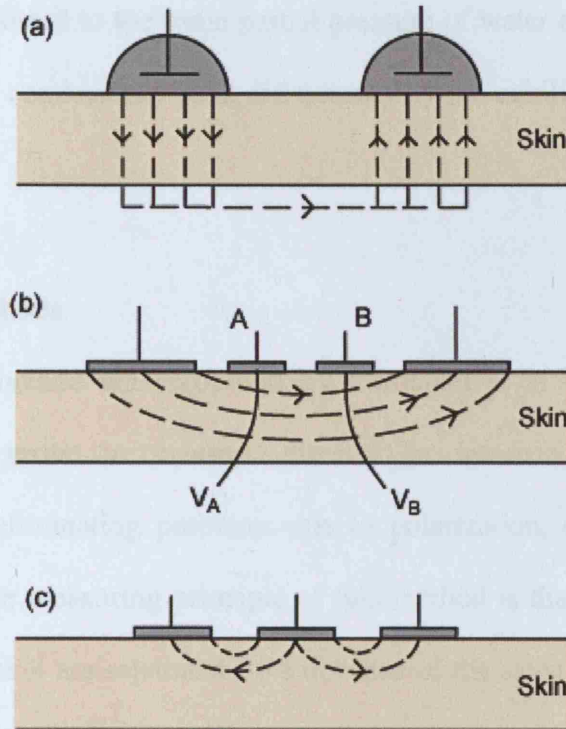
Fig 2.7 Schematic diagram of electrical field lines in the skin produced by electrical
measurements (a) low frequency method, (b) four electrodes method,
(c) high frequency method.

Low frequency methods

Low frequency current penetrates into the viable portion of the skin (Fig 2.7a), hence it

measures the properties of the SC over its entire thickness, and the distribution of the

electrical field within the SC is simple. However, this method suffers from technical

difficulties such as the influence of applied pressure between the electrode and the skin

surface, accumulation of water underneath the electrode resulting from transepidermal

water loss (TEWL), and polarisation of the electrodes.

The method developed by Clar et al. (1975) is a well known low-frequency method,

involving the measurement of the impedance and relaxation time of the α dispersion of the skin. They used an electrode filled with a conductivity joint liquid, which consisted of various proportions of sodium chloride solution (NaCl), polyethylene glycol (PEG) and water (H_2O), adjusted to the same partial pressure of water as the ambient relative humidity, so that the conductivity joint did not modify the equilibrium of water on the skin surface.

Four electrodes methods

This measurement method was proposed by Campbell et al. (1977) and it uses a four-microelectrode probe to measure directly an intrinsic parameter, electrical conductivity, while eliminating problems due to polarization, contact resistance and sample geometry. The measuring principle of this method is that if the electrodes that apply current to the skin are separated by a distance of the same order as the thickness of the SC, the field lines will pass through this layer. Two inner electrodes are placed between the outer electrodes to read the values of the local potentials (Fig 2.7b).

High frequency methods

General dielectric studies of skin have shown that experiments conducted at higher frequencies provide information on deeper layers of the skin. However, penetration of waves into the skin does not depend solely on their frequency, but also on the way they are generated on the skin according to the electrodes used and their respective spacing (Leveque and de Rigal, 1983). Specifically, if the applied electrodes are placed very close together, they can maintain the electrical field in the superficial portion of the skin (Fig 2.7c). Using high frequency current, there is no problem of polarization of the electrodes.

Very high frequency methods

The γ dispersion observed at very high frequencies, i.e. at several GHz, is due to the relaxation of free water. One of the very high frequency methods found in the literature (Jacques, 1997) used an interdigitated electrode, which enabled the electrical field to be maintained at a depth of 3 μm from the skin surface. A linear relationship between the electrical parameters and the water content of the SC was measured.

Guidelines for using electrical methods to assess the SC hydration have been published by a European group (Berardesca, 1997). They analysed the variables related to measurements and current instrumentation, and standardisation of measurements was suggested. The main topics of discussion related to the electrical methods are summarised below:

● The area of contact between the probe and the skin surface will depend on the pressure applied, and thus pressure between the probe and the skin may affect the results

● Distribution of the electric field through the different skin layers cannot be calculated adequately because of the complexity of the geometry and the composition of the materials involved. All electrical instruments give results that are an integration over depth, with the dependence on depth varying from instrument to instrument and also from skin site to skin site

● Instruments that are available on the market work at different frequencies and use various probe sizes that apply different pressures on the skin

In summary, electrical measurements can be used to estimate the water content of the superficial layers of the skin with the following drawbacks: (1) Agents other than water (e.g. salts and urea) can lower the impedance of the SC; (2) Occlusion of the test skin

site by the probes can affect measurements; (3) Variation of probe pressure against the skin can alter impedance, and (4) Measurement depth is ambiguous, making it more complicated to understand. Therefore such techniques may not be suitable for measurement on over-hydrated skin, in particular.

2.4.2 Near infrared spectroscopy

NIR spectroscopy is a point-measurement method that uses a fibre optic probe to transport light to and from the skin (Martin, 1993). The absorption spectrum of the skin is then produced and expressed as absorbance, (log 1/R, where R is reflectance) against wavelength. Spectroscopy techniques can be used to determine the concentration of absorbers within a tissue sample, and this concentration (c_a) can be considered to be directly proportional to the absorbance (A) at a given wavelength according to an equation based on the Beer-Lambert's law (Wang and Wu, 2007):

$$A = \varepsilon \cdot c_a \cdot d \ldots\ldots\ldots\ldots\ldots\ldots\ldots \text{Equation 2.2}$$

where A is absorbance, ε is the specific extinction coefficient, c_a is the concentration and d is the distance that the light travels through the material (the path length).

In the NIR spectrum (1100 – 2500 nm), water molecules show two clear absorption bands at 1450 and 1936 nm which are easily identified in the spectrum of the human skin *in vivo*. The NIR region is sensitive to hydrogen-bonding differences, and so it can distinguish different types of water (see below); and the scattering effects can be used to determine changes in the character of the skin surface. Attas et al. (2001) used two digital imaging systems equipped with the NIR instrument, to produce images that show the degree of skin hydration as a function of location.

de Rigal et al. (1993) used NIR reflectance on *in vitro* skin to demonstrate that the water

peak intensities are proportional to the water content, and *in vivo*, they found a strong correlation between water peak intensities and clinical scores for skin 'dryness'. The scores were evaluated by a trained expert describing the appearance of the skin using different criteria (inflammation, roughness, and presence of flakes and scales) with a score of 0 to 4 according to the degree of severity.

Martin (1993) compared the log 1/R spectrum of skin with that for water, and inferred the existence of four types of water in the skin: water associated with the lipid phase within the SC, bulk water below the SC, secondary and primary water of hydration on SC keratin.

The depth of penetration of optical radiation into the skin depends on several factors. When NIR radiation impinges on skin, it undergoes regular reflectance, absorption, internal scattering and diffuse reflectance. The degree to which each occurs depends on the structure, refractive index, absorptivity and the scattering coefficient of the skin, as well as the wavelength of the incident NIR light. Arimoto et al. (2005) implemented a Monte Carlo simulation to investigate the relationship between the NIR penetration depth in the skin and experimental conditions, such as the wavelength of the NIR light and the geometry of the optical fibre probes. They found that the measurement depth depends on the geometry of the optical fibre probe used for radiating and detecting light on skin. A larger source-detector separation and a thicker optical fibre resulted in a greater measurement depth.

By using NIR spectroscopy, skin spectra or images can be collected *in vivo* without the need to have the probe in contact with the skin surface, i.e. non-occlusive measurements can be made. However, when it comes to quantifying water content in the skin, the

technique is not specific enough; the output spectrum gives information about many compounds that exist in the skin rather than water alone. Therefore it has to be calibrated by the use of other techniques on the reference samples (skin), in order to extract information about the water concentration in the skin.

2.4.3 Evaporimetry

The SC *in vivo* is always partially hydrated (Scheuplein and Blank, 1971). The concentration of water near the lowest cell layer must be high because of the adjacent water-filled cells of the viable epidermis. As the ambient relative humidity is always less than 100%, water is continuously transferred outward by diffusion. Under normal equilibrium, the total amount of water lost from the human body is the sum of this continuous diffusion of water vapour through the epidermis and the secretion of sweat through the sweat glands, and this is termed transepidermal water loss (TEWL). Under many conditions, the level of sweat gland activity is negligible, in which case the only contribution to TEWL is water that has evaporated from the skin having diffused up through the epidermis.

Confusingly, people have used a variety of descriptors in the literature, and different authors have sometimes used the same phrase to describe different quantities. The term 'TEWL' has also often been used to describe the evaporation of water from skin which has become over-hydrated by occlusion with baby diapers, incontinence pads and test patches of various materials. This is inappropriate as the excess water given off when over-hydrated skin is opened to the atmosphere cross from the SC and does not, therefore, cross the epidermis. In this thesis, the term 'water vapour flux density' is used to describe any water loss from the skin surface while TEWL is reserved for water which leaves the skin having diffused across the epidermis. In the interests of providing

a coherent literature review, previous work is described using the consistent phrasing described above, rather than that used by the various authors.

2.4.3.1 Open-chamber evaporimetry devices

Nilsson (1977) invented the open-chamber method of measuring water vapour flux in the 1970s. In the absence of forced or natural air convection, a boundary layer develops around the skin (approximately 10 mm high) in which a water vapour gradient exists between the skin surface and ambient air (Nilsson, 1977). If the vapour pressure of the boundary layer is known, the evaporative water loss can be expressed in terms of the vapour-pressure gradient, which can be represented by Fick's 1st law of diffusion:

$$J = -D_w \cdot \frac{\partial c}{\partial z}$$ ………..…………….. Equation 2.3

where J is the water vapour flux density, D_w is the diffusion coefficient of water vapour in air at the ambient temperature, c is water vapour concentration, z is the distance measurement, therefore $\frac{\partial c}{\partial z}$ is the water vapour concentration gradient (Fig 2.8).
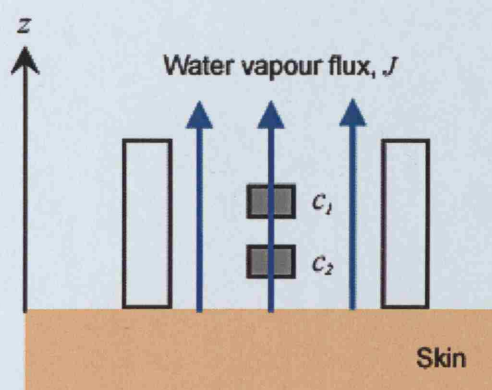
Fig 2.8 Illustration of the Fick's law of diffusion used in the open-chamber technique.

Nilsson's invention has developed into a commercial instrument (Evaporimeter, Servo Med AB, Sweden). It utilises a probe with an open, cylindrical measurement chamber that is placed on the skin site to be measured. A pair of sensor units (each comprising a

hygrosensor - transducers whose resistance varies with humidity, and a thermistor) for determining the relative humidity and temperature, and hence the water vapour concentration at two fixed levels above the skin (Fig 2.9). This information – together with the known distance between the sensors - is used to estimate the concentration gradient, and hence the water vapour flux.
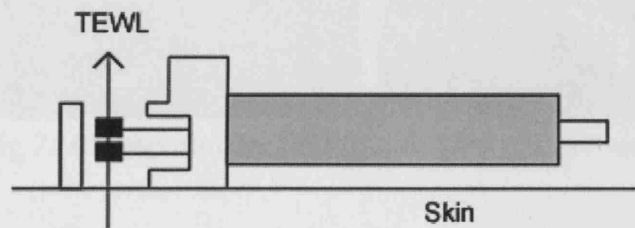
Fig 2.9 Evaporimeter probe showing the geometry of the measurement diameter
and the positions of the sensors (shaded black in figure).
(reproduced from Nilsson, 1977)

Today, open-chamber instruments for measuring water vapour flux are available from Cortex Technology, Denmark (DermaLab), and Courage and Khazaka Electronic, Germany (Tewameter), but Servo Med AB appears to have ceased trading at the time of writing. The following sections provide a description of the three commonly used open-chamber devices: Evaporimeter EP2, DermaLab and Tewameter TM300, reviewing their physical dimensions, data gathering methods, probe checking methods and special functions.

Evaporimeter EP2

The Evaporimeter (Fig 2.10) was the only commercially available evaporimetry instrument between the 1970s and 1990s. It consists of a probe containing two pairs of hygrosensors and thermistors positioned in an open cylindrical chamber to take measurements at 3 mm and 9 mm above the skin. The probe weighs 104 g and has a chamber of diameter of 12 mm and height 15 mm. A gold-plated cover is provided to be

placed over the surface of the chamber that is in contact with the skin to facilitate cleaning.
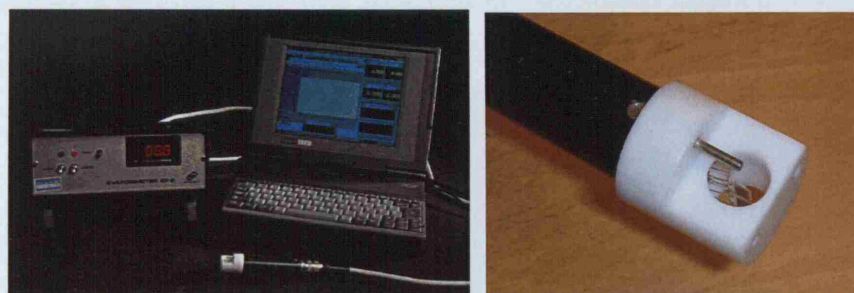
Fig 2.10 Evaporimeter EP2 (Servo Med AB, Sweden).

The instrument is supplied with standard software to measure mean flux values in $g \cdot m^{-2} h^{-1}$ based on the information from the sensors, over different time periods.

It is advised that between measurements, the Evaporimeter reading should be allowed to settle to zero, rather than adjusting the offset button, in case water vapour is trapped in the probe and a false zero is obtained (Pinnagoda et al. 1990).

An instrumental checking program is recommended for daily use to ensure that the instrument is functioning correctly. It is necessary for the Evaporimeter to be switched on for at least 15 minutes prior to use to equilibrate to ambient room temperature and relative humidity before calibration can take place. The probe is turned sideways so that the axis of the chamber is horizontal, making the two sensors sample the same ambient air at the same level, and the flux reading should settle to zero if the sensors are in calibration.

DermaLab

The DermaLab (Fig 2.11) also applies the open-chamber vapour pressure gradient

estimation to calculate water vapour flux. The two combined humidity / temperature sensors are mounted at 4 mm and 8 mm above the skin in the diffusion chamber. The probe weighs 53 g and has a chamber diameter of 10 mm and height of 22 mm.
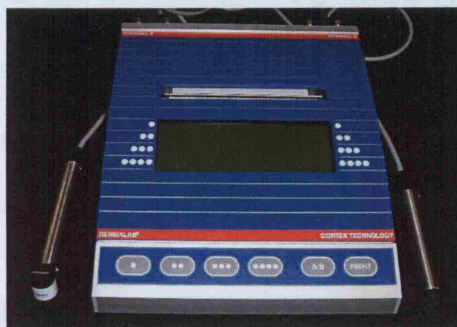
Fig 2.11 DermaLab (Cortex Technology, Denmark).

The main feature of the device is that it may accommodate one or two measurement channels, i.e. measurements from the two channels can be recorded and synchronised simultaneously. It is fully menu driven with a LCD panel and built-in printer. Parameter settings are automatically saved in memory, and reports with graphics may be printed in full or reduced form either automatically at the end of a measurement or manually by pushing a button. The printed report also carries the date and time of recording. The ambient relative humidity and temperature can be read from the LCD display by selecting 'Environmental Check' from the menu.

The device can also be connected to a computer to export measurements either as individual readings, or by using the continuous mode. In continuous mode, a maximum of 5 minutes of raw data are transferred in real-time to the program, enabling graphical and numerical monitoring of ongoing measurements using the device. The measurement can be set to stop automatically after a preset time (within 5 minutes) or when a preset standard deviation on the mean reading has been achieved.

Tewameter TM300

The Tewameter (Fig 2.12) is also an open-chamber evaporimetry device with two pairs of sensors (temperature and relative humidity), which take measurements 3 mm and 8 mm above the skin surface, and the data are analyzed by a microprocessor. The probe weighs 90 g and has a chamber diameter of 10 mm and height 20 mm. The Tewameter can be equipped with up to three additional probes with the Multi Probe Adapter (MPA) to measure at different skin sites simultaneously.
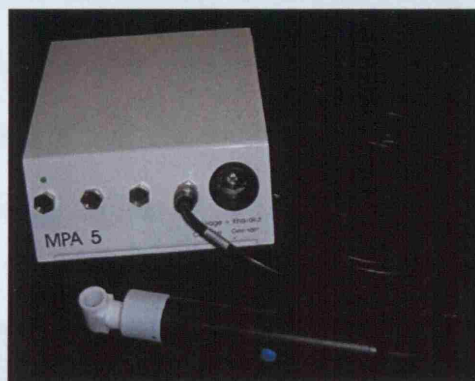
Fig 2.12 Tewameter TM300 (Courage and Khazaka Electronic, Germany).

A start / stop green button is positioned on the side of the probe handle and, when measurement starts, the water vapour flux values, mean flux values, standard deviation and the temperature and humidity of the two sensors in the probe can be selected to be displayed and stored by the software. The measurement is stopped when the green button is pressed, or the preset stopping criterion is reached (at a certain standard deviation or measuring time).

A pre-heating function is available with the Tewameter TM300. When it is selected, the two pairs of sensors in the chamber will be heated to 3 °C above ambient, making the sensor temperature closer to skin temperature, hence reducing the time taken to reach a stable measurement from about 60 s to less than 20 s (CK electronic GmbH).

The calibration of the probe can be checked by the supplied calibration unit TCC-300. The probe is fixed in position on the calibration unit with a small cap on the probe head, creating a closed measuring chamber (Fig 2.13), which is left undisturbed for one hour to check calibration. The temperature and humidity from the probe sensors and the calibration unit are measured for 3 minutes and then compared. A report of the state of the probe with suggested action is generated, e.g. perform a zero calibration by clicking the 'Reset' button on the software to zero the value of the probe when it sits in the calibration checking unit; or the humidity sensors are giving values out of tolerance and 'Regaining' is needed. In the latter case, the sensors are then heated to let impurities evaporate from the probe. If the checked values remain out of tolerance after the suggested actions have been performed, the device will need to be sent for recalibration by the manufacturer.
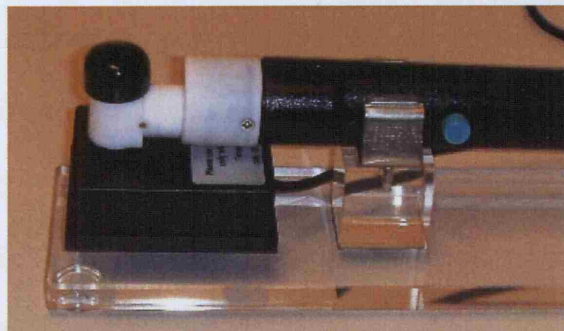
Fig 2.13. Tewameter on the calibration unit.

2.4.3.2 Limitations of the open-chamber devices

As the use of evaporimetry to characterise skin barrier function became more common, guidelines for the measurement of water vapour flux using open-chamber devices were published (Pinnagoda et al., 1990 and Rogiers, 2001). Focusing particularly on TEWL measurement on normal skin, they identified three main sets of variables that can affect measurements, related to: (i) the *individual* (the subject whose skin is being investigated); (ii) the *environment*; and (iii) the *instrument*. The variables, rationales and

the recommendations are summarised in Table 2.2. This practical guidance aimed to enable users of open-chamber devices to achieve repeatable results.

It has also been noted (Pinnagoda et al., 1990) that during measurement, the presence of the open-chamber probe may restrict the water vapour flux it is attempting to measure, causing an underestimation of unimpeded water vapour flux, particularly at high evaporation rates. It has been reported (Wheldon and Monteith, 1980) that at evaporation rates of about 20 $g \cdot m^{-2} h^{-1}$ the underestimation is about 10%, but at around 75 $g \cdot m^{-2} h^{-1}$ - a value easily reached for fully over-hydrated skin - the underestimation may be about 50%.

2.4.3.3 Closed-chamber evaporimetry

Recognition of the limitations of open-chamber devices – particularly their sensitivity to ambient and body-induced airflows near the probe, room temperature and ambient humidity – has led to the development of instruments which seek to address these problems. They make use of different measurement principles, but a closed measurement chamber is a key feature in all of them: the unventilated-chamber instruments (Model H4300, Nikkiso-Ysi Co Ltd, Japan; and VapoMeter, Delfin Technologies Ltd, Finland) and the condenser-chamber instrument (AquaFlux, Biox Systems Ltd., UK). Since the use of the H4300 device is limited in the literature and its commercial availability is unknown at time of the study, this section provides a description of just the other two closed-chamber evaporimetry devices: the VapoMeter and the AquaFlux, reviewing their physical dimensions, data gathering and probe checking methods.

Table 2.2 Summary of individual-related, environment-related and instrument-related variations when using open-chamber evaporimetry devices.

	Variables	Rationale	Recommendation
Individual	Age	TEWL varies with age: premature infants have greater and more variable TEWL than mature infants; for adults, a slightly decreased TEWL has been found in aged individuals as compared with mid-adulthood values.	Homogenous groups of subjects with respect to sex and age should be used.
	Anatomical sites	Skin structure and, therefore, TEWL varies across the body.	The skin site for measurements should be recorded accurately. Volar forearm is a preferred skin site.
	Sweating	Physical, thermal and emotional sweating needs to be controlled for accurate TEWL measurements.	Subjects should be acclimatised and rested for 15-30 min in a temperature-controlled room at about 20 °C prior to measurements.
	Skin surface temperature	TEWL increases with skin surface temperature, with a steep slope at around 28-30 °C.	
Environment	Air convection	Air movement is the main sources of disturbance which produces fluctuations in TEWL measurements.	Measurements should be performed in a controlled environment room with limited air circulation.
	Ambient air temperature	Temperature of the ambient air influences the skin temperature, and hence the TEWL value.	Recommended temperature is 20-22 ± 1 °C and relative humidity is < 60%.
	Ambient air humidity	TEWL changes with ambient air humidity and the relationship is not linear, it is a complex and important variable in TEWL measurements.	
	Direct light	Light sources should be avoided as they affect the ambient air temperature close to the subject and create air convection.	Direct and close light sources should be avoided.

.... Continuation of Table 2.2

Instrument			
	Zero drift	After measurement, the temperature and humidity of the probe is higher than that at its 'pre-use' equilibrium with the room conditions.	Allow time for the sensors to equilibrate with the ambient conditions and return to the 'zero' water evaporation level as indicated in the unused position, between experiments.
	Probe temperature changes	The warmth of operator's hand influences the amplifiers in the probe handle, and hence TEWL values.	Measuring probe should not be touched immediately before and during measurements.
	Probe contact pressure	Variation in contact pressure between probe head and skin changes the distance between the skin and sensors and hence TEWL values	Measuring surface should be in horizontal plane and the probe applied perpendicular to the surface with constant and light contact pressure.
	Probe surface plane	Skin surface is warmer than the environment, causing an increased upward natural convection of air close to the skin surface.	

VapoMeter

The most commonly used unventilated closed chamber device is the VapoMeter (Fig 2.14). It is a battery-operated, orientation-independent and portable device. The VapoMeter weighs 150 g with a chamber diameter of 11 mm and height of 18.4 mm. A single humidity and temperature sensor pair is located in the centre of the measurement chamber, which is directly integrated into a hand-held microprocessor-controlled electronic unit with a digital readout for the TEWL, relative humidity and temperature values.
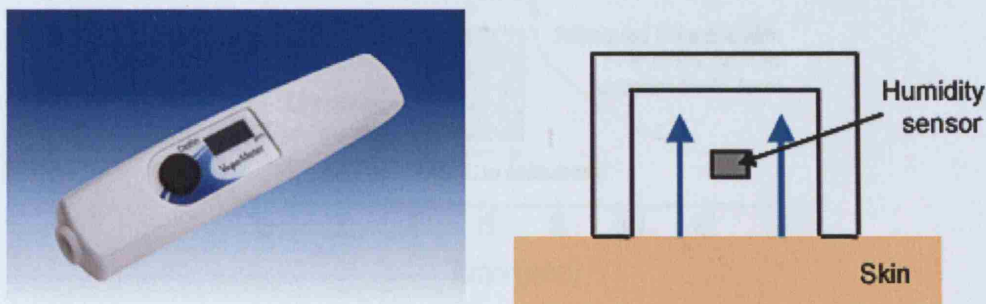
Fig 2.14 VapoMeter (Delfin Technologies Ltd, Finland).

One end of the measurement chamber is closed and the other end has a measurement orifice that is placed in contact with the skin. Water vapour from the skin is collected in the chamber from which it cannot escape. This causes the humidity to rise with time, slowly at first, but approximately linearly after a few seconds, as illustrated in Fig 2.15. The flux density of water evaporation from the skin is calculated from the gradient of the linearly rising part of the curve (as shown in Fig 2.15) using the relative humidity and temperature measured by the sensors.

The measurement is operated by a one push-button. There are tone signals to guide the measurement process. The VapoMeter is placed on the skin after pressing the button, the device is then held in contact with the skin until a tone signal indicates that the

measurement is finished (with a measuring time of 7-16 s). Readings of water vapour

flux in $g \cdot m^{-2} h^{-1}$, ambient relative humidity and temperature are displayed on the device.

After the measurement is completed, the chamber needs to be lifted from the skin to

allow the accumulated water vapour to escape before the next measurement can be

commenced.
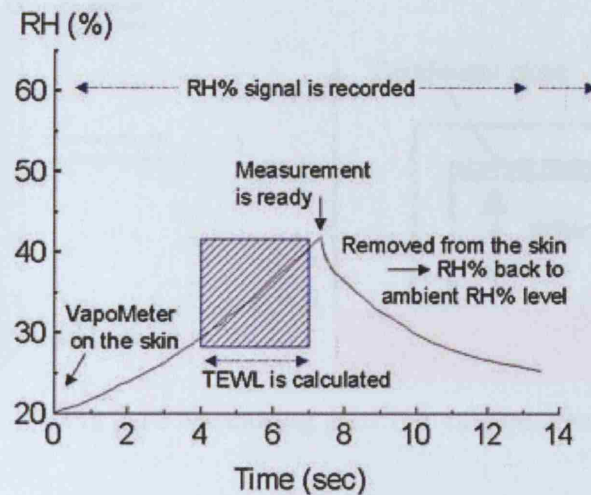
Fig 2.15 Measuring principle of VapoMeter
(adapted from Delfin Technologies Ltd).

The device can be equipped with a data interface to a computer, so that the data are

collected according to customized program protocols via a wireless data receiver.

The VapoMeter is factory calibrated. Each calibration holds for up to 2 years unless the

device is used in very variable conditions or continually on a daily basis (VapoMeter

user manual). Recalibration is recommended every other year or once a year for units in

heavy use.

AquaFlux

Very recently, Imhof at el. (2002) developed a new device for measuring water vapour

flux called the AquaFlux, which is based on Nilsson's invention discussed in Section

2.4.3.1. It uses a closed measurement chamber containing a single temperature / humidity sensor and an electronically cooled condenser opposite to the measurement orifice. Being closed, the chamber shields the sensor from the effects of external air currents and provides measurements independent of ambient temperature and humidity.
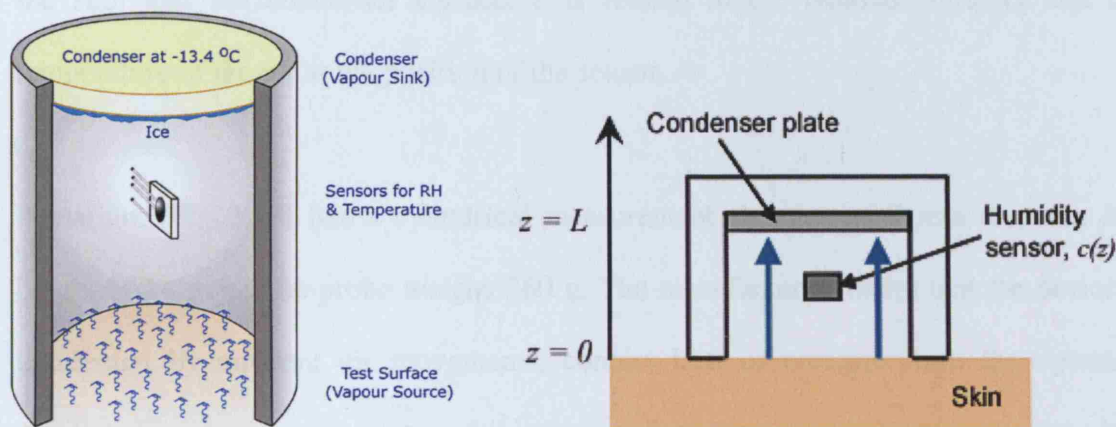
Fig 2.16 Measuring principle of AquaFlux.

During measurement, water vapour travels from the skin surface towards the opposite end of the measurement chamber, where it is removed by freezing onto the condenser surface which is maintained at -13.4°C. As illustrated in Fig 2.16, skin is at $z = 0$ and emits a flux of water vapour. The condenser surface is at $z = L$. In the absence of mass air movements, the concentration of water vapour $c(z)$ at any point within the chamber can be calculated from Fick's first law of diffusion (Eq 2.3). In steady state, the water vapour flux evaporated from the skin is equal to the flux condensing onto the condenser surface, $\frac{\partial J}{\partial z} = 0$. Applying this to Eq 2.3 gives $D_w \frac{\partial^2 c}{\partial z^2} = 0$. This expression can then be solved to give an expression for the flux of water vapour in terms of the concentration of water vapour at any point within the chamber:

$$J = D_w \cdot \frac{c(z) - c(L)}{L - z} \qquad \ldots\ldots\ldots\ldots\ldots \text{Equation 2.4}$$

This equation forms the basis of the technique. If the condenser surface temperature is low enough, $c(L)$ can be approximated to zero and a measurement of water vapour concentration at any one position z will be sufficient to determine J. This can be done by means of a single relative humidity / temperature sensor located about halfway between the skin and the condenser surface; c is related to the relative humidity and the temperature of the air at the position of the sensor.

AquaFlux (Fig 2.17) has a cylindrical measurement chamber of 7 mm diameter and height of 14 mm. The probe weighs 260 g. The manufacturers claim that the device is unaffected by ambient air movements, contact heat or pressure from the operator; site-hopping measurements are possible (pauses between measurements are not needed) and it can be used in any surface orientation (AquaFlux user manual).

(a)   (b)
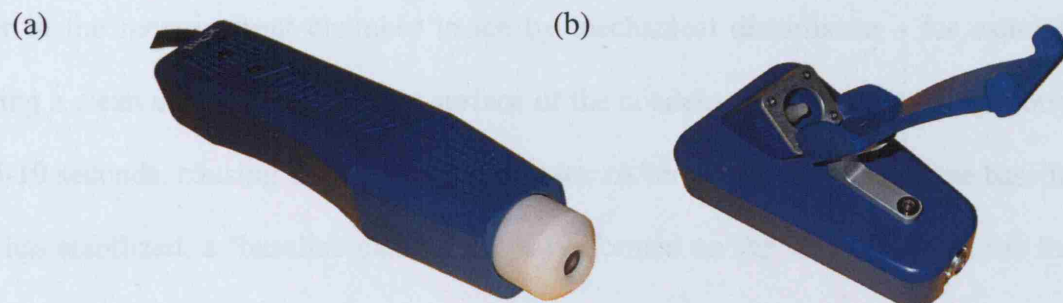
Fig 2.17 (a) Hand-held probe and (b) base unit of
AquaFlux AF100 (Biox Systems, U.K.).

The base unit of the device provides an interface to a computer and the measurement process is operated by the software. Two main types of measurement can be performed: TEWL spot measurement and time-series continuous measurement. The outcome of a TEWL spot measurement is a single value representing the mean water vapour flux density escaped from the skin surface when it has reached equilibrium. The outcome of

a time-series continuous measurement is graph of water vapour flux density against time. The measurement ends after a pre-set time and the data are saved in a spreadsheet-compatible format.

Two calibration processes are implemented in the software: baseline calibration and flux density calibration. The baseline calibration needs to be performed every time the instrument is switched on, because of the hysteresis properties of the humidity sensor. When the device is switched on, the aluminium condenser is maintained at below the freezing temperature of water at -13.4 °C. It is then fitted with a calibration cap which closes the measurement chamber, hence the air within it is protected from the ambient conditions. The flux reading decreases towards zero as the humidity sensor settles, the water in the chamber desorbs and the materials in the vicinity of the condenser reach thermal equilibrium. Priming the condenser is then needed to convert the super-cooled water in the measurement chamber to ice by mechanical disturbance – for example, moving a clean dental stick over the surface of the condenser in a light scribing motion for 5-10 seconds, causing ice crystals to nucleate. After priming, and once the baseline flux has stabilized, a 'baseline calibration' is performed on the software to set the flux reading to zero. The device is then ready to use.

The flux density calibration is recommended to be performed at 3-6 month intervals using the 'droplet method' and the micro-syringe supplied. A 1 mg droplet of water is dispensed into the calibration near the centre of the calibration cap. The cap is then applied to the probe, and the flux recorded as a function of time until the droplet has evaporated. The calibration factor can then be calculated from the area under the flux-time curve, since the true area is known to be equivalent to 1 mg of water.

2.4.3.4 Limitations of closed chamber devices

Unventilated closed-chamber methods for measuring water vapour flux were not recommended by the guidelines for TEWL measurement published in 1990 (Pinnagoda et al., 1990). The closed-chamber devices available at the time were not capable of making continuous measurements. This is because water evaporating from the skin gradually built up in the chamber, so interfering with the evaporation of further water. However, the two commercially available close-chamber instruments described above have shown that this problem can be overcome. VapoMeter uses a short measurement time to minimise the impact of the chamber on the evaporation process (Alanen et al., 2003). The condenser within the AquaFlux measurement chamber freezes the incoming water vapour to ice, making it possible to measure water vapour flux density continuously without water vapour build up due to occluding the skin.

Table 2.3 presents a summary of the recommendations provided by the guidelines (Pinnagoda et al., 1990 and Rogiers, 2001) and how they apply to the two close-chamber instruments. It is apparent that the devices are not affected by most of the conditions recommended for the open-chamber devices, which gives them advantages for use in clinical settings, e.g. in nursing homes where the ambient air conditions cannot be controlled.

2.4.3.5 Methodology for using evaporimetry on over-hydrated skin

Most studies of over-hydrated skin have aimed to measure or compare the impact of various occlusive materials and products using evaporimetry techniques. However, in the review that follows, the focus is on the methodologies used, rather than the outcomes of the studies, reflecting the primary interest of the current project.

Table 2.3 Summary of the recommendations on evaporimetry measurements by Pinnagoda et al. (1990) and Rogiers (2001) and their application to closed-chamber devices.

Variables	Guidelines recommendations	Closed-chamber device applicability
Ambient air conditions	Perform measurements in a controlled environment room with limited air circulation. Recommended temperature is between 20-22 ± 1 °C and relative humidity is lower than 60%.	Ambient air conditions have no effect on closed-chamber measurements. The recommendations are valid for all measurements as they provide conditions that can avoid surface moisture and sweat gland activity of the subjects.
Post measurement recovery	Allow time for the sensors to equilibrate with the ambient conditions and return to the 'zero' water evaporation level as indicated in the unused position, between experiments.	**VapoMeter:** The humidity in the measurement chamber needs to return to ambient humidity before the next measurement can be started. **AquaFlux:** Recovery time is not necessary before starting the next measurement, because of the controlled microclimate.
Probe temperature changes	Measuring probe should not be touched before and during measurements. Recommended to handle with the electrical wire, a coating or by wearing gloves.	**VapoMeter:** TEWL values were found to increase significantly with probe temperature (De Paepe et al., 2005). **AquaFlux:** The probe can be held in whatever way is comfortable.
Probe contact pressure	The contact pressure of the probe onto the skin should be kept low and constant.	No measurable contact pressure effect has been found with either closed-chamber devices.
Probe surface plane	The measuring surface should be placed in a horizontal plane, and the probe applied parallel to this surface.	Closed chambers do not suffer the same interference from convection air movements as open-chamber instruments do. They can therefore be used with all surface orientations.

Zimmerer et al. (1986) published the first substantial study to characterise skin that had been over-hydrated by occlusion with wet diaper materials, a study that included extensive water vapour flux density measurements. In preliminary work on adult volar forearms, they established that although a wear time of two hours was needed to achieve full over-hydration of the skin, a saturation level of 95% was reached in an hour. Accordingly, they used two hours for adults but - for convenience – just one hour for babies. Thirty-two male babies wore cloth or disposable diapers loaded with 0, 50, 100 or 150 ml of synthetic urine (dyne solution) for one hour and had the water vapour flux density from their suprapubic skin measured on diaper removal.

In a parallel study, patches cut from the same two brands of diaper were held on the volar forearms of adult volunteers for two hours with elastic mesh bandage, having been preloaded with the volunteers' own urine to various saturation levels. As with the babies, water vapour flux density from their occluded skin was measured on patch removal. All water vapour flux density measurements were taken with the Servo Med Evaporimeter EP1 and each measurement involved determining the maximum flux value during a 20 seconds logging period. For adults and a limited number of the babies, a first water vapour flux density reading was taken immediately after patch removal, followed by periodic readings until the flux density returned to its background value (after 15-20 minutes). Water vapour flux density was then plotted against time – having first subtracted the background value – and the area under the graph up to 20 minutes was determined as an estimate of the amount of Skin Surface Water Loss (SSWL) in grams per square meter ($g.m^{-2}$) caused by contact with the wet diaper material.

For most of the babies, a single flux density measurement was taken two minutes after patch removal (when the rate of fall in the flux reading had abated somewhat). Analysis

of data from the entire desorption curves recorded for some of the babies revealed that a spot reading at two minutes after diaper removal correlated quite well with the area under the desorption curve up to 20 minutes, and was much easier to obtain.

A number of other studies have based their methods on those used by Zimmerer et al. (1986), but there has been considerable variation in components of the method. The variations are discussed below with a particular focus on the methods of hydrating the skin and the procedure for logging and processing data to obtain some measure of skin wetness. Twelve studies were identified and they are listed in Tables 2.4 and 2.5, which summarise their key features. All used a Servo Med Evaporimeter (in its various models) for measurements.

Table 2.4 shows the characteristics of the subjects included, the various skin sites used and the different methods of hydrating the skin in the studies. A variety of test fluids was used, for example, subject's own urine was used with known (Zimmerer et al., 1986) or unknown masses – whatever the subject had voided (Davis et al., 1989 and Berg et al., 1994); *saline* with known (Wilson and Dallas, 1990; Dallas and Wilson, 1992; Shafer et al., 2002; and Fader et al, 2007) or unspecified masses (Grove et al., 1998 and Akin et al., 1997); immersion of the patches (a piece of material that was used to occlude the skin) in distilled water (Hatch et al. 1992 and 1997; Markee et al., 1993 and Cameron et al., 1997); or different masses of dyne solution (Zimmerer et al., 1986). These test fluids were then applied to either whole diaper products (Zimmerer et al., 1986; Davis et al., 1989; Berg et al., 1994; Grove et al., 1998; Akin et al., 1997; and Shafer et al., 2002); patches cut from diapers (Wilson and Dallas, 1990; and Dallas and Wilson, 1992); or different fabric materials (Hatch et al. 1992 and 1997; Markee et al., 1993; Cameron et al., 1997; and Fader et al., 2007).

In most studies, fluid loading was insufficient to achieve full saturation and, except in the studies by Hatch et al. (1992 and 1997), Markee et al. (1993) and Cameron et al. (1997) there was no attempt to distribute sub-saturation fluid loading uniformly throughout a test piece. Accordingly, the environment experienced by skin will have varied with position beneath a given patch, and from patch to patch in different experiments under nominally identical conditions. Likewise, diapers which were loaded naturally by their infant wearer may have varied greatly in the environment they provided for occluded skin, depending on how much urine the infant voided and when. Although such methods have often proved capable of detecting differences between products (e.g. diapers with and without SAP) a more reliable way of hydrating the skin is needed to examine the repeatability of evaporimetry measurements.

Table 2.5 shows the methods and conditions of logging and analysing evaporimetry data. The environmental conditions under which evaporimetry measurements were made varied between studies (temperature from 20 to 30 °C and relative humidity from 30 to 75 %) but they were sometimes not recorded (Zimmerer et al., 1986; Davis et al., 1989 and Berg et al., 1994). Similarly, the acclimatisation time (the time for conditioning the subjects to the environment) before taking measurements varied from 10 min to 1 hour and was sometimes not recorded (Zimmerer et al., 1986; Davis et al., 1989; Wilson and Dallas, 1990; Dallas and Wilson, 1992; Berg et al., 1994 and Akin et al., 1997). Perhaps most importantly, the procedure for logging and processing data to obtain some measure of skin wetness varied greatly between studies. This is most easily reviewed by considering an example desorption curve for very wet skin (Fig 2.18).

Table 2.4 Subjects, sites and methods of hydrating the skin found in the literature on evaporimetry measurements.

Authors (year)		No. subjects; gender	Skin site for measurement	Diaper / patch material	Patch held in place by	Fluid load	Diaper / patch wear time
Zimmerer (1986)	Expt 1	?N adults ?Gender	Volar forearm	1 disposable, 1 cloth diaper	Elastic mesh bandage	1-6 times dry patch weight of subject's own urine	2 h
	Expt 2	32 male babies	Suprapubic area	Whole disposable or cloth diapers (one variant of each)	N/A	0, 50, 100, 150 ml of Dyne solution	1 h
Davis et al. (1989)		150 Infants Gender mix	Buttock	4 disposable diapers; 2 with SAP*, 2 without.	N/A	Whatever infant had voided (measured on diaper removal)	Variable
Wilson & Dallas (1990)		80 adults ?Gender	Volar forearm	Patches cut from 16 brands of diapers; 7 washable; 9 disposable (5 with SAP*, 4 without).	Elastic mesh retainer	7 ml of 1% saline with 0.025% Triton in 6.3 x 6.3 cm patch (= "moderate loading")	2 h
Dallas & Wilson (1992)		33 adults ?Gender	Volar forearm	Patches cut from 20 brands of continence products; 3 washable; 17 disposable (10 with SAP*, 7 without)	Knitted wrap retainer	7 ml of 1% saline with 0.025% Triton in 6.3 x 6.3 cm patch (= "moderate loading")	2 h

... continuation of Table 2.4

Hatch et al. (1992 - TRJ) & Markee et al. (1993)	5 adults males	Volar forearm	3 knitted fabrics (1 cotton; 2 PET)	Occlusive chamber	At regain (cotton and 1 PET); 38.6% saturated (just cotton); or fully saturated (all 3 fabrics). 3 x 3 cm patches immersed in distilled water, put through ringer with chromatography paper either side to give uniform distributions: once to give saturated samples; twice for 38.6% saturated.	1, 2, 5, 10, 20, 30, 45, or 60 min
Berg et al. (1994)	1601 infants ?Gender	Suprapubic area and buttock (thigh for background TEWL)	8 diaper brands; 1 washable; 7 disposable	N/A	Whatever infant had voided.	Variable.
Hatch et al. (1997)	5 adults males	Volar forearm	2 different fabrics	Occlusive chamber	3 x 3 cm patches immersed in distilled water, put through ringer with chromatography paper either side to give uniform distributions of ~ 35 (PET fabric), 44 or 75 (cotton fabric) % saturation	30 and 60 min
Cameron et al. (1997)	35 adults female	Volar forearm	16 different fabrics	*Hilltop* chamber	2.5 x 2.5 cm patches immersed in distilled water, put through ringer with chromatography paper either side to give uniform distribution.	40 min
Grove et al. (1998)	? N adults female	Volar forearm	3 disposable diapers: all with SAP*; one with a microporous backing, two without	Tape and nylon netting.	Normal Saline delivered into *in situ* diaper to simulate micturition. Fluid loading level unclear.	1 h

... continuation of Table 2.4

Akin et al. (1997)	?N infants Gender mix	Suprapubic area	3 disposable diapers: all with SAP*; one with a microporous backing, two without	N/A	Normal Saline delivered into *in situ* diaper to simulate micturition. Fluid loading level unclear.	1h
Shafer et al. (2002)	10 adults females	Volar forearm	Whole menstrual pad with standard backing or vapour-permeable.	Elastic mesh bandage	3 ml of Physiological saline (except for dry pads worn for 3h as controls) in product centre	1, 3 or 6h
					3 ml of saline	3h
Fader et al. (2007)	11 adults females	Volar forearm and hip	Hydro-entangled rayon	Fabric cuff (forearm); tape (hip)	Patch fully saturated with Normal Saline	20 min (forearm); 60 in (hip)

*SAP: superabsorbent polymer.

Table 2.5 Methods and conditions of logging, timing and analysing evaporimetry data found in literature.

Authors; (year);		Temp; RH	Acclimatisation time	TEWL probe held in place by	Timing of flux density measurement(s)	Flux density outcome variable(s)
Zimmerer (1986)	Expt 1	?	?	By hand?	'Precise intervals' until background (~20 min). Max reading over 20s taken as flux value.	Area under curve above background
	Expt 2	?	?	By hand?	Periodically until background (~15 min) at 2 min after patch removal. Max reading over 20s taken as flux	Value at 2 min after patch removal (primarily)
Davis et al. (1989)		?	?	By hand?	Data logged at 1Hz for 2 min straight after diaper removal.	Area under drying curve over first two min
Wilson & Dallas (1990)		75°F (24°C) 40%	?	By hand?	First reading over 2 min straight after patch removal. Six further 2 min readings, each separated by 2 min rest. Means over each 2 min taken as flux value.	Difference between 1st and 6th flux reading = ESW (Excess skin wetness).
Dallas & Wilson (1992)		74°F (23°C) 42%	?	By hand?	2 min flux density at 2 min after patch removal; 2nd 2 min SSWL after 2 min rest. Background TEWL (on adjacent skin) taken between the two sets. Means over each 2 min taken as flux value.	Difference between 2nd flux reading and background = ESW (Excess skin wetness).
Hatch et al. (1992) & Markee et al. (1993)		21°C 65%	Dry skin 30 min; 80% hydrated skin 1h	Hilltop chamber	30 s flux density starting 2 min after patch removal. Highest value in 30s noted. Flux readings corrected for skin temperature using Mathias (1981) method	Difference between max from 30s logs after "treatment" minus (mean) background value.

... continuation of Table 2.5

Reference	Conditions	Time	Method	Procedure	Flux calculation
Berg et al. (1994)	?	?	By hand?	Immediately after diaper removal and at 60s and 120s.	Mean of flux at all times - background = skin wetness.
Hatch et al. (1997)	21°C 65%	30 min	By hand?	1 flux reading of 30 sec taken 2 min after patch removal. Max reading in 30s taken as flux value.	Max value minus background (on adjacent skin) = "change in EWL".
Cameron et al. (1997)	20°C 65%	10 min	By hand	Mean of 2 min flux taken immediate after patch removal, but discarded first 30 s of data.	Mean minus background (taken on nearby skin).
Grove et al. (1998)	22°C 40%	15 min	Probe holder	Background: average of data from last 15 s of 30 s logging period. After diaper removed: Mean of 2 min logging period	Mean - background
Akin et al. (1997)	?22C ?40%	?	By hand	Background: Mean of 2 min logging period. After diaper removed: Mean of 2 min logging period.	Mean - background
Shafer et al. (2002)	20°C, 30% 25°C, 50% 30°C, 75%	30 min	By hand?	Immediately after patch removal, flux density logged for 45s where centre of pad (with fluid loading) was.	Maximum flux value between 15 and 45s. Background TEWL not subtracted.
Fader et al. (2007)	23°C 50%	20 min (forearm); 60 min (hip)	Probe holder	Background: mean for last 2 min of 2.5 min logging. On patch removal, blot surface water, log flux density for 10 min.	Area under drying curve (0-10 min) having subtracted background.
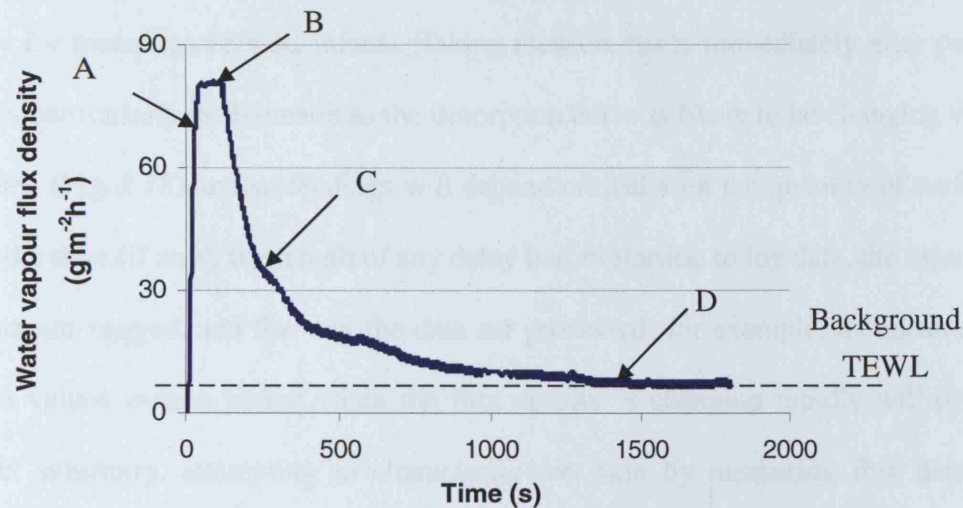
Fig 2.18 Example of desorption curve for over-hydrated skin.
A – steep increase due to machine response; B – surface water evaporation;
C – water loss from the SC; and D – background TEWL value re-attained.

Initially, a steep increase appears when the machine responds to the change in humidity inside the measurement chamber (A). The evaporation of water from the surface of the skin then dominates, resulting in the high value, low gradient portion of the curve (B). If the skin is not very wet or surface water has been blotted away prior to data logging, this element of the curve may be much shorter or completely absent. Once surface water has evaporated, water loss from within the SC dominates (C) and, as the SC dries out, the flux density value falls – initially very rapidly – until the background TEWL level recorded for the skin prior to over-hydration is re-attained (D).

The approach of Zimmerer et al. (1986) – who recorded the whole desorption curve and measured the area beneath it having subtracted background TEWL - would seem to be the most robust and defensible on theoretical grounds, although their decision to log water vapour flux density for only 20 seconds is likely to have introduced substantial errors to their readings (see below). Other approaches were probably developed primarily to reduce the time and difficulty of capturing whole desorption curves –

especially for measurements on infants. Taking measurements immediately after patch removal is particularly problematic as the desorption curve is likely to be changing very rapidly then (Fig 2.18) and so readings will depend critically on the quantity of surface water on the skin (if any), the length of any delay before starting to log data, the time for which data are logged, and the way the data are processed; for example, the mean and maximum values over a period when the flux density is changing rapidly will differ greatly. In summary, attempting to characterise wet skin by measuring flux density immediately after patch removal is subject to several difficulties and sources of error.

Another important factor is that the Evaporimeter probe is known to take of the order of 30-45 seconds to achieve a stable reading in measuring background TEWL under equilibrium conditions on the volar forearm and palm (Blichmann and Serup, 1987 and Hatch et al., 1987). It seems unlikely that the device will deliver reliable readings in less than this time under the non-equilibrium conditions associated with skin drying curves. Accordingly, the two minute logging period chosen for most wet skin studies is likely to have been too short. For some work the logging period was 30 seconds or less (Zimmerer et al., 1986 and Hatch et al., 1997), a practice likely to have yielded particularly inaccurate data. Notably, Cameron et al. (1997) logged for two minutes but discarded data from the first 30 seconds of logging. Another important feature of these studies (Zimmerer et al., 1986 and Grove et al., 1998) is that none of them appears to have conducted repeat experiments on the same subjects under the same conditions and, certainly, none report such data. Accordingly, the repeatability of the methodologies used is unknown.

There have been several other studies reported in the literature with the Evaporimeter which, although they did not involve skin over-hydrated by contact with wet materials,

report some methodologically interesting details (Hatch et al., 1987; Pinnagoda et al., 1989 and Hatch et al., 1990). Hatch et al. (1987) adhered to their earlier practice (Hatch et al., 1992; Markee et al., 1993 and Hatch et al., 1997) of normalising their flux readings to a skin temperature of $30^{\circ}C$ following the method described by Mathias et al. (1981) (where the skin specimens were placed between modified diffusion chambers, and the chamber was heated by a water bath of $30^{\circ}C$). In their second study (Hatch et al., 1990) – which involved women exercising under hot humid conditions wearing garments made from various materials – they blotted sweat from the skin before logging the flux density. Pinnagoda et al. (1989) used a probe clamp to avoid heat from the operator's hand interfering with flux readings, and reduced the impact of air currents by using a draught shield. Agner and Serup (1993) had their operator wear an insulating glove.

It is evident from this review that techniques and methods have varied widely in studies on over-hydrated skin and that a robust methodology needs to be established for further work.

2.4.3.6 Comparisons between evaporimetry devices

There are no published studies in which devices other than Servo Med Evaporimeter have been used for evaporimetry on skin that has been over-hydrated by occlusion with wet patches or products. However, a number of papers report on comparison between various devices for measuring the water vapour flux density in other situations. These papers aimed at comparing the technical descriptions of the instruments, and evaluating the accuracy, reproducibility, sensitivity, and range of flux density measurements.

Barel and Clarys (1995) compared the Evaporimeter EP1 and the Tewameter TM210 by

taking measurements on 12 adults in a 20°C, 45%RH environment, in which they had been acclimatised for at least 30 minutes. Flux density was measured from skin that had been occluded for two hours with surgical tape; tape stripped; or received no treatment, generating flux values in the range 0-100 $g \cdot m^{-2} h^{-1}$. The authors do not record how long the flux density was logged for in taking each measurement or how soon measurements began after tape stripping or after occlusion had been removed. The Evaporimeter was handheld while a probe holder was used to apply the Tewameter to the skin. Both instruments showed good repeatability in measuring background TEWL from normal skin giving coefficients of variation of 3-8% for measurements at the same skin site of the same individual. There was good correlation between Evaporimeter and Tewameter readings across the entire flux density range tested but values from Evaporimeter were generally a little lower and the difference was particularly apparent at low flux readings; for example, readings for normal volar forearm skin from Evaporimeter were about half of those for the Tewameter. The authors noted that it took 10-15 minutes for the Tewameter probe temperature (which is displayed) to reach equilibrium with the skin temperature during a measurement, an important factor given that the flux reading increased by about 0.6 $g \cdot m^{-2} h^{-1}$ for each degree Centigrade rise in temperature. They also found that increasing the load on probes from 100 to 300 gram force increased flux readings by about 10% for both devices. Finally, they noted that Tewameter readings were less sensitive to air movements in the vicinity of the probe and they attributed this to the smaller diameter probe chamber (10 mm compared with 12mm for the Evaporimeter).

Grove et al. (1999) compared the Evaporimeter and the DermaLab by measuring the flux density from the volar forearms of 11 adults, whose skin had been occluded with soap solutions for 24 hours, giving rise to flux readings over the range 0-25 $g \cdot m^{-2} h^{-1}$.

Test conditions were 23.5°C and 34%RH. In addition, they measured water vapour

transmission rates through membranes over various aqueous salt solutions. In the *in*

vitro experiments the coefficients of variation for repeat measurements with the

Evaporimeter and DermaLab were about 7% and 4%, respectively. Readings from the

two devices correlated well but values from Evaporimeter were typically 2-3 $g \cdot m^{-2} h^{-1}$

lower. Correlation was also strong for *in vivo* readings. This time, readings from

Evaporimeter were lower, but this was attributed to the use of a cover plate (6-7 mm

thick) on the face of the probe that had not been used in *in vitro* measurements.

Tagami et al. (2002) compared the DermaLab with a closed chamber device: the

Nikkiso-YS1 Model H4300. They measured background TEWL on the untreated cheek,

volar forearm and leg skin of 14 healthy adults and also on the lesion sites of seven

adults with atopic dermatitis or psoriasis. Test conditions were 21°C and 50%RH and

TEWL values fell in the range 0-50 $g \cdot m^{-2} h^{-1}$. Correlation between measurements from

the two devices was high but the Nikkiso device gave substantially lower readings –

about 30% lower at 50 $g \cdot m^{-2} h^{-1}$.

Nuutinen et al. (2003) compared the DermaLab with the VapoMeter by measuring water

vapour flux rates from water baths. They found that although readings from the

VapoMeter correlated well with gravimetric results over the entire range tested (0-250

$g \cdot m^{-2} h^{-1}$), the correlation for the DermaLab was good only up to about 125 $g \cdot m^{-2} h^{-1}$,

after which the DermaLab increasingly under-estimated the gravimetric measurements.

Below 125 $g \cdot m^{-2} h^{-1}$, readings from DermaLab were about 15% lower than those from

the VapoMeter.

De Paepe et al. (2005) compared the Tewameter TM210 with the VapoMeter SWL-2.

They measured water vapour flux density from the volar forearm of 16 adult females whose skin had been subjected to tape stripping; an application of cream; an insult with sodium lauryl sulphate; or no treatment, leading to flux readings in the range 0-40 $g \cdot m^{-2} h^{-1}$. Test conditions were $20.9°C$ and $52.9\%RH$ and subjects acclimatised for at least 30 minutes before measurements. For readings with the Tewameter, the probe was held against the skin adjacent to the test site until it had reached skin temperature before it was transferred to the test site for readings. Background TEWL values for normal skin were about twice as high for the Tewameter as the VapoMeter. Ten repeat measurements were taken at the same site of the same subject with the VapoMeter and readings increased by about 40% from the 1st to the 10th repeat, and the 7th to 10th readings were significantly higher than the first. No repeat measurements appear to have been made with the Tewameter. After 20, 30, 40 and 50 tape stripping, the flux readings with the Tewameter were about 6 $g \cdot m^{-2} h^{-1}$ higher than those using the VapoMeter. Slightly higher differences were found between the two devices for measurements on skin that has been exposed to cream and for skin that had received an insult with sodium lauryl sulphate: typically, 8% and 10%, respectively. Readings from the VapoMeter were found to be sensitive to probe temperature: background TEWL for untreated skin typically rose from 7 to 15 $g \cdot m^{-2} h^{-1}$ if the probe was warmed by $6°C$ before application to the measurement site. However, VapoMeter readings were not changed significantly by increasing (by an unspecified amount) the pressure on the probe.

Finally Shah et al. (2005) compared the Tewameter and VapoMeter SWL-3 by measuring background TEWL from normal skin at three volar forearm and three forehead sites of nine adult subjects. Test conditions were $20-21°C$ and $40-48\%RH$. No significant differences were found between the two devices when measuring background TEWL from forearms but the VapoMeter produced significantly higher

readings for background TEWL from the forehead: differences were of the order of 4

$g \cdot m^{-2} h^{-1}$ (~30%).

2.4.3.7 Calibration methods

For TEWL measurements on normal skin where the measured water vapour has diffused

across the epidermis to the skin surface, the water vapour flux is controlled by the SC

barrier. Therefore, with the assumption that the device measurement head itself is not

significantly affecting the flux density it is aiming to measure, all evaporimetry

instruments should then give the same readings, if they are correctly calibrated.

Traditionally, the open-chamber devices have been calibrated using a 'wet-cup method'

as described in ASTM-E96 Standard (ASTM-E96, 1995), which was originally

developed for characterising materials for the building industry and plastic films -

materials with quite low permeability. They use a membrane-covered Petri dish filled

with some water or salt solution. The water loss through the uncovered wet-cup

membrane can be determined gravimetrically, from the weight loss of the cup with time

(Fig 2.19a). A evaporimetry probe is then placed on the membrane with light pressure

for measuring the water loss from the dish (Fig 2.19b). The instrument is then calibrated

by equating J_G with J_H.

This calibration method assumes the flux entering the evaporimetry measurement

chamber is the same as the gravimetrically determined flux through the uncovered

membrane. Although both the wet-cup and actual skin measurement have a membrane

to limit water loss, the difference is that for skin the lower surface of the SC is in

contact with condensed liquid water, and for the wet-cup method, the membrane is

separated from the water reservoir by an air gap, i.e. water vapour is on both sides of the

membrane. In short, the wet-cup method is about water vapour transport while the actual skin measurement involves liquid water. The relative resistance to water transmission of the membrane and the measurement head will be different in the two situations. Therefore, this traditional method of calibration is not suitable for the open-chamber devices.

(a) Flux density J_G

Membrane

Water or salt solution

(b) Flux density J_H

Evaporimetry measurement head

Membrane

Water or salt solution
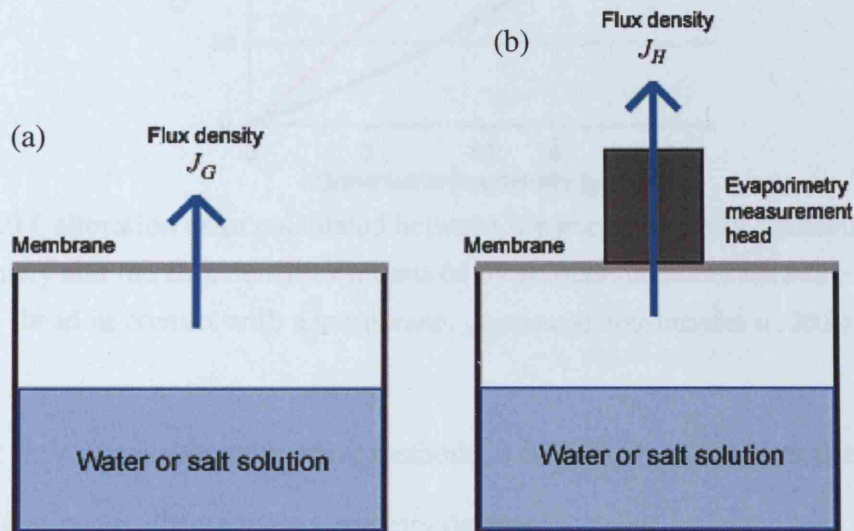
Fig 2.19 Wet-cup method for calibration of open-chamber devices.
(a) Gravimetric measurement of flux J_G from cup weight loss;
(b) Calibration of open-chamber device, assuming $J_G=J_H$.

Imhof et al. (2004) developed a mathematical model for this wet-cup calibration method for open-chamber measurement heads. They used Fick's law to calculate a calibration error as the percentage deviation between the flux densities measured by an open-chamber measurement head in contact with the membrane and the gravimetrically determined flux density. Their results are shown in Fig 2.20. The boundary layer shown on the graph is the height of the layer of air between the membrane and liquid. It shows that when the gravimetric flux density is about 5 $g \cdot m^{-2} h^{-1}$, i.e. the value typically achieved for background TEWL of the volar forearm, the calibration error is about 13% for a 3.5 mm boundary layer and 6% for a 13 mm boundary layer; the predicted error increases substantially with the flux.
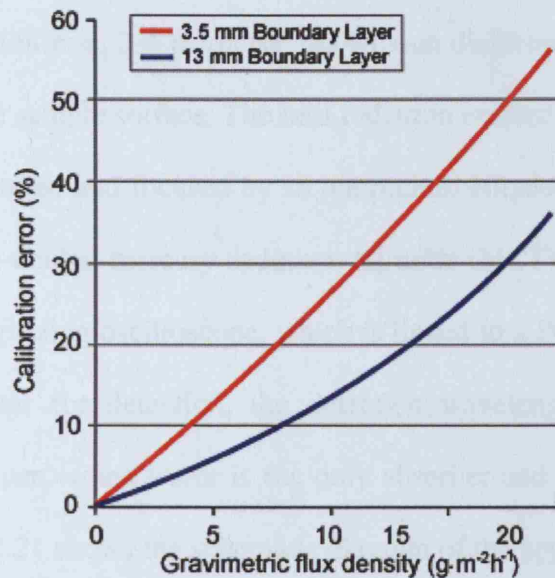
Fig 2.20 Calibration error calculated between the gravimetrically determined flux density and the flux densities measured by an open-chamber measurement head in contact with a membrane. (reproduced from Imhof et al., 2004)

Due to the lack of reliable calibration methods, it is difficult to correlate data and make comparison between different evaporimetry devices.

In summary, evaporimetry has been particularly widely used for charactering the water barrier function of the skin. However, the above literature review suggests that there is a need for a standard methodology for making accurate evaporimetry measurements. Furthermore, a number of evaporimetry devices have come on to the market recently and there has been little work to measure the repeatability of their measurements, or to compare and contrast their strengths and limitations when used for work on over-hydrated skin.

2.4.4 Opto-Thermal Transient Emission Radiometry (OTTER)

Opto-Thermal Transient Emission Radiometry (OTTER) is a new approach to measuring the hydration level of the SC (Xiao and Imhof, 1996). OTTER uses a Q-switched Er:YAG pulsed laser (with excitation wavelength at 2.94µm, 100 ns pulse

duration, 5 Hz repetition rate, 3-4 mJ/pulse and ~1 mm diameter laser spot size) as the heat source to heat the sample surface. The heat radiation emitted by a sample due to the temperature rise is filtered and focused by an aluminium ellipsoidal mirror onto a high speed, liquid-nitrogen-cooled mercury cadmium telluride (MCT) detector. The signal is then captured by a digitizing oscilloscope, which is linked to a PC for analysis. OTTER uses a band-pass filter for detection, the detection wavelength for skin hydration measurement is 13.1 μm, when water is the only absorber and has strong emission at this wavelength. Fig 2.21 shows the schematic diagram of the apparatus used for in vivo skin hydration measurement.
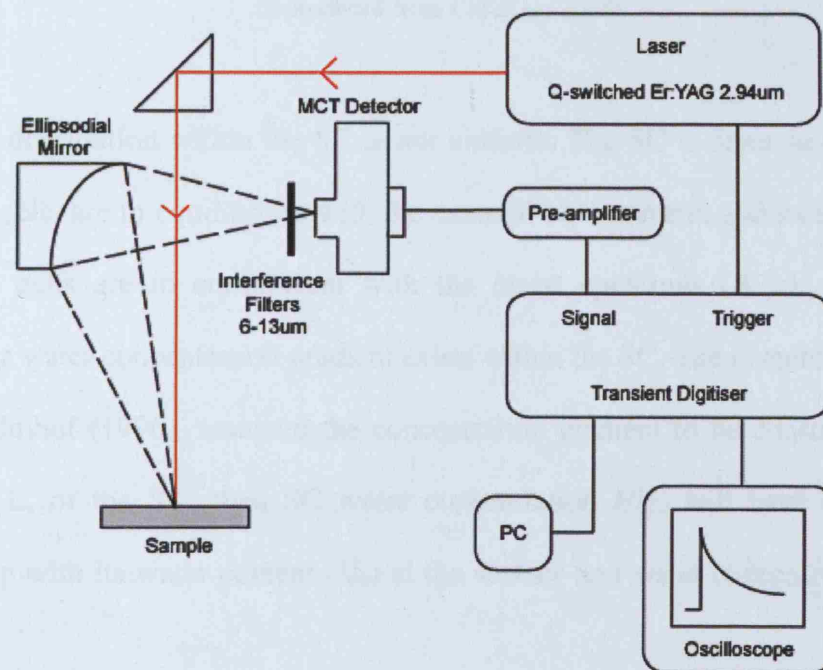
Fig 2.21 Schematic diagram of OTTER apparatus

Fig 2.22 shows the schematic diagram of an OTTER measurement, a pulsed laser heats the sample and an infrared emission signal detected. Information about the water within the SC is in the shape of the signal detected.
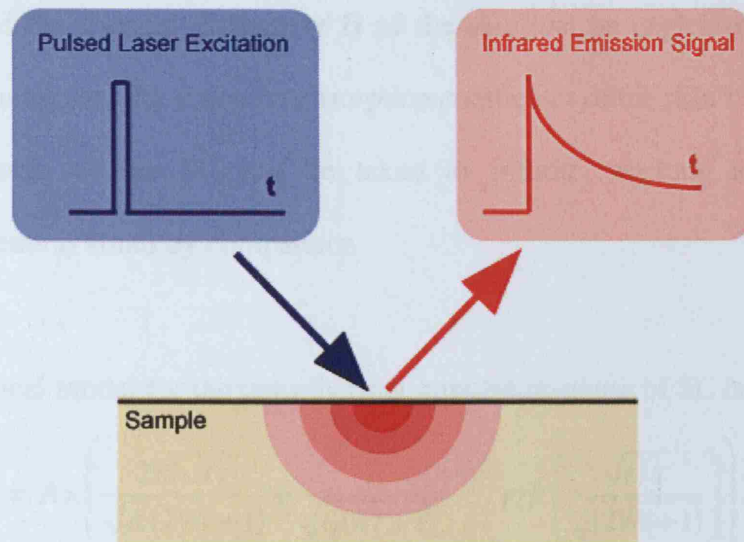
Fig 2.22 Schematic diagram of an OTTER measurement, where t = time.

(reproduced from Cui et al., 2005)

The water distribution within the SC is not uniform. The SC is dryer near the surface, where the cells are in equilibrium with the external environment; and wetter at its base, where the cells are in equilibrium with the moist epidermis (Blank et al., 1984). Therefore a water concentration gradient exists within the SC. The inventors of OTTER, Xiao and Imhof (1996), assumed the concentration gradient to be constant across the thickness, L, of the SC; then SC water concentration $H(z)$ will have the following relationship with its water content (H_0) at the surface and water concentration gradient (W):

$$H(z) = H_0 + Wz , \quad 0 \leq z \leq L$$
$$H(z) = H_1, \qquad z \geq L$$

$$\text{............. Equation 2.5}$$

where $W = \dfrac{H_1 - H_0}{L}$.

A mathematical model for the opto-thermal signal was built by Xiao and Imhof (1996) with the following assumptions:

(a) The thermal reflections within the material can be neglected

(b) Changes of the thermal diffusivity D of the skin can be neglected in comparison

with the changes of the emission absorption coefficient of the skin's surface β

(c) The thickness of the SC can be taken as infinite, as long as the depth of

measurements is small by comparison

The mathematical model for the opto-thermal impulse response of SC is:

$$S(t) = A \times \left(\frac{2W\sqrt{t\tau}}{\sqrt{\pi}(2Wt+1)} + \frac{1}{\sqrt{(2Wt+1)}} e^{\frac{t/\tau}{2Wt+1}} erfc\left(\frac{\sqrt{t/\tau}}{\sqrt{(2Wt+1)}} \right) \right) \dots \text{ Equation 2.6}$$

where A is a constant that is dependent on laser energy, measurement geometry, and

detector sensitivity, $erfc$ is the complementary error function, τ is the surface lifetime of

the OTTER signal (defined by $\tau = 1/\beta_0^2 D$), D is the thermal diffusivity and β_0 is the

emission absorption coefficient of the skin's surface.
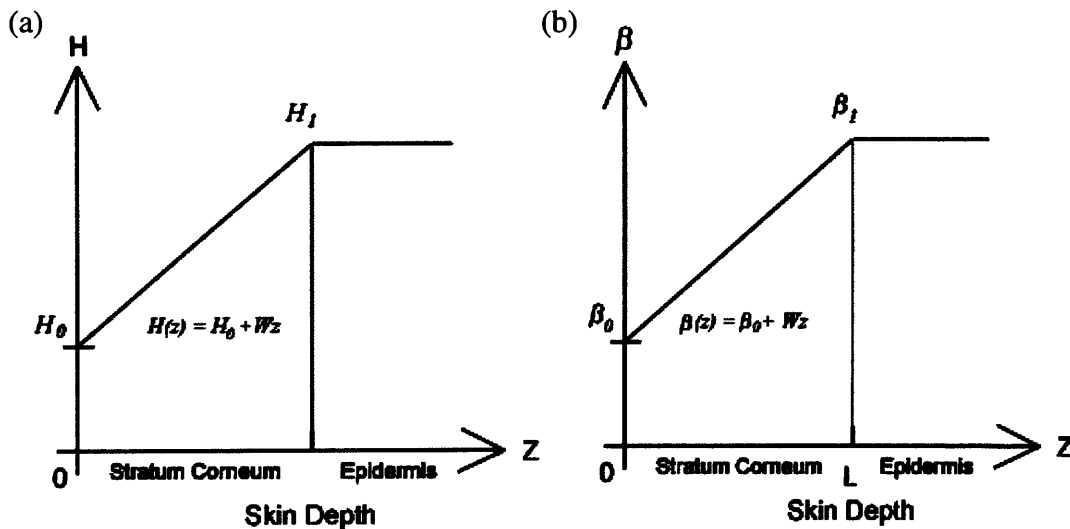
Fig 2.23 (a)Water concentration profile within skin, and (b) its mathematical model.
(adapted from Xiao and Imhof, 1996)

Measured values of τ and W can be converted to water content, if a linear relationship

with β is assumed (Fig 2.23b), i.e:

$$\beta_H = H \times \beta_W + (1-H) \times \beta_d \quad \dots\dots\dots\dots\dots \text{ Equation 2.7}$$

where β_H is the emission absorption coefficient of skin of fractional volume hydration H, β_w is the emission absorption coefficient of water and β_d is the emission absorption coefficient of dry skin.

A best fit surface lifetime τ and effective water concentration gradient W can then be produced from the model (Eq 2.8); which can be interpreted in terms of surface water content H_0 and the sub-surface water concentration gradient W using the following equations (Xiao and Imhof, 1999):

$$H_0 = \frac{\beta_0 - \beta_d}{\beta_w - \beta_d} = \frac{\sqrt{\frac{1}{\tau D}} - \beta_d}{\beta_w - \beta_d} \quad ; \quad w_w = \frac{H_1 - H_0}{L_{SC}} = \frac{W}{D(\beta_w - \beta_d)} \quad \ldots\ldots \text{Equation 2.8}$$

2.4.4.1 Measurements of OTTER on skin

OTTER is a non-movable bench-top apparatus that is based in the PhotoPhysics Group of London South Bank University, so most of the literature on it has been published by the same group of researchers. The first publication on OTTER was by Imhof et al. (1984), reporting the development of this new technique. Thereafter, many publications have followed applying the technique to different research areas, but the main focus has been on the hydration properties of the SC.

The model (Eq 2.8) for measuring the surface hydration (H_0) and the water concentration gradient (W) using OTTER was verified by Xiao and Imhof (1999). They used the model to measure the drying out of *in-vivo* and *in-vitro* hydrated SC. For *in-vitro* tests, a SC sample was taken from the sole of a volunteer's foot and hydrated by soaking in water overnight. OTTER measurements were taken at intervals for 2 hours immediately after the sample was withdrawn from the water and excess water shaken

off. For the *in-vivo* test, an area on the volar forearm was occluded by a plastic film for 3 days. OTTER measurements were performed at intervals for 4 hours immediately after the film was removed, to observe the recovery of the treated site. The surface hydration and the hydration gradient were then plotted against time and, by comparing the two graphs the authors concluded that when skin was fully hydrated, the SC lost its barrier function, which was represented by the low hydration gradient. Therefore, the barrier recovery proceeded at a different rate from that of the drying of the skin, i.e. there was a time lapse prior to barrier recovery.

Xiao et al. (2001) demonstrated that the depth profiles of externally applied substances diffusing through the skin could be produced from the opto-thermal signals measured by the OTTER. They measured the hydration depth profiles of different skin sites along the volar forearm, drying of skin after a 3-day occlusion, and ethylene glycol (EG) diffusion in the volar forearm skin.

By choosing a suitable excitation wavelength for OTTER measurement where the contrast between a topically applied substances and the normal skin was the greatest, the disappearance of different applied substances (e.g. sunscreen, natural dye and barrier cream) from the skin could be monitored.

Imhof et al. (1990) measured the rate of disappearance of sunscreen from the skin of fingers by taking OTTER measurements prior to the application of the sunscreens, immediately afterwards and periodically thereafter, over a 2 day period. Reasonable care was taken to avoid contact with water, rubbing or contamination of the skin during this period. By observing the change of decay time of the opto-thermal signals, it was found that the treated skin recovered over a 43 hour period.

Cowen et al. (2001) measured the SC renewal time of different skin sites by applying a natural dye to the skin and measuring its disappearance. The dye was spread on to the volar forearm and left overnight (at least 14 hours), and OTTER measurements were taken over a 21 day period after application. It was found that there was little change during the first 17 days, and by day 21, the signals indicated that the dye had been exfoliated. The measured SC renewal times were found to vary between 19 and 21 days on volar forearm, compared with reported values of 13.3 ± 1.5 days, 17.2 days and >21 days in the literature. The authors explained that the present study was limited to make comparisons, but the technique for measuring the SC renewal time using OTTER was developed.

The residence time of barrier cream on skin was studied by Guo et al. (2001). A thin layer of cream was applied on the dorsal finger skin by rubbing for a few seconds with another finger. The thickness of the cream was measured with OTTER under protected and unprotected conditions at intervals for 24 hours. In protected conditions, the test site was not washed and care was taken to avoid abrasion of the test site during the test period. In unprotected conditions, the test site was washed as normal, and no precautions were taken to avoid abrasion. Similar results were obtained from protected and unprotected test sites, and it was found that the thickness of the cream decreased exponentially with time after application with a $1/e$ disappearance time of about 60 minutes.

The literature cited above shows that the OTTER is a potential technique for making *in-vivo* skin measurement, but the apparatus setup has a restriction to make measurement only on fingers or forearm of the human body. Pascut et al. (2001) developed a fibre optic opto-thermal hand held probe, which used only one fibre to

deliver the excitation radiation to the sample surface and another fibre to collect the infrared radiation before sending it to the infrared detector. They used this hand held probe to take measurements from different sites of the human body (chest, leg and face), and hydration measurements were performed on a finger. The authors showed that this hand held probe could achieve 'adequate' signals from the skin and were able to take measurements from different sites of the human body.

Finally, of most direct relevance to the work in this thesis, Xiao et al. (2007) combined the OTTER and evaporimetry to study the SC water concentration distribution, water binding status in the SC, SC thickness and the swelling effects, and SC water-holding capabilities. The authors plotted the water concentration gradient against the surface water content measured during the drying process of occluded skin (30-60 min occlusion of plastic film) (Fig 2.24a). Results showed that the water changes its state from bound water to free water at different surface water contents for different skin sites, i.e. the water content below this threshold is bound water and above it is free water (Fig 2.24a). They also studied the swelling effect of SC by calculating the thickness of SC at different water concentration levels by using the information obtained from the OTTER data. Results indicated that the SC thickness increased linearly as the water concentration increased, but the increase varies between the skin sites (Fig 2.24b). The SC water–holding capabilities were then investigated by correlating the OTTER and evaporimetry measurements (made using the AquaFlux) during skin recovery from immersive hydration on finger skin. The two measurements were performed side by side on the same skin sites before soaking and about every 5 min over a period of about 40 min after the skin sites were padded dry using soft tissues. The linear models indicated differences between the relationships at the two skin sites (Fig 2.25).
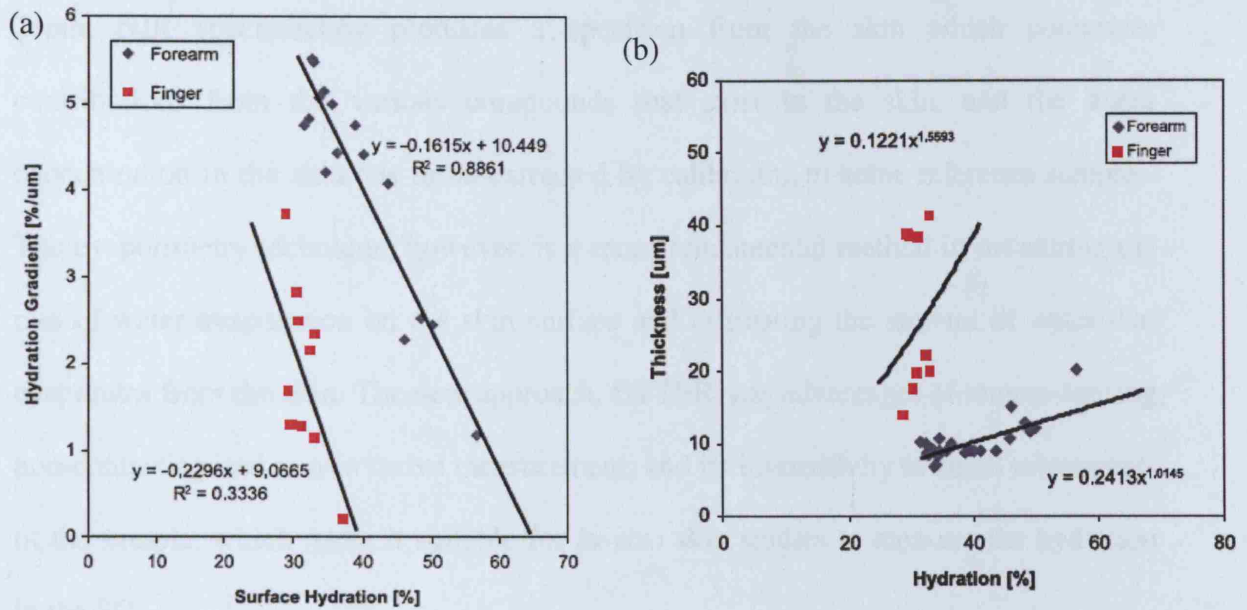
Fig 2.24 (a) Relationship between surface water content of SC and the water concentration gradient at two sites during skin recovery from occlusion. (b) Swelling effects of SC at two different skin sites. (adapted from Xiao et al., 2007)
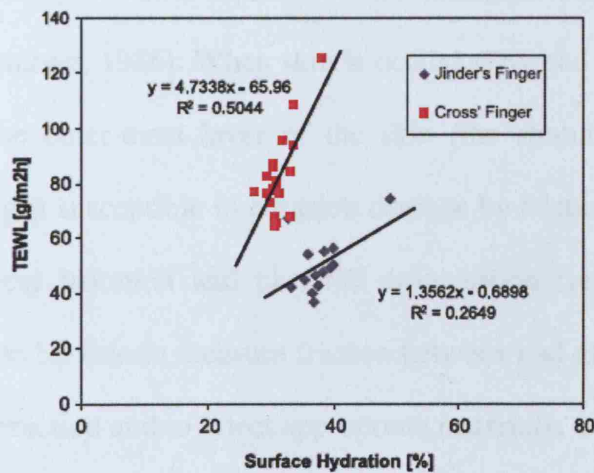
Fig 2.25 Water-holding capabilities of SC by using OTTER and AquaFlux. (adapted from Xiao et al., 2007)

In summary, the water content within the SC can be measured by various techniques, such as electrical measurements and NIR spectroscopy. It has been noted that electrical measurements suffer from technical difficulties: probe in contact with the skin surface during measurement – accumulation of water underneath the probe due to TEWL; and the sampled depth of SC being difficult to determine since it gives an integration over

depth. NIR spectroscopy produces a spectrum from the skin which comprises contributions from the various compounds that exist in the skin, and the water concentration in the skin has to be extracted by calibrating to some reference samples. The evaporimetry technique, however, is a more fundamental method in measuring the rate of water evaporation on the skin surface and estimating the amount of water that evaporates from the skin. The new approach, OTTER, has advantages of remote-sensing, non-contacting and non-invasive measurement, and its insensitivity to small movements of the sample, which make it suitable for *in-vivo* skin studies to measure the hydration in the SC.

2.5 Skin friction

Wearers of incontinence pads often experience skin damage, soreness and discomfort in the *diaper area* (Zimmerer, 1986). When skin is occluded by pad materials – especially if they are wet – the outer-most layer of the skin (the stratum corneum) becomes over-hydrated making it susceptible to abrasion damage by friction against the pad and vulnerable to chemical irritation and bacterial colonisation (see Section 2.2). It is, therefore, important to be able to measure friction between pad materials and skin both to understand the interaction and to select appropriate materials.

2.5.1 Friction between surfaces

Friction is defined as a force that acts parallel to an interface between two surfaces to oppose any applied tangential force. In 1699, the French physicist Amontons (1663-1705) published two important findings on friction:

(1) the frictional force for two subjects in sliding contact is proportional to the normal force of the object being moved

(2) the frictional force is independent of the macroscopic surface area of contact

between the two surfaces

With these results, Amontons developed the empirical law of friction now known by his name:

$$F = \mu \cdot N \quad \dotfill \text{Equation 2.9}$$

where F is the force of friction, μ is the constant of proportionality called the coefficient of friction, and N is the normal force, i.e. the force perpendicular to the contacting surfaces.

The coefficient of friction (μ) depends on (1) the materials in contact, (2) the geometry of their surfaces, and (3) the cleanliness of the interface. Different μ values can be achieved for the same materials depending on their surface roughness, and also different μ values may be found for different materials with different surface roughness. The higher the μ value is, the higher the friction.

Later, Coulomb (1736-1806) proposed that the force of friction is independent of the velocity of movement by the object. He also distinguished between static and dynamic friction, where:

(1) **Static friction** occurs when the two objects are not moving relative to each other; it is the initial force to get an object moving. In this case the ratio of friction to normal force is called the coefficient of static friction (μ_s)

(2) **Dynamic (or kinetic) friction** occurs when the two objects are moving relative to each other and rub together. It is the force required to sustain the motion of one object past another at a constant velocity. In this case the ratio of friction to normal force is called the coefficient of dynamic friction (μ_k) and is usually less than μ_s.

In 1956, Bowden and Tabor (Bowden and Tabor, 1956) of Cambridge University determined that the real area of contact is much smaller than the geometrical contact area, focusing initially on metal-metal interfaces. The real contact area is formed by asperities, where atom-to-atom contact takes place. They found that the number of asperities (i.e. the area of contact) increases with the normal force, and showed that the frictional force is independent of the geometrical contact area, but dependent on the real contact area with the following equation:

$$F = s \cdot A_R \quad \text{................................... Equation 2.10}$$

where s is the shear stress at the contacting surface, and A_R is the real contact area.

They subsequently showed that in adhesive wear, the asperity junctions in the interface deform plastically above a critical shear stress – equal to the shear strength of the adhesive bond (or one of the bonding materials, if weaker) - which determines the adhesive force between the two contacting surfaces. Therefore, if all asperities are plastically deformed, the real area of contact between asperities increased in proportion to the normal force (N), and because the frictional force is proportional to the real contact area (Eq. 2.10), F is proportional to N as found in Amontons' law (Eq 2.9).

Friction can be regarded as the energy dissipated per unit sliding distance. For a deformable substrate, work is expended at both the interface and in the bulk of the material when a rigid sphere slides over it (Bowden and Tabor, 1964). The total frictional force, F_{total} can be expressed as the sum of two non-interacting terms – a deformation term, $F_{deformation}$, and an interfacial adhesion term, $F_{adhesion}$:

$$F_{total} = F_{adhesion} + F_{deformation} \quad \text{................... Equation 2.11}$$

2.5.2 Measurements of friction between the skin and other materials

The first modern attempt to measure skin friction was published by Naylor (1955). He found that the coefficient of friction between skin and polythene can be varied by a large amount by changing the skin surface conditions. His findings have drawn attention from many research areas, such as skin physiology, skin care products, the textile industry, human friction-dependent activities and skin friction-induced injuries. Numerous papers followed his work describing instruments for measuring friction and / or providing data. Dowson (1997) and Sivamani et al. (2003) have provided useful reviews of work up to 1997 and 2003, respectively.
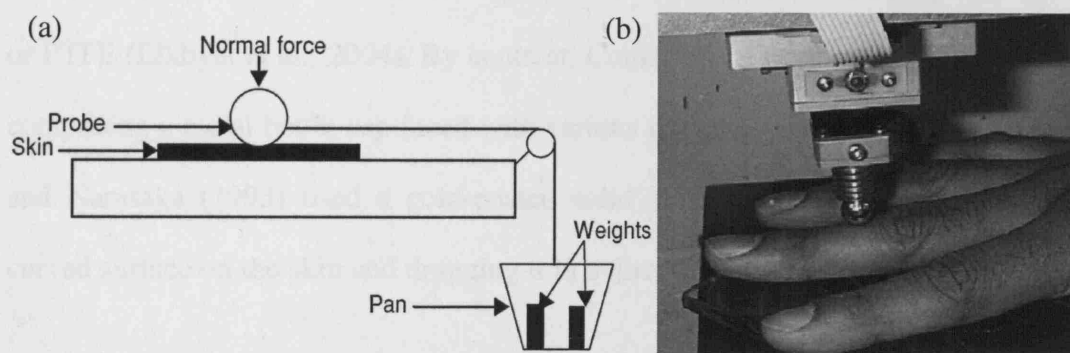
Fig 2.26 Illustration of the (a) linear and (b) rotational approaches
found in the literature for measuring friction on skin.
(adopted from Comaish and Bottoms, 1971; and Gitis and Sivamani, 2004)

There have been two main approaches to measuring friction against skin. In the first (as illustrated on 2.26a), a probe or slider is dragged across the skin in a straight line and the force required to initiate or sustain constant velocity motion is divided by the normal force to give the coefficient of static or dynamic friction, respectively (Amontons' law, (Amontons, 1706)). Table 2.6 summarises the key features of the work which has used this linear approach.

In Naylor's original study (Naylor, 1955), he used a reciprocating device to drag an 8 mm diameter polyethylene hemisphere back and forth across a skin site. Sulzberger et al. (1966), Johnson et al. (1990) and Hills et al. (1994) took similar approaches but using a leather-faced probe of un-described geometry, a convex glass lens and a polymethylmethacrylate disc, respectively. In early unidirectional devices linear motion was achieved using a pulley and dead weights (Comaish and Bottoms, 1971) but in more recent work, more controlled motion was achieved using tensometers or various custom-built mechanised devices (see Table 2.6). Most of these studies used a spherical or hemispherical probe which was made from glass (Koudine et al., 2000; Elkhyat et al., 2004), ruby (Asserin et al., 2000), steel (Sivamani et al., 2003 and Elkhyat et al., 2004) or PTFE (Elkhyat et al., 2004). By contrast, Comaish and Bottoms (1971) used a probe comprising a metal bottle cap faced with various polymers and fabrics, while Nakajima and Narasaka (1993) used a gold-coated solid aluminium hemicylinder, placing the curved surface on the skin and dragging it in a direction perpendicular to its axis.

Others have used methods based on the friction element of the series of devices developed by Kawabata and colleagues (1989) to evaluate clothing fabrics (KES frictional feel analyzer). Rather curiously, Egawa et al. (2002a) used the Kawabata friction probe - which is designed to simulate the human finger tip in friction measurements on cloth - to measure friction against the skin. The 10 mm square face of the probe is made from 20 lengths of 0.5 mm diameter piano wire lined up side by side with their axes perpendicular to the direction of motion. Kondo et al. (2002) faced the same probe (and a variant with twice the surface area) with various fabrics to measure friction against skin. Hong et al. (2005) took the novel approach of facing a probe with a circular flat face of radius 5mm with sheep skin and dragging it across four nonwoven fabrics commonly used as diaper coverstocks. Finally, Kenins (1994) measured the

force needed to drag 35 mm wide strips of various fabrics over the forearm or finger of volunteers. It was not possible, however, to extract coefficients of friction from the data because of the complex distribution of forces.

The second major category of devices (as illustrated on 2.26b) involve applying a rotating probe to the skin and measuring the friction force required to initiate or to sustain rotational motion, and dividing it by the normal force between probe and skin to give the coefficient of static or dynamic friction, respectively. Table 2.7 summarises the key features of the work which has used this rotational approach. Most studies have used the Newcastle skin friction meter (Comaish et al., 1973; Nacht et al., 1981; Elsner et al., 1990; Cua et al., 1990 and Cua et al., 1995) or similar (Zhang and Mak, 1999) which applies the face of a rotating annular ring to the skin. The ring may be made from a monolithic material like PTFE or Nylon but may be faced with a fabric. By contrast, Loden et al. (1992) and Sulzberger et al. (1966) used probes with solid circular faces made from steel and rubber, respectively, while El-Shimi (1977) used stainless steel hemispheres. Finally, Highley et al. (1977) chose a nylon disc rotating with its axis parallel to the skin surface and its periphery touching the skin.

Table 2.6 Key features of published methods using the linear approach to measuring skin friction.

Author (year)	Probe size and shape	Probe material	Maintenance of normal load	How force is applied	Test skin site(s)	Coefficient(s) of friction measured
Naylor (1955)	8 mm diameter sphere	Polyethyene	Static weights	?	Anterior surface of tibia	Dynamic
Sulzberger et al. (1966)	?	Leather (linear)	Static weights	?	Palm	N/A
Comaish and Bottoms (1971)	14 mm - 18 mm diameter metal bottle cap	PTFE, Nylon, Polyethylene, Wool, Terylene	Static weights	Dead weight and pulley	Dorsum of hand, palm, mid tibia, and mid-abdominal area of cadavers	Static and dynamic
Nakajima and Narasaka (1993)	20 mm long and 20 mm diameter semicylinder	Teflon	Computer controlled	Tensometer ?	Volar forearm	Static
Johnson et al. (1993)	8 mm radius of curvature lens	Glass	Static weights	Tensometer	Volar forearm	Dynamic
Kenins (1994)	35 mm wide fabric strip	Coarse wool, Cashmere, Wool, Cotton, Polyester, Base wool fabric	Static weights	Tensometer ?	Forearm and finger	Static and dynamic
Hills et al. (1994)	8 mm diameter circular base	Polymethylmethacrylate	Static weights	Tensometer ?	Porcine skin	Dynamic

... continuation of Table 2.6

Koudine et al. (2000)	Half-sphere lens	Glass	Static weights	Dead weight and pulley	Volar and dorsal forearm	Static and dynamic
Asserin et al. (2000)	3 mm diameter sphere	Ruby	Static weights and Balloon under the arm	Dead weight and pulley	Volar forearm	Static
Egawa et al. (2002a)	100 mm² square (KES frictional feel analyser)	20 steel piano wires	Static weights	Tensometer	Ventral forearm	Dynamic
Kondo (2002)	100 mm² square and 200 mm² rectangle (KES frictional feel analyser)	KES probes faced with: cotton, wool, silk, Rayon, polyester, Nylon	?	Tensometer	Inside of forearm	Dynamic
Sivamani et al. (2003)	10 mm diameter sphere	Stainless steel	Computer controlled	Tensometer	Dorsal skin of finger	Dynamic
Elhkyat et al. (2004)	3 mm diameter sphere	Ruby	Static weights and Balloon under the arm	Dead weight and pulley	Volar forearm	
Hong et al. (2005)	10 mm diameter disc	Four types of nonwoven (NB the skin (sheepskin) was on the probe)	Static weights	Dead weight and pulley	Soft sheepskin	Dynamic

Key of table: ? – not stated in paper.

Table 2.7 Key features of published methods using the rotational approach to measuring skin friction.

Author (year)	Probe size and shape	Probe material	Maintenance of normal load	Test skin site(s)	Coefficient(s) of friction measured
Sulzberger et al. (1966)	?	Eraser on pencil	Static weights	Palm	N/A
El-Shimi (1977)	12 mm diameter hemisphere	Highly polished and roughened stainless steel	Static weights	Volar forearm	Static and dynamic
Highley et al. (1977)	Wheel (axis parallel to skin)	Nylon	Spring load	Volar forearm	Dynamic
Nacht et al. (1981)	Newcastle skin friction meter (designed by Comaish et al., 1973). An annular ring with outer diameter 15 mm and inner diameter 5.5 mm			Volar forearm	
Zimerer et al. (1986)				Volar forearm and infant's lower abdomen	
Elsner et al. (1990)		PTFE	Spring load	Vulvar skin (hair shaved at middle third of labia majora), and volar forearm	Dynamic
Cua et al. (1990 and 1995)				Forehead, upper arm, volar and dorsal forearm, postauricular, palm, abdomen, upper and lower back, thigh, ankle	

... continuation of Table 2.7

	Circular plate	Steel	?	Dorsam of hand, lower back and volar forearm	Dynamic
Loden et al. (1992)					
Zhang and Mak (1999)	Annular ring with outer diameter 16 mm and inner diameter 10 mm	Aluminium, Nylon, silicone, Pelite, cotton sock	Monitored by spring balance	Dorsum of hand, palm, anterior and posterior side of forearm, anterior and posterior leg	Dynamic

Key of table: ? – not stated in paper

Most researchers have made *in-vivo* friction measurements on human skin and, although a great diversity of sites have been studied, the volar forearm has been by far the most common (Table 2.6 and 2.7). A minority have used skin from cadavers (Comaish and Bottoms, 1971), pigs (Hills et al., 1994) or sheep (Hong et al., 2005).

Almost all studies have been performed on normal 'dry' skin. Several have investigated multiple sites and, by measuring skin hydration at the same sites, established that the coefficient of friction of skin increases with increasing hydration (Elsner et al., 1990; Cua et al., 1990; Loden et al., 1992; Nakajima and Narasaka, 1993; and Kondo, 2002). Many papers report on the influence of water on skin friction. Table 2.8 summarises the methodologies that have been used for hydrating the skin and removing surface water in key skin friction studies to date. It is difficult to compare data across studies as a wide range of techniques were used to apply the water; for example, immersion of the skin in water for an extended period prior to testing (Johnson et al., 1993); applying controlled quantities of water (typically a few mg/cm^2) to the skin surface immediately prior to testing (Highley et al., 1977; Nacht et al., 1981 and Egawa et al., 2002a), or dripping water on to the interface between skin and probe during friction measurements (Sulzberger et al., 1966). Nevertheless, a broadly consistent picture emerges: damp skin has a higher coefficient of friction than both dry skin and skin that is very wet. Of less significance to the work in this thesis, some studies describe the impact of lubricants (Comaish and Bottoms, 1971; Highley et al., 1977 and Johnson et al., 1993) or emollients / moisturisers (Nacht et al., 1981; Hills et al., 1994; Koudine et al., 2000 and Kondo, 2002) on skin friction.

Table 2.8 Summary of hydration methods in skin friction studies.

Author	Hydration method	Manner of surface water removal (if used)
Naylor (1955)	'A trace of water' applied to skin surface with a camel-hair brush	-
Sulzberger et al. (1966)	0.04 and 1.94 ml / min tap water delivered to rubbing interface by perfusion pump	-
Comaish and Bottoms (1971)	Hand immerse in water at 37°C for 30 min	Hand dried 'carefully'
Highley et al. (1977)	50 ul of distilled water applied to one-square-inch area	-
El-Shimi (1977)	Arm 'rinsed' with water	Excess water blotted away
Nacht et al. (1981)	2 mg of water per cm^2 of skin	-
Johnson et al. (1993)	Immersed in water for 120 seconds	-
Kenins (1994)	Water applied to the skin 'so that it glistened'	-
Egawa et al. (2002a)	2 ml/cm^2 distilled water applied	-
Kondo (2002)	Apply cream combining urea on the friction materials	-
Sivamani et al (2003)	'water was added to skin samples'	-
Hong et al. (2005)	10 ml dripped onto the sample at a speed of 1.25 ml/minute	-

2.5.3 Investigations of Amontons' law

Amontons' law holds that the coefficient of friction is independent of the normal force between two surfaces (Amontons, 1706) and there have been a number of investigations in the literature to discover whether or not this holds true for various materials on the skin. Data from studies that used probes whose faces were not flat are difficult to interpret quantitatively as such probes do not deliver a uniform pressure and, furthermore, the area of (nominal) contact between skin and probe changes with loading.

However, all these studies have reported either no change in coefficient of friction over the load range investigated (Naylor, 1955 and Asserin et al., 2000) or an initial fall in coefficient of friction with increasing load, reaching a plateau beyond some threshold load (Comaish et al., 1973; Nakajima and Narasaka, 1993; and Koudine et al., 2000).

Data from flat-faced probes are more useful (Comaish and Bottoms, 1971; Zhang and Mak, 1999; Egawa et al., 2002a; and Kondo, 2002). Comaish and Bottoms (1971) reported that the coefficient of static friction between polyethylene and the skin of a single subject was approximately constant for normal pressures greater than about 15 kPa but rose with decreasing pressure below this threshold. Zhang and Mak (1999) found that the coefficient of dynamic friction (with a probe of unreported material) for their ten subjects fell approximately linearly by an average of about 10% when the normal pressure was raised from 2 kPa to 8 kPa. Kondo (2002) – experimenting over an overlapping pressure range of 0.5-5 kPa with a Nylon fabric on three subjects – found no systematic change in dynamic coefficient of friction. Finally, Egawa et al. (2002a) reported no change in the dynamic coefficient of friction between the Kawabata (piano wire) probe (1989) and the skin of a single subject over the pressure range of 2.5-5 kPa.

In summary, literature suggested that there are differences amongst researchers about the apparatus setup and the techniques and methods for hydrating the test skin sites for friction measurements. In order to develop absorbent pads that cause less abrasion damage to skin, a robust method for hydrating the skin and measuring the coefficient of friction between skin and pad materials is needed.

2.6 Project aims

The overall aim of this work was to pave the way for improved incontinence pads by developing, validating and using methodologies (i) for measuring the quantity and distribution of water in SC that has been occluded by wet materials, and (ii) for measuring the coefficient of friction between skin (wet or dry) and nonwoven materials. Specific aims relating to the three primary methodologies were:

2.6.1 Evaporimetry study aims

● Develop a methodology for uniformly hydrating the volar forearm skin

● Develop a robust methodology for measuring the water vapour flux density using the five most widely used evaporimetry devices

● Compare and investigate the findings from the five devices

● Identify the strengths and limitations of the five devices

● Establish quantitative parameters that can be used in subsequent mathematical modelling of desorption of water from over-hydrated skin

2.6.2 OTTER study aims

● Develop a methodology for measuring the saturation profile of water within the SC using OTTER

● Develop a methodology for examining the relationship between the desorption curves of over-hydrated skin (measured by evaporimetry) and the water content of the SC (measured by OTTER) during the recovery of the skin

● Investigate the relationship between the water vapour flux density evaporated from the over-hydrated skin and the water content within the SC in order to establish quantitative parameters that can be used in subsequent mathematical modelling of desorption of water from over-hydrated skin

2.6.3 Friction study aims

- Develop a method for measuring the coefficient of friction between nonwoven materials and the skin (wet and dry)

- Validate the method by performing measurements on different subjects

- Apply the method to investigate Amontons' law for skin (wet and dry) and nonwoven material

Chapter 3

GENERAL METHODS

This chapter describes the general methods that had to be selected / developed before systematic work on skin measurements could begin. Specifically, it was necessary to:

1. Decide on appropriate test subjects and skin site(s) for experiments.

2. Define a subject acclimatisation procedure and test conditions (temperature and relative humidity).

3. Develop a methodology for hydrating skin sites reproducibly for wet skin measurements.

3.1 Test subjects and skin sites for experiments

In reality, the problem area of incontinence sufferers' skin is around the diaper area, but for the purpose of this work – to develop methodologies for charactering skin wetness and friction – it was necessary to choose a simple test site; that is, one that is flat and (relatively) hair free.

It is known that the properties of skin can differ considerably between two sites just a few centimetres apart, therefore results of skin tests obtained from one skin site are not directly comparable to another. In order to be consistent and to be able to compare results from different measurements, a specific skin site on the volar forearm was chosen for all experimental work in this thesis.

The volar forearm is easy to hold in any desired orientation, it is relatively free of hair

(particularly for females), readily accessible, and has often been used in studies of skin hydration relating to incontinence products (see Section 2.4.3.5 and 2.5.2). Since much is already known about volar forearm skin from studies on incontinence pad materials it would be valuable to be able to develop methodology for characterising wetness and friction there too. However, differences in background TEWL measured between skin sites on the volar forearm also exist (Rodrigues and Pereira, 1998), and so measurements in this thesis were focused on the flat area 100 mm distal to the elbow crease of subjects. This choice avoided the regions around the wrist and elbow creases which are rich in sweat glands and where transepidermal water loss can vary substantially over short distances.

A homogeneous group of young female subjects were recruited for this work since females tend to have less hair on the volar forearm, and wrinkles can be avoided in young subjects. Table 3.1 shows the description of the subjects and the experimental work they participated in.

Table 3.1. Description of the test subjects and the experiments in which they participated.

Subject	Age (y)	Right or left handed	Experiments		
			Evaporimetry (Chapter 4)	Evaporimetry and OTTER (Chapter 5)	Friction (Chapter 6)
I	25	Right	X	X	X
II	18	Left			X
III	44	Right			X
IV	23	Right			X
V	19	Right			X
VI	28	Right		X	
VII	23	Right		X	

All clinical work in this thesis was conducted with the approval of the Local Research Ethics Committee (Appendix A).

3.2 Test conditions and subject acclimatisation

As discussed in Section 2.4.3, subjects' skin condition and evaporimetry experiments are influenced by the environmental condition in which the measurements are performed. Therefore environment-related variables were controlled, according to published recommendations (Pinnagoda et al., 1990). Measurements on skin wetness and friction were carried out in a controlled environment room, where standard conditions of 23°C and 50% RH were chosen. These are similar to those chosen by previous workers (Table 2.5) and seem likely to avoid problems from either chilling or sweating of the subjects.

Subjects were asked not to apply any creams to their arms for 24 hours before the measurement, and not to take a bath or shower on the morning of the experiments. The reason for this was to minimize data noise from confounding variables that are known to have an effect on skin properties i.e. cream and water immersion.

Upon arrival, subjects were rested and acclimatized to the temperature and humidity in the measurement room for at least 30 minutes with their skin test sites on the volar forearm exposed.

3.3 Methodology for uniformly hydrating the skin

The methodology developed to achieve repeatable, uniform hydration of the skin at a test site was based on that devised by Fader et al. (2007). They hydrated the skin by applying patches of wet material to it under controlled conditions. Their method is

described below, along with modifications developed for the current work.

3.3.1 Wet patch material

Fader et al. (2007) used a hydro-entangled rayon fabric (code R200 ORV Manufacturing SpA, Italy) as a patch material for hydrating the skin. It has an area density of 200 g·m^{-2} and a nominal thickness of 1 mm. It is homogeneous and compliant enough to conform readily to curved skin surfaces. Its absorption capacity for water is about 1.3 kg·m^{-2}. Fader et al. (2007) showed that the skin would experience a constant environment throughout the skin hydration period by comparing the absorption capacity of the fabric (1.3 kg·m^{-2}) with the mass of excess water evaporated from the over-hydrated volar forearm skin on patch removal (about 5 g·m^{-2}). Patches were backed with rectangles (20 mm greater in length and width than patches) of waterproof material (Nylon / polyurethane) to prevent them drying out by evaporation.

However, due to the problem of obtaining a consistent supply of this hydro-entangled rayon fabric, it was only used as a patch material in the preliminary work described here, and in the experiments of characterising skin friction for Subject I described in Chapter 6.

A more reliable alternative was found to be used as patches for all other hydration experiments in this thesis, since it is more readily available to a consistent specification. Rectangles of filter paper (17 Chromatography, Whatman plc, England) were used instead of hydro-entangled rayon R200. It has an area density of 400 g·m^{-2}; a nominal thickness of 0.92 mm; and an absorption capacity for water of about 1.2 kg·m^{-2}. Table 3.2 shows the characteristics of the two patch materials. The 17Chr is stiff when dry, but is compliant enough to conform to curved volar forearm skin surfaces when it is wet.

Table 3.2 Characteristics of the two patch materials used to hydrate skin in this thesis (R200 and 17Chr).

Material	Area density (g·m^{-2})	Thickness (mm)	Absorption capacity for water (under low pressure) (kg·m^{-2})	Max. absorbency (kg·m^{-2})
R200	200	1.00	1.3	1.1
17Chr	400	0.92	1.2	1.0

Fader et al. (2007) performed several tests on R200 to discover how uniformly it distributed a certain quantity of water. Similar tests were carried out on 17Chr and the results compared with R200. R200 and 17Chr patches (50 x 70 mm) were first fully submerged in water for one minute, lifted up horizontally and weighed on a balance. By taking away the dry masses from the fully saturated masses of the patches, it was found that just less than 3 g of water was retained in patches of both materials. Therefore 3.5 ml of water was chosen to be sure to fully saturate patches.

The redistribution of water in fully saturated patches under gravity was investigated. This is important because subjects are not able to keep their arms absolutely horizontal when their skin is being hydrated from wet patches. Rectangles of the two patches (50 x 70 mm) were uniformly wetted to full saturation using 3.5 ml of water. They were then suspended vertically from two pins for 20 minutes with the 50 mm edges horizontal, and then cut into three equal rectangles (50 x 23 mm) which were weighed wet. They were then dried in the atmosphere and reweighed, the mass of water in each per unit dry weight measured. Three repeats were performed, and the results are shown in Table 3.3.

The water content of the upper and lower thirds of both R200 and 17Chr were about 9% above and below the mean. This is acceptable since, during patch wearing, the subjects

were allowed to walk about within the environment controlled room, but they were asked to keep their hydrating arm roughly horizontal during the wear period. Therefore, when in use, the patches should be tipped at angles to the vertical very much less than 90°, so the water redistribution under gravity should not introduce major differences in wetness of the patch across its interface with the skin, and hence the wetness across the test skin site should be evenly distributed.

Table 3.3 Water distribution in the wet patch materials when hung vertically.

Patch material	Sections	Mass water / unit dry mass (g/g)			% deviation from mean		
		R#1	R#2	R#3	R#1	R#2	R#3
R200	upper	2.32	2.40	2.35	-8.0	-7.8	-6.9
	middle	2.53	2.51	2.60	+0.4	-2.1	-1.1
	lower	2.70	2.65	2.76	+7.2	+8.0	+6.2
17Chr	upper	2.52	2.47	2.57	-7.9	-3.3	-5.8
	middle	2.32	2.46	2.41	+1.6	-4.9	-0.6
	lower	2.09	2.21	2.25	+6.2	+9.0	+5.3

The tests above showed that the performance of 17Chr is as good as the hydro-entangled rayon R200, but with consistent supply.

3.3.2 Holding the wet patch in place

The same simple cuff designed by Fader et al. (2007) was adopted in this project (Fig 3.1) for holding the wet patch in contact with the skin. The cuff was made from cotton fabric and it was held in place with *Velcro* strips.

Fig 3.1 A simple cuff used for holding the wet patch on skin.

The wetted patch was placed against the skin and backed with a rectangle (20 mm greater in length and width than patches) of waterproof material (nylon / polyurethane) to prevent it drying out by evaporation. An 11 mm thick piece of foam was placed over the wetted patch and waterproof material, before the cuff was positioned on the forearm and secured using Velcro (Fig 3.2).
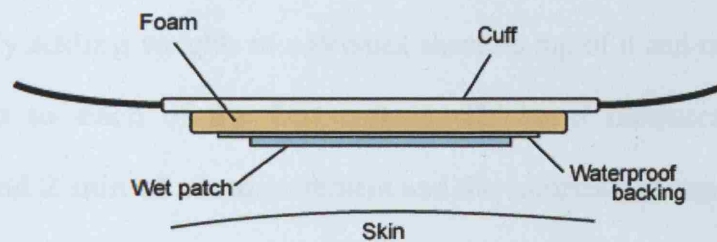
Fig 3.2 Arrangement of wet patch with the use of the cuff on skin.

Fig 3.3 shows the positions on the volar forearm of wet patches for hydrating the skin for characterising wetness, measurement of hydration profile of the skin, and for friction measurements described in chapters 4, 5 and 6, respectively.
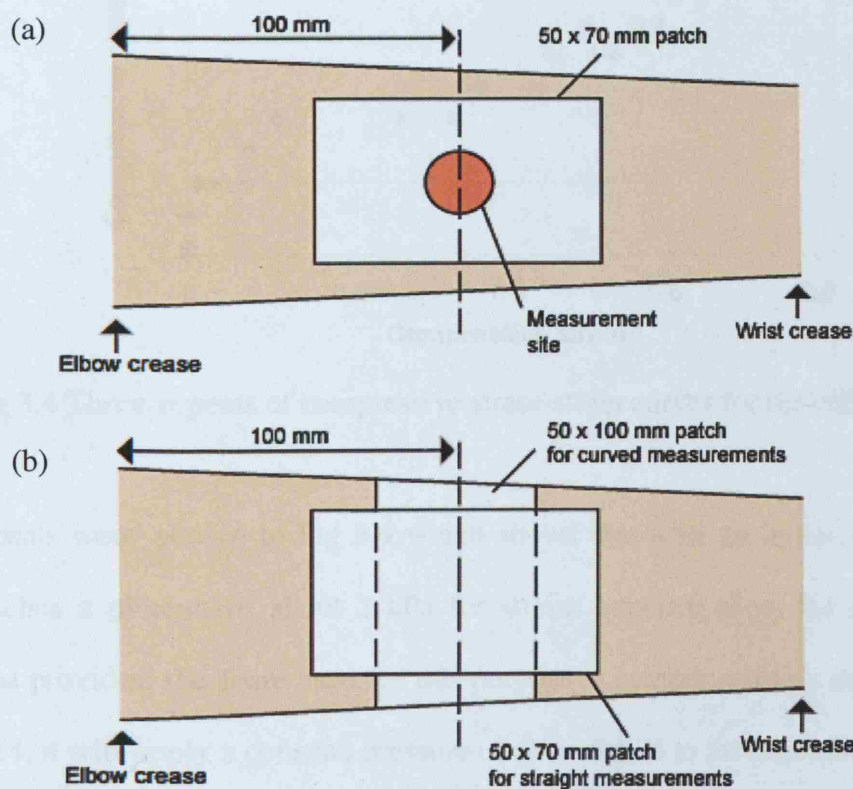
Fig 3.3. Positions on the volar forearm of wet patches for hydrating the skin for (a) evaporimetry and OTTER measurements and (b) friction measurements.

The foam in the cuff (Fig 3.2) was chosen to be hard enough to ensure that the wet patch was held in firm contact with the skin over the whole target area, but soft enough to avoid large differences in pressure between areas in which it was compressed to slightly different degrees. Fader et al. (2007) produced three repeats of the compressive stress-strain curve for the foam (Fig 3.4). It was measured on a 75 mm square of foam by progressively adding weights to a Perspex sheet on top of it and measuring the foam thickness close to each of the four corners. Thickness measurements were made between 30 s and 2 min of a load increment and the compressive strain under each load was calculated using the average of the four thicknesses (t), and the foam thickness under zero load (t_o).

$$\text{Strain} = (t_o - t)/ t_o \quad \text{.....................} \quad \text{Equation 3.1}$$
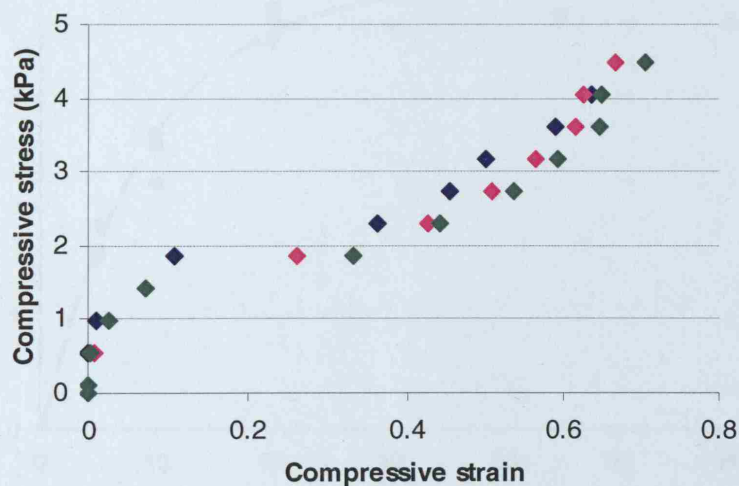
Fig 3.4 Three repeats of compressive stress-strain curves for the cuff foam.

Three repeats were shown in Fig 3.4 which shows that after an initial steep rise, the stress reaches a plateau of about 2 kPa for strains between about 0.1 and 0.4. This means that provided the foam used for this purpose is compressed to a strains between 0.1 and 0.4, it will apply a constant pressure of about 2 kPa to the constraining surfaces. A pressure of 2 kPa is low compared to the pressures beneath supine and seated people (Cottenden et al., 1998) but sufficient to achieve the purpose of achieving contact

between patch and skin over the whole nominal interface area.

3.3.3 Patch wear time

In order to choose appropriate patch wear times, it was important to establish the impact of patch wear time on skin hydration level. Patches of 17Chr filter paper soaked in normal saline were applied to the volar forearm of Subject I for different times between 5 and 60 minutes. On patch removal, surface water was blotted (see next section) and the SSWL in the skin ($g \cdot m^{-2}$) due to patch wearing, was estimated by measuring the area under the desorption curve logged for 30 minutes by a Servo Med Evaporimeter EP2, following the method described in Section 4.3.2.
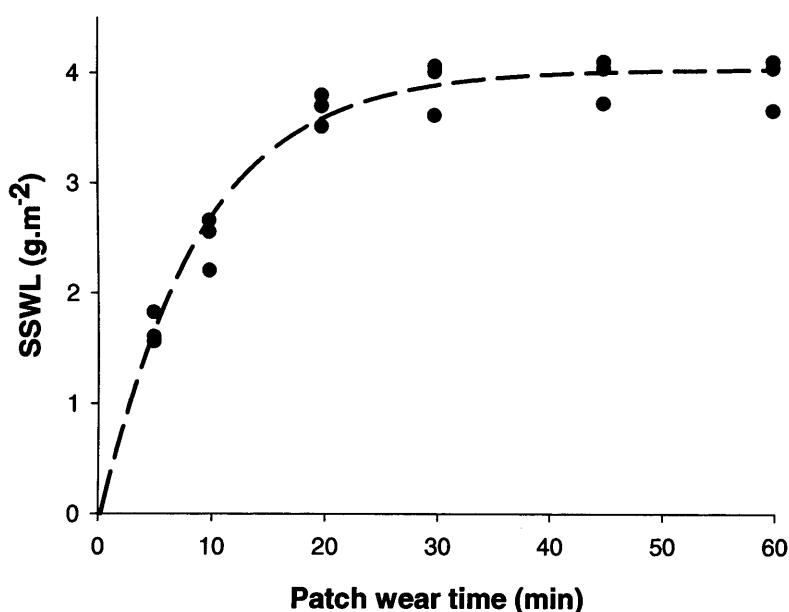
Fig 3.5. The impact of patch wear time on skin hydration.

It was established that the volar forearm skin hydrated to an increasing extent for patch wear times up to 20 minutes but increased only slightly from 20 to 60 minutes (Fig 3.5). Good reproducibility could be achieved for skin hydration measurements if a patch wear was extended to correspond with the plateau region of the SSWL (Fig. 3.5).

Wearing the wet patch for 60 minutes would ensure that the volar forearm skin was fully hydrated, so 60 minutes patch wear time was chosen to be used for making the skin wetness measurements described in Section 4.3 and 5.3. However, for large sample size experiments with short data gathering time (i.e. the skin friction measurements described in Section 6.5) a 20 minutes patch wear time was used to shorten the experiment time.

3.3.4 Dealing with skin surface water

When a wet patch is removed from the skin, it leaves behind a visible film of surface water and the amount of water depends on how the patch was removed. Fig 2.18 in Section 2.4.3.5 shows a desorption curve of an over-hydrated skin measured with an Evaporimeter (see Section 4.3 for method) with surface water left in place. The curve shows a high plateau value (B) corresponding to the evaporation of surface water from the wet skin surface. Once the surface water has gone, the SC itself begins to dry out, giving the desorption curve (C) in the graph. The length of the plateau depends on the amount of surface water present. This potential source of variability was addressed by blotting surface water from the skin by applying a piece of dry filter paper (Whatman N°1 filter paper, Whatman plc., England) to the wet area for two seconds immediately after patch removal and before measurement began. The methods for applying the filter paper to the skin for the wetness and friction measurements are described in Section 4.2.4 and 6.4.3.2, respectively.

3.3.5 Final methodology

Detailed instructions for managing test subjects, producing uniformly wetted patches, and applying them to the subject's skin are described below.

1. Take the test subject into the environment controlled room with their test skin site
    uncovered to start acclimatising for 30 minutes.

2. Check the temperature and relative humidity in the controlled environment room to
    ensure conditions are within the acceptable range of 23 ± 2 °C and 50 ± 5 % RH.

3. Cut a stock of 50 mm x 70 mm (or 50 mm x 100 mm for curved friction
    measurements) rectangles of R200 / 17Chr with the 70 mm (or 100 mm) edges
    parallel to the machine direction (grain) of the material for consistency.

4. Cut a stock of 70 x 90 mm (or 70 x 120 mm) rectangles of water-proof plastic film
    for backing the patches.

5. Place a R200 / 17Chr patch on a smooth, flat, level surface (check with a spirit
    level), then draw 3.5 ml of normal saline into a 10 ml pipette.

6. With the tip of the pipette about 10 mm above the centre point of the patch, release
    the 3.5 ml of fluid. Touch the pipette tip to the patch to get rid of the last drip.

7. Transfer the wetted patch from bench to the test skin site shown in Fig 3.2 (keep it
    as horizontal as possible to avoid fluid dripping out), cover the patch with the
    water-proof backing, foam and cotton cuff. Secure the cuff to the forearm using
    Velcro.

8. Leave the wet patch on the skin for 60 minutes for skin wetness experiments
    (Chapter 4 and 5) and 20 minutes for skin friction measurements (Chapter 6).
    During this wear time, allow the subject to walk about in the environment
    controlled room while keeping their forearm roughly horizontal.

9. Remove the wet patch, blot surface water by applying a piece of dry filter paper to
    the wet skin for two seconds (using the methods described in Section 4.2.4 and
    6.4.3.2), before measurement begins.

Chapter 4

CHARACTERISING SKIN WETNESS USING EVAPORIMETRY

Although a variety of instruments and techniques have been used in attempts to measure the water content of SC, devices for measuring water vapour flux density from the skin have been the most commonly used. Accordingly, they are the focus of the work described below. The initial focus was on developing a robust methodology for making measurements on over-hydrated skin. This was then used to compare measurements made using the five most widely used evaporimetry devices on the market.

Water vapour flux density measurements were supplemented by work with OTTER (described in the next chapter) to measure the saturation gradient within the SC during desorption, in order to elucidate the drying process.

4.1 Equipment

Five commonly used evaporimetry devices were selected to be compared by developing methods for estimating the amount of excess water (SSWL) within the SC after over-hydration under carefully controlled conditions. The five devices and the reasons for the choices are:

● Evaporimeter EP2 (Servo Med AB, Sweden)

  - It was the only available device on the market between the 1970s and 1990s, and was used in most of the early studies.

● DermaLab (Cortex Technology, Denmark)

- Commonly used open-chamber device that is still available on the market.

● Tewameter TM300 (Courage and Khazaka Electronic, Germany)

- Most commonly used open-chamber device nowadays.

● VapoMeter SWL4 (Delfin Technologies Ltd, Finland)

- A commonly used closed-chamber device.

● AquaFlux AF100 (Biox Systems, U.K.)

- A relatively newly available device with a new measuring principle.

4.2 Methodology development

In this section, a series of experiments were performed to develop a reproducible and reliable final methodology for measuring the skin wetness using the five different evaporimetry devices. Table 4.1 summarises this approach.

4.2.1 Environment conditions

As discussed in Section 3.2, it was necessary to control the environment conditions for measurements as it will certainly influence the since subjects' skin condition and evaporimetry experiments.

Measurements were performed in a small room instead of an open laboratory area because open-chamber devices are very sensitive to air movement, which can result in substantial fluctuations in measurements (Pinnagoda et al., 1990). An enclosed room has less problems with drafts.

Therefore, all of the work described in this chapter was carried out in a controlled environment room with a temperature of 23°C and 50% relative humidity to avoid chilling or sweating of the subjects.

Table 4.1 Structure of the methodology development section.

Section	Goal
4.2.1 Environment conditions	Ensure the environment condition can be controlled within a suitable range for evaporimetry measurements.
4.2.2 Software	Establish suitable procedures for using the software associated with each of the evaporimetry devices.
4.2.3 Evaporimetry probe setup	Develop a method for applying evaporimetry probes to the skin without affecting the measurements.
4.2.4 Preparation of over-hydrated skin	Devise a method for removing the film of surface water left behind on the skin by the wet patch.
4.2.5 Calibration method and checks	Devise and use methods for checking the calibration of the open chamber evaporimetry devices.
4.2.6 Comparison of measurement monitoring time and characterising parameters used in the literature	Summarise and compare the wide variety of different evaporimetry methodologies reported in the literature for taking measurements and analysing data.
4.2.7 Selection of measurement monitoring time and characterising parameter	Based on Section 4.2.6, define a suitable methodology for the current work.
4.2.8 Measurement with the AquaFlux	Investigation of the recently developed instrument that produced an unexpected desorption curve.

4.2.2 Software

All devices were supplied with software that allows measured data to be displayed and stored on a computer, in a format that can be exported into a spreadsheet for analysis. The Evaporimeter came with standard software to measure mean water vapour flux densities over different time periods, for example,

- mean and standard deviation of the last 15 s of a 45 s measurement period,

- the last 30 s of a 90 s measurement period,

- the last 30 s of a 2 minutes measurement period

However, these time periods were too short to capture the entire SC desorption curve. Accordingly, software that allowed water vapour flux densities to be logged continuously over extended periods was commissioned from the manufacturer, and a description of the procedure is listed in Appendix C1.

The DermaLab software only allows water vapour flux densities to be logged for a maximum of 5 minutes, and an upgrade of the software (to overcome this limitation) is only available from the manufacturer when an upgrade of the device is purchased. Therefore for the purpose of this work – capturing the SC desorption curve for 30 minutes – 5 minutes of logged data were repeatedly transferred to a text file and the program restarted immediately until 30 minutes had been captured (see Appendix C2 for a detailed description of the procedure).

The procedures for using the software associated with the other three evaporimetry devices (Tewameter, VapoMeter and AquaFlux) are described in Appendices C3, C4 and C5, respectively.

4.2.3 Evaporimetry probe setup

In order to apply the open-chamber probe to the skin:

(1) with constant / reproducible contact pressure to avoid changes in the distance between skin and sensors,

(2) avoiding artefacts due to the movement, hot hand or warm, damp breath of the researcher, and

(3) in a horizontal plane parallel to the skin to avoid interference from convection air movements.

Fader et al. (2007) designed and built a wooden beam and probe holder (Fig 4.1) for the Evaporimeter. The same holder was used in the work described here.
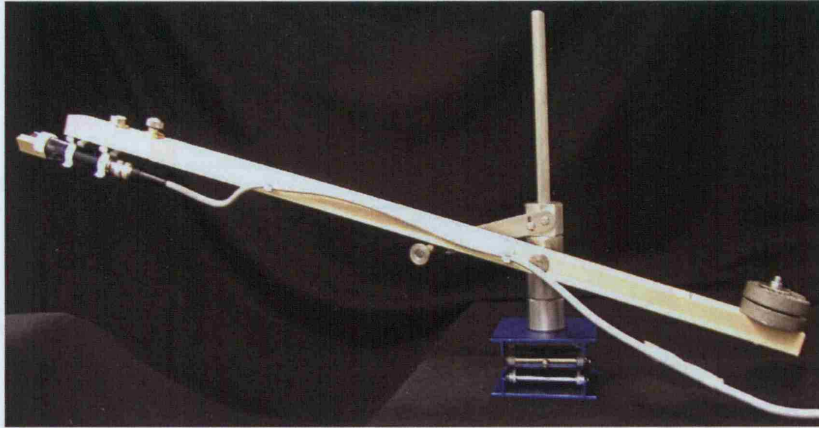
Fig 4.1 Wooden beam and probe holder for Evaporimeter.
(designed and built by Fader et al. (2007))

With this wooden beam, the probe application pressure could be set to any desired value by adjusting the distance of a counterweight from the fulcrum (Fig 4.1). The height of the wooden beam could be adjusted for different subjects and the probe holder was equipped with a bulls-eye spirit level to ensure that it was always horizontal when taking measurements. The beam also had a 'parking station' into which it could be placed when not in use, to hold it clear of the subject.

Similarly, new probe holders for all the other evaporimetry devices were designed and built. For the two other open-chamber devices, the DermaLab and Tewameter, probe holders were built in the same way as the Evaporimeter (Fig 4.2), since their probes are similar in design.

The VapoMeter and AquaFlux measurement heads have rather different geometries and so a different approach was needed to making suitable probe holders (Fig 4.3 and 4.4). They were machined from Delrin. Two screw holes in the back of the VapoMeter

provided convenient location points for a pair of pins in the probe holder (Fig 4.3). A

movable barrier with a finger gnurled knob was used to secure the device during

measurements.
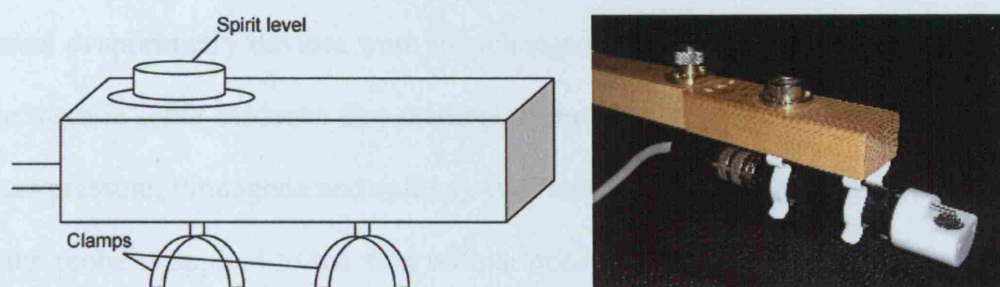
Fig 4.2 Drawing and picture of the probe holder for the Evaporimeter,
DermaLab and Tewameter.
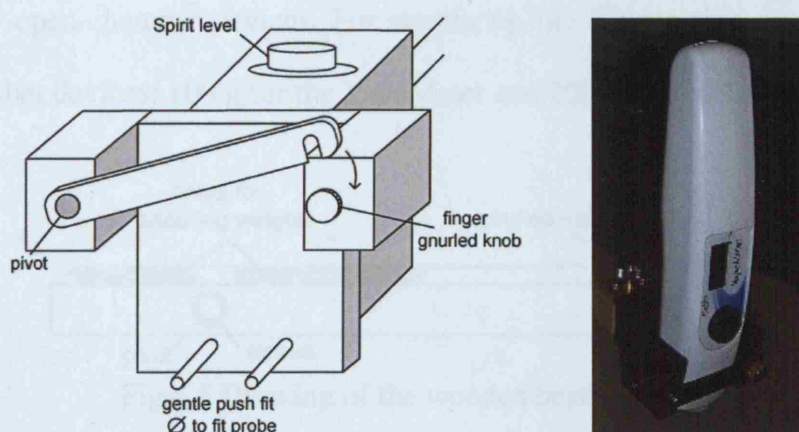
Fig 4.3 Drawing and picture of the probe holder for the VapoMeter.
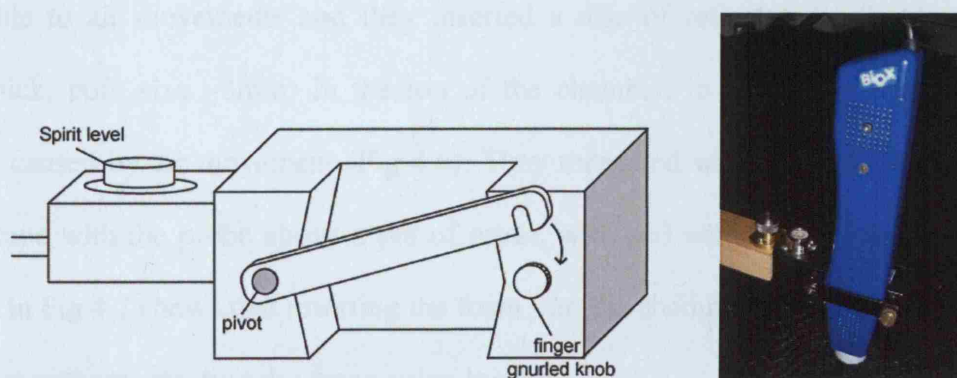
Fig 4.4 Drawing and picture of the probe holder for the AquaFlux.

For AquaFlux, the probe holder was built in the shape of the probe (Fig 4.4), with a movable barrier and a gnurled knob to secure the device during measurement.

The wooden beam was also improved for this work so that probe holders for the different evaporimetry devices were interchangeable on one end of the beam (Fig 4.5). Since there is some evidence that readings from open-chamber devices are affected by contact pressure, Pinnagoda and colleagues (Pinnagoda et al., 1990) have recommended that the probe is applied to the skin with a 'constant light pressure'. However, they do not provide quantitative guidelines. In the absence of such guidelines, it was decided to use the probe pressure corresponding to the mass of the probe (50 g) resting on the skin for all three open-chamber devices. For simplicity, the same action was used for the closed-chamber devices: 100 g for the VapoMeter and 200 g for the AqauFlux.
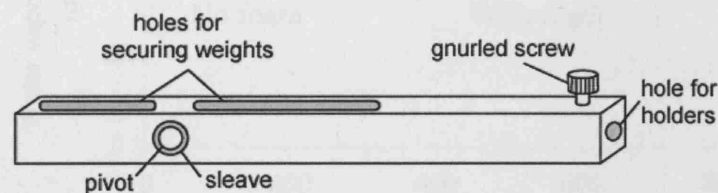
Fig 4.5 Drawing of the wooden beam design.

Fader et al. (2007) reported that readings using the Evaporimeter were particularly susceptible to air movements and they inserted a disc of reticulated polyester foam (6mm thick, pore size ~3mm) in the top of the chamber, to reduce the variation in readings caused by air movement (Fig 4.6). They measured water vapour flux density against time with the probe above a pot of water, with and without the foam in place. The plot in Fig 4.7 shows that inserting the foam into the chamber greatly reduced noise in the data without affecting the mean value logged.

This foam was left in place in the Evaporimeter for all measurements reported in this

thesis. Another open-chamber devices – DermaLab – was supplied with a similar disc of foam (although of a smaller pore size) *in situ*. The third open-chamber device (Tewameter) had no such foam.

Fig 4.6 A piece of foam in the Evaporimeter probe chamber.
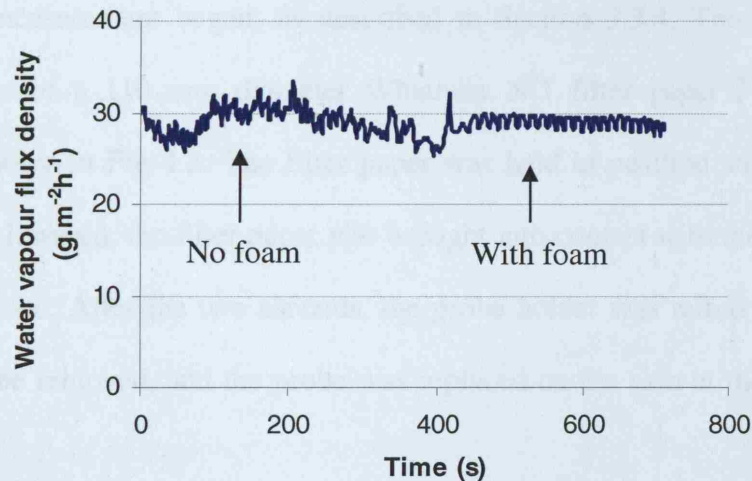
Fig 4.7: Comparison of water vapour flux density of a pot of water with and without foam (Adopted from Fader et al. (2007)).

The gold-plate protection cover provided for use with the Evaporimeter to facilitate cleaning was removed for the work, as only healthy skin sites were being used for measurements in this study.

As described on Section 2.4.3.1, the Tewameter came with a heating up option that preheats the sensors inside the measurement chamber to a temperature close to that of the skin, which considerably decreases the response time of the instrument. This

function was not applied in this project in order to make the Tewameter comparable with all other evaporimetry devices.

4.2.4 Preparation of over-hydrated skin

In order to measure and compare the amount of SSWL in over-hydrated skin using the devices, the procedure for uniformly hydrating the skin described in Section 3.3.5 was used.

After patch removal, dry filter paper was applied for two seconds to blot any surface water before measurement began, as described in Section 3.3.4. This was achieved using a quarter of a 110 mm diameter Whatman N°1 filter paper (Whatman plc., England) as shown in Fig 4.8. The filter paper was held in position so that when the probe arm was lowered, the filter paper was brought into contact with the skin and held there by the probe. After the two seconds, the probe holder was raised briefly for the filter paper to be removed, and the probe was replaced on the skin at the same site for measurement.
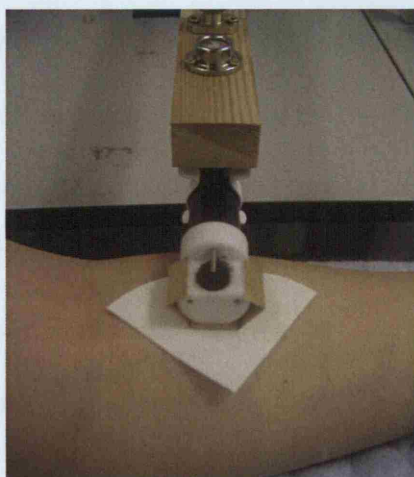
Fig 4.8 Evaporimeter probe showing filter paper in place
for blotting of surface water.

4.2.5 Calibration method and checks

All devices were calibrated by their manufacturers / suppliers at the start of the work, except for the Evaporimeter. The DermaLab was calibrated by Cortex Technology, Denmark; the Tewameter was calibrated before it was leased from EnviroDerm Services, UK; the VapoMeter and AquaFlux were newly bought at the beginning of the study. The manufacturer of the Evaporimeter was out of business at the time of this study, and the probe was no longer available on the market. It was, therefore, sent to a biomedical research instruments specialist company called cyberDERM (US) for calibration.

Currently, the method used by manufacturers for calibrating the open-chamber devices is based on the 'wet-cup method' from the ASTM-E96 Standard (ASTM-E96, 1995), and this calibration method has several limitations, as discussed in Section 2.4.3.7. However, as this method is commonly used by manufacturers, it was used in this work in order to compare the devices as they are usually used.

One of the evaporimetry devices used in this work, the AquaFlux, is supplied with instructions and equipment for periodic flux density calibration by the user (see Section 2.4.3.3 for details). This involves placing a one microlitre (0.001 g) droplet of water in a cap screwed to the open face of the chamber and logging the water vapour flux from it until it has all evaporated. Calibration is achieved by setting the area under the flux / time curve multiplied by the cross-sectional area of the chamber to equal the known mass of water evaporated, i.e. 0.001 g.

A similar procedure was adopted for all the open-chamber devices with the aim of checking the calibration by the wet cup method. The lower face of each chamber was occluded with a sheet of polyethylene fixed to the chamber face with silicone rubber

(Fig 4.9). A microlitre of water was placed near the centre of the polyethylene disc, through the top of the chamber and the water vapour flux logged until all the water had evaporated.
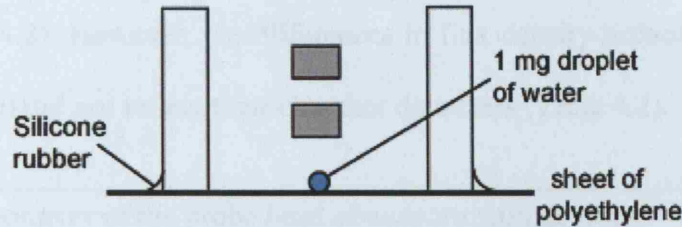
Fig 4.9. Experiment setup for droplet calibration of the open-chamber devices.

The mass of water measured by each device (in g) was calculated by multiplying the area under the flux / time curve (in $g \cdot m^{-2}$) by the cross-sectional area of the device measurement chamber (in m^2), and compared with the known mass of water evaporated. Three repeat measurements were taken with each of these four devices, and an example plot is shown in Fig 4.10. It was not possible to use this procedure with the VapoMeter as it provides only spot measurements of flux and the chamber needs to be flushed of water vapour between measurements.
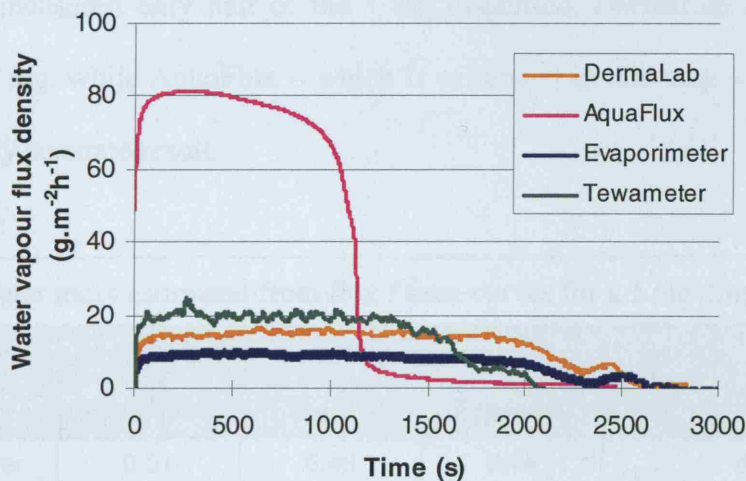
Fig 4.10. Water vapour flux density curves of the 1 mg of water evaporated and measured by the four devices.

Fig 4.10 shows that the AquaFlux produced a larger area under the curve and a much

higher maximum flux density (~80 $g{\cdot}m^{-2}h^{-1}$) than those of the three open-chamber

devices (between $10 - 20$ $g{\cdot}m^{-2}h^{-1}$). The higher flux density from the AquaFlux could be

predicted given the low humidity inside its chamber and its smaller cross-section

chamber (Table 4.2). However, the differences in flux density between the other three

devices (Fig 4.10) did not reflect their chamber diameters (Table 4.2).

Table 4.2 Geometry of the probe head of evaporimetry devices.

Devices	Height from the skin to the lowest sensor (mm)	Chamber diameter (mm)	Volume of chamber (mm^3)
Evaporimeter	3	12	339.3
DermaLab	4	10	314.2
Tewameter	3	10	235.6
AquaFlux	7	7	269.4

Table 4.3 shows the mass of evaporated water measured by each of the devices when 1

mg of water had evaporated in the experiment shown in Fig 4.9. If the devices were

correctly calibrated and working (i.e. the instrument reporting correctly what actually

happened), they should measure 1 mg of water. However, the results shows that the

Evaporimeter measured only half of the 1 mg dispensed, DermaLab and Tewameter

about 2/3 of 1 mg, while AquaFlux – which is calibrated in this way – unsurprisingly,

produced a very accurate result.

Table 4.3 Water mass estimated from flux / time curves for a 1 mg droplet

Device	Measured water mass (mg)			Mean as a % of 1 mg
	Repeat #1	Repeat #2	Repeat #3	
Evaporimeter	0.51	0.48	0.44	47.5
DermaLab	0.71	0.79	0.66	71.9
Tewameter	0.76	0.73	0.73	73.8
AquaFlux	1.01	0.94	1.02	99.2
VapoMeter	Measurement not possible			

However, the evaporation of water from a point source is rather different from evaporation from the whole chamber floor, as happens in taking measurements on skin. It might be that water vapour from a droplet is not uniformly distributed across the cross sectional area of the chamber (Fig 4.11) when it reaches the sensors. In that case, flux measurements would depend on the diameter of the chamber and the height of the sensors – especially the lowest one. Therefore another approach using wet filter paper disc was developed to address this limitation.
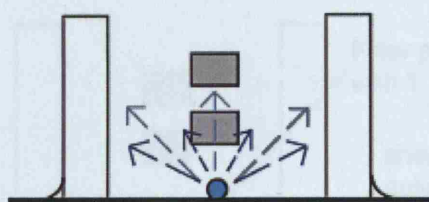
Fig 4.11. Illustration of water evaporation from the droplet
inside the measurement chamber.

Discs of filter paper (Whatman N°1 filter paper, Whatman plc., England) were cut, placed on a polyethylene sheet on a balance, and sufficient water added to them to just achieve full saturation. The mass of water was noted and the device being calibrated was placed over the wet disc to log the water vapour flux from it till the filter paper was fully dry. Initial experiments revealed that this took some few hours for the larger discs – an impractically long time – and so a variation on the technique was developed.

Discs were fully saturated as before, but allowed to partially dry out in the atmosphere while being left on the balance. Once a pre-determined mass of water was left in the disc, the device being calibrated was placed over it as before. The same effect would not have been achieved by dropping a sub-saturation quantity of water on to filter paper discs as this would not had achieved uniform distribution.

Before each open-chamber device was placed on top of the filter paper, grease (silicon vacuum grease, Beckman Instruments, US) was spread across the annular underside of the measurement chamber to ensure a good seal between the device and the polyethylene sheet (Fig 4.12). A quick test was performed with no filter paper in place to confirm that no water evaporated from the grease alone. Water vapour flux density was then logged in the setup shown in Fig 4.12, until all the water had evaporated from the filter paper.
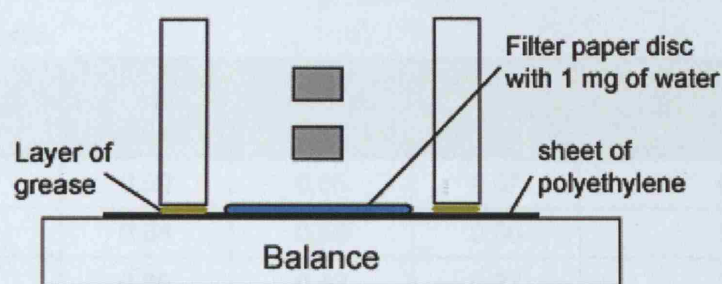
Fig 4.12. Experiment setup of the calibration using filter paper for the open-chamber devices.

Filter paper discs were made in three different diameters with the biggest disc close to the chamber diameter and the other two of smaller arbitrary diameter: the Evaporimeter (6, 8 and 10 mm), the DermaLab (5, 6 and 8 mm) and the AquaFlux (3.5, 5 and 6 mm). The results are shown in Table 4.4, 4.5 and 4.6, for the Evaporimeter, DermaLab and AquaFlux, respectively. Again, measurement was not possible for the VapoMeter since it is unable to make continuous measurements. The Tewameter – which had been rented for earlier work – was no longer available at the time of test.

Table 4.6 shows the AquaFlux measured very close to the correct mass of water for all filter paper disc diameters. By contrast, the Evaporimeter and DermaLab underestimated the true mass of evaporated water for all filter paper disc diameters measured (Table 4.4 and 4.5, respectively). However, the magnitude of the

underestimate increased with increasing filter paper disc diameter. When the diameter of the discs (10 mm for Evaporimeter and 8 mm for DermaLab) were close to the diameter of the chamber (12 mm for Evaporimeter and 10 mm for DermaLab on Table 4.2), the devices only measured ~40% and ~55% of the water evaporated from the filter paper disc, respectively. These results show that the Evaporimeter underestimated the most, which agrees with the droplet experiments (Table 4.3).

Table 4.4 Water mass measured using the Evaporimeter for different diameter wet filter paper discs.

Diameter of disc	Measured water mass (mg)			Mean as a % of 1 mg
	Repeat #1	Repeat #2	Repeat #3	
6 mm	0.60	0.65	0.67	63.9
8 mm	0.58	0.52	0.60	56.7
10 mm	0.38	0.43	0.37	39.7

Table 4.5 Water mass measured using the DermaLab for different diameter wet filter paper discs.

Diameter of disc	Measured water mass (mg)			Mean as a % of 1 mg
	Repeat #1	Repeat #2	Repeat #3	
5 mm	0.86	0.94	0.83	87.6
6 mm	0.66	0.65	0.62	64.4
8 mm	0.53	0.50	0.62	55.1

Table 4.6 Water mass measured using the AquaFlux for different diameter wet filter paper discs.

Diameter of disc	Measured water mass (mg)			Mean as a % of 1 mg
	Repeat #1	Repeat #2	Repeat #3	
3.5 mm	1.05	1.06	0.96	102.4
5 mm	1.06	1.03	0.89	99.4
6 mm	0.89	1.06	1.03	99.0

According to this calibration study, the error of the measured water mass may be more

than 50% for both the Evaporimeter and the DermaLab in the case of the evaporimetry

work in this thesis, where the whole diameter of the chamber was covered by the test

skin site. However, the reason for the increase in underestimation with increasing filter

paper disc diameter is still unclear. If it was determined purely by the cross sectional

area of the evaporation source, the data from droplet experiments would be expected to

be consistent with the data from filter paper experiments, i.e. the droplet should

represents a small diameter on Fig 4.13, and therefore a higher percentage of the

evaporated mass would be expected than was measured.
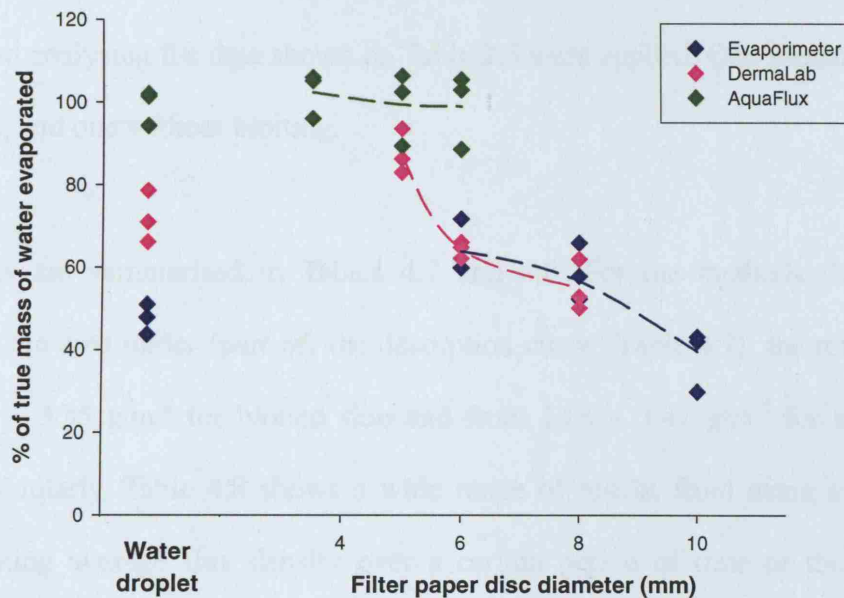
Fig 4.13 Summary of the results from droplet and filter paper calibration experiments
with the Evaporimeter, DermaLab and AquaFlux.

4.2.6 Comparison of measurement monitoring time and characterising parameters used in the literature

Different methodologies that have been used for applying the evaporimetry technique

on over-hydrated skin in the literature are reviewed in Section 2.4.3.6, and they were

found to have varied widely, not only in the methods used for hydrating the skin (Table

2.4) but in how evaporimetry data was logged and analysed (Table 2.5). Experiments

were carried out with the Servo Med Evaporimeter on the volar forearm of Subject I

(Table 3.1), in order to demonstrate the variation in the results that are produced using

the various methods of logging and processing the data found in literature.

Prior to the hydration measurement, a background TEWL that represents the rate of

water loss evaporating from the skin surface under normal conditions was measured. If

the method was described in the literature then it was used, if no method was specified

the one in Section 4.3.1 was used. The skin was then hydrated with the method

described in Section 3.3.5 for 60 minutes. Upon removal of the wet patch, methods of

logging and analysing the data shown on Table 2.5 were applied. One measurement was

taken with, and one without blotting.

The results are summarised in Tables 4.7 and 4.8. For the methods that involved

measuring the area under (part of) the desorption curve (Table 4.7), the results ranged

from $0.95 - 3.35$ g·m^{-2} for blotted skin and from $1.06 - 3.47$ g·m^{-2} for skin without

blotting. Similarly, Table 4.8 shows a wide range of results from using methods that

involve taking average flux density over a certain period of time or the peak, as a

measure of skin wetness. The results ranged from $8.02 - 40.65$ g·m^{-2}h^{-1} for blotted skin

and from $6.57 - 56.79$ g·m^{-2}h^{-1} for skin without blotting. These findings confirm that

widely different values for 'skin wetness' will be generated depending on the details of

the method used. Therefore a standard, validated method is needed.

Table 4.7 Results from repeating the methods described in the literature that measured the area under a portion of desorption curves.

Authors (year)	Method for measuring flux density	Method for measuring background TEWL	Measured result with blotting (g·m⁻²)	Measured result without blotting (g·m⁻²)
Zimmerer (1986)	'Precise intervals' until ~20 min. Max reading over 20s taken as flux value. Area under curve above background TEWL calculated	Given: 4.3 g·m⁻²·h⁻¹	0.95	1.06
Davis et al. (1989)	Area under drying curve over 2 minutes straight after patch removal	-	1.17	1.86
Fader et al. (2007)	On patch removal, blot surface water, log flux for 10 min. Area under desorption curve (0-10 min) having subtracted background.	Mean for last 2 min of 2.5 min logging	3.35	3.47

Table 4.8 Results from repeating the methods described in the literature that the averaged flux density over a certain periods of time or took the peak value as a measure of skin wetness.

Authors (year)	Method for measuring flux density	Method for measuring background TEWL	Measured result with blotting (g·m⁻²·h⁻¹)	Measured result without blotting (g·m⁻²·h⁻¹)
Wilson & Dallas (1990)	2 min reading straight after patch removal, six further 2 min readings, each separated by 2 min rest. Means over each 2 min taken as flux value. Difference between 1st and 6th flux reading = ESW (Excess skin wetness).	-	28.84	49.15

Table 4.7 Results from repeating the methods described in the literature that measured the area under a portion of desorption curves.

Authors (year)	Method for measuring flux density	Method for measuring background TEWL	Measured result with blotting ($g \cdot m^{-2}$)	Measured result without blotting ($g \cdot m^{-2}$)
Zimmerer (1986)	'Precise intervals' until ~20 min. Max reading over 20s taken as flux value. Area under curve above background TEWL calculated	Given: $4.3 \ g \cdot m^{-2} h^{-1}$	0.95	1.06
Davis et al. (1989)	Area under drying curve over 2 minutes straight after patch removal	-	1.17	1.86
Fader et al. (2007)	On patch removal, blot surface water, log flux for 10 min. Area under desorption curve (0-10 min) having subtracted background.	Mean for last 2 min of 2.5 min logging	3.35	3.47

Table 4.8 Results from repeating the methods described in the literature that the averaged flux density over a certain periods of time or took the peak value as a measure of skin wetness.

Authors (year)	Method for measuring flux density	Method for measuring background TEWL	Measured result with blotting ($g \cdot m^{-2} h^{-1}$)	Measured result without blotting ($g \cdot m^{-2} h^{-1}$)
Wilson & Dallas (1990)	2 min reading straight after patch removal, six further 2 min readings, each separated by 2 min rest. Means over each 2 min taken as flux value. Difference between 1st and 6th flux reading = ESW (Excess skin wetness).	-	28.84	49.15

...continuation of Table 4.8

Dallas & Wilson (1992)	2 min flux, starting 2 min after patch removal; second 2 min flux after 2 min rest. Means over each 2 min taken as flux value. Differences between 2nd flux reading and background = ESW (Excess skin wetness).	Taken on adjacent skin during the 2 min rest.	8.02	6.57
Hatch et al. (1992 and 1993)	Max value during 30 s flux density, 2 min after patch removal, difference between the max value - background	Mean for last 30 s of 5 min logging	11.55	16.52
Berg et al. (1994)	Immediately after diaper removal and at 60 and 120s. Mean of flux density at all times minus background = skin wetness.	Mean for last 30 s of 5 min logging	19.21	33.04
Hatch et al. (1997)	Max value of 30 s flux density taken 2 min after patch removal, minus background = "change in EWL".	Taken on adjacent skin	12.69	17.19
Cameron et al. (1997)	Mean of 2 min flux density straight after patch removal, but discarded first 30 s of data, minus background.	Taken on adjacent skin	33.46	54.93
Grove et al. (1998)	Mean of 2 min logging period straight after patch removal minus background	Mean of last 15 s of 30 s logging period	32.26	52.64
Akin et al. (1997)	Mean of 2 min logging period straight after patch removal minus background	Mean of 2 min logging period	30.89	50.95
Shafer et al. (2002)	45 s flux density reading straight after patch removal. Maximum flux density between 15 and 45 s.	-	40.65	56.79

4.2.7 Selection of measurement monitoring time and characterising parameter

In order to develop a standard method for measuring the excess water from over-hydrated skin, the monitoring time of experiments needed to be decided such as to strike a balance between capturing as much information as possible without causing discomfort to the subjects.

Once a wet patch is removed from the skin, the excess water which was caused by the patch starts to evaporate immediately. The sensors of the evaporimetry device that are applied to the skin require a short period to react to the change in humidity inside the measurement chamber, as shown in Fig 4.14. Therefore the flux density during the reaction time of the sensors cannot be measured accurately. However, this reaction time is relatively short (<60s for open-chamber devices and ~60s for AquaFlux (it was not possible to estimate the reaction time for the VapoMeter spot measurements)) compared to the monitoring time of the desorption curve in this work (30 minutes). Hence the error is small.
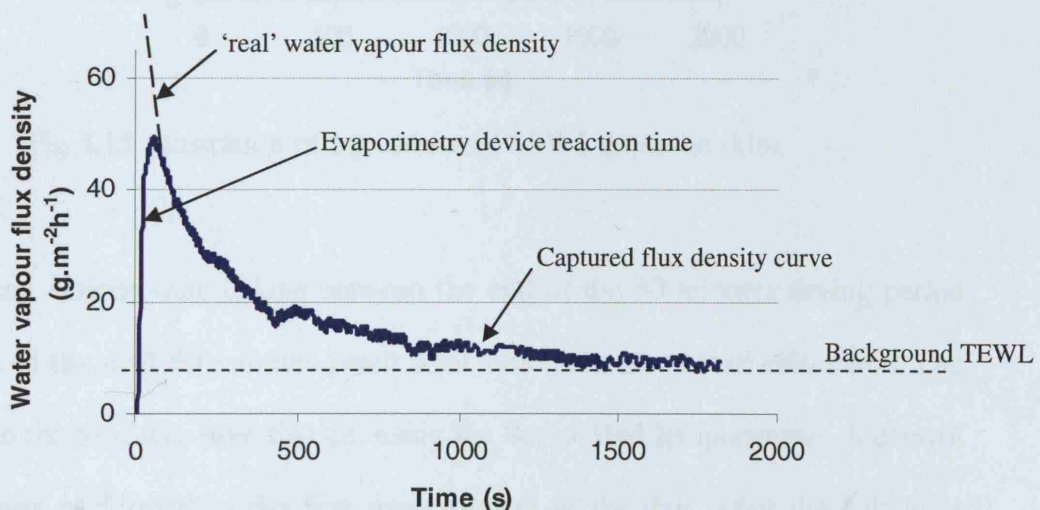
Fig 4.14 Illustration of the 'real' desorption curve.

The water vapour flux density was logged continuously for 30 minutes (Fig 4.14). This was not usually quite long enough for the readings to return to the background TEWL

value (see example plots on Fig 4.25 in Section 4.4.2). However, it was long enough to

log most of the curve and represented a reasonable compromise between capturing as

much of the desorption curve as possible, and limiting the length of the time for which

the subject needed to keep their arm still. Flux density in $g{\cdot}m^{-2}h^{-1}$ was plotted against

time in seconds (as illustrated on Fig 4.14).

The background TEWL value was then subtracted from the desorption curve and the

area under the resultant curve between 0 and 30 min calculated to give an estimate of

the SSWL from the skin ($g{\cdot}m^{-2}$) which the wet patch had caused (Fig 4.15).
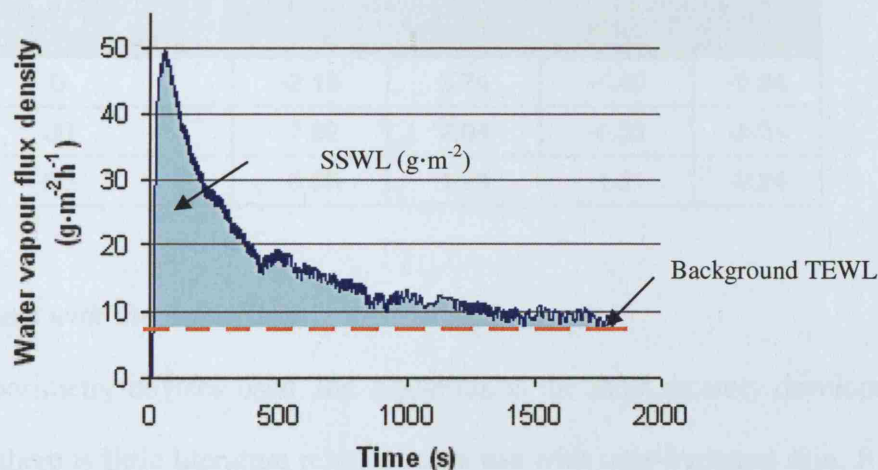
Fig 4.15 Illustration of the estimated SSWL from the skin.

By introducing various time delays between the end of the 30 minutes drying period

and the start of the next 60 minutes patch wear time, any carry-over effect from one

experiment to the next was investigated, using the Servo Med Evaporimeter. A control

experiment was performed as the first measurement of the day. After the half hour

measurement period, the skin was rested for a period (chosen at random from 0, 30 and

60 min) before the skin was rehydrated for an hour, and the desorption curve again

measured 30 minutes. Several hydration / drying cycles per day were achieved like this.

The areas under the desorption curves were compared with the control as shown on Table 4.9. It was established that there was no measurable carry-over from one experiment to the next, even with no time delay, i.e. the area under the desorption curve was not affected by the length of the time delay between the end of the previous desorption cycle and the application of the wet patch. Therefore, after a desorption curve was finished, the skin could be rehydrated immediately, ready for the next measurement.

Table 4.9 Results of time delay experiments with the Evaporimeter.

Time delay since previous measurement (min)	% difference in the area under the desorption curve from the control			
	Repeat #1	Repeat #2	Repeat #3	Mean
0	-2.15	3.74	-4.40	-0.94
30	-7.82	2.04	-6.33	-4.04
60	-6.05	1.24	-1.91	-2.24

4.2.8 Measurement with the AquaFlux

Of the five evaporimetry devices used, the AquaFlux is the most recently developed instrument, and there is little literature relating to its use with over-hydrated skin. It is also a device that uses a new measuring principle to measure evaporimetry, therefore particular attention was paid to the AquaFlux.

Preliminary experiments of measuring the flux density from over-hydrated skin was logged continuously for 30 minutes with AquaFlux, yielded curves with readings fell below background after around 20 minutes; Fig 4.16 shows an example curve, in which background TEWL measured on the normal skin before the hydration test, has been subtracted from the flux density.
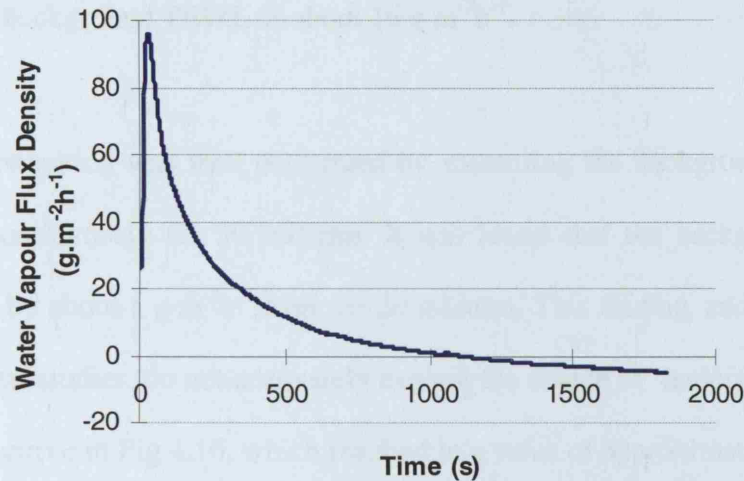
Fig 4.16 Example desorption curve measured by the AquaFlux which fell below background after ~20 minutes.

Since the condenser within the AquaFlux measurement chamber has a very low temperature, -13.4 °C, it creates a low humidity inside the chamber (~12% RH in equilibrium, measured by the sensor that is located at 7 mm from the skin surface within the chamber), a 'drying effect' of the skin from the low humidity was concerned. A study of the effect of skin exposure to a dry environment (10 %RH) was found in the literature (Egawa et al., 2002b), they measured the TEWL values on the normal forearms and cheeks of three volunteers 10 minutes after the subjects went in the room of 10 %RH, 3h later and 6h later. There was a drop of about 18% in TEWL values between the first two readings, but since they are point measurements (average of a 2 minutes measurement), it was not clear if the change was linear with respect to time.

Another study was performed by the manufacturer of AquaFlux (Ciortea et al., 2002), they left the measurement chamber on the normal volar forearm for about 3 hours, and a TEWL reading and OTTER reading were taken every 30 minutes. They found a linear drop in TEWL value with time, amounting to about 16% over 3 hours. According to this value, for a 30 minutes measurement, a drop of about 0.5 $g \cdot m^{-2} h^{-1}$ is

expected for a background TEWL of about 16 $g \cdot m^{-2}h^{-1}$.

A similar investigation was then performed by measuring the background TEWL on normal skin continuously for 30 minutes. It was found that the background TEWL value dropped by about 1 $g \cdot m^{-2}h^{-1}$ over the 30 minutes. This finding, and the results of the two previous studies, do not adequately explain the degree of 'undershoot' found in the desorption curve in Fig 4.16, which resulted in a value of approximately -5 $g \cdot m^{-2}h^{-1}$. However, the desorption curve was measured on over-hydrated skin whereas the two literatures above were performed on normal skin. Therefore, it is possible that over-hydrated skin suffers a bigger drop in background TEWL than normal skin when exposed to low RH.

Another hypothesis was that the 'undershoot' might be caused by the properties of the skin being changed by the over-hydration cycle. Two experiments were developed to test this hypothesis. First, the impact of the duration of skin exposure to the wet patch was investigated. The patch wear time experiment described in Section 3.3.3 was repeated with the AquaFlux, it was found that the undershoot was similar for all patch wear times in the range of 5 – 60 minutes (Fig 4.17).

Second, an experiment was carried out with no AquaFlux in place; that is, after the wet patch was removed from the skin and surface water was blotted with filter paper, the forearm was left to dry under the environment conditions for 30 minutes, and then background TEWL was measured at the test site with AquaFlux. The value found was similar to the background TEWL measured before the experiment, which indicated that the undershoot effect only happened when the AquaFlux was in place during the drying period. Following these investigations, efforts were made to capture desorption curves

by monitoring flux density with AquaFlux for short periods, separated by rest periods

in which the AquaFlux was removed from the skin.
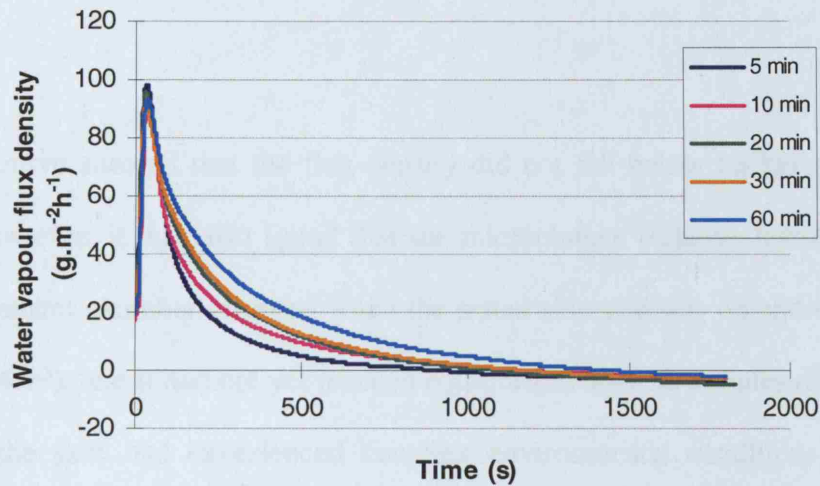
Fig 4.17 Desorption curves measured by the AquaFlux with different patch wear times.
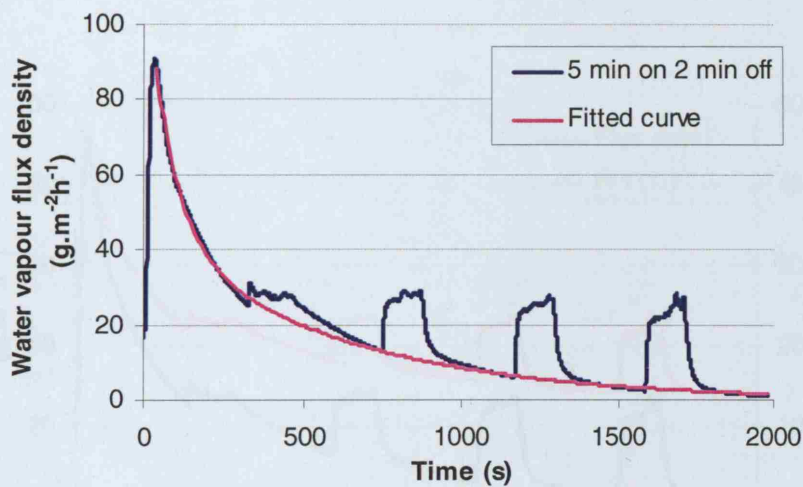
Fig 4.18 Intermittent experiments with the AquaFlux alternatively on skin for 5 min
then off for 2 min. An exponential decay curve was fitted to the data set to calculate the
area under the estimated, simple desorption curve.

Flux density was logged for periods of five minutes separated by rest periods of two

minutes (for a total of at least 30 minutes duration), during which the probe was held

clear of the skin before being returned to the same measurement site to provide data

sets like the one shown in Fig 4.18. A complete desorption curve was then estimated

from such data sets by fitting an exponential decay curve (Fig 4.18) to the data, the background TEWL subtracted, and the area under the resultant curve between 0 and 30 min calculated as before to give an estimate of the SSWL ($g \cdot m^{-2}$), which the wet patch had caused.

The fitted curve showed that the flux density did not fall below background for this method. However, it was also found that the microclimate (relative humidity) within the measurement chamber changed when the tested skin site was on and off from the probe (Fig 4.19), and it had not yet reached equilibrium after 30 minutes of experiment. Therefore the skin had experienced complex environmental conditions during the intermittent experiment, and the findings were thought to be unreliable, and difficult to interpret.
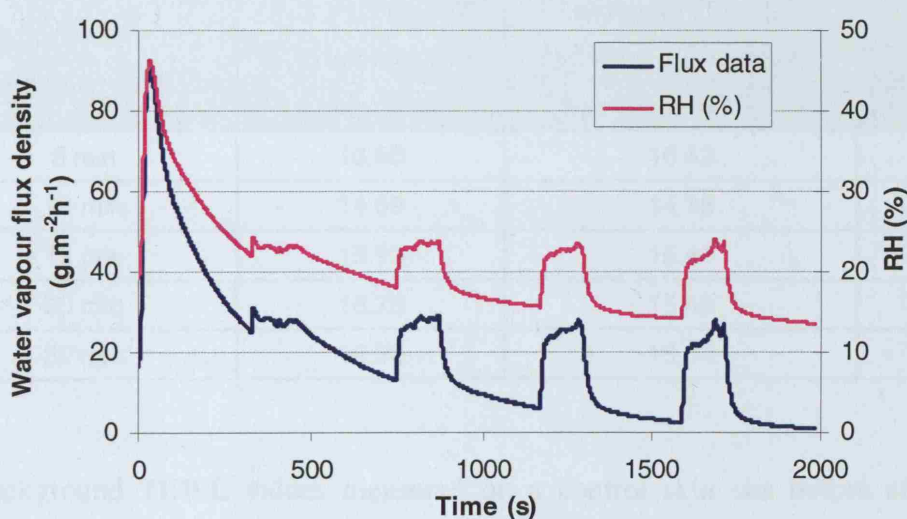
Fig 4.19 Intermittent desorption curve measured and the relative humidity (RH) recorded within the AquaFlux measurement chamber during the experiment.

Since the undershoot effect only appeared when the AquaFlux was in place for measurement, another approach was developed to investigate how long the AquaFlux had to be in contact with the skin before it triggered the undershoot effect. Apart from

the usual measurement skin site, an adjacent skin site was used as a control. The background TEWL was measured on both skin sites at the beginning, then the measurement site was hydrated with the wet patch for one hour while the control skin site was left open to the environment. When the patch was removed and surface water blotted, the flux density was measured by AquaFlux on the hydrated skin for different durations in a series of five experiments (5, 10, 15, 20, 30 min). Once the measurement was finished, the AquaFlux was placed on the adjacent control skin site immediately to measure the background TEWL again. This value was then compared with the background TEWL of the same skin site measured at the beginning, i.e. before the AquaFlux was applied to the over-hydrated skin.

Table 4.10 Background TEWL measured on a control skin site before and after hydration measurements of different durations at an adjacent site, using AquaFlux.

Hydration measurement duration	Background TEWL in beginning $(g \cdot m^{-2} h^{-1})$	Background TEWL after hydration measurement $(g \cdot m^{-2} h^{-1})$	% decreased
5 min	16.50	16.42	0.5
10 min	14.69	14.18	3.5
15 min	15.93	15.41	3.3
20 min	16.78	15.49	7.7
30 min	16.26	15.34	5.7

The background TEWL values measured on a control skin site before and after a hydration measurement of different duration are shown in Table 4.10. The background TEWL values on the control skin site decreased by at least 3.3% for all hydration measurements, except for the 5 min hydration measurement, which only decreased by ~0.5%. The scatter of the background TEWL values measured in normal circumstances by the AquaFlux is reported in Section 4.4.1, where the C.V. is less than 3.2% for five repeats. The findings in Table 4.10 indicate that after the AquaFlux had been applied to

a very wet site (over-hydrated skin) for more than 5 minutes, the instrument tended to produce a lower TEWL value.

At this point, all the AquaFlux findings to date were presented to its manufacturer for discussion. It was concluded that there may be a problem with the start-up procedure of the device. Since the measuring principle of the AquaFlux depends on the microclimate within the measurement chamber created by the layer of ice on the condenser (see Section 2.4.3.3), it is important to convert any super-cooled water to ice within the chamber, before the baseline calibration is performed to set the zero flux value. If the zero flux value was set before the flux stabilised or when there was super-cooled water in the measurement chamber, all findings would be shifted or inaccurate (private communication with R.E. Imhof). A revised start-up procedure was then provided by the manufacturer (see Appendix C5 for detailed start up procedure for the AquaFlux.).

The primary change in the procedure was that: a longer time was needed before and after priming the condenser for the super-cooled water to convert into ice (see Appendix C5). This start-up procedure was then used to measure a desorption curve from over-hydrated skin and an example curve with background TEWL subtracted is shown on Fig 4.20. The curve still fell below zero with the improved start-up procedure, although it was evident after approximately 25 minutes, compared to the earlier finding of 20 minutes (Fig 4.16).

In summary, it was found that:

● The 30 minutes desorption curve measured by the AquaFlux fell below zero when the background TEWL was subtracted

- The 'drying effect' caused by the low humidity inside the measurement chamber was small (the background TEWL value dropped by ~1 $g \cdot m^{-2} h^{-1}$ over 30 minutes)

- Reducing the patch wear time (i.e. different durations for skin exposure to the saline) had little impact on the effect

- With no AquaFlux in place, the flux density measured after the patch had been removed and the skin exposed to the ambient environment for 30 minutes, was similar to the background TEWL measured before the experiment

- Capturing the desorption curve using intermittent measurements was not appropriate for the AquaFlux

- The device measured a lower background TEWL value on an adjacent control skin site immediately after desorption measurements of different durations

- The 30 minutes desorption curve measured by AquaFlux still fell below zero (although taking longer to do so) when the start-up procedure of the instrument had been improved.
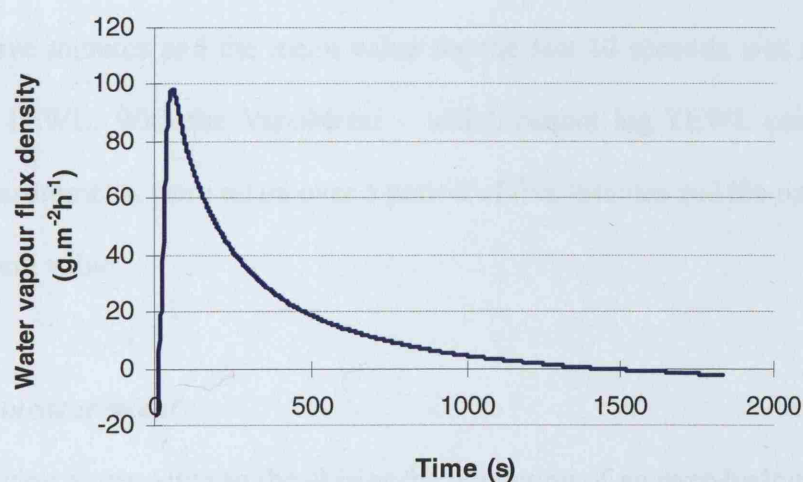
Fig 4.20 Example desorption curve measured by the AquaFlux
with improved start-up procedure.

Work continues to resolve this problem, but the procedure developed had reduced the

'undershoot' effect sufficiently to provide adequately accurate data for the planned comparative study.

4.3 Final methodology

All measurements were made in a controlled environment room at 23 ± 2 °C and 50 ± 5 %RH. All experiments were conducted on one subject (Subject I, Table 3.1) all experiments were performed on her left volar forearm at a point 100 mm from her elbow crease (Fig 3.3). On arrival, the subject acclimatized in the measurement room for at least 30 minutes with her volar forearm skin sites exposed.

Two sets of experiments were conducted for all of the devices: background TEWL on normal skin and the SSWL from over-hydrated skin. Details are as follows.

4.3.1 Background TEWL measurement

For all of the devices except the VapoMeter, background TEWL from normal skin was logged for five minutes and the mean value for the last 30 seconds was taken as the background TEWL. With the VapoMeter – which cannot log TEWL continuously – five spot measurements were taken over a period of five minutes and the mean taken as the background value.

4.3.2 SSWL measurement

Prior to applying a wet patch to the skin at the beginning of an over-hydration / drying cycle, background TEWL for the normal skin was measured as described above. The subject's skin was then hydrated for 60 minutes with the wet patch using the method described in Section 3.3.5, the evaporimetry probe applied to the skin site immediately after the wet patch had been removed and the surface water had been blotted. For the

three open-chamber devices and the AquaFlux, the flux density was logged continuously for 30 minutes. The background TEWL value was then subtracted from the desorption curve and the area under the resultant curve was calculated to give an estimate of the SSWL $(g \cdot m^{-2})$ which the wet patch had caused.

Another procedure was needed for the VapoMeter as it could not be used to log the flux density continuously. Instead, spot measurements were taken as frequently as flushing the chamber between measurements would allow (typically ~1 minute between readings, depending on the humidity inside the chamber). Background TEWL was subtracted from these readings and the area under the resulting desorption curve between 0 and 30 minutes was calculated.

For each of the background TEWL and SSWL measurements, two types of experiments were performed. In the first, each device was used to measure the background TEWL / SSWL five times at the same skin site on the same day, i.e. one device (five repeats) per day, to study the repeatability of measurements from each of the devices under conditions as nearly constant (same skin site, same day) as practicable. In the second experiments, the five devices were each used once in a random order on each of five days to study the reproducibility of each device on the same skin site from day to day. This second approach is important as studies to determine the impact of a treatment compared with a control often involve measurements on different days on the assumption that skin properties do not change much from day to day. These two types of measurements are referred to as *same day* and *different days*.

From the methodology development (Section 4.2.7), it was found that there was no

measurable carry over from one hydration experiment to the next with no time delay. Accordingly, for the SSWL measurements, the skin site was rehydrated again as soon as the desorption curve from the previous experiment was completed.

It should be noted that during the *different days* measurements, the undershoot effect on AquaFlux was under investigation, so this device was not included in the experiments with the other four devices. The *different days* measurements were made in another occasion for the AquaFlux.

4.4 Results

4.4.1 Background TEWL measurement

Graphs for the background TEWL experiments measured using each of the five evaporimetry devices on *same day* are shown in Fig 4.21, and the results measured on *different days* are shown in Fig D1 in Appendix D. One example graph of background TEWL measurements from each of the five devices is plotted in Fig 4.22 for comparison.

DermaLab

Tewameter

VapoMeter
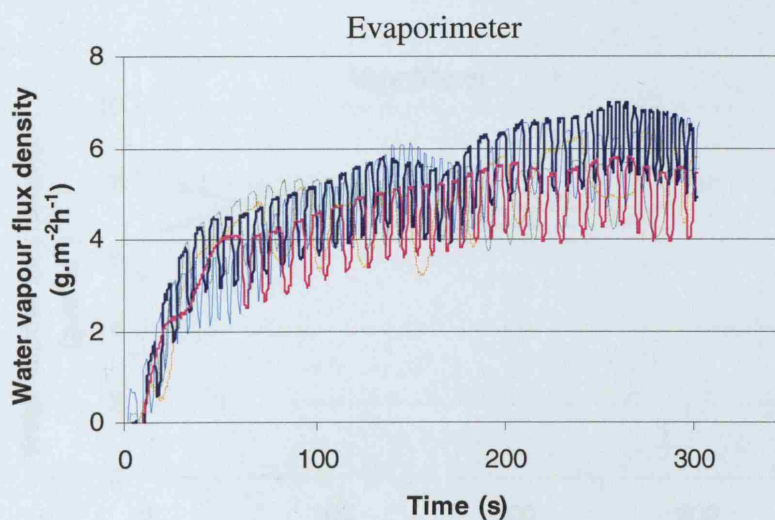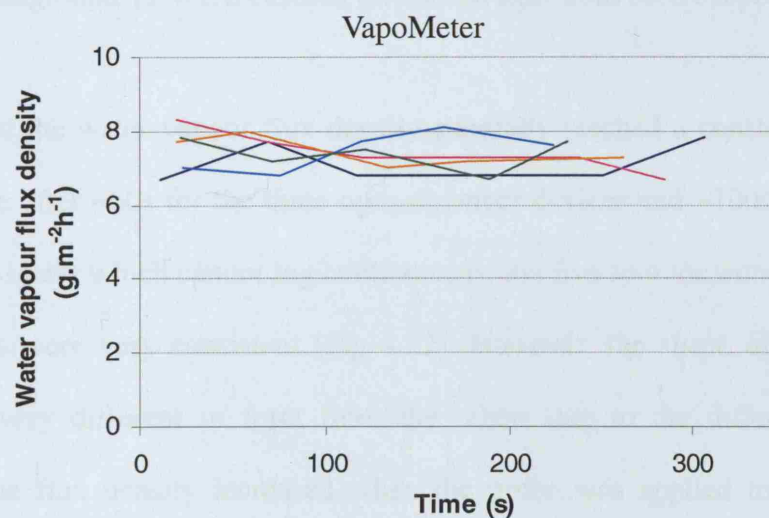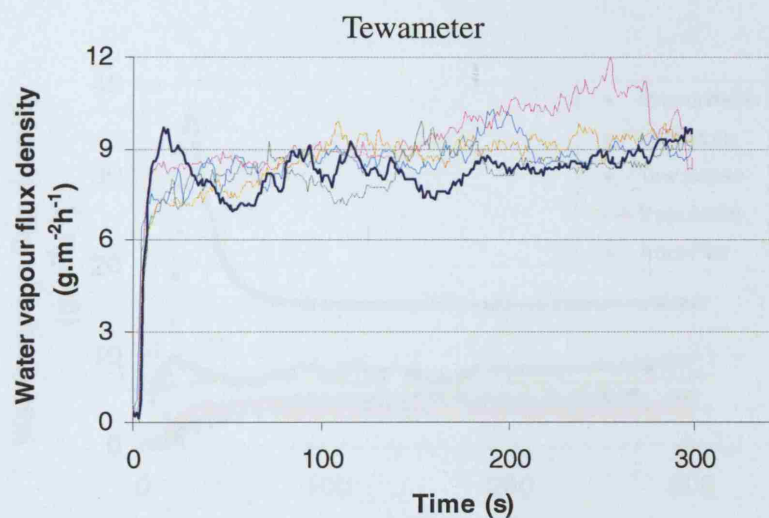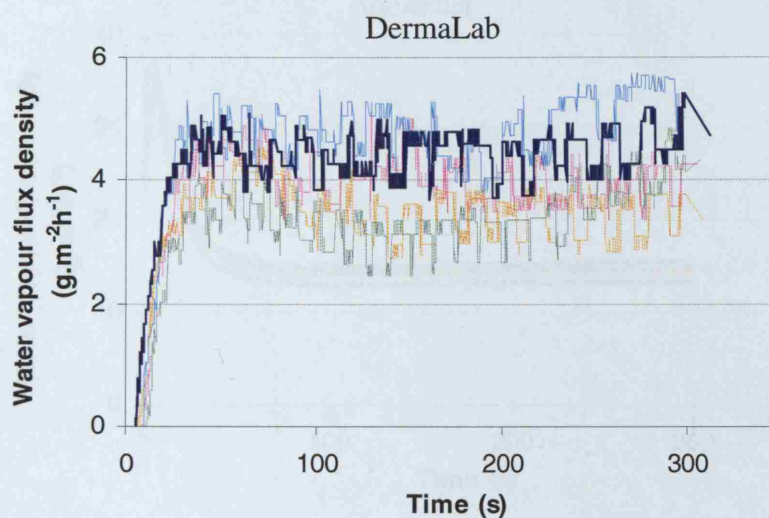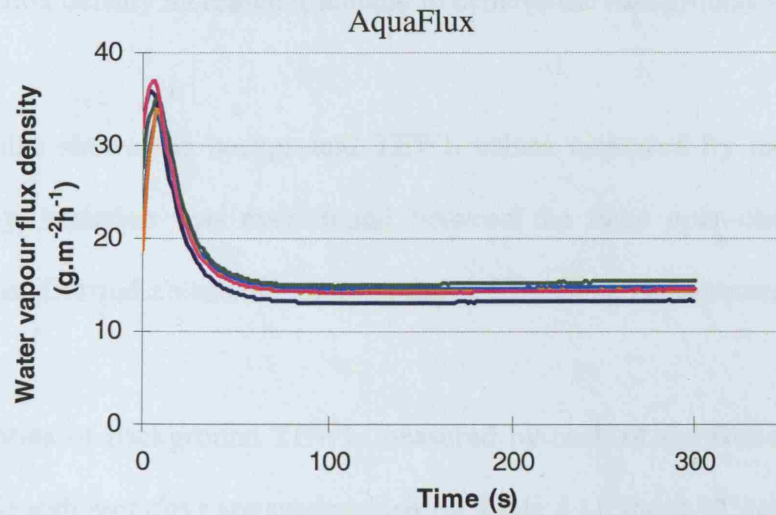
Fig 4.21 Results of background TEWL measured on the *same day* on Subject I.
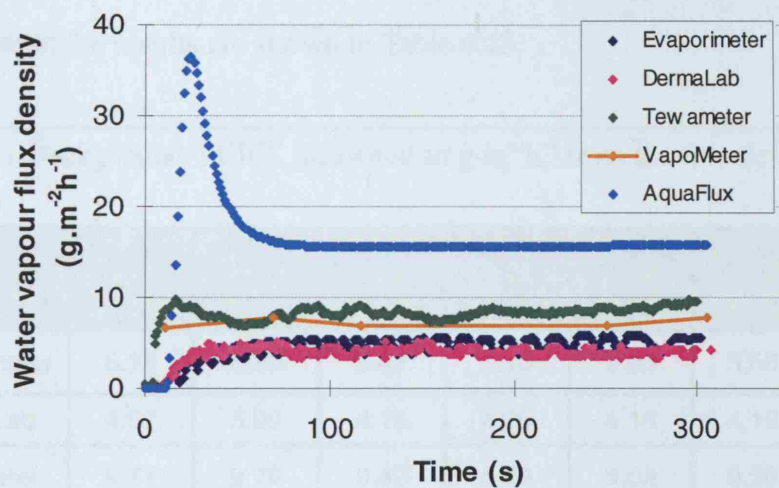
Fig 4.22 Background TEWL measured on normal skin from each evaporimetry device.

It shows that the water vapour flux density generally reached a constant background TEWL value after ~60s for the three open-chamber devices and ~100s for AquaFlux; for the VapoMeter which cannot log continuously, the five spot measurements over the five minutes were very consistent (Fig 4.22). However, the shape of the AquaFlux curve was very different in form from the others due to the different measuring principle: the flux density increased when the probe was applied to the skin then decreased to achieve the background TEWL; whereas with the three open-chamber

devices, the flux density increased gradually to achieve the background TEWL value.

The graph also shows the background TEWL values measured by the five devices differ greatly, variation was even found between the three open-chamber devices (Evaporimeter, DermaLab and Tewameter) that use the same measurement principle.

The five repeats of background TEWL measured by each of the five devices on the *same day* and *different days* are summarised on Table 4.11 and 4.12, respectively, and Fig 4.23 summarises all the data on a graph. Paired sample T-tests were performed on the data measured from the five evaporimetry devices on *same day*, *different days* and all data together; the results are shown in Table 4.13.

Table 4.11 Background TEWL measured in $g \cdot m^{-2} h^{-1}$ from the five devices on the *same day*.

Device	Repeat #1	Repeat #2	Repeat #3	Repeat #4	Repeat #5	Mean	C.V. (%)
Evaporimeter	6.18	4.99	5.47	5.10	6.06	5.56	9.8
DermaLab	4.57	3.95	4.16	4.05	4.16	4.18	5.6
Tewameter	9.17	9.79	9.42	8.89	9.02	9.26	3.9
VapoMeter	7.23	7.56	7.13	7.26	7.34	7.30	2.2
AquaFlux	16.63	16.62	16.89	16.26	15.54	16.39	3.2

Table 4.12 Background TEWL measured in $g \cdot m^{-2} h^{-1}$ from the five devices on *different days*.

Device	Repeat #1	Repeat #2	Repeat #3	Repeat #4	Repeat #5	Mean	C.V. (%)
Evaporimeter	5.54	5.58	6.30	5.35	6.32	5.82	7.9
DermaLab	5.18	4.94	4.62	4.90	5.84	5.10	9.0
Tewameter	9.77	10.95	10.01	9.01	9.73	9.90	7.1
VapoMeter	6.82	7.98	7.70	7.44	7.74	7.54	5.9
AquaFlux	16.92	16.62	15.97	16.65	15.93	16.42	2.7

The results show that the agreement between *same day* and *different days* data was very good for all devices. The coefficients of variation were low, between 2.2 and 9.8% for all five devices with the two closed chamber instruments (VapoMeter and AquaFlux) having the lowest C.V., between 2.2 and 5.9%. The mean background TEWL varied within the range of $4.2 - 16.4$ $g \cdot m^{-2} h^{-1}$, in which the AquaFlux produced significantly higher values than the others (Fig 4.23 and Table 4.13), and within the three open-chamber devices, the Evaporimeter and DermaLab gave similar ranges of background TEWL values, while the Tewameter produced systematically higher values. Table 4.13 of paired sample t-test shows differences between all pairs of devices were significant ($p < 0.05$) for *same day* and *different days* and all data together.
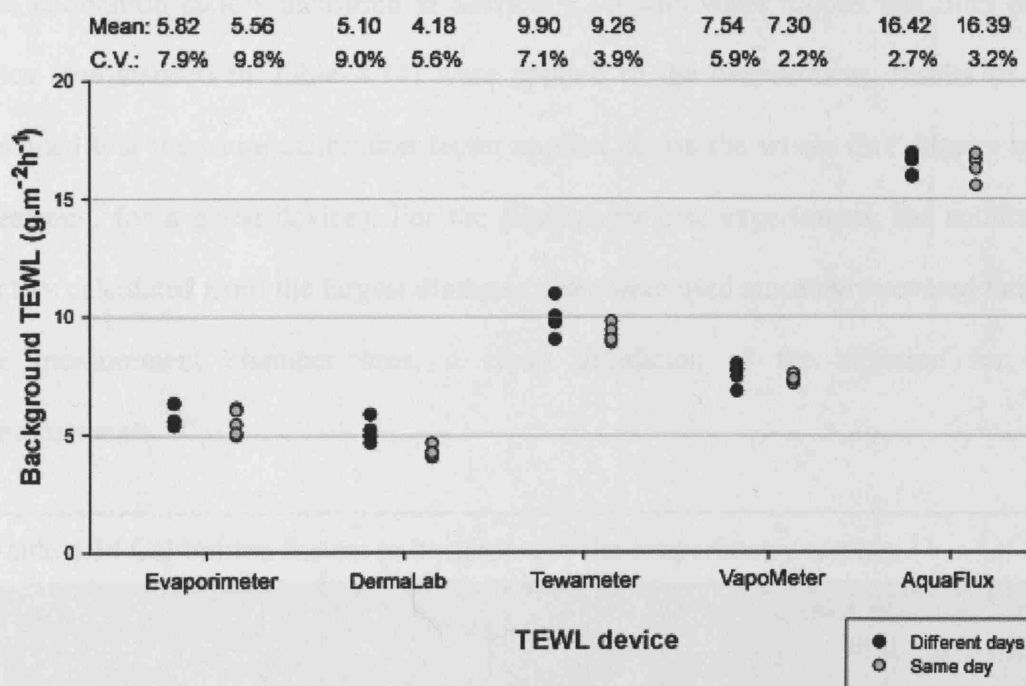
Fig 4.23 Background TEWL estimated for all five devices for measurements on the *same day* and *different days*.

Table 4.13 Paired sample t-test on *same day*, *different days* and all
data for background TEWL measurements.

Comparison			p values		
			Same day	Different days	All
Evaporimeter	vs	DermaLab	p<0.001	p<0.05	p<0.001
Evaporimeter	vs	Tewameter	p<0.001	p<0.001	p<0.001
Evaporimeter	vs	VapoMeter	p<0.01	p<0.001	p<0.001
Evaporimeter	vs	AquaFlux	p<0.001	p<0.001	p<0.001
DermaLab	vs	Tewameter	p<0.001	p<0.001	p<0.001
DermaLab	vs	VapoMeter	p<0.001	p<0.001	p<0.001
DermaLab	vs	AquaFlux	p<0.001	p<0.001	p<0.001
Tewameter	vs	VapoMeter	p<0.001	p<0.001	p<0.001
Tewameter	vs	AquaFlux	p<0.001	p<0.001	p<0.001
VapoMeter	vs	AquaFlux	p<0.001	p<0.001	p<0.001

The calibration factors measured in Section 4.2.5 with water droplet and filter paper
discs (summarised in Table 4.14) were applied to the evaporimetry results (it was
assumed that the same calibration factor applied across the whole flux density range
measured, for a given device). For the filter paper disc experiments, the calibration
factors calculated from the largest diameter discs were used since they covered most of
the measurement chamber area, a close simulation of the situation for skin
measurements.

Table 4.14 Calibration factors to be applied to the evaporimetry results.

Evaporimetry device	Calculated calibration factor from droplet experiments				Calculated calibration factor from experiments with the largest diameter filter paper discs			
	Repeat #1	Repeat #2	Repeat #3	Mean	Repeat #1	Repeat #2	Repeat #3	Mean
Evaporimeter	1.96	2.09	2.29	2.11	2.61	2.31	2.67	2.53
DermaLab	1.41	1.27	1.51	1.40	1.89	1.99	1.61	1.83
Tewameter	1.32	1.37	1.38	1.36	-	-	-	-
AquaFlux	0.99	1.06	0.98	1.01	1.13	0.95	1.07	1.05

These calibration factors were applied to the *same day* and *different days* data of background TEWL measurements, and the results are given in Table 4.15 and 4.16, and Fig 4.24 which show the background TEWL data from the four evaporimetry devices measured on *same day* and *different days*, with and without calibration factors applied. The data points represent the mean $\pm$ 1 standard deviation for the three correction factors.

By applying the calibration factors to the background TEWL data, the range of results between the devices reduced slightly, but the agreement between the background TEWL values measured by the four devices was still very poor.

Table 4.15 Background TEWL measured in $g{\cdot}m^{-2}h^{-1}$ on the *same day* with and without calibration factors applied.

Evaporimetry device	No correction		Droplet calibration correction		Filter paper calibration correction	
	Mean	sd	Mean	sd	Mean	sd
Evaporimeter	5.56	0.54	11.76	1.32	14.08	1.56
DermaLab	4.18	0.24	5.84	0.52	7.65	0.80
Tewameter	9.26	0.36	12.55	0.50	-	-
AquaFlux	16.39	0.53	16.54	0.79	17.18	1.37

Table 4.16 Background TEWL measured in $g{\cdot}m^{-2}h^{-1}$ on *different days* with and without calibration factors applied.

Evaporimetry device	No correction		Droplet calibration correction		Filter paper calibration correction	
	Mean	sd	Mean	sd	Mean	sd
Evaporimeter	5.82	0.46	12.30	1.21	14.73	1.43
DermaLab	5.10	0.46	7.13	0.79	9.33	1.15
Tewameter	9.90	0.70	13.41	0.91	-	-
AquaFlux	16.42	0.45	16.57	0.75	17.21	1.34
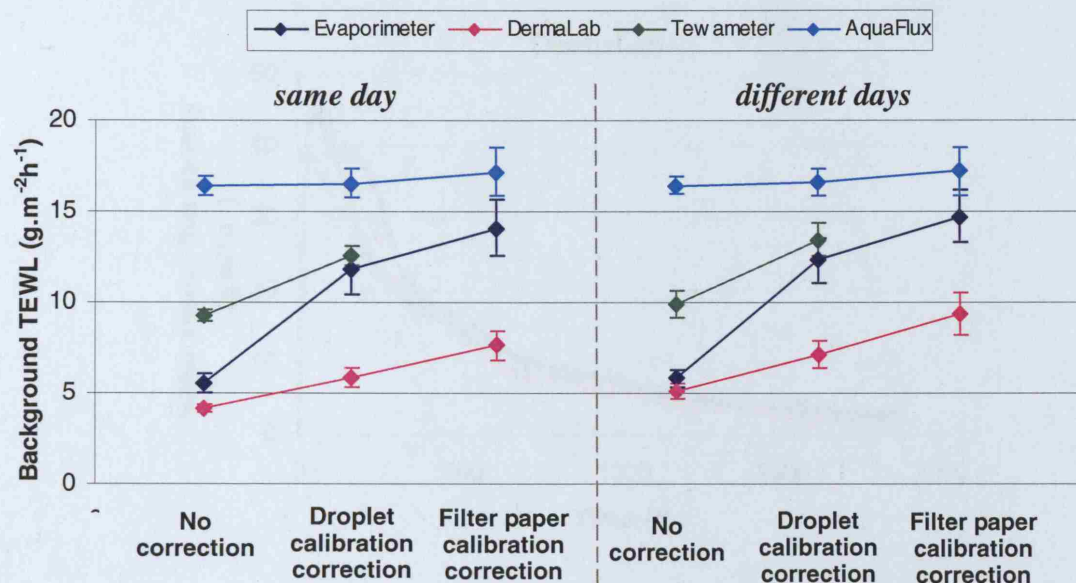
Fig 4.24 Background TEWL measurements on the *same day* (left) and *different days* (right) with no correction and corrected using calibration factors calculated from droplet and from filter paper experiments (Filter paper calibration not available for Tewameter).

4.4.2 SSWL measurement

All desorption curves (with the background subtracted) from the five evaporimetry devices measured on *same day* are shown in Fig 4.25, and an example of each is plotted on Fig 4.26 for comparison.

DermaLab

Tewameter

VapoMeter
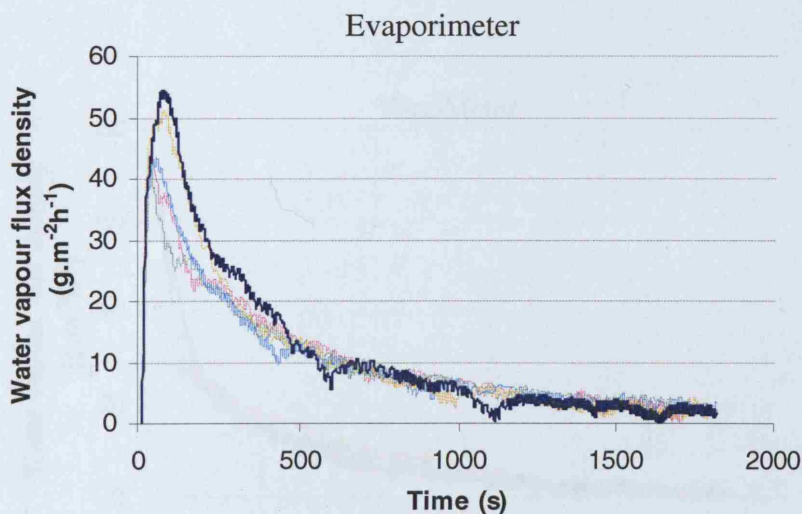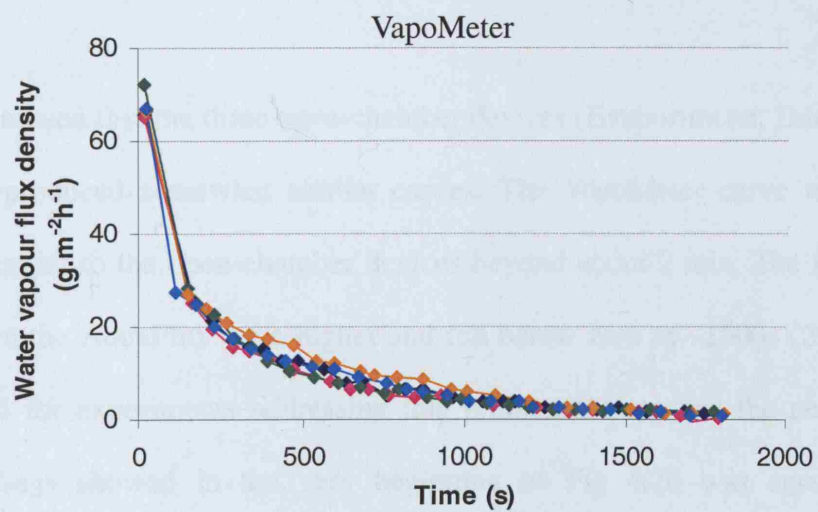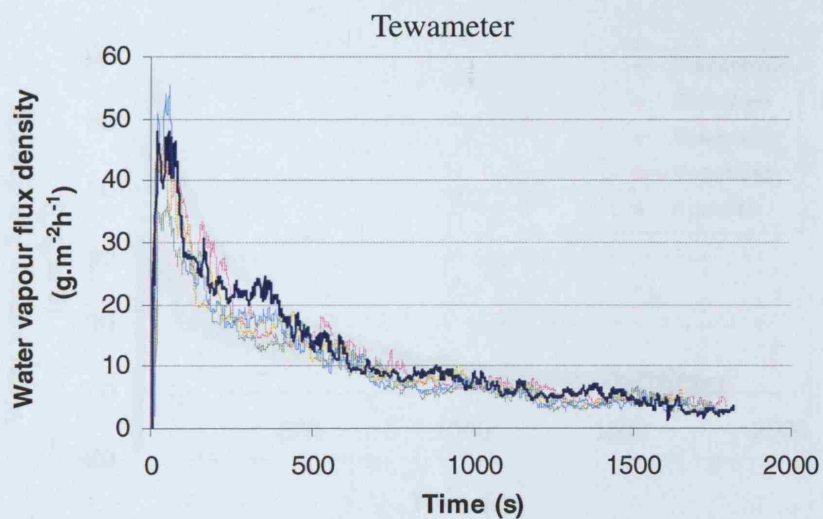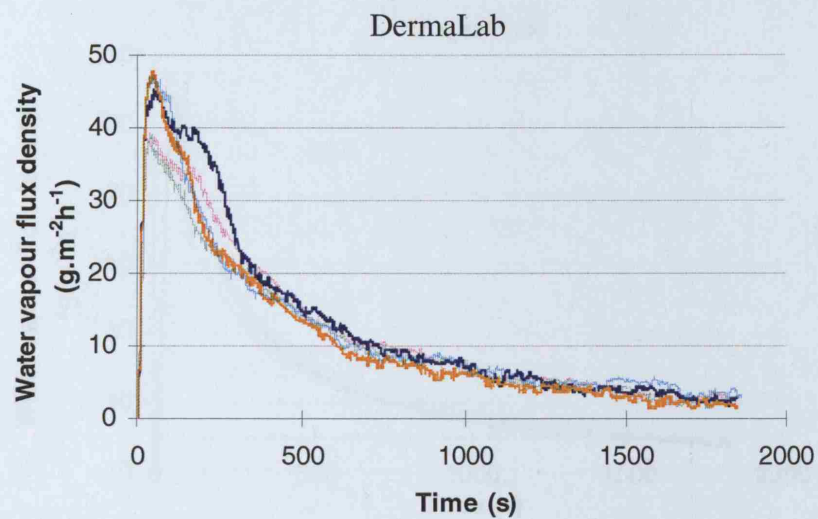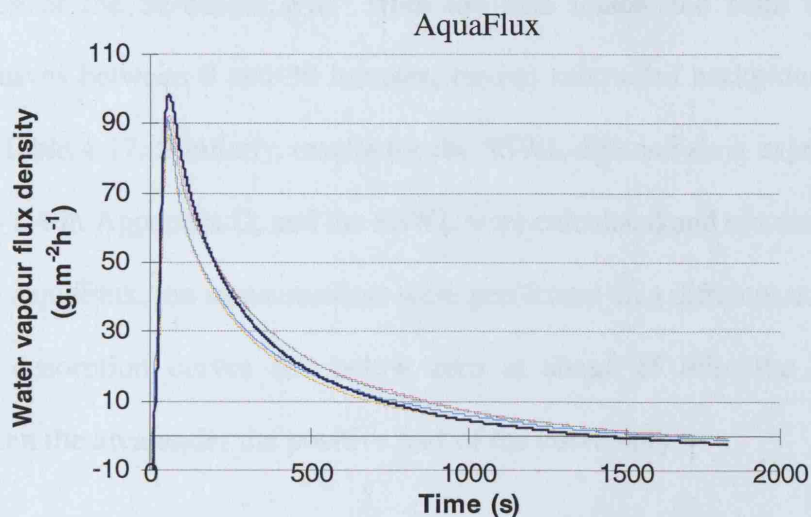
Fig 4.25 Results of SSWL measured on the *same day* on Subject I.
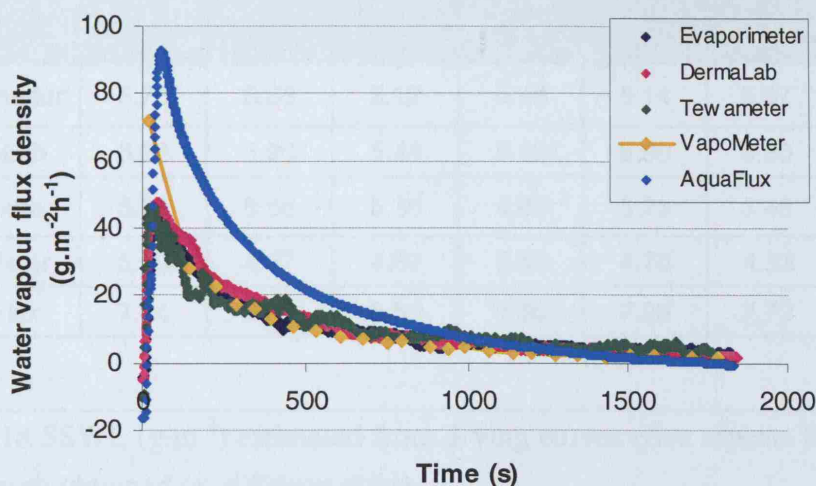
Fig 4.26 An example desorption curve of over-hydrated skin from each
evaporimetry device.

The results showed that the three open-chamber devices (Evaporimeter, DermaLab and Tewameter) produced somewhat similar curves. The VapoMeter curve was initially higher but similar to the open-chamber devices beyond about 2 min. The flux density readings from the AquaFlux were higher and fell below zero at ~1500s (25 min) (see Section 4.2.8 for experiments addressing this problem). Note that the negative flux density readings showed in the very beginning of Fig 4.26 was caused by the subtraction of the background TEWL from the flux density reading.

The estimates of the SSWL in $g \cdot m^{-2}$ from the skin (calculated form areas under desorption curves between 0 and 30 minutes, having subtracted background TEWL), are given in Table 4.17. Similarly, results for the SSWL *different days* experiments are shown in Fig D4 in Appendix D, and the SSWL were calculated and tabulated on Table 4.18. For the AquaFlux, the measurements were performed on a different occasion, and because the desorption curves fell below zero at about 25 min, the SSWL was calculated from the area under the positive part of the curve only.

Table 4.17 SSWL ($g \cdot m^{-2}$) estimated from drying curves (five repeats for a given device, each obtained on the *same day*).

Device	Repeat #1	Repeat #2	Repeat #3	Repeat #4	Repeat #5	Mean	C.V. (%)
Evaporimeter	5.78	5.33	5.12	5.48	5.14	5.37	5.1
DermaLab	6.33	5.90	5.44	5.42	5.90	5.80	6.5
Tewameter	5.91	5.88	5.36	4.86	5.25	5.45	8.2
VapoMeter	5.00	4.57	4.85	5.52	4.70	4.93	7.5
AquaFlux	7.74	8.63	8.50	6.50	7.23	7.72	11.5

Table 4.18 SSWL ($g \cdot m^{-2}$) estimated from drying curves (five repeats for a given device, each obtained on *different days*).

Device	Repeat #1	Repeat #2	Repeat #3	Repeat #4	Repeat #5	Mean	C.V. (%)
Evaporimeter	5.15	4.65	4.23	4.57	4.03	4.52	9.5
DermaLab	6.64	7.60	5.60	5.31	5.09	6.05	17.4
Tewameter	6.05	6.13	5.74	5.70	5.42	5.81	5.0
VapoMeter	6.18	5.89	4.57	4.87	4.99	5.30	13.1
AquaFlux	7.93	7.61	8.93	8.62	8.16	8.25	6.4

Fig 4.27 summarises the SSWL calculated from the area under the desorption curves from the five devices for both *same day* and *different days* data. It shows little differences between the two sets of data for all the devices except the Evaporimeter,

for which the *same day* data were slightly higher than *different day* data. The mean of the SSWL ($g \cdot m^{-2}$) from four of the devices was similar, within the range of 4.52 – 6.05 $g \cdot m^{-2}$, but the AquaFlux produced higher values (range of 7.72 – 8.25 $g \cdot m^{-2}$). The coefficients of variation were generally good (<10%) except for DermaLab *different days* (17.4%), VapoMeter *different days* (13.1%) and AquaFlux *same day* data (11.5%).
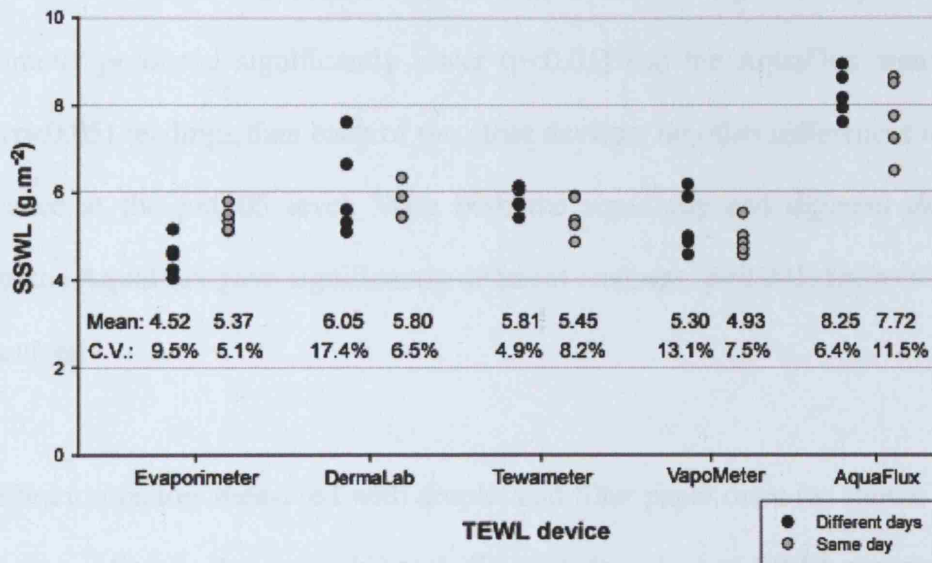
Fig 4.27 SSWL estimated from all five devices for measurements on the *same day* and *different days*.

Table 4.19 Paired sample t-test on *same day*, *different days* and all data for SSWL measurements (highlighted cells are not statistically significant i.e $p > 0.05$).

Comparison			p values		
			Same day	Different days	All
Evaporimeter	vs	DermaLab	p<0.05	p<0.05	p<0.001
Evaporimeter	vs	Tewameter	p>0.05	p<0.001	p<0.05
Evaporimeter	vs	VapoMeter	p<0.05	p<0.05	p>0.05
Evaporimeter	vs	AquaFlux	p<0.05	p<0.001	p<0.001
DermaLab	vs	Tewameter	p>0.05	p>0.05	p>0.05
DermaLab	vs	VapoMeter	p<0.05	p>0.05	p<0.001
DermaLab	vs	AquaFlux	p<0.001	p<0.05	p<0.001
Tewameter	vs	VapoMeter	p>0.05	p>0.05	p<0.05
Tewameter	vs	AquaFlux	p<0.001	p<0.001	p<0.001
VapoMeter	vs	AquaFlux	p<0.001	p<0.001	p<0.001

Paired sample T-tests were performed on the data measured from the five evaporimetry devices on *same day*, *different days* and both sets of data, the results are shown on Table 4.19. For measurements taken on the *same day*, differences between the Tewameter and the Evaporimeter, the DermaLab and the VapoMeter were not significant (p>0.05) while the AquaFlux produced readings significantly greater (p<0.01) than readings with each of the other devices. With *different days* results, the Evaporimeter produced significantly lower (p<0.01) and the AquaFlux significantly higher (p<0.05) readings than each of the other devices; no other differences achieved significance at the p<0.05 level. With both the *same day* and *different days* data together, the AquaFlux gave significantly different readings (p<0.001) from each of the other devices.

The calibration factors measured with droplet and filter paper discs (as shown in Table 4.14) were applied to the *same day* and *different days* data of SSWL measurements. The results are shown in Table 4.20, 4.21 and summarised on Fig 4.28. It shows the SSWL results from the four evaporimetry devices with and without calibration factors applied. The data points represent the mean , and the error bars are $\pm$ 1 standard deviation for the correction factors.

Table 4.20 SSWL ($g \cdot m^{-2}$) measured on the *same day* with and without calibration factors applied.

Evaporimetry device	No correction		Droplet calibration correction		Filter paper calibration correction	
	Mean	sd	Mean	sd	Mean	sd
Evaporimeter	5.37	0.27	11.36	0.92	13.60	1.08
DermaLab	5.80	0.38	8.11	0.77	10.61	1.16
Tewameter	5.45	0.44	7.39	0.57	-	-
AquaFlux	7.72	0.89	7.79	0.88	8.09	1.05

Table 4.21 SSWL (g·m^{-2}) measured on *different days* with and without calibration factors applied.

Evaporimetry device	No correction		Droplet calibration correction		Filter paper calibration correction	
	Mean	sd	Mean	sd	Mean	sd
Evaporimeter	4.52	0.43	9.56	1.05	11.45	1.25
DermaLab	6.05	1.05	8.46	1.50	11.07	2.05
Tewameter	5.81	0.29	7.87	0.39	-	-
AquaFlux	8.25	0.53	8.33	0.59	8.65	0.82

The range of the *same day* data is increased when the calibration factors are applied (Fig 4.28), while the range is reduced slightly for the *different days* data. However, the agreement between the SSWL values measured by the four devices is still poor. It is interesting to note that after applying the calibration factors, the SSWL results from the AquaFlux were no longer the highest but the lowest of the four devices used, while the Evaporimeter results had become the highest.
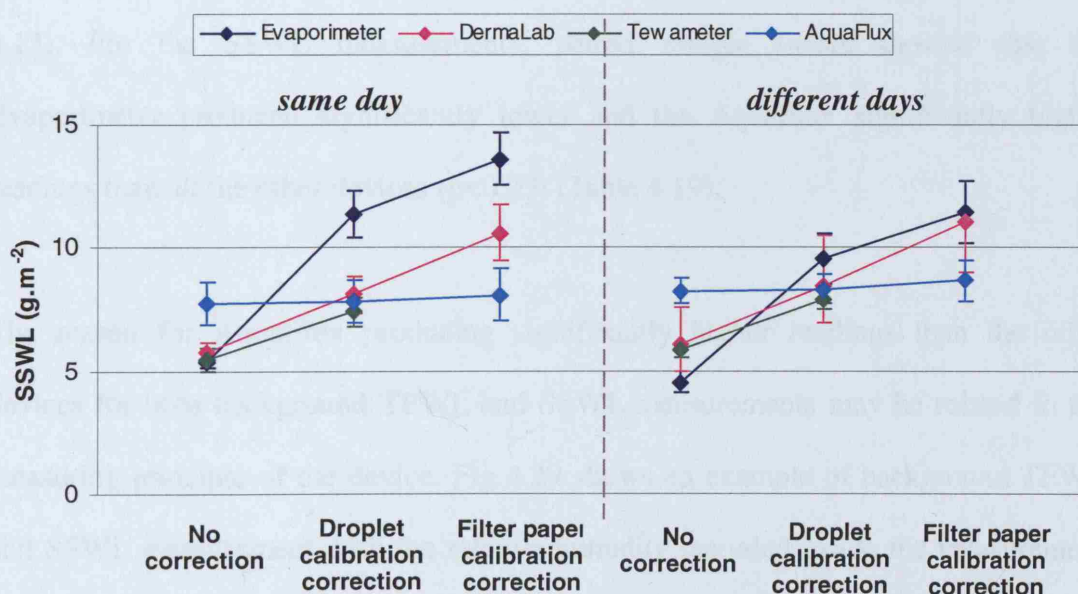
Fig 4.28 SSWL measurements on the *same day* (left) and *different days* (right): with no correction and corrected using calibration factors calculated from droplet and from filter paper experiments. (Filter paper calibration not available for Tewameter).

4.5 Discussion

Methods have been developed for measuring background TEWL on normal skin and the SSWL in over-hydrated skin using the five evaporimetry devices. The repeatability of all five devices was good for both background TEWL and SSWL measurements on the *same day*, with only a slight increase in the coefficient of variation for five repeats on *different days* data, due to variation in the subject's skin between days (Fig 4.23 and 4.26).

For the background TEWL measurements shown on Fig 4.23, Evaporimeter and DermaLab gave similar results while the Tewameter, another open-chamber device, gave slightly higher values. The VapoMeter data were between those for the Tewameter and the other two open-chamber devices, while the AquaFlux produced significantly higher background TEWL values than all the others. Paired sample t-tests showed the differences between all pairs of devices were significant ($p<0.05$) (Table 4.13). For the SSWL measurements, paired sample t-tests showed that the Evaporimeter produced significantly lower and the AquaFlux significantly higher readings than all the other devices ($p<0.05$) (Table 4.19).

The reason for AquaFlux producing significantly higher readings than the other devices for both background TEWL and SSWL measurements may be related to the measuring principle of the device. Fig 4.29 shows an example of background TEWL and SSWL measurement with the relative humidity recorded inside the measurement chamber. The presence of the condenser creates a low relative humidity inside the measurement chamber, 12 %RH was recorded at a location of 7 mm from the skin surface when background TEWL has stabilised and at the end of the SSWL measurement on Fig 4.29. The skin experiences a dryer environment during the

measurement with the AquaFlux than the other devices (for example, the sensors inside the Tewameter measurement chamber recorded a RH of 48% at the lower sensor (3 mm from the skin surface) and 47% at the upper sensor (8 mm from the skin surface)).
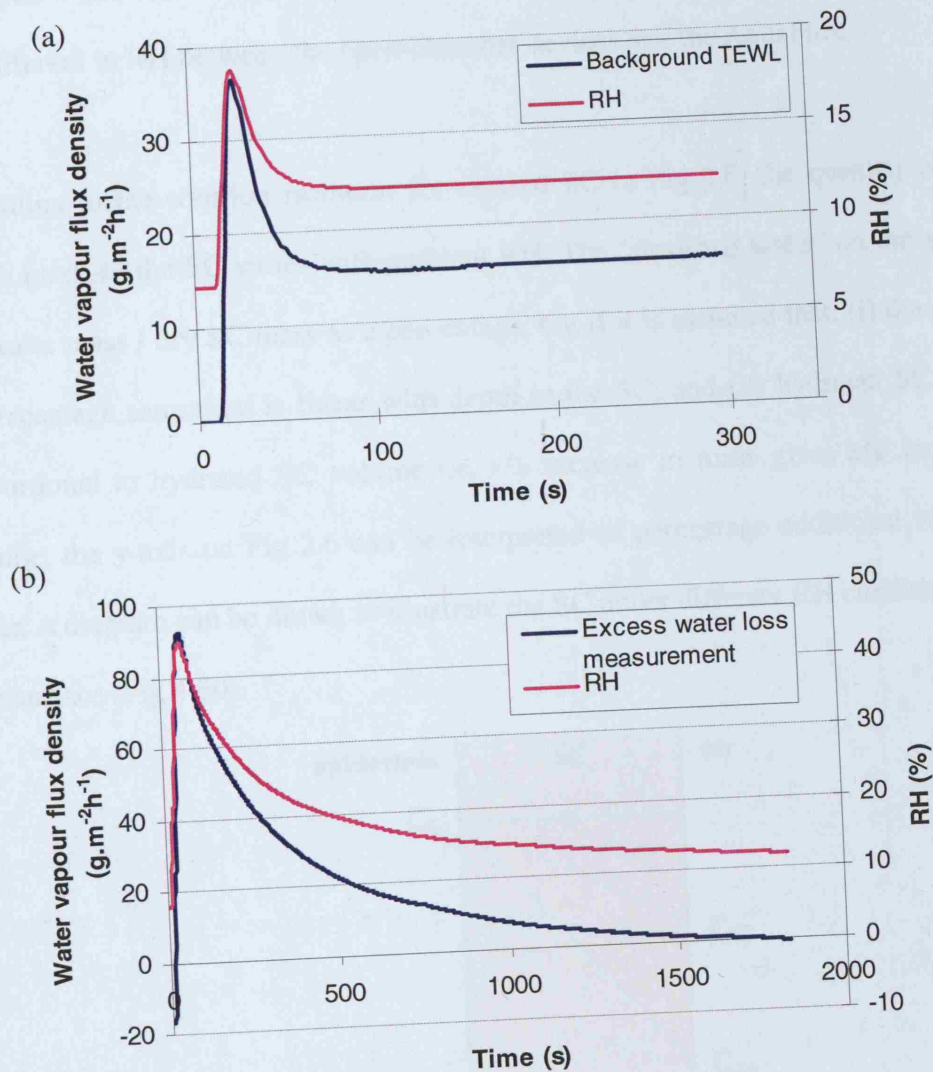
Fig 4.29 An example of (a) background TEWL and (b) SSWL measurement using the AquaFlux, showing the change in relative humidity inside the measurement chamber.

Although the RH recorded by the sensors inside the measurement chambers were at a distance from the skin surface, the lower sensor of the open-chamber device is close to the skin surface (3 mm above) and the differences between upper and lower sensors is

small, therefore it can be assumed that the RH at skin surface is ~50%. For the

AquaFlux, the sensor is located half way inside the chamber, at 7 mm above the skin.

If we assume a linear relationship between RH and distance, RH = 0% at the condenser

plate, RH = 12% at 7 mm, and 24 %RH is assumed at the skin surface. Therefore, there

is a different in RH between the open-chamber devices and the AquaFlux.

According to the sorption isotherm for excised SC in Fig 2.6, the quantity of water

which binds to the SC varies with ambient RH. The 'absorbed water' on the y-axis is

the water mass / dry SC mass as a percentage, but if it is assumed that: (i) the gradient

of percentage saturation is linear with depth in the SC; and (ii) hydrated SC mass is

proportional to hydrated SC volume i.e. x% increase in mass gives x% increase in

volume; the y-axis on Fig 2.6 can be interpreted as percentage additional volume of

water. A diagram can be drawn to illustrate the SC under different RH conditions at the

skin surface (Fig 4.30).
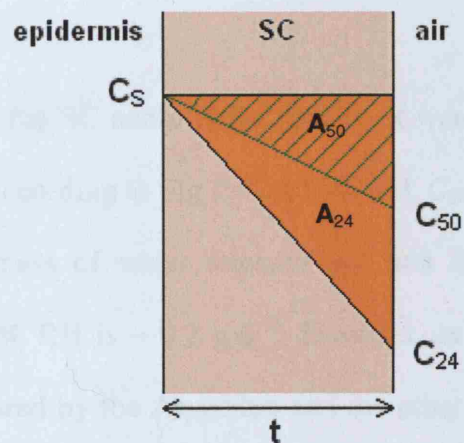
Fig 4.30 Diagram illustrating the sorption isotherm calculation for the
AquaFlux and other evaporimetry devices

Fig 4.30 illustrates that when the SC is fully over-hydrated, the saturation level is C_S

throughout its depth. When fully over-hydrated SC equilibrate with an atmosphere of

50%RH, the saturation in the SC will vary linearly from C_S at its base to C_{50} at its

surface, then the volume of water lost per unit area of SC can be represented by the right-angled triangle area shaded in green, A_{50}. Similarly, when the outside RH is 24% (represented by C_{24}), the volume of water loss per unit area of SC can be represented by the area of the orange right angled triangle, A_{24}.

By determining the differences between the two areas, A_{24} - A_{50}, the extra amount of water loss induced by the lower RH on the skin surface (as it was within the measurement chamber of the AquaFlux) can be estimated:

A_{50} = Volume of water per unit area of SC when the RH outside is 50% $= (C_S - C_{50})\dfrac{t}{2}$

Mass of water lost per unit area of SC at 50% RH $= (C_S - C_{50})\dfrac{t}{2} \cdot \rho$

A_{24} = Volume of water per unit area of SC when the RH outside is 24% $= (C_S - C_{24})\dfrac{t}{2}$

Mass of water lost per unit area of SC at 24% RH $= (C_S - C_{24})\dfrac{t}{2} \cdot \rho$

where t is the thickness of the SC and ρ is the density of water. If t $= 10^{-5}$ m (typical value), $\rho = 10^6$ g·m^{-3}, and according to Fig 2.6 at 50% RH, C_{50} ~ 10%, at 24% RH, C_{24} ~ 6%, the difference in mass of water released per unit area of SC for ambient conditions of 50% and 24% RH is ~ 0.2 g·m^{-2}. However, as shown in Fig 4.25, the difference in SSWL measured by the AquaFlux and the other devices was ~3 g·m^{-2} – far too much to be explained by the estimates calculated from the sorption isotherm above (~0.2 g·m^{-2}).

One possible reason for the SSWL measured by AquaFlux being higher than for the other devices, is that the low humidity in its chamber may have led to faster desorption.

By contrast, for the other devices flux density had not fallen quite to background TEWL after 30 minutes and so the area beneath the tail in desorption curves beyond 30 minutes will have been excluded. However, it seems unlikely that these excluded areas will have been big enough to account for the large difference between AquaFlux and the other devices.

Due to the measurement principle of the VapoMeter, it was not possible to check the calibration of this particular device, but experiments to check the calibration of the AquaFlux and the open-chamber devices using known masses of water (as droplets or dispersed in filter paper discs) were informative. While the AquaFlux produced accurate readings in all experiments, the open chamber devices underestimated water masses by up to 60%. Furthermore, the magnitude of underestimates increased with increasing filter paper disc diameter and also varied between filter paper disc and water droplet experiments. The explanation for those differences is unclear.

These data were then used to calculate calibration correction factors for the different devices which were then applied to background TEWL and SSWL results. The correction factors based on both water droplets and filter paper discs produced minimal improvement in agreement between background TEWL results from the different devices. However, they reduced the level of agreement of the SSWL results.

Overall, the five evaporimetry devices used in this work were compared by measuring the background TEWL on normal skin and the SSWL on over-hydrated skin of one subject. The repeatability of each device was good, but the agreement between them was poor, with AquaFlux having the highest results on both set of experiments; that is, three and two times higher than the Evaporimeter (the device which produced the

lowest values) in background TEWL and SSWL measurements, respectively.

Several reasons were identified for the disagreement between devices:

1. Different calibration methods – the calibration of the instrument is the basis of making comparable measurements, without a reliable / suitable calibration method, the reliability of measurements is not assured.

2. Differences in device measurement heads – it is impossible to measure evaporimetry from the skin in a non-contacting way, i.e. a probe has to be placed onto the skin for measurement, which will occlude the skin that is in contact with the rim of the probe. This may restrict the water vapour flux it is attempting to measure. Also, the presence of the sensors within the measurement chamber may disturbed the natural evaporation / diffusion of the water vapour flux from the skin.

3. The undershoot effect of the AquaFlux desorption curves – because of this, the SSWL value was calculated from the positive part of the curve only, and also it has been noted that the desorption curve appears to be still decreasing after the 30 minutes monitoring time (see Fig 4.20). More thorough investigation is needed to understand the reason(s) behind the 'undershoot' effect.

4. The different measuring principle of devices makes it difficult to compare results, especially for the AquaFlux, which uses a measuring principle that creates a different measurement environment than the other devices.

The method developed for measuring background TEWL on normal skin, and the SSWL in over-hydrated skin by using the five evaporimetry devices, are robust for comparing readings made with the same device, but the actual value obtained should be interpreted with caution until the reasons for differences between devices have been more fully explained.

A summary of the strengths and limitations of each of the evaporimetry devices used in this work is provided in Table 4.22. It should be noted that the strengths and limitations of the instruments were identified from the view point of the specific work described in the thesis.

Table 4.22 Personal views on the strengths and limitations of the five evaporimetry devices used in this work.

Evaporimetry device	Strengths	Limitations
Evaporimeter	• Most published studies have used it	• Open-chamber device that suffers from many restrictions in clinical use (e.g. the device is sensitive to uncontrolled ambient environment conditions, see Table 2.2 for details) • Old equipment which is now unsupported • Calibration can only be done by another company. The manufacturer no longer exists • Repair or replacement of parts is no longer possible • No foam in measurement chamber to minimise air movement effect • Not compatible with new PC • Original software can only log the mean TEWL over some time period • Cannot record ambient or sensors' T and RH • Gives generally lower TEWL value than other devices
DermaLab	• Can log data from two probes (TEWL or others) • New version is available	• Open-chamber device that suffers from many restrictions in clinical use • The old version of the software can

		• only log data continuously for 5 min • Cannot record sensors' T and RH
Tewameter	• Start and stop button on probe handle, more convenient • Base unit can log data from multiple probes • Many parameters can be recorded from each sensor • Preset stopping criteria • Preheat function • Can choose from spot or continuous measurements • Calibration check equipment available	• Open-chamber device that suffers from many restrictions in clinical use (e.g. the device is sensitive to uncontrolled ambient environment conditions, see Table 2.2 for details) • No foam in measurement chamber to minimise air movement effect
VapoMeter	• Start and stop button on probe, more convenient • Battery operated and digital readout on probe • Wireless data transfer • Different sizes of measurement heads available	• Cannot log data continuously • Cannot record sensors' T and RH • Software not very user-friendly • Slightly heavy probe • Need time in between measurements for ventilating the measurement chamber
AquaFlux	• Can choose from spot or continuous measurements • Many parameters can be recorded from the sensor • Good and helpful support from the manufacturer • Sophisticated and reliable calibration method • Different sizes measurement heads available • New version is available	• Long and careful starting up time and procedure • Cause of undershoot effect in desorption curve is still unclear • Heavy probe

N.B. A new version of the DermaLab and of the AquaFlux devices have become available more recently.

Chapter 5

MEASUREMENT OF HYDRATION PROFILE OF THE

STRATUM CORNEUM USING OTTER

A new approach, OTTER, has demonstrated its capability to measure skin hydration *in-vivo* with the advantages of remote sensing, non-contacting, non-invasive measurement, and its insensitivity to small movements of the sample (Section 2.4.4). By combining this technique with the evaporimetry measurements, a more thorough understanding of the distribution of water in the SC after occlusion with wet materials should be achieved. This chapter describes work to develop and use a methodology for measuring the hydration profile within the SC using OTTER, and relate the data to the desorption curves for over-hydrated skin measured using the evaporimetry technique.

5.1 Equipment
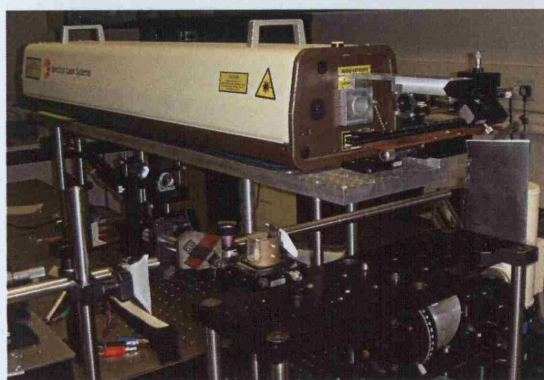
Fig 5.1 Picture of the OTTER apparatus.

When a sample is excited by a laser pulse, the absorbed energy changes rapidly to heat, causing the temperature near the surface to rise steeply and subsequently decline. OTTER measures this change of heat radiation emitted by the sample in order to relate

to the optical and thermal properties of the near-surface region of the sample. Fig 5.1 shows the OTTER that is based in the London South Bank University. Details of the laser are described in Section 2.4.4.

5.2 Methodology development

All measurements were conducted at London South Bank University in a room in which temperature was controlled (at $23^{o}C$) but not the relative humidity, it was recorded on the day of measurements that the RH was in the range of 45 - 55 %.

The area of the volar forearm described in Section 3.1 of Subject I (Table 3.1) was used in preliminary measurements. Upon arrival, the subject was acclimatised in the measurement room for 30 minutes before any experiments.
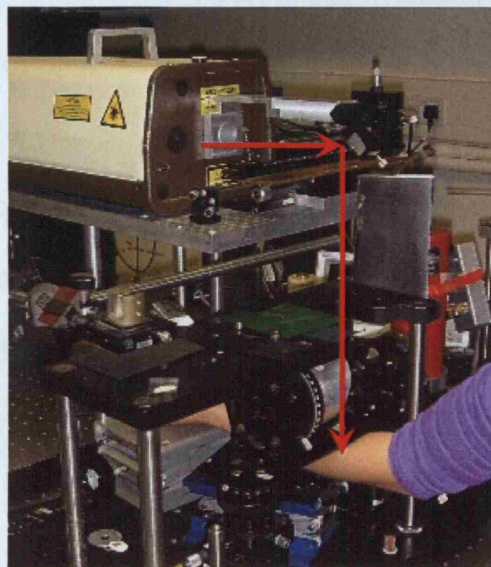
Fig 5.2 Volar forearm in position for OTTER measurement.

For making OTTER measurements, the volar forearm was positioned under the laser as shown in Fig 5.2, and by using the dedicated software the signals received by the detector were recorded. A detection wavelength of 13.1 µm was used since water is the only strong absorber in skin at this wavelength. The detailed procedure for using the

software is described in Appendix E.

Two evaporimetry devices were chosen to make measurements for correlating with OTTER data: the open-chamber Evaporimeter, the most commonly used evaporimetry instrument in published papers; and the condenser-chamber AquaFlux, an instrument that came onto the market recently. The devices are described in Section 2.4.3.

The OTTER data were then analysed using the dedicated program described in Appendix E. It incorporates a gradient model (Eq. 2.6) to yield the best fit surface lifetime of the OTTER signal (τ) and the effective gradient (W), and then calculate the water concentration at the surface of the SC (H_0), and the water concentration gradient in the SC (w_w), using Eq. 2.8. with $\beta_w = 2.9 \times 10^5 \, \mathrm{m}^{-1}$, $\beta_d = 1 \times 10^4 \, \mathrm{m}^{-1}$ and $D = 1.47 \times 10^{-7} \, \mathrm{m}^2 \mathrm{s}^{-1}$ (Xiao and Imhof, 1999). The percentage hydration level in the SC can then be plotted as a function of time.

In the development work, three methods were investigated in order to develop an efficient, reproducible and reliable method to correlate flux density with the surface hydration of the SC. At the end of this section, a final method was chosen to be performed on three subjects.

5.2.1 Method I

In this early work, OTTER measurements and the desorption curves measured by the two evaporimetry devices were made on different occasions, and the skin was hydrated for 20 minutes instead of 60 minutes adopted later to ensure maximum over-hydration, since this was performed with the aim of developing the methodology rather than gathering very accurate results: a 20 minute hydration period helps to shorten the

experiment time.

For OTTER measurements, the volar forearm was positioned under the laser immediately after the wet patch had been removed and the surface water blotted. Eight consecutive measurements were performed in rapid succession, each averaging the response to 50 laser pulses (signals). Measurements were then performed at 5 min intervals up to a period of 30 minutes. Each measurement was an average of 100 signals. Averaging more signals would have reduced noise but at the expense of having a longer measurement period, i.e. it takes ~30s to average 50 signals, and ~45s to average 100. Therefore a shorter measurement period was chosen near the beginning of the desorption curve in order to capture the rapidly changing hydration level. For the whole 30 minutes of experiments, the forearm remained still in the measurement position. The data were then analysed using the OTTER program, and the SC surface hydration level was plotted against time (Fig 5.3). Three repeat runs were conducted on the same day (shown in three different colours), and the results show three very similar desorption curves.
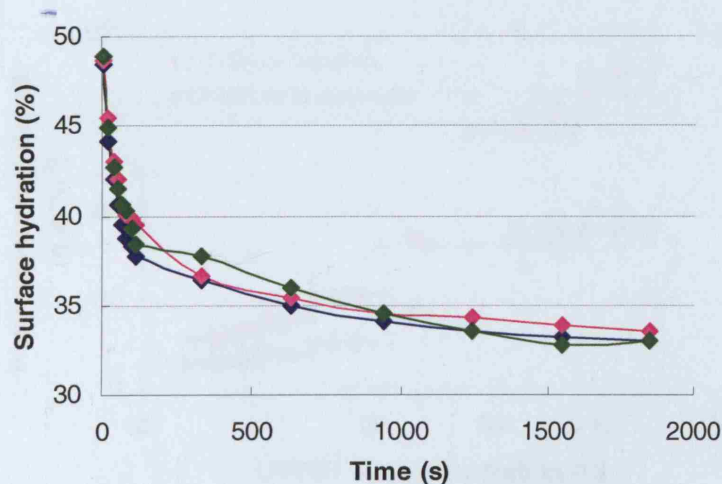
Fig 5.3 Three repeats desorption curves for over-hydrated skin from OTTER.

For desorption curves measured using the evaporimetry devices, the skin was, again,

hydrated for 20 minutes and flux density was logged for 30 minutes following removal of the wet patch and surface water blotting. Three repeats were run on the same day for each device, and the flux density was plotted against time (Fig 5.4). Results show the three desorption curves (shown in three different colours) were very similar for each device, although there were substantial differences in the temporal profiles between devices.
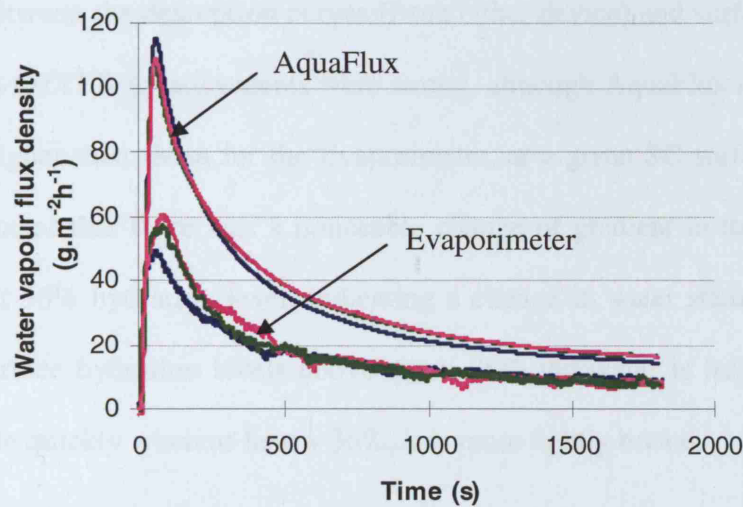
Fig 5.4 Desorption curves for over-hydrated skin from the Evaporimeter and the AquaFlux.
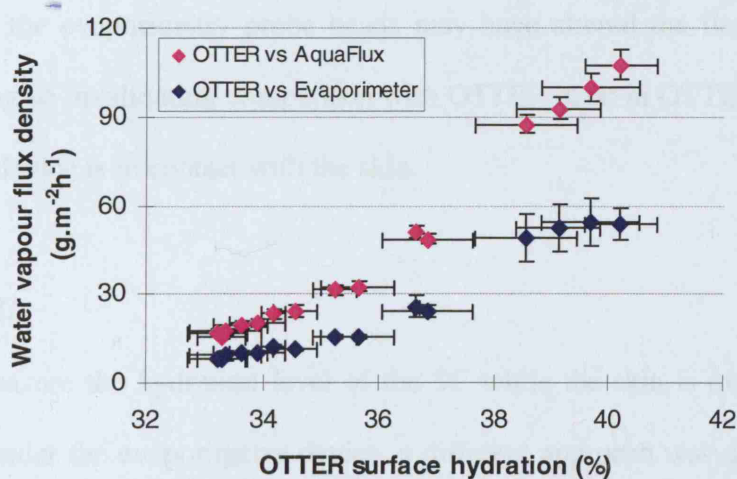
Fig 5.5 Flux density (measured with the Evaporimeter and the AquaFlux) against the estimated hydration level of the SC at the skin surface, based on OTTER measurements. Error bars are ± one standard deviation.

The desorption curves were then related to the OTTER data by averaging the three repeat flux values at the times (after patch removal) at which OTTER measurements were made. These average flux values were then plotted against the average OTTER hydration level, as shown in Fig 5.5.

Correlations between the desorption curves (from either device) and surface hydration estimated from OTTER measurements were strong, although AquaFlux readings were substantially higher than those for the Evaporimeter, at a given SC surface hydration level. It was found that there was a noticeable change of gradient in the drying flux values at about 36% hydration level, indicating a change in water status. It suggests that for SC surface hydration levels above about 36% the water is largely free, and evaporates quite quickly whereas below 36%, it is more tightly bound.

However, it should be noted that the desorption curves measured using OTTER and evaporimetry devices were evaluated on different occasions and, as discussed in Section 2.4.3, the evaporimetry probe heads may have altered the flux density they were measuring so invalidating comparison with OTTER data: in OTTER experiments no part of the device is in contact with the skin.

5.2.2 Method II

In order to measure the hydration level of the SC while the skin is experiencing the environment under the evaporimetry device, a different approach was developed. The drying of over-hydrated skin was measured using OTTER and the evaporimetry devices within the same hydration/drying cycle; that is, measurements alternated between OTTER and evaporimetry device.

After the forearm had been hydrated for 60 minutes (see Section 3.3.3) the wet patch was removed and surface water blotted, the evaporimetry probe was applied to the skin and logging started. During the measurement, the forearm was removed from the probe and positioned under the laser for one OTTER measurement incorporating an average of 100 signals (which took about 45 seconds), before returning to the evaporimetry probe at the same test site. OTTER measurements were made intermittently at times 0, 1, 2, 3, 4, 5, 7, 10, 15, 20, 25 and 30 minutes after patch removed. Fig 5.6 shows an example of the intermittent flux density measured by each evaporimetry devices during the 30 minutes.
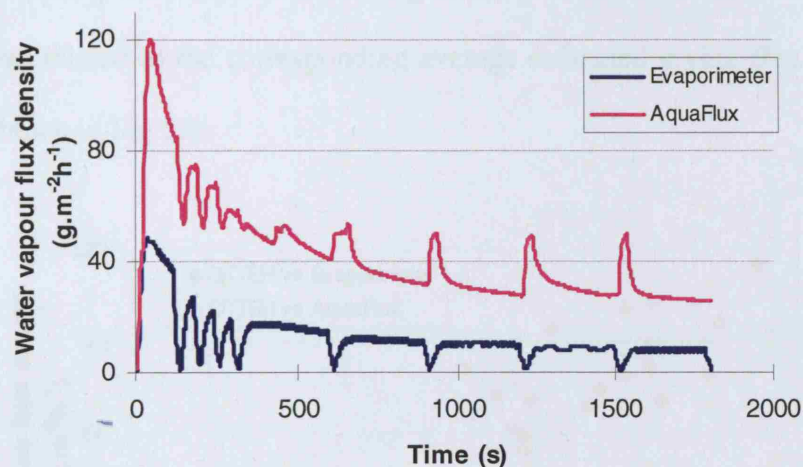
Fig 5.6 Example plot of intermittent desorption curves measured by the Evaporimeter and the AquaFlux.

In order to correlate the desorption curves with OTTER hydration data, the data was interpolated linearly in the periods during which the OTTER measurements were performed (as illustrated on Fig 5.7). The flux value in the middle of each line was extracted to relate to the corresponding OTTER data.
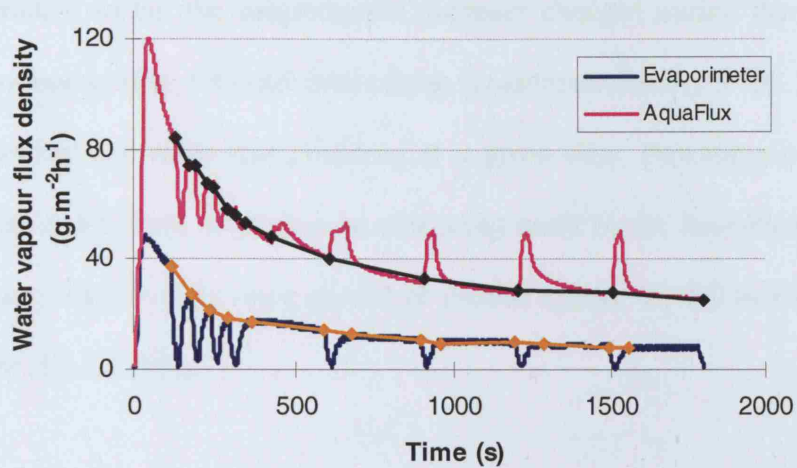
Fig 5.7 Illustration of the flux value estimated from lines fitted
to the desorption curves.

Four repeats were performed for each evaporimetry device and the average OTTER

hydration was related to the corresponding average estimated drying flux values, and

results are shown in Fig 5.8.
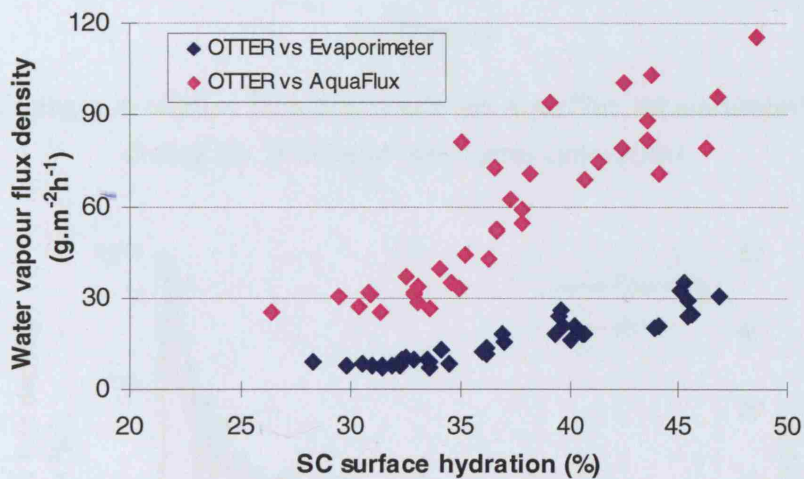
Fig 5.8 Flux density against the estimated hydration level of the SC
at the skin surface using Method II.

For this method, the OTTER measurements were made on skin that had been subjected

to the environment under the two evaporimetry probes. However for the AquaFlux, the

relative humidity within the measurement chamber changed during the 30 minutes, both for continuous (Fig 5.9) and intermittent measurements (Fig 5.10). Therefore, a different flux density value was produced at a given time, depending on whether a continuous or intermittent measurement was being made by the AquaFlux; hence it is difficult to determine which value should be plotted against the SC surface hydration data measured by OTTER.
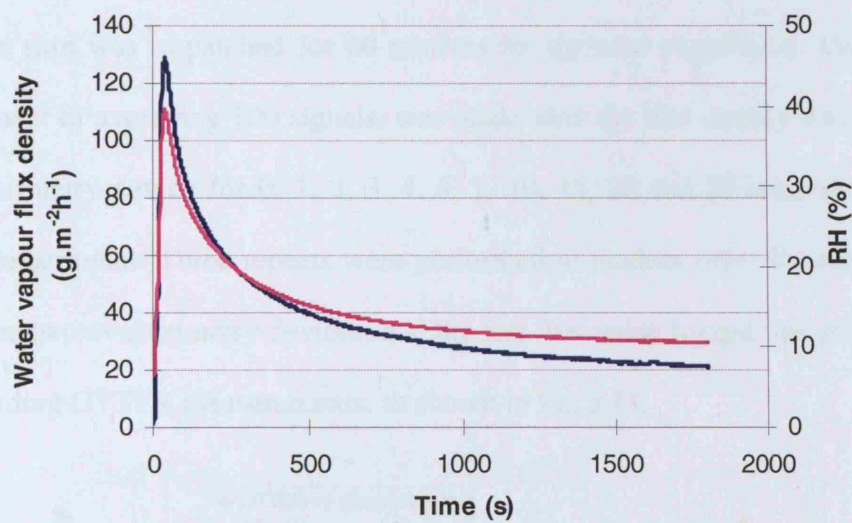
Fig 5.9 Changes in relative humidity inside the AquaFlux measurement chamber during the 30 minute continuous experiment.
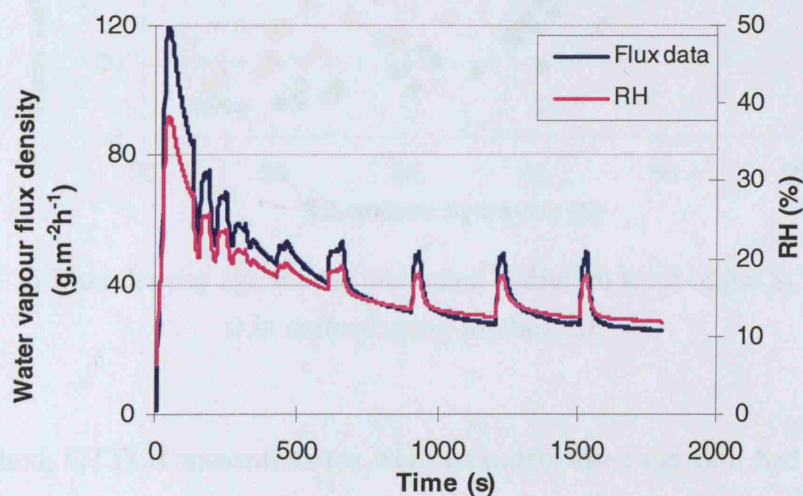
Fig 5.10 Changes in relative humidity inside the AquaFlux measurement chamber during the 30 minute intermittent experiment in Method II.

5.2.3 Method III

Another approach was then developed to overcome the problem of skin experiencing complex environment conditions under the evaporimetry devices when they were placed on and off the skin over the 30 minutes. One OTTER measurement was made at a certain time into the desorption curve, i.e. the flux density was logged for a certain time, namely 20 minutes after removal of the wet patch and surface water blotted, the forearm was then immediately placed under the OTTER to make one measurement before the skin was re-patched for 60 minutes for the next experiment. One OTTER measurement of averaging 100 signals, was made after the flux density was logged by the evaporimetry device for 0, 1, 2, 3, 4, 5, 7, 10, 15, 20 and 30 minutes, each in a separate experiment. Three repeats were performed in random order for each time for each of the two evaporimetry devices, and the last flux value logged was related to the corresponding OTTER measurements, as shown in Fig 5.11.
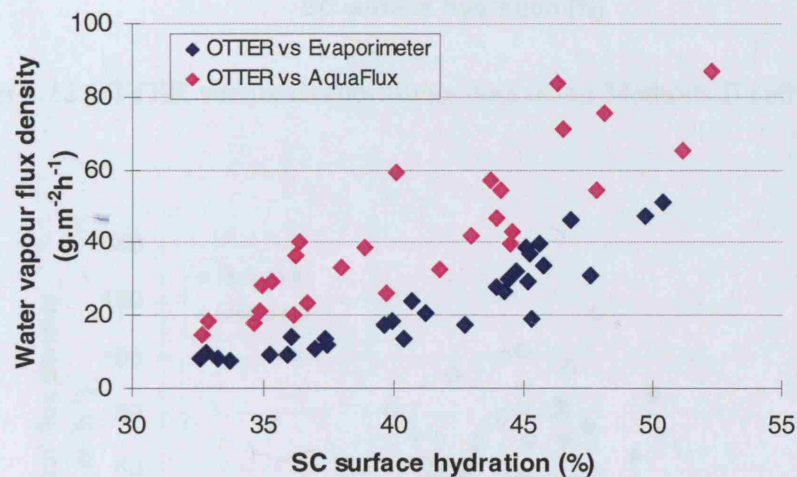
Fig 5.11 Flux density against the estimated hydration level of the SC at the skin surface using Method III.

In this method, OTTER measurements were recorded when the skin had experienced the environment created by the evaporimetry device continuously for a certain time since the wet patch removed. Therefore the surface hydration level measured by

OTTER should correlate to the flux density measured by the evaporimetry devices at that time into the desorption curve. The results showed that the plot of OTTER versus Evaporimeter data was non-linear in nature, with a distinct change in gradient in the drying flux value at about 37% hydration level. By contrast, the data in the plot of OTTER versus AquaFlux data were more variable and the relationship appeared more linear in form without any distinct change in the gradient (Fig 5.11).
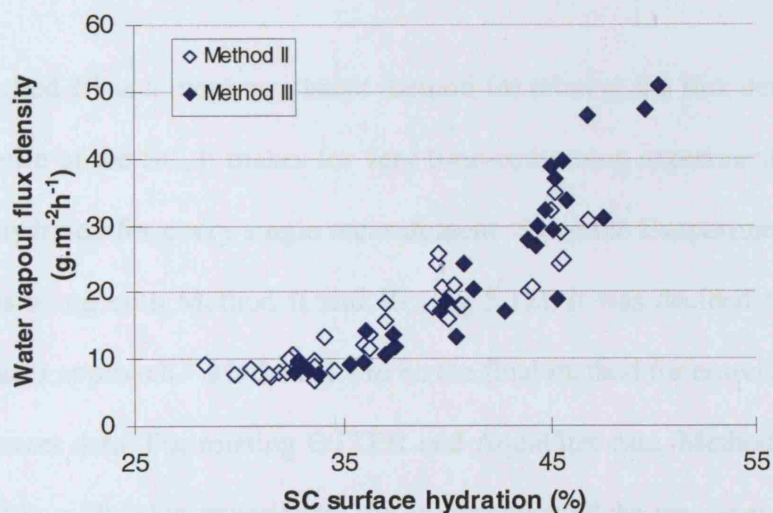
Fig 5.12 OTTER versus Evaporimeter data using Methods II and III.
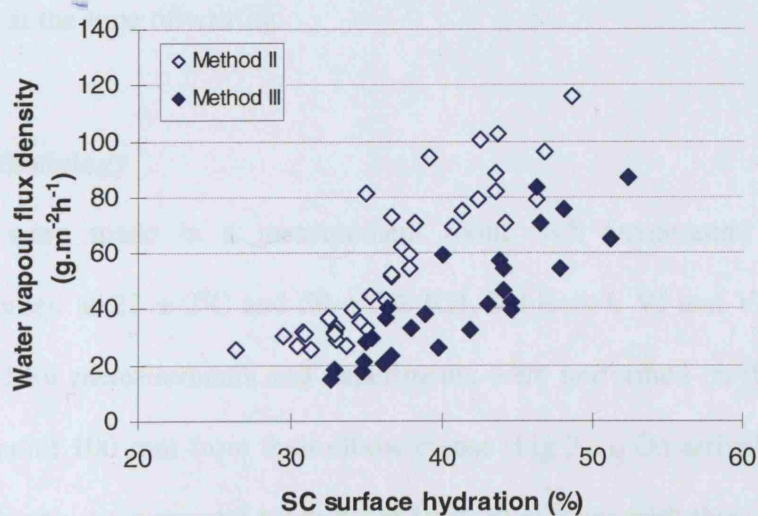
Fig 5.13 OTTER versus AquaFlux data using Methods II and III.

Data from Methods II and III for OTTER versus Evaporimeter and OTTER versus AquaFlux data are plotted for comparison in Figs 5.12 and 5.13, respectively. They show that data from the two methods agreed very well for the Evaporimeter, but for the AquaFlux, data from Method II produced higher flux readings than Method III. This is thought to be due to the variation in the microclimate within the measurement chamber of the AquaFlux in Method II (Fig 5.10).

Although Method III is a more consistent method for relating the flux density and the hydration profile of the SC, it makes for very time-consuming experiments as the skin has to be re-hydrated for every single measurement. Since the Evaporimeter produced similar results using both Method II and III (Fig 5.12), it was decided to choose the practically easier approach – Method II – to be the final method for correlating OTTER and Evaporimeter data. For relating OTTER and AquaFlux data, Method III seems to be more reliable as the skin experiences the environment of the measurement chamber continuously before the AquaFlux probe is removed from the skin for OTTER measurement. Unfortunately, there was not enough time to perform experiments with the AquaFlux at the time of writing.

5.3 Final methodology

Experiments were made in a measurement room with temperature and relative humidity recorded at $22 \pm 2°C$ and $50 \pm 5\%$ RH. Subjects I, VI and VII (Table 3.1) were recruited for measurements and experiments were performed on their left volar forearm at a point 100 mm from their elbow crease (Fig 3.3). On arrival, the subjects acclimatized in the measurement room for at least 30 minutes with their test skin sites exposed.

Out of the three methods developed in the last section, Method II using the Evaporimeter was chosen to be reliable and practically easier approach for relating OTTER and Evaporimeter measurements.

The procedure for uniformly hydrating the skin described in Section 3.3.5 was used. After patch removal, dry filter paper (a quarter of a 110 mm diameter Whatman N° 1 filter paper, Whatman plc., England) was applied for two seconds to blot any surface water before measurement began, as addressed in Section 3.3.4.

The Evaporimeter probe was then positioned on the skin and logging started. During measurements, the forearm was removed from the probe and positioned under the laser for one OTTER measurement incorporating an average of 100 signals, at times 0, 1, 2, 3, 4, 5, 7, 10, 15, 20, 25 and 30 minutes, before the Evaporimeter probe was located on the identical skin site.

In order to correlate the desorption curves with the OTTER hydration data, the data was interpolated linearly in the periods during which the OTTER measurements were performed (as illustrated on Fig 5.7), and the flux values in the middle of each line were extracted to relate to the corresponding OTTER data. Three repeats were performed on each subject on the same day.

5.4 Results

The flux density measured by the Evaporimeter is plotted against the hydration level at the skin surface measured by OTTER for the three subjects in Fig 5.14. It shows that Subject I and VII produced similar results. The relationship between the flux density and skin surface hydration was non-linear, with changes in gradient in the drying flux

value at about 34% hydration level for Subject I, and about 37% for Subject VII. By

contrast, the relationship found for Subject VI was linear in nature, with no evidence of

an apparent change in the drying flux gradient.
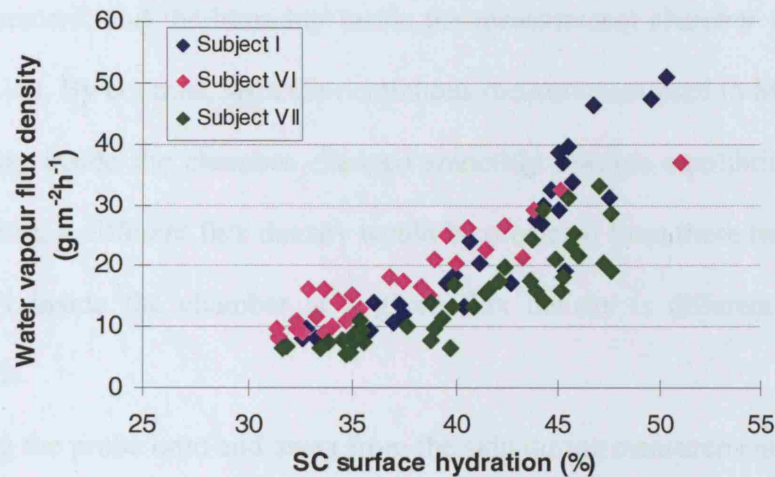
Fig 5.14 Flux density against the estimated hydration level of the SC at the skin surface for three subjects.

5.5 Discussion

In the preliminary experiment using Method I, a change of gradient of the correlation

plot was observed at about 36% hydration level (Fig 5.5), indicating a change in water

status during the drying of over-hydrated skin. Thus, for SC surface hydration levels

above about 36% the water is largely free, and evaporates quickly whereas below 36%

it is more tightly bound and hence evaporates at a slower rate. This finding agrees

impressively well with Berardesca (1997), who found three binding state of water

molecules to the keratin chains by using electrical measurements, in which 'tightly

bound water' was between water content of 0 - 7%; 'bound water' was between about

7 – 35 %; and 'free water' was above 35 % (see Section 2.4.1).

It was found during the method development that the AquaFlux produced different

readings between Methods II and III (Fig 5.13). There are various possible reasons:

(i)   the continuously changing humidity environment within the measurement chamber of the AquaFlux: in Method II, the measurement was made in an intermittent manner, such that – the probe was placed on and off the skin during measurement, and the humidity inside the measurement chamber was disturbed (Fig 5.10). By contrast, with the continuous measurement used in Method III, the humidity inside the chamber changed smoothly towards equilibrium (Fig 5.9). Therefore, a different flux density would be predicted from these two methods as the RH inside the chamber at a given flux density is different for the two methods.

(ii)   Moving the probe onto and away from the skin during measurement in Method II, is likely to have created air movement around the test skin site that may have enhanced the evaporation of SSWL.

For the above reasons, Method III was considered to be the most reliable method for correlating OTTER and evaporimetry data from both evaporimetry devices during the desorption curve. However, the duration of this experiment is rather long, which is not ideal when performing the test on volunteer subjects; and no difference was found between Method II and III for the Evaporimeter (Fig 5.12). Therefore, Method II was used in the final methodology to correlate the surface hydration with flux density measured by the Evaporimeter on three subjects. Results showed (Fig 5.14) a change of gradient in Subject I and VII at 34% and 37%, respectively; but the data from Subject VI appeared to be linear, i.e. no change in gradient was found. These differences may be attributed to the fact that Subject VI is a nurse who washes her arm frequently everyday, possibly disrupting the barrier function of the SC.

In conclusion, strong correlation was found between the surface water level measured by the new non-contacting technique – OTTER – and the flux density during the drying of over-hydrated skin. This correlation is thought to indicate changes of SC water holding capabilities during the drying process. The experimental data presented in this chapter will be used to develop a mathematical model for modelling the desorption curve of over-hydrated skin (beyond the scope of this thesis).

Chapter 6

CHARACTERISING SKIN FRICTION

As discussed in Section 2.5.2, there is a lack of a standard method for measuring friction between skin and fabric material. This chapter describes the development and validation of a robust and reliable methodology for measuring the coefficient of friction between skin and incontinence pad materials, particularly the coverstock, the water-permeable nonwoven material that lays against the skin.

6.1 Theory for measuring friction between skin and pad materials

In general, a greater force is required to overcome static friction than dynamic and so it is the former that needs to be measured to determine the maximum shear forces generated between incontinence pads and skin. As described in Section 2.5.2, although the rotational methods used to measure friction need a smaller flat area of skin than linear methods, they deliver a complex load distribution to the skin. Linear methods also have their constraints: they require reasonably large area of flat skin that can be maintained in a horizontal position. The volar forearm is an ideal test site since it has a reasonably large flat area, it is readily accessible and easy to hold in any desired orientation.

The test configuration adopted by Gwosdow et al. (1986) and Kenins (1994) was adopted in this work, where the force required to drag a strip of nonwoven material across the forearm was measured, as shown in Fig 6.1b. This curved configuration is geometrically more complex (Fig 6.1a) and is not such a pure configuration in that the normal

pressure varies with angular position, which would lead to complexities if the coefficient of friction varied with the normal pressure, i.e. if Amontons' law did not hold.
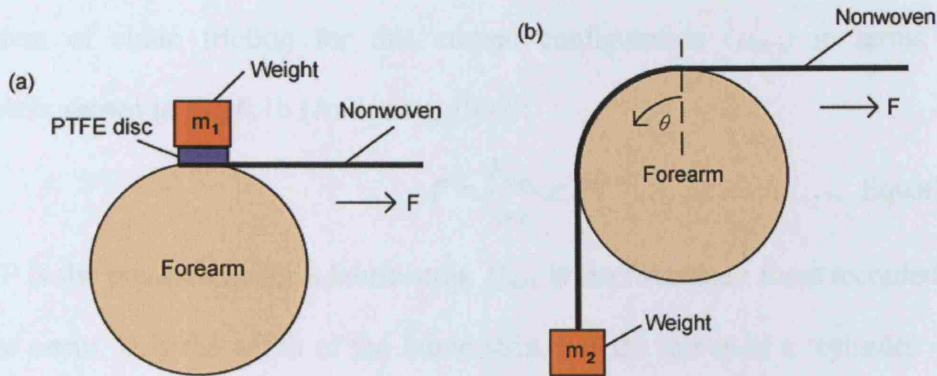
Fig 6.1 (a) Flat and (b) Curved friction measurement configurations.

However, as Gwosdow et al. (1986) have pointed out, an analytical solution exists for the geometrically analogous situation of friction in band brakes in which the coefficient of friction is assumed to be invariant with the normal force (Shigley, 1956) and the same solution has also been applied to an inextensible rope or drive belt around a rigid, cylindrical capstan (Fig 6.2) (Shames, 1996):

$$\mu_s = \frac{1}{\beta}\left(\ln\frac{F_1}{F_2}\right) \quad \ldots\ldots\ldots\ldots\ldots\ldots\ldots\text{ Equation 6.1}$$

where: μ_s = coefficient of static friction; β = angle of contact between belt / rope and capstan; F_1 and F_2 are the leaving and incoming tensions at the point of slippage, respectively.
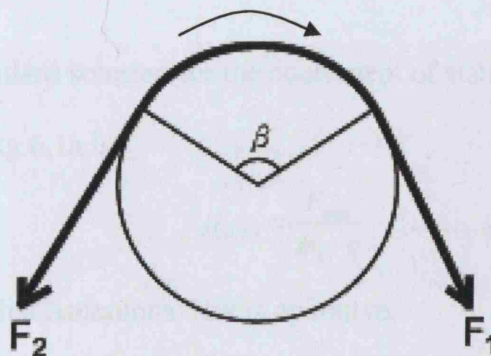
Fig 6.2 Belt friction.

Modelling the arm as a rigid cylinder, assuming the nonwoven fabric to be inextensible

and prescribing a value for β of $\pi/2$, the same analysis yields expressions for the

pressure distribution between fabric and skin when slipping occurs and for the

coefficient of static friction for this curved configuration ($\mu_{s(c)}$) in terms of the

parameters shown in Fig 6.1b (Anderson, 1997):

$$P = \frac{F_{max}}{w.r}.e^{-\mu_{s(c)}.\theta} \quad\dots\dots\dots\dots\dots\dots\dots\dots \text{Equation 6.2}$$

where P is the pressure under a fabric strip, F_{max} is the maximum force recorded before

slippage occur, w is the width of the fabric strip, r is the radius of a 'cylinder' used in

the setup, and θ is the angle measured about the axis of the arm from the point of

contact between the horizontal portion of the nonwoven strip and the skin (Fig 6.1b).

6.2 Strategy for measuring friction between skin and pad materials

By applying the Eq 6.1 to the curved configuration of Fig 6.1b, the coefficient of static

friction between skin and pad materials can be estimated. When the arc of contact by the

fabric is $90°$ (i.e. $\pi/2$ radians), the incoming force F_2 is the weight $m_2 g$, and F_1 is the

maximum leaving force (denoted F_{max}), the coefficient of static friction for the curved

configuration ($\mu_{s(c)}$) of Fig 6.1b is:

$$\mu_{s(c)} = \frac{2}{\pi}\ln\left(\frac{F_{max}}{m_2.g}\right) \quad\dots\dots\dots\dots\dots\dots\dots\dots \text{Equation 6.3}$$

For comparison, the standard solution for the coefficient of static friction for the flat

configuration ($\mu_{s(f)}$) of Fig 6.1a is:

$$\mu_{s(f)} = \frac{F_{max}}{m_1 \cdot g} \quad\dots\dots\dots\dots\dots\dots\dots\dots \text{Equation 6.4}$$

Both equations assume that Amontons' law is operative.

Experimentally, the flat configuration (Fig 6.1a) is more difficult to perform than the curved configuration (Fig 6.1b), since it requires balancing the weights on a limited skin site on the forearm. Moreover, a piece of material is needed between the fabric and weight (Fig 6.1a) to avoid / minimise the interference of the load with friction measurements (see Section 6.4.2), and the choice of this material may have an influence on the resulting coefficient of friction.
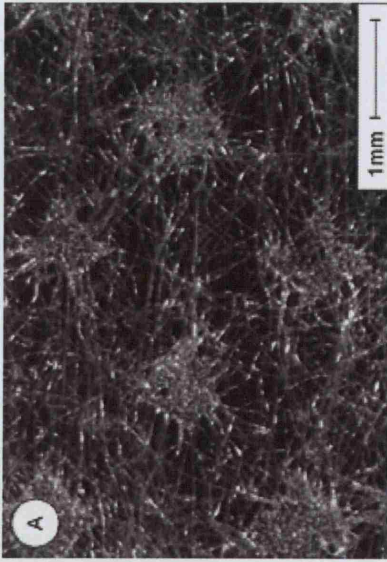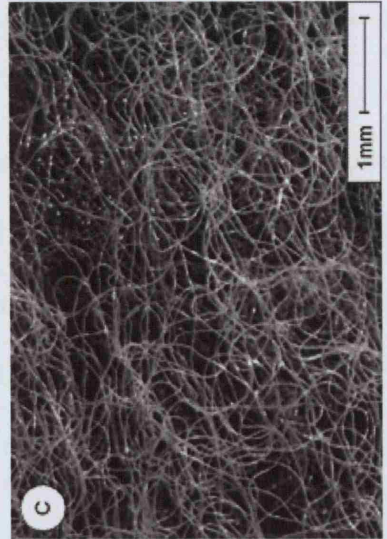
The strategy of the work was to determine whether the values for the coefficient of static friction between skin and nonwovens calculated with Eq 6.3 using the experimentally simpler but mathematically more complex curved configuration ($\mu_{s(c)}$) agreed with those from Eq 6.4 using the mathematically simpler but experimentally more difficult linear configuration ($\mu_{s(f)}$). In the rest of the thesis the two kinds of experiments / measurements are referred to using the shorthand terms: *curved friction* and *flat friction*.

6.3 Materials and subjects

Three nonwoven materials were selected for the work and their details are given in Table 6.1. All three are commonly used as coverstocks in absorbent hygiene products: A for incontinence pads; B for feminine hygiene pads; and C for feminine hygiene pads and baby diapers.

Friction measurements were made on the left volar forearms of five female volunteers (Subjects I, II, III, IV and V in Table 3.1).

Table 6.1 Characteristics of the three nonwovens used in friction measurements.

Nonwoven code	A	B	C
Area density (g·m⁻²)	17.0	26.0	25.0
Fibre polymer(s)	Polypropylene	Copolymer	Bicomponent (Polyethylene sheath and Polypropylene core) + 1% cotton
Bonding technique	Thermal calendered Spun laid web	Thermobonded Carded web	Through-air bonded Carded web
Manufacturer	Unknown	BBA Fiberweb	Unicharm
Optical micrographs			

6.4 Methodology development

In order to obtain repeatable and reliable data from flat and curved friction measurements on normal and over-hydrated skin, it was necessary to establish a standard well-defined procedure. The methodology development described below was performed on one subject (Subject I on Table 3.1).

6.4.1 Curved friction

The method development work on measuring skin friction was based on the experimental set up devised by SCA Hygiene Products AB, Sweden (Fig 6.3). They used a standard tensometer that is widely used to measure the tensile strength of materials in industry, called the Dia-Stron Miniature Tensile Tester 170 (MTT170), to measure the force applied to overcome friction between fabric and skin. A trough holder in which the arm rested was built to be used with the tensometer, a strip of test material is placed across the volar forearm and mounted on the tensometer cross-head (Fig 6.3). This cross-head moves at a constant velocity horizontally at 150 mm/min, and the force applied to the fabric is measured.
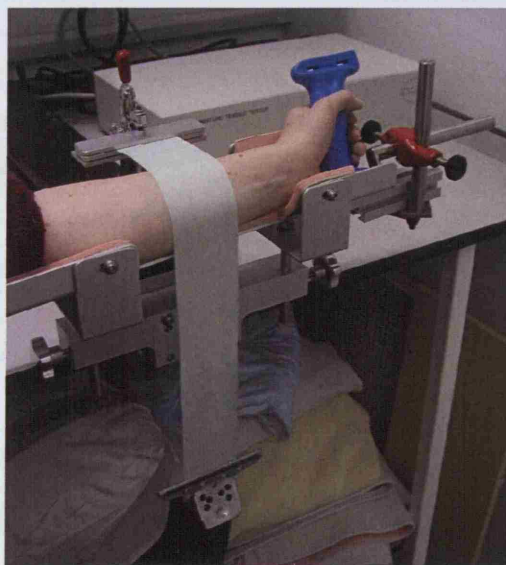
Fig 6.3 Experimental set up devised by SCA Hygiene Products: the arm rest and Tensometer with coverstock strip in place.

Data was then recorded on the *Mttwin* software that comes with the Tensometer for analysis. The setting of the software is described in Appendix F.

6.4.2 Flat friction

In preliminary experiments with the flat configuration, a rubber disc was used in between the test fabric and weights (in place of the PTFE shown in Fig 6.1a). It was suspected that the disc material may affect the friction measurement as the fabrics used were of low density containing many large pores. Therefore three different disc materials were tested for this purpose: rubber, cupro-nickel and PTFE. Three repeat flat friction measurements were performed on normal skin with the same fabric (Nonwoven A on Table 6.1) for each material disc, and the coefficient of static friction was measured. Table 6.2 shows that the $\mu_{s(s)}$ values measured using the three different disc materials were not significantly different. PTFE was chosen in this project since it has the lowest coefficient of friction measured, hence if there is any interference from the material to the measurement, it will be kept to a minimum.

Table 6.2 Mean, standard deviation and coefficient of variation of $\mu_{s(s)}$ measured using the flat configuration using discs made from three different materials between the nonwoven and the weights.

Material	Mean $\mu_{s(s)}$	sd	C.V.
Rubber	0.38	0.03	8.0%
Cupro-Nickel	0.42	0.04	9.6%
PTFE	0.38	0.02	5.3%

6.4.3 Preparation of over-hydrated skin

Skin was over-hydrated following the standard procedure described in Section 3.3.5. Patches – 50 x 70 mm for flat friction measurements and 50 x 100 mm for curved – were positioned on the volar forearm as shown in Fig 3.3b.

6.4.3.1 Impact of skin hydration history

For convenience several friction measurements were conducted on the forearm in one session. However, the skin loses water to the air by evaporation once the patch is removed and water is also lost into the strips of (initially dry) nonwoven fabric. Accordingly, the skin had to be rehydrated before every measurement. This was achieved by wearing a fresh patch for 20 minutes without first waiting for the skin to dry fully from the previous experiment. To establish that this procedure adequately rehydrated the skin, repeat friction measurements were conducted on one volar forearm (Subject I on Table 3.1) with one nonwoven fabric (Nonwoven A on Table 6.1), using each of the test configurations (flat and curved, Fig 6.1) and a range of mass values (m_1 or m_2, Fig 6.1).
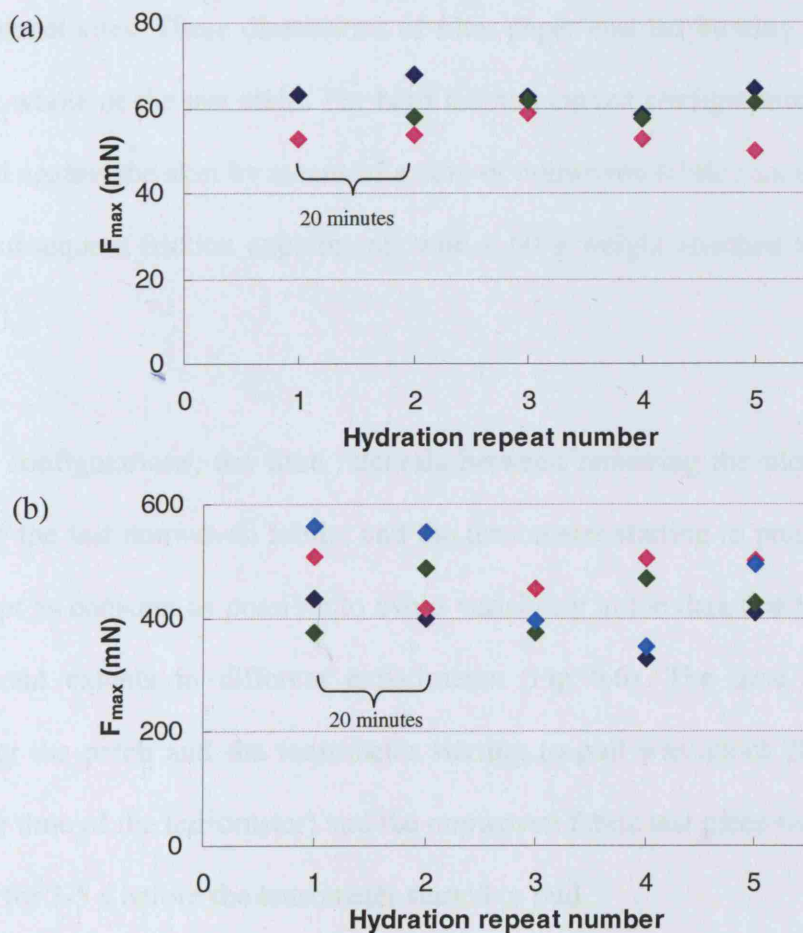
Fig 6.4. Example plots of re-hydration experiments on (a) flat friction with $m_2 = 30$ g and (b) curved friction with $m_1 = 40$ g, after 1-5 hydration cycles.

Three series of experiments were conducted, each on a different day. After each friction measurement in a series the skin was rehydrated for 20 min before the next friction measurement. There was no evidence of friction measurements changing systematically with repeated partial drying out and rehydration: example sets of data are shown in Fig 6.4 (repeats are shown as different colours on the graphs).

6.4.3.2 Skin preparation after patch removal

As discussed in Section 3.3.4, after a wet patch is removed the surface water left on the skin needs to be blotted in order to address this potential source of variability. A quadrant of 55 mm radius filter paper was used on sites to be used for flat friction measurements, and a 45° sector of 92.5 mm radius filter paper for curved friction measurement sites. These dimensions of filter paper enabled blotting the surface water over the whole of the test areas. For both flat and curved configurations the filter paper was held against the skin by means of a strip of nonwoven fabric (not the one to be used in the subsequent friction experiment) with a 60 g weight attached to its vertical end (Fig 6.5).

In both configurations, the time intervals between removing the blotting filter paper, applying the test nonwoven fabric, and the tensometer starting to pull on the test-piece were kept as constant as possible to avoid variability in the data due to skin drying out to different extents in different experiments (Fig 6.6). The time interval between removing the patch and the tensometer starting to pull was about 20 s (fixed by the response time of the tensometer) and the nonwoven fabric test piece was in contact with the skin for 3-5 s before the tensometer started to pull.
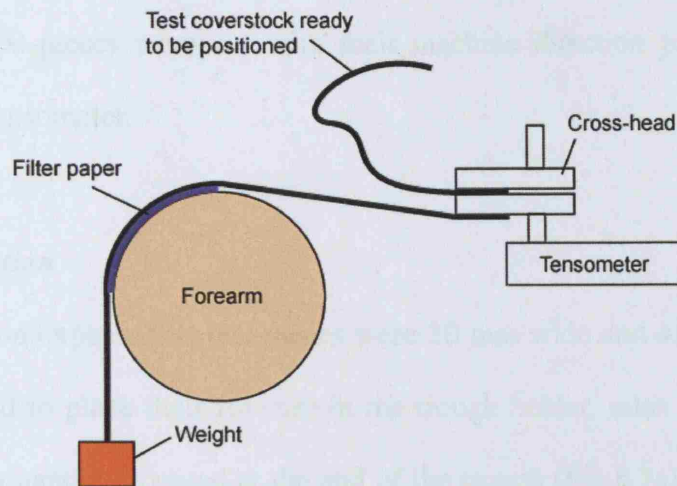
Fig 6.5 Blotting configuration for friction measurements.
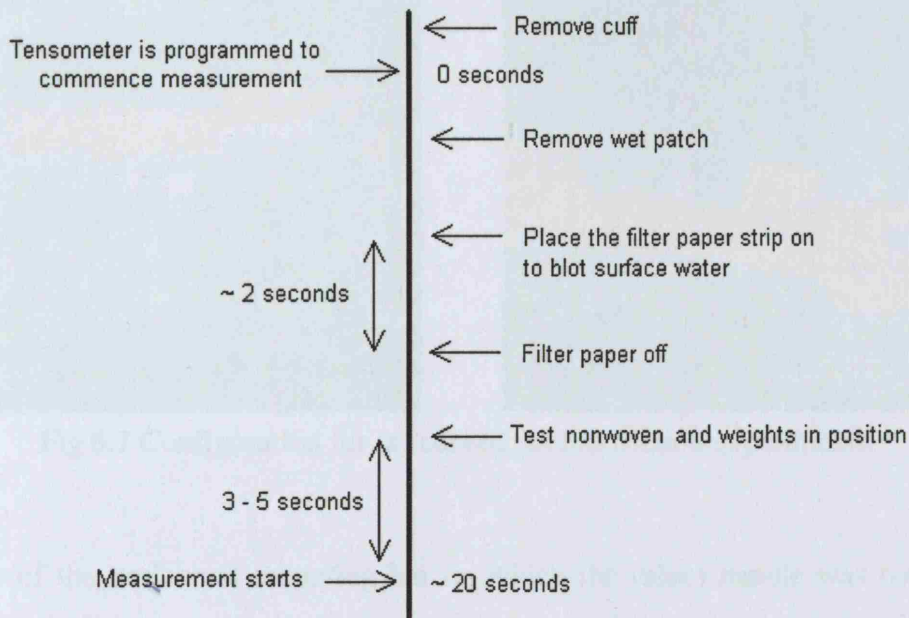
Fig 6.6 Timeline of the hydration / friction measurement procedure.

6.5 Final Methodology

In experiments on the first subject (Subject I on Table 3.1), over-hydration of the skin was achieved using rectangles of hydro-entangled rayon fabric (R200) soaked in normal saline (as described in Section 3.3.1). In experiments with the subsequent four subjects (Subject II, III, IV and V on Table 3.1), rectangles of filter paper (17Chr) were used instead, for the reason explained in Section 3.3.1.

All nonwoven test-pieces were cut with their machine direction parallel to the pull direction of the tensometer.

6.5.1 Curved friction

For curved friction experiments test-pieces were 30 mm wide and 450 mm long. Each subject was asked to place their forearm in the trough holder, relax their arm muscles and lightly grip a handle mounted at the end of the trough (Fig 6.7a), to avoid changes of muscle tone during measurement.
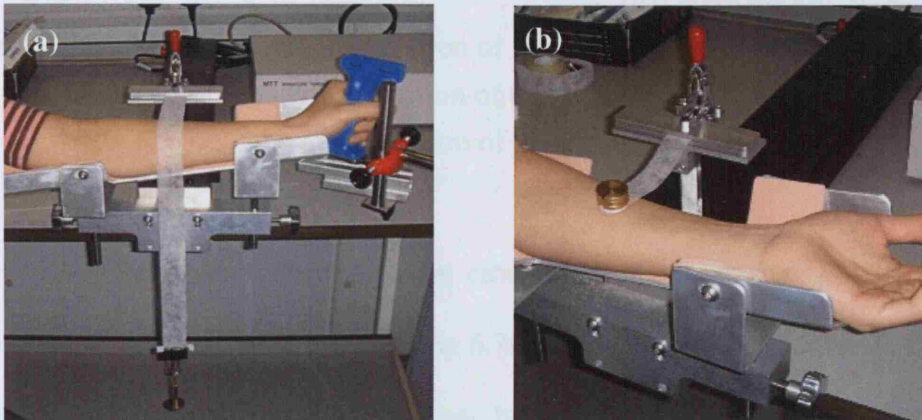
Fig 6.7 Configuration for (a) curved (b) flat friction experiments.

The axis of the horizontal mounting bar on which the (blue) handle was constrained always to be parallel with the length of the trough in which the forearm rested, but was allowed to be adjusted in the same parallel direction to accommodate arms of different lengths. This adjustment was needed to ensure that the fabric to be passed over the arm coincided with the area of the skin that had been hydrated. By then defining the orientation of the primary plane of the handle about its mounting bar (45° anticlockwise from the vertical was chosen) the geometry of the rig could be defined very simply and adjusted to the same settings for a given subject in successive experiments. The angle and height of the trough and the position of the handle were adjusted before each set of measurements to ensure that (i) the upper surface of the subject's arm was horizontal

and at the same height as the clamp in the cross-head of the tensometer and (ii) the

plane of the vertical section of the test piece was perpendicular to the pull direction of

the tensometer (Fig 6.8).

F ←

Arm
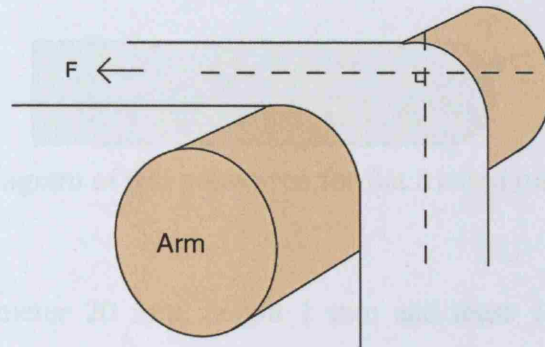
Fig 6.8 Diagram to illustrate the position of the arm in curved friction experiments.
The plane of the vertical portion of the fabric was perpendicular to
the pull direction of the tensometer.

The nonwoven strip was attached to the cross-head of the tensometer with a weight

(mass m_2) attached to the vertical part (Fig 6.7a) and pulled by the crosshead. Force was

plotted against displacement (proportional to time) and the maximum force (F_{max})

registered as that needed to overcome static friction. Measurements were repeated for a

range of values of m_1 and the gradient of the plot of m_1 against F_{max} used to calculate

$\mu_{s(c)}$ from Eq 6.3. At least three sets of repeats per subject were performed on both

normal and over-hydrated skin, for each of the three nonwoven materials.

6.5.2 Flat friction

For flat friction measurements, nonwoven test pieces were 125 mm long and 20 mm

wide with the end which was to be in contact with skin trimmed to form a semicircle of

radius 10 mm (Fig 6.9). Subjects were asked to place their forearm in the trough holder

transverse to the pull direction of the tensometer with the test site of their arm in line

with the cross-head clamp (Fig 6.7b) and relax the muscles to avoid changes of muscle

tone during measurement. In order to ensure the nonwoven test-piece was horizontal when pulled, the trough holder was adjusted so that the target skin area was horizontal and at the same height as the clamp in the cross-head of the tensometer.

Semicircle of radius 10 mm
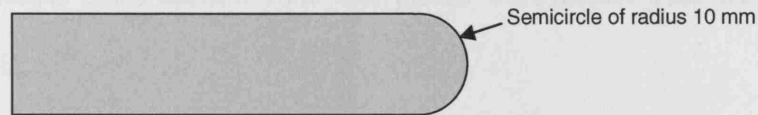
Fig 6.9 Diagram of test nonwoven for flat friction measurements.

A PTFE disc of diameter 20 mm, height 1 mm and mass 1.4 g was placed at the trimmed end of the nonwoven test-piece followed by a stack of brass weights of total mass m_1. The use of the PTFE disc was to minimize any interference of the load delivery system with the friction measurements (Section 6.4.2).

Force was plotted against displacement (proportional to time) and the maximum force (F_{max}) registered as that needed to overcome static friction. Measurements were repeated for a range of values of m_1 and the gradient of the plot of m_1 against F_{max} used to calculate $\mu_{s(f)}$ using Eq 6.4. At least three sets of repeats per subject were performed on both normal and over-hydrated skin, for each of the three nonwoven materials

6.5.3 Additional experimental and theoretical work on arm skin friction

The friction work described in this thesis resulted in two projects which aimed to explain and extend the findings. Cottenden developed a mathematical model for the friction between a strip of fabric and a convex prism of any cross-section, without the requirement of the prism or the material being rigid (Cottenden, 2007). This work is described in Appendix G.

Secondly, the current author initiated, designed and co-supervised an MSc project

(Karavokiros, 2007), in which friction measurements were made on surrogate arms of a variety of cross-sectional shapes to test the model (Cottenden, 2007). Most surrogate arms were made from Plaster of Paris covered in Neoprene. Cylinders, elliptical cross section prisms and circular cross section cone test pieces were made. This work is described in Appendix H.

To facilitate this work (Karavokiros, 2007) each subject who participated in this friction work was asked to have their arms scanned, so that surrogate arms could be a representation of the dimensions of real arms. The laser scans were performed in the Photographic Unit at the UCL Ear Institute, using the portable laser scanner (FastSCAN Handheld Laser Scanner) shown in Fig 6.10a. Fig 6.10b shows an example of a scan image of one of the arms. Results from this additional work are included in the discussion in Section 6.7.
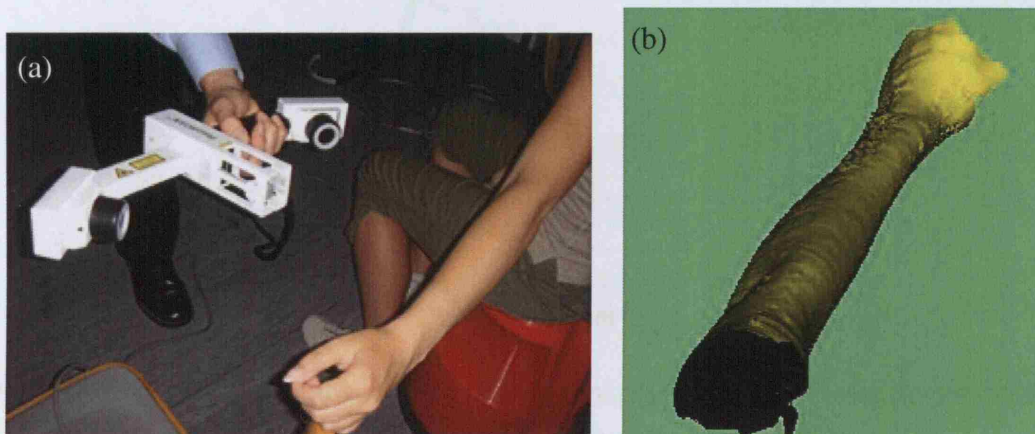
Fig 6.10 (a) Arm scanning with FastSCAN Handheld Laser Scanner;
(b) Scan image of an arm.

6.6 Results

Example sets of data from both flat and curved friction measurements on normal and over-hydrated skin are shown in Figs 6.11 and 6.12, respectively. For both configurations when measured on normal skin (Figs 6.11a and b), the applied force

increased to a maximum (F_{max}) to overcome static friction, enabling the material to move. Since the test site for flat configuration experiments was limited, the stack of weights fell to the ground as the material started to move (Fig 6.11a). For the curved configuration, when F_{max} was reached, dynamic friction occurred and the applied force decreased from that to overcome static friction to a constant value (Fig 6.11b).

(a)

(b)
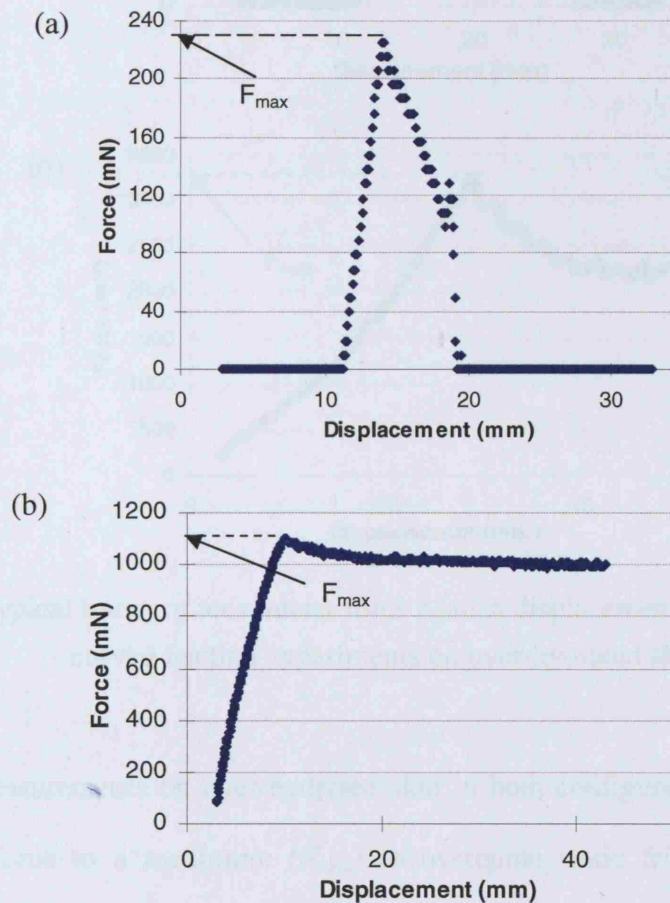
Fig 6.11 Typical traces of tensometer force against displacement of nonwovens for (a) flat and (b) curved friction experiments on normal skin.
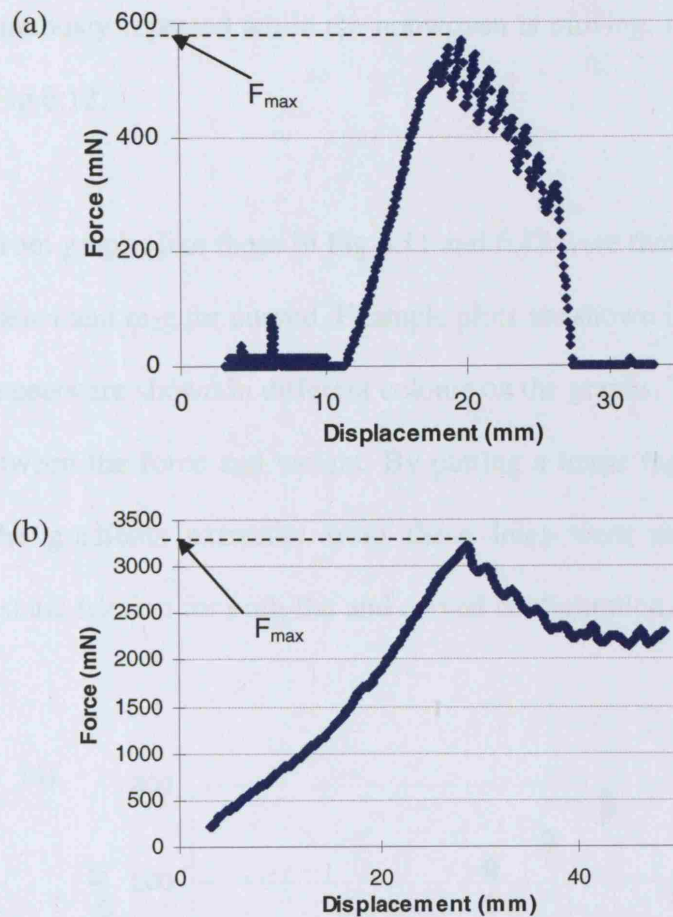
Fig 6.12 Typical traces of tensometer force against displacement for (a) flat and (b) curved friction experiments on over-hydrated skin.

Similarly, measurements on over-hydrated skin in both configurations also showed an increase in force to a maximum (F_{max}) to overcome static friction and enable the movement of material (Fig 6.12a and b). A stick-and-slip effect was noticed in both configurations. The motion of the material on over-hydrated skin was intermittent because of the difference between μ_s and μ_k. When static friction overcomes the dynamic friction, the force is not sufficient to maintain the shear strain that the skin and fabric have been subjected to, so a relocation (slip) occurs very rapidly. When static contact is re-established the stress is much lower, but again begins to increase as the fabric is pulled (without slipping) across the skin. Shear strain (and thus stress) continue to increase (stick) until static friction again fails, causing the cycle to repeat. This

process is continuously repeated while the nonwoven is moving, i.e. the stick and slip

effect seen on Fig 6.12.

F_{max} obtained from graphs like those in Fig 6.11 and 6.12 were then plotted against m_1g

for flat experiments and m_2g for curved. Example plots are shown in Figs 6.13 and 6.14,

respectively. Repeats are shown in different colours on the graphs. They showed a linear

relationship between the force and weight. By putting a linear regression line on each

set of data, the gradients extracted from these lines were used to calculate the

coefficients of static friction for both flat and curved configuration, using Eq 6.4 and 6.3

respectively.
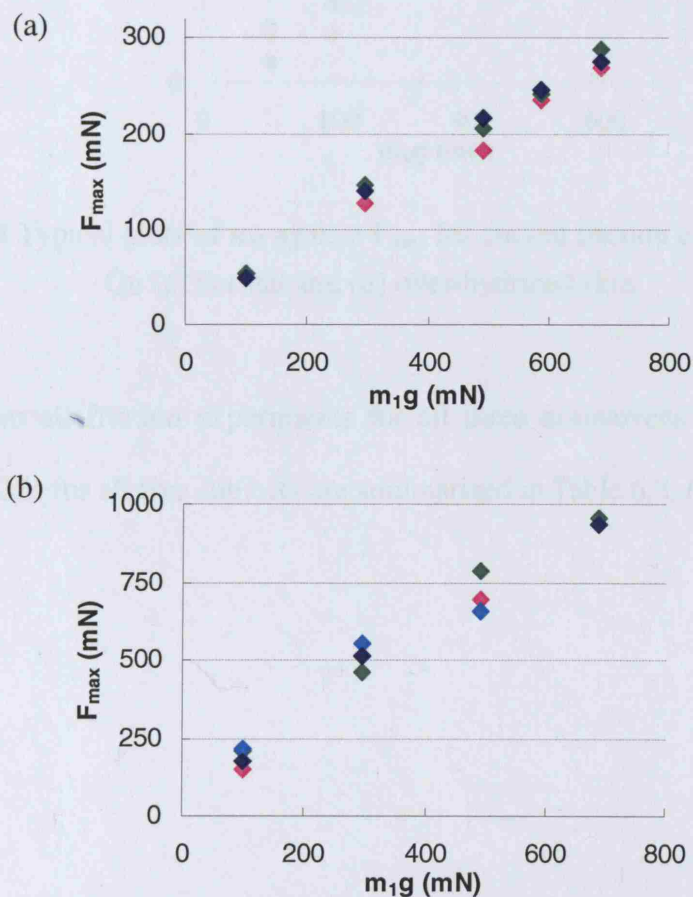
Fig 6.13 Typical plots of m_1 against F_{max} for flat friction experiments.
On (a) normal and (b) over-hydrated skin.

(a)

(b)
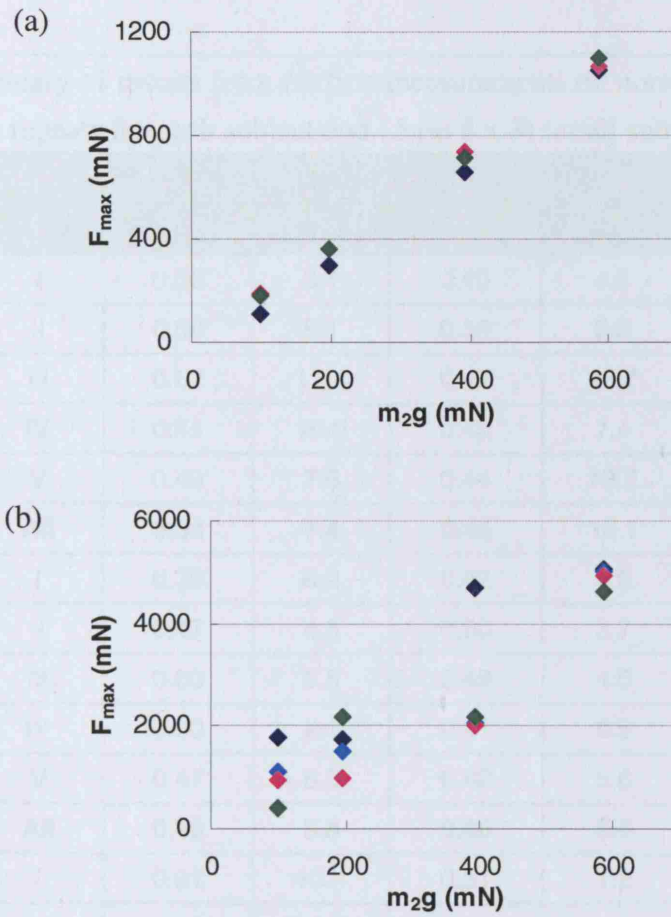
Fig 6.14 Typical plots of m_2 against F_{max} for curved friction experiments.

On (a) normal and (b) over-hydrated skin.

The results from all friction experiments for all three nonwovens on normal and on over-hydrated skin for all five subjects are summarised in Table 6.3, 6.4 and Figs 6.15.

Table 6.3 Summary of results from friction measurements on normal skin. Means are based on three repeats for each subject and 15 (ie 5 x 3) for all subjects together.

| Nonwoven | Subject | Flat friction | | Curved friction | | Difference: |
		Mean $\mu_{s(f)}$	CV (%)	Mean $\mu_{s(c)}$	CV (%)	$(\mu_{s(c)}-\mu_{s(f)})/\mu_{s(f)}$ (%)
A	I	0.38	3.1	0.40	4.5	5.3
	II	0.50	5.1	0.55	5.0	10.0
	III	0.67	11.4	0.47	15.7	-29.9
	IV	0.45	10.0	0.42	7.4	-6.7
	V	0.49	7.6	0.44	18.2	-10.2
	All	**0.50**	**7.4**	**0.45**	**10.1**	
B	I	0.39	6.2	0.42	4.8	7.7
	II	0.47	4.5	0.50	3.7	6.4
	III	0.60	5.5	0.49	4.0	-18.3
	IV	0.50	4.1	0.41	6.9	-18.0
	V	0.47	8.6	0.49	5.6	4.3
	All	**0.48**	**5.8**	**0.46**	**5.0**	
C	I	0.31	10.4	0.31	1.2	0.0
	II	0.36	19.7	0.40	8.7	11.1
	III	0.36	6.4	0.33	2.9	-8.3
	IV	0.36	1.1	0.38	4.1	5.6
	V	0.28	5.6	0.34	21.5	21.4
	All	**0.33**	**8.7**	**0.35**	**7.7**	

Table 6.4 Summary of results from friction measurements on over-hydrated skin. Means are based on three repeats for each subject and 15 (ie 5 x 3) for all subjects together.

Nonwoven	Subject	Flat friction		Curved friction		Difference:
		Mean $\mu_{s(f)}$	CV (%)	Mean $\mu_{s(c)}$	CV (%)	$(\mu_{s(c)}\text{-}\mu_{s(f)})/\mu_{s(f)}$ (%)
A	I	1.26	10.9	1.27	1.5	0.8
	II	0.95	5.3	1.14	4.9	20.0
	III	1.09	16.4	1.09	6.9	0
	IV	1.46	6.1	1.53	5.4	4.8
	V	1.16	13.7	1.17	6.0	0.9
	All	**1.18**	**10.5**	**1.24**	**4.9**	
B	I	1.33	5.1	1.33	4.2	0.0
	II	0.90	8.8	0.91	7.3	1.1
	III	1.29	15.0	0.84	8.4	-34.9
	IV	1.30	5.2	1.20	3.7	-7.7
	V	1.52	5.3	1.32	13.1	-13.2
	All	**1.27**	**7.9**	**1.20**	**7.4**	
C	I	1.16	15.7	1.09	4.1	-6.0
	II	0.74	12.3	0.63	2.1	-14.9
	III	0.93	19.2	0.72	18.9	-22.6
	IV	0.75	1.4	0.77	2.4	2.7
	V	0.94	20.5	1.10	34.9	17.0
	All	**0.90**	**13.8**	**0.86**	**12.5**	0.8

Summary for Nonwoven A

Summary for Nonwoven B
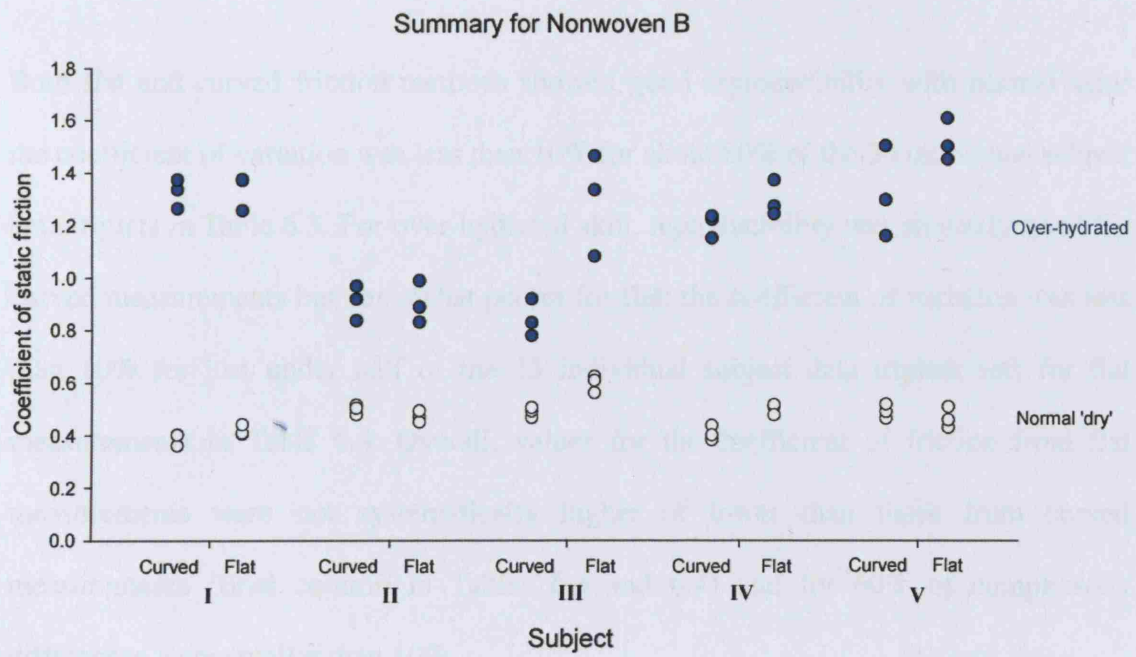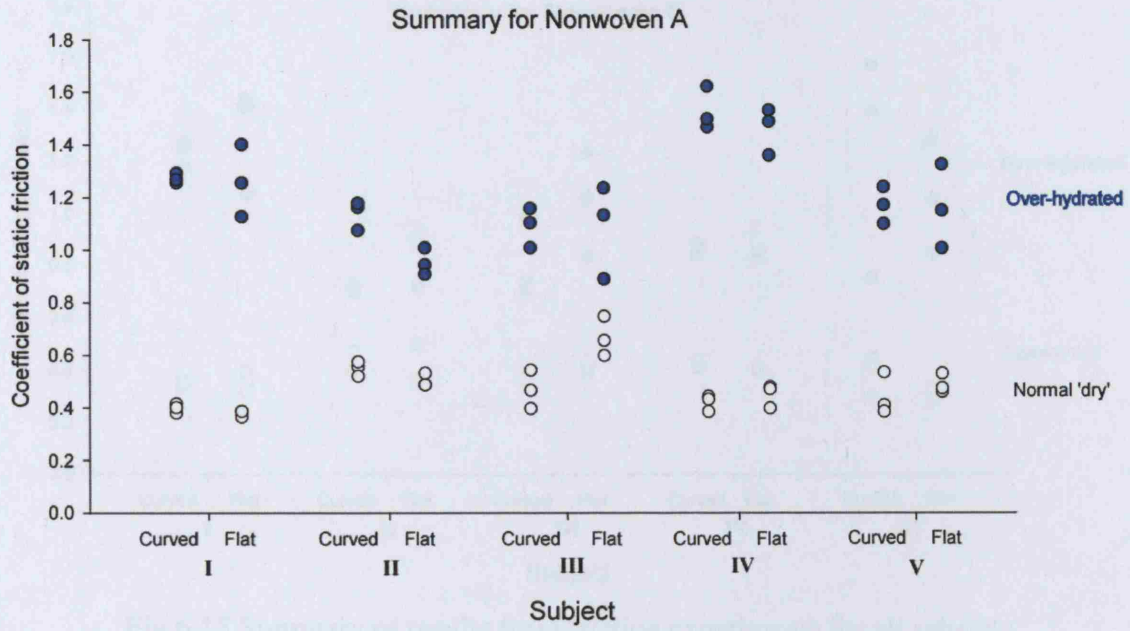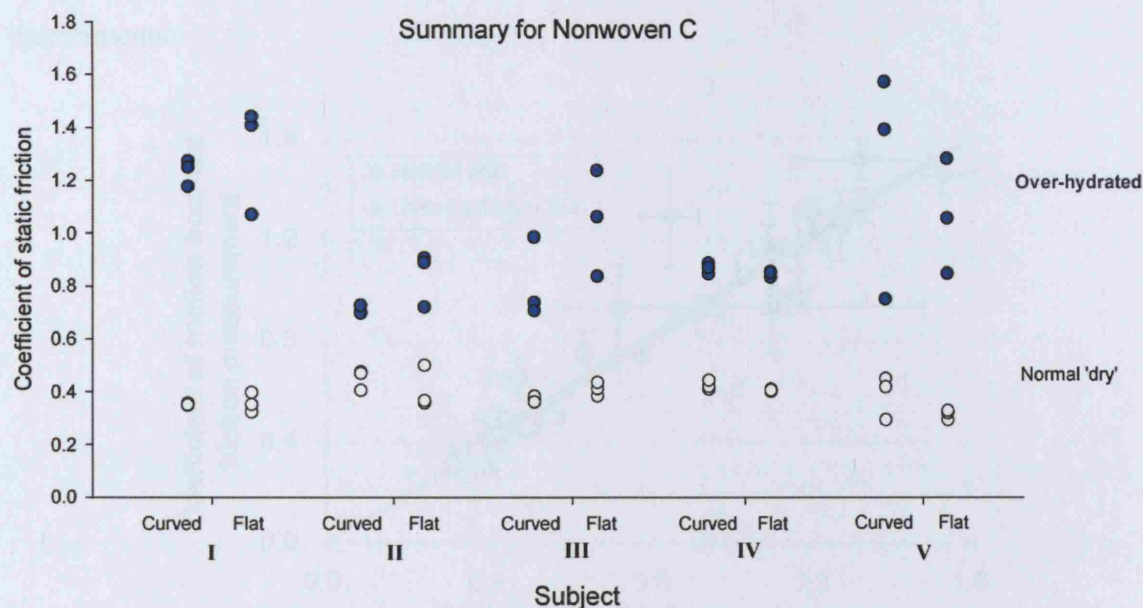
Fig 6.15 Summary of results from friction experiments for all subjects
and nonwoven A, B and C.

Both flat and curved friction methods showed good reproducibility with normal skin: the coefficient of variation was less than 10% for about 80% of the 30 individual subject data triplets in Table 6.3. For over-hydrated skin, reproducibility was similarly good for curved measurements but somewhat poorer for flat: the coefficient of variation was less than 10% for just under half of the 15 individual subject data triplets sets for flat measurements in Table 6.4. Overall, values for the coefficient of friction from flat measurements were not systematically higher or lower than those from curved measurements (final column in Tables 6.3 and 6.4) and for 60% of comparisons differences were smaller than 10%.

Differences exceeded 20% for only five comparisons, four of them relating to subject III. In all four of these cases, the coefficient of friction from flat measurements exceeded that from curved (see Section 6.7 for a discussion of the probable explanation). Fig 6.16 shows coefficient of friction values calculated from flat and from curved experiments plotted against each other for all nonwovens. Correlations were strong: R = 0.95 for all

experiments.
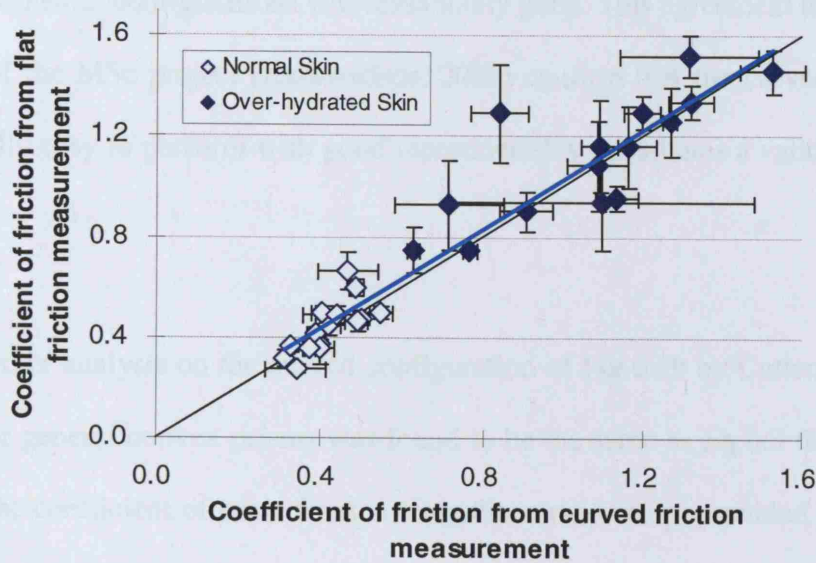
Fig 6.16 Coefficient of friction values calculated from flat and from curved experiments plotted against each other for all nonwovens and all subjects. Error bars are $\pm$ 1 standard deviation. The blue line is a regression line through the data while the thin line is the line of equality between measurements using the two configurations.

As predicted, coefficients of friction for over-hydrated skin exceeded those for normal skin for all three nonwovens and all subjects (Tables 6.3, 6.4 and Fig 6.16). Values for nonwoven C were generally lower than those for nonwovens A and B, which yielded similar results. There were often considerable differences between the coefficient of friction for different subjects. For example, subject I generally had the highest values of all the subjects for all three nonwovens when the skin was over-hydrated whereas subject II generally had the lowest. Interestingly, however, subject I generally had lower values than the other subjects for dry skin.

6.7 Discussion

Considering the simplifying assumptions that were made in deriving Eq 6.3 (modelling the arm as a rigid cylinder and assuming the nonwoven fabric to be inextensible) the

agreement found between measurements of coefficient of friction using the flat and curved experimental configurations was remarkably good. This agreement together with the results of the MSc project (Karavokiros, 2007) confirm that the curved method is experimentally easy to perform with good reproducibility constitutes a validation of the method.

From the further analysis on the curved configuration of Fig 6.1b by Cottenden (2007), a solution for general convex prisms was found to be the same as Eq 6.3 that was used for finding the coefficient of static friction from the curved setup, provided angles were measured appropriately. This general solution showed that it can be used to extract μ on any convex prism arm (see Appendix G). The experimental data from the MSc project supports this general solution: elliptical prisms in three orientations with fabric angle of contact varying from $70°$ to $120°$, and with weights from 98mN – 686 mN were used, all giving good agreement with the mathematical model. This provides a rationale for the good agreement between the flat and curved configurations on real arms in this work.

The linearity of plôts like those in Fig 6.13 for flat measurements indicates that Amontons' assumption, that the coefficient of friction is independent of normal pressure, is valid for the pressure range used in these experiments (0.36-2.23 kPa). The linearity of plots like those in Fig 6.14 for curved experiments enables this conclusion to be extended. In this configuration, the pressure between skin and nonwoven material varies with angular position (Eq 6.2) and Eq 6.3 is derived on the assumption that the coefficient of friction is independent of pressure over the range encountered. Assuming an arm radius of 30 mm, Eq 6.3 predicts that this pressure will have varied over the ranges of 0.1-0.2 kPa and 0.9-1.6 kPa for the minimum and maximum values, respectively, of m_2 for experiments on normal skin, and 0.1-1.6 kPa and 1.1-8.2 kPa for

over-hydrated skin. Taken together, these results suggest that the coefficients of friction measured were independent of normal pressure over the range of 0.1-8.2 kPa.

This conclusion is consistent with the studies of Kondo (2002) and Egawa et al. (2002a), who reported no dependence on pressure of the dynamic coefficient of friction of various materials against skin over pressure ranges of 0.5-5 and 2.5-5 kPa, respectively. However, it is inconsistent with earlier work by Comaish and Bottoms (1971) who found that the coefficient of static friction fell with decreasing pressure below 15kPa and Zhang and Mak (1999) who reported that the coefficient of dynamic friction rose approximately linearly by about 10% when the normal pressure was reduced from 8 kPa to 2 kPa.

Measurements of the coefficient of static friction for normal and over-hydrated skin varied in the ranges of about 0.3-0.5 and 0.9-1.3, respectively, for the three nonwovens (Tables 6.3 and 6.4). The friction values of normal skin are similar to those reported by Zhang and Mak (1999) who measured the coefficient of dynamic friction between cotton sock material and the dry volar forearm of 10 subjects and recorded values in the range 0.4-0.7. Similarly, Comaish and Bottoms (1971) measured a value of about 0.4 for the coefficient of static friction between wool and the dorsum of the hand of one subject when dry. However, their value for wet skin (0.6) was rather lower than those reported here for nonwovens.

Four of the five poorest agreements between coefficient of friction values measured using flat and curved configurations related to subject III (Tables 6.3 and 6.4) and in all four cases, the coefficient of friction from flat measurements exceeded that from curved. Inspection of volar forearms revealed that this subject had rather more skin hair than the

other four subjects. Furthermore, while hairier skin could be avoided when making flat measurements (which involved a smaller contact area between nonwoven and skin) this was not possible for curved measurements. It seems likely that the (often substantially) lower values for coefficient of friction recorded in curved measurements on subject III were a consequence of this hair acting as a lubricant by helping to hold the nonwoven test piece away from her skin. However, the plot on Fig 6.16 still showed a strong correlation between the coefficient of friction from flat and curved measurements for all subjects with R = 0.95.

In conclusion, a new method for measuring the coefficient of static friction between nonwovens and volar forearm skin has been developed and validated. It proved simple to perform and produced results with good reproducibility. It can now be used for further studies of friction between skin and nonwovens.

Chapter 7

DISCUSSION, CONCLUSIONS, AND FUTURE WORK

The motivation for this research has its roots in a lack of standard methods that could support the development of better incontinence pads in the aspect of skin health. In particular, there is a need to understand the impact of over-hydrated skin on (i) the hydration of the SC, and (ii) friction between the skin and nonwoven materials.

Detailed discussions of various topics can be found at the end of each relevant chapter (section 4.5 for evaporimetry; section 5.5 for OTTER and section 6.7 for friction). This chapter summarises the key issues found in various topics and highlights the need for future research.

7.1 Characterising skin wetness using evaporimetry

The literature was reviewed and it was established that there is a lack of methodology for both hydrating the skin and for logging, timing and analysing evaporimetry data. In this work, a standard method was developed for fully and uniformly hydrating the skin, by choosing a suitable material as the wet patch, establishing a suitable patch wear time in order to hydrate the skin fully, and removing surface water after patch removal.

Five different evaporimetry devices were chosen for the work, three of them use the same measuring principle – open-chamber (Evaporimeter, DermaLab and Tewameter), and the other two use different methods (closed chamber for the VapoMeter, and closed

chamber with condenser plate for the AquaFlux). Methodology for measuring background TEWL on normal skin, and the SSWL in over-hydrated skin by using evaporimetry was developed, validated and used to compare the performances of the five different devices.

In preliminary experiments, an undershoot effect was found with the newly available evaporimetry device, the AquaFlux. Flux density was logged on over-hydrated skin for 30 minutes after the wet patch was removed, when the background TEWL was subtracted from the flux density data in order to calculate the SSWL from the skin. The flux density measured after 20 minutes was lower than the normal flux of liquid water diffusing through the normal skin. A series of tests was performed to investigate the source of this undershoot effect. Although the effect was reduced after a slight change in the start-up procedure, with the undershoot occurring at about 25 instead of 20 minutes, the source of this effect is still unclear.

Results showed each of the five devices yielded good repeatability for background TEWL measurements on normal skin: with a C.V. of between 2.2 and 9.8%; and for SSWL measurements on over-hydrated skin: the C.V. was between 4.9 and 17.4%. However, there were some significant differences found between measurements made with different devices. Paired sample t-tests showed the differences between all pairs of devices were significant (p<0.05) for background TEWL measurements, and the AquaFlux produced readings significantly higher (p<0.009) than readings with each of the other devices for SSWL measurements.

Possible causes for these discrepancies were investigated by checking the calibration of each evaporimetry device. The droplet calibration method supplied by the AquaFlux

was adapted and improved (as filter paper calibration), to check the calibration of the

three open-chamber devices. This method was not possible for the VapoMeter as it

involves capturing the water vapour continuously. Underestimations were found in all

three of the devices, despite the fact that they had been calibrated by either their own

manufacturer or a specialist company before the work. The calibration factors obtained

from these calibration checking procedures were applied to the background TEWL and

SSWL measurements. This reduced the differences between devices to some extent, but

some significant differences still remained.

Another possible cause for the differences found between devices, especially for the

significantly high readings obtained by the AquaFlux, was investigated. Since the

AquaFlux uses a different measuring principle to measure evaporimetry, by use of a

condenser plate inside a closed measurement chamber, the RH at the skin surface was

different from that of other devices (~24% for the AquaFlux and 50%RH for

open-chamber devices). An approximation, based on the sorption isotherm presented by

Lévêque (2004), showed that the differences in mass per unit area of SC between 50%

and 24% RH was about 0.2 $g \cdot m^{-2}$, which is not enough to explain the differences found

between AquaFlux and other devices.

It is concluded that the methodology developed for using the five devices could be used

with confidence to compare readings made with the same device, but that it would be

unwise to trust the absolute values obtained until the reasons for differences between

devices have been more fully explained. By using patches made from a portion of an

absorbent pad (rather than pieces of filter paper), companies could use the developed

method to measure the TEWL and SSWL to investigate the change in SC barrier

function and the amount of excess water in the skin that is caused by using absorbent

pads, so helping them to develop pads that are more skin-friendly. Some further

development of the methodology is also needed to be able to conduct evaporimetry on

the buttocks area, where the pads are used in the clinical setting.

Future work

The next step of this work is to investigate further the causes for the differences found

between evaporimetry devices, by performing measurements on more subjects to

examine whether the differences were not solely attributable to the individual subject

used in the present study. Data should then be used to develop a mathematical model

describing the kinetics of each device during measurement.

In this evaporimetry work, 30 minutes was used to capture the desorption curve, which

is considered too long for most subjects to cope with in practice. Therefore, it would be

beneficial for studying evaporimetry, especially in clinical settings (nursing homes,

hospitals etc.), if a complete desorption curve could be predicted using a mathematical

model based on a limited amount of experimental data, for example, capturing the

desorption curve for 10 minutes instead of 30 minutes.

7.2 Measurement of hydration profile of the SC using OTTER

A new approach for measuring the water distribution within the SC - OTTER - was

adopted in this work. It has the advantages of taking non-contact and specific

measurements of water within the SC. A methodology was developed for measuring the

saturation profile within the over-hydrated SC during desorption. The relationship

between the saturation of the SC at the surface (measured using OTTER) and the water

vapour flux from over-hydrated SC (measured using evaporimetry) was investigated

using the volar forearms of three young female subjects. The two evaporimetry devices

used were the Evaporimeter and the AquaFlux.

A method for relating the SC saturation at the surface and the evaporimetry results was developed, and as predicted, a strong correlation was found with a change of gradient in the plot at about 35% saturation, which is thought to indicate the change in water holding capacity in the SC. This finding was consistent with the transition between loosely and tightly bound water reported by Berardesca (1997). However, no such change in gradient was found in the correlation plot of the SC saturation and evaporimetry for one subject, which might be attributable to the fact that as a nurse she is required to wash her arm frequently and this has may have disrupted the barrier function of her epidermal tissue.

Future work

A continuation of this work could involve examining the correlation between other electrical methods for measuring SC water content and evaporimetry (as with the OTTER and evaporimetry correlation performed in this work). The resulting data could be used to inform mathematical modelling on the SC saturation at the skin surface and the water flux evaporated from the skin during hydration and dehydration.

7.3 Characterising skin friction

The literature was reviewed and it was established that there is a lack of standard methodology for measuring friction between skin and fabric materials. Two methods were developed for friction measurement between both normal and over-hydrated skin, and nonwovens materials. The *flat* and *curved* methods were performed on the volar forearms of five young female subjects, to measure the friction between their normal and over-hydrated skin, and three nonwoven materials that are commonly used as

coverstocks in absorbent hygiene products.

The results showed that Amontons' law held in the pressure range used in this work (0.36 - 2.23 kPa) and, as expected, coefficients of friction for over-hydrated skin exceeded those for normal skin for all three nonwovens tested. The repeatability of the result was good for measurements on normal skin, with C.V. < 10 % for 80 % of the data. For over-hydrated skin, repeatability was similarly good for curved measurements but somewhat poorer for flat configurations with less than 50% of the data exhibiting a C.V. < 10 %.

It was noticed that four of the five poorest agreements between coefficient of friction values measured using flat and curved configurations related to one of the subjects - subject III; and in all four cases, the coefficient of friction from flat measurements exceeded that from curved. The volar forearm of this subject was then inspected and it was found that she had rather more skin hair than the other four subjects. It was suggested that the skin hair was acting as a lubricant by helping to hold the nonwovens away from the skin during curved measurements, and the tested area for flat friction was smaller and further away from the skin hair; therefore higher friction coefficient values were obtained from flat than curved measurements for subject III.

Remarkably good agreement were found between the two methods - R = 0.95 for all experiments - considering the assumptions that were made in deriving the solution for the *curved friction* (modelling the arm as a rigid cylinder and assuming the nonwoven fabrics to be inextensible). Additional theoretical work (by Cottenden (2007)) and experimental work on surrogate arms made based on laser scans of real arms (in a MSc project, Karavokiros (2007)) were made to explain and extend the findings. The

theoretical analysis showed that the mathematical solution for a cylindrical arm holds for any convex prism, and the experimental work supported the solution very well. It was concluded that a repeatable, accurate method for measuring friction coefficients on curved anatomical surfaces had been developed and validated.

The developed method could be used by pad manufacturers to characterise the friction between dry or wet skin and different coverstock materials, to help them develop pads that are more skin-friendly. However, the present method was developed on the volar forearm and this needs to be extended to other body sites, in particular the buttocks which is the most appropriate to the clinical problem.

Future work

A suggestion of immediate future work on skin friction is to understand the cause of the results obtained from this work: why does the coefficient of friction for a given nonwoven on a given skin site have the value that it does. Increase understanding in this area would help in the development of nonwovens with more skin friendly properties.

Furthermore, all measurements in this work were performed on two extreme cases of the skin, either normal or fully over-hydrated. However, in reality there is a hydration process before the normal skin becomes fully over-hydrated; it would be interesting to apply the curved method developed in this work to measure friction between nonwovens and skin at different stage of the hydration process, to reflect real use.

7.4 Summary

This work has achieved the primary aim of developing, validating and using methodologies (i) for measuring the quantity and distribution of water in SC of

over-hydrated skin, and (ii) for measuring the friction between skin (normal or over-hydrated) and nonwoven materials. One of the main areas of future work will involve applying the developed methodologies to improve the understanding of the underlying mechanisms based on reliable data. However, some of the methods, especially the evaporimetry, need further development before they can be used to obtain reliable quantitative data.

Publications resulting from this PhD

Wong, W.K.R., Cottenden, A.M., Xiao, P., Ciortea, L.I., Zheng, X. and Imhof, R.E. **Stratum corneum hydration and TEWL measurements during the drying process of an over-hydrated skin site.** Abstract from the stratum corneum V conference 2007. *International Journal of Cosmetic Science*, 29(3), 2007, 236.

Cottenden, A.M., Wong, W.K.R., Cottenden, D.J. and Farbrot, A. **Development and validation of a new method for measuring friction between skin and nonwoven materials.** *Journal of Engineering in Medicine* (In press).

Cottenden, A.M., Cottenden, D.J., Karavokiros, S. and Wong, W.K.R. **Development and experimental validation of a mathematical model for friction between fabrics and a volar forearm phantom.** *Journal of Engineering in Medicine* (In press).

Fader, M., Clarke-O'Neill, S., Wong, W.K.R., Runeman, B. and Cottenden, A.M. **Review and development of methods for quantifying excess water in over-hydrated skin using evaporimetry.** *Skin Research and Technology* (Submitted).

Cottenden, A.M., Wong, W.K.R. **Measuring transepidermal water loss (TEWL) from over-hydrated skin: a comparison of five evaporimeters.** *Skin Research and Technology* (In preparation).

Conference presentations

The influence of skin hydration on friction with incontinence pad materials.

Incontinence: The Engineering Challenge V, Institute of Mechanical Engineers, London, 2005.

A new method for measuring friction between nonwoven materials and skin.

EDANA's Nonwoven Research Academy, Leeds, 2007

Stratum corneum hydration and TEWL measurements during the drying process of an over-hydrated skin site.

Stratum Corneum V in association with The International Society for Bioengineering and the Skin (ISBS), Cardiff, 2007

Poster presentations

1. Estimating the excess water content of over-hydrated skin by measuring evaporative water loss desorption curves: a comparison of five devices.

2. Development and validation of a new method for measuring the coefficient of friction between fabrics and skin.

10th Anniversary EPUAP Open Meeting, European Pressure Ulcer Advisory Panel, Oxford, 2007.

Incontinence: The Engineering Challenge VI, Institute of Mechanical Engineers, London, 2007.

Appendix A

Ethics approval for this work

UCL
GRADUATE
SCHOOL

The Graduate School
University College London
Gower Street London WC1E 6BT

Professor David Bogle   Tel: (
Head of the Graduate School   Fax: (
                                                                 Email:

26 July 2005

Dr /
UCL
Continence and Skin Technology Group
Departments of Medicine/Medical Physics and Bioengineering
UCL Archway Campus
Clerkenwell Building
Highgate Hill
London N19 5LW

Dear

Re: Notification of Ethical Approval

Project ID: 、 ˙ .0507/001: Physics of Wet Skin

The above research has been given ethical approval following review by the UCL Committee for the Ethics of non-NHS Human Research for a period of 12 months from the commencement of the project (1 August 2005).

Approval is subject to the following conditions:

1. It is a requirement of the Committee that research projects which have received ethical approval are monitored annually. Therefore, you must complete and return our 'Annual Continuing Review Approval Form' PRIOR to the **1 August 2006**. If your project has ceased or was never initiated, it is still important that you complete the form so that we can ensure that our records are updated accordingly.

2. You must seek Chair's approval for proposed amendments to the research for which this approval has been given. Ethical approval is specific to this project and must not be treated as applicable to research of a similar nature. Each research project is reviewed separately and if there are significant changes to the research protocol you should seek confirmation of continued ethical approval by completing the 'Amendment Approval Request Form'.

The forms identified above can be accessed by logging on to the ethics website homepage: http://zzz.grad.ucl.ac.uk/ethics/ and clicking on the button marked 'Key Responsibilities of the Researcher Following Approval'.

3. It is your responsibility to report to the Committee any unanticipated problems or adverse events involving risks to participants or others. Both non-serious and serious adverse events must be reported.

Letter to Dr Cottenden 26/7/2005

Reporting Non-Serious Adverse Events.

For non-serious adverse events you will need to inform Ms Helen Dougal, Ethics Committee Administrator   within ten days of an adverse incident occurring and provide a full written report that should include any amendments to the participant information sheet and study protocol. The Chair or Vice-Chair of the Ethics Committee will confirm that the incident is non-serious and report to the Committee at the next meeting. The final view of the Committee will be communicated to you.

Reporting Serious Adverse Events

The Ethics Committee should be notified of all serious adverse events via the Ethics Committee Administrator immediately the incident occurs. Where the adverse incident is unexpected and serious, the Chair or Vice-Chair will decide whether the study should be terminated pending the opinion of an independent expert. The adverse event will be considered at the next Committee meeting and a decision will be made on the need to change the information leaflet and/or study protocol.

4. On completion of the research you must submit a brief report (a maximum of two sides of A4) of your findings/concluding comments to the Committee, which includes in particular issues relating to the ethical implications of the research.

Yours sincerely

Chair of the UCL Committee for the Ethics of Non-NHS Human Research

Cc: Wing Kei Rebecca Wong, Continence and Skin Technology Group, UCL

UCL GRADUATE SCHOOL

26 July 2006

Dr /
Department of Medical Physics and Bioengineering
UCL

Dear

Re: Annual Continuing Review Approval

Project ID: 0507/001: Physics of Wet Skin

I am pleased to inform you that the Chair of the UCL Research Ethics Committee has approved your study for the remaining period of the project. Please see attached signed copy of the Approval Form for your records.

On completion of the research, please submit a final report to the Committee (a maximum of two sides of A4) of your findings/concluding comments, which includes in particular, issues relating to the ethical implications of the research.

With best wishes

Yours sincerely

Secretary, UCL Research Ethics Committee

Enc.

UCL RESEARCH ETHICS COMMITTEE

Annual Continuing Review Approval Form

It is a requirement of the UCL Research Ethics Committee that research projects which have received ethical approval by the Committee are monitored annually. Therefore, this form must be completed and returned **PRIOR** to the date that the current approval expires. If your project has ceased or was never initiated, it is still important that you complete this form so that we can ensure that our records are updated accordingly.

1	**ID Number:**	**Principal Investigator:**
	0507/001	Dr. Alan Cottenden

2	**Project Title:**
	Physics of Wet Skin

3	**Current Approval Expires:**
	01/08/2006

4	**Project Status:** (please tick relevant box)	☑ Active ☐ Terminated
	01/08/2005	

5	**Current Status of Human Participant Use:**	
	Number being used: 4	Participant use completed? ☐ Yes ☑ No
	Number will be used: 15	
	Total Number enrolled to date: 4	Date completed: Not applicable
	Beginning date: December 2005	Total number enrolled: Not applicable

6	**Human participants will no longer be used. Please explain:**
	Not applicable

7	If funded study, please indicate:	Agency: SCA Hygiene AB (Sweden)
		Project Period: Oct 2004 – Oct 2007
		Agency Award Number: /

8	Number of participants who withdrew from the project: /
	Please provide reasons for withdrawal:
	Not applicable

9	**Have you modified your research since your last review?**		Yes ☐	No ☑

If so, you are required to submit a revised application form to the Committee for review.

10	**Please provide with this form a brief report describing the progress of your study thus far.**

Include a description of any **adverse or unforeseen circumstances** arising out of the research project (e.g. a complaint by a participant, an incident endangering a research worker taking a questionnaire out to a population study, etc) together with a summary of any recent literature, findings, or other relevant information associated with your study.

The aim of this study is to develop standard methodologies for measuring skin wetness and friction, identify strengths and limitations of different Trans-epidermal Water Loss (TEWL) devices, which measure the skin wetness, and build mathematical models on skin wetness and friction measurements.

For skin wetness measurements:
➤ The four different TEWL devices have been commissioned and calibrated
➤ Procedures for conducting and analyzing TEWL measurements for each device have been developed and practiced on one subject
➤ Three repeats experiments on each device under identical conditions on one subject have been measured
➤ Up to 8 young and 8 old subjects will be recruited for further measurements

For skin friction measurements:
➤ Methodologies for measuring skin friction have been developed and validated
➤ Measurements performed on four young subjects and results were investigated
➤ Up to 5 young and 8 old subjects will be recruited for further measurements

There was no adverse circumstances, subjects were and will be recruited as described on the application form.

Print Name:	**Signature:**	**Date:**
Dr Alan Cottenden		17/7/06

FOR OFFICE USE ONLY:

Approval

The continuing monitoring of this protocol has been reviewed and approved by the Committee. The re-approval date is .....1. AUGUST. 06.......... and is valid for 1 year from this date.

Date: 26/7/06

Please return completed form to:

Ms H
Secretary of the UCL Research Ethics Committee
Graduate School
North Cloisters, Wilkins Building
Gower Street
London
WC1E 6BT

Appendix B

Data protection for this work

UCL

UNIVERSITY COLLEGE LONDON
ESTATES AND FACILITIES DIVISION
RECORDS OFFICE
Gower Street, London WC1E 6BT

23 June 2005

Miss Rebecca Wong,
Department of Medical Physics & Bioengineering,
3rd Floor, Clerkenwell Building,
Archway Campus,
Highgate Hill,
London
N19 5LW

Dear Miss Wong,

Data Protection Registration

Thank you for your application for Data Protection Registration for your Project: "Physics of Wet Skin"

I am pleased to confirm that your Research Project will be covered by the UCL Data Protection Registration, reference no. Z6364106/2005/6/40, Section 19 Research: Medical Research.

Yours sincerely,

Records Manager, Data Protection Officer & FOI Officer

Appendix C

Evaporimetry device software

The following are description of the procedures for taking evaporimetry measurements using the software provided with each of the evaporimetry devices.

C1. Evaporimeter

1. Check that the Evaporimeter is **zero** on the LCD of the base unit before measurement

2. Open the **Workbench PC for Windows** program

3. Select **File**, and open the **Runsave.wbw** on the program

4. Select **Experiment, Experiment Setup** and change the frequency to **1 Hz**.

5. Select **File, Write File** to save the data to a desired path and filename.

6. Press **ON** on the Datalog window below the graph

7. Measurement can then be commenced by pressing the **Play button (▶)** on the top menu bar

8. Press the **Stop button (■)** to finish the experiment

9. The data will then be saved to your pre-selected path and filename

10. Process the data by opening the file in WordPad

11. Replace all commas with stops, then save the file

12. The file can now be opened with Excel for analysis

C2. DermaLab
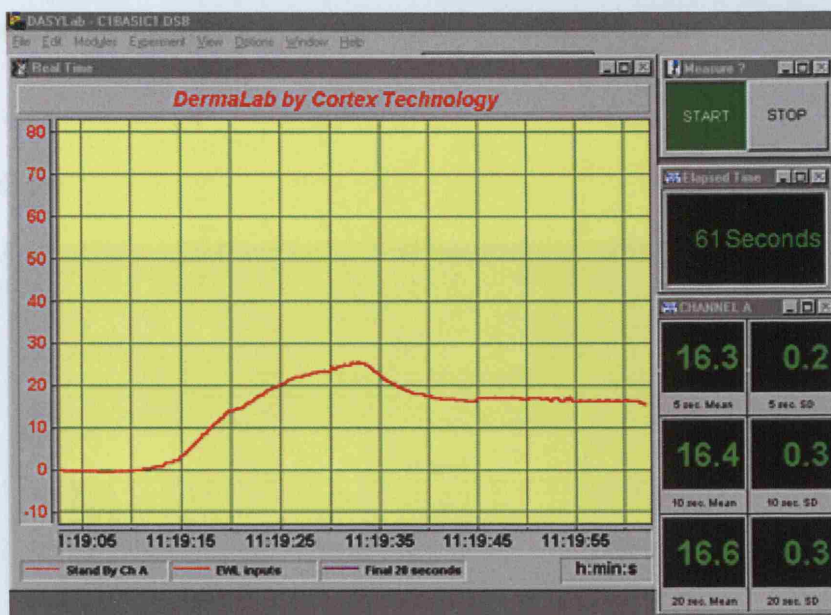
1. Open the **DASYLab** program

2. Select **File**, and open the file **cbasic1.dsb** on the program

3. Select **Experiment, Experiment Setup** and change the frequency to **1 Hz**.

4. Press **START** on the top right hand window to start collecting data from the probe, but you should not be able to see any change in number on the screen yet, even if you put your finger below the probe.

5. Go to the base unit of the DermaLab and press **START,** now you should be able to see fluctuations on the screen when you put your finger below the probe. However, the data is only showing on the screen and has not been recorded

6. Choose the duration you want the software to log data for from the drop-down window below the **START / STOP** window, the maximum continuously measurement allowed is 5 minutes

7. Measurement can then be commenced by pressing the **COLLECT** button on the top right hand window

8. The experiment will end when the time is up or the **STOP** button is pressed

9. A list of raw data will then appeared, put the cursor on top of the list and right click, select **Edit**, and **List to clipboard**

10. Open a Notepad file, paste the data and save the file

11. Measurement can be continued by repeating from **step 6**

12. The data saved on Notepad can be opened with Excel for analysis.

C3. Tewameter
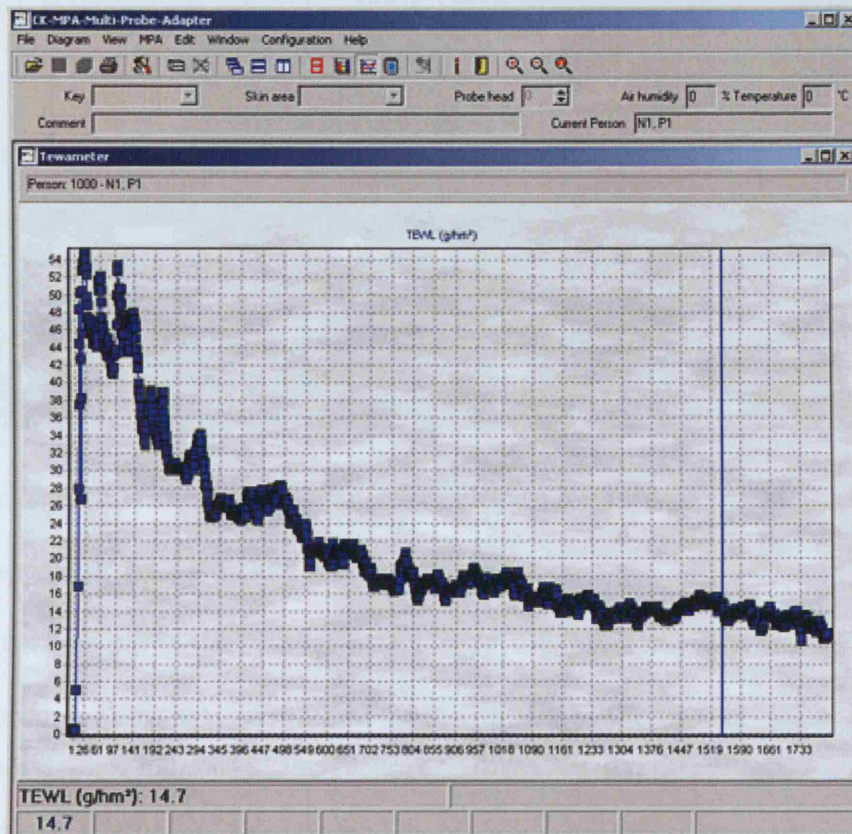
1. Open the **MPA** program, it will then recognise the probe(s) connected to the base unit

2. Select **Configuration**, **Options**. Under the **Tewameter** tab, choose **Normal** measuring mode; **continuous measurement** in measurement type, and the duration of the experiment can be pre-selected here in Stop events.

3. The heating option should not be registered in this study

4. Measurement can be started by pressing the green button on the side of the probe

5. Press the same side button to stop the experiment if no stop event has been selected

6. The cursor in the graph on the screen indicates the lowest standard deviation value from the data

7. Select **File, Save** to save the data in Excel format on your desired path and

filename.

C4. VapoMeter
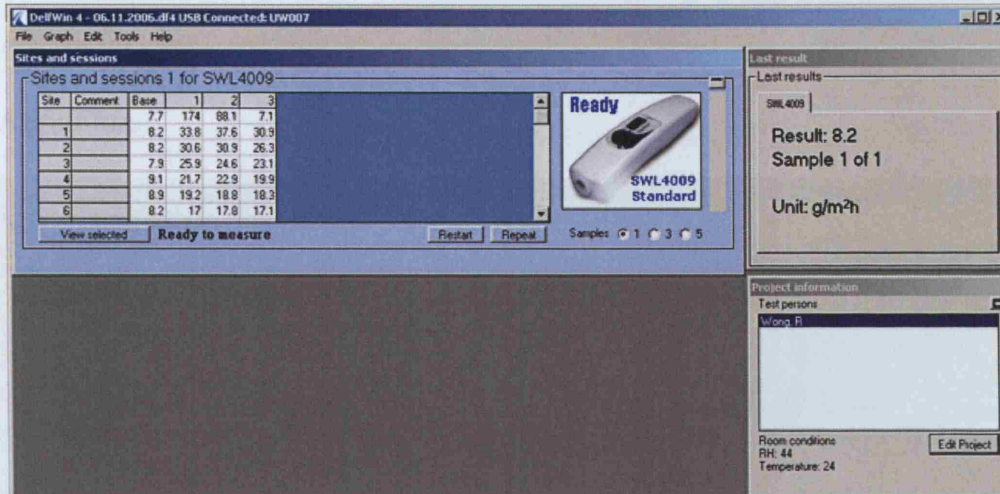
1.   Open the **DelfWin** program, then select **Create New Project**

2.   Choose the desired path and filename for the data

3.   You can then put in the details of the test person, project details and test sites

4.   The program will ask you to add an instrument to the project, select **VapoMeter,** put in the serial number of the probe, and press **Ready**

5.   A table of details you just put in will appear and you are allowed to change them here, when finished click **Close Edit**. Measurement is ready to commence.

6.   The program will look like the screenshot above, with a table of data to be measured

7.   Click on one of the cells in the table, start measurement by pushing the button on the probe

8.   When it finished, the result will appear on the cell and also be displayed on the right of the screen

9.   Repeat measurements can be selected below the VapoMeter picture, when selected, 3 or 5 measurements will be taken and averaged to be displayed on the selected cell on the table

10. The data can be exported into Excel for analysis by selecting **File, Export as, Excel file / Excel file with comments / Detailed excel file / Text file**. Excel file

and text file contain only averages of multiple samples. Excel file with comments contains comments for each measurement. Detailed excel file contains all individual measurements.

11.   The filename and the path of the exported file are shown on the screen. Click **OK**.

C5. AquaFlux
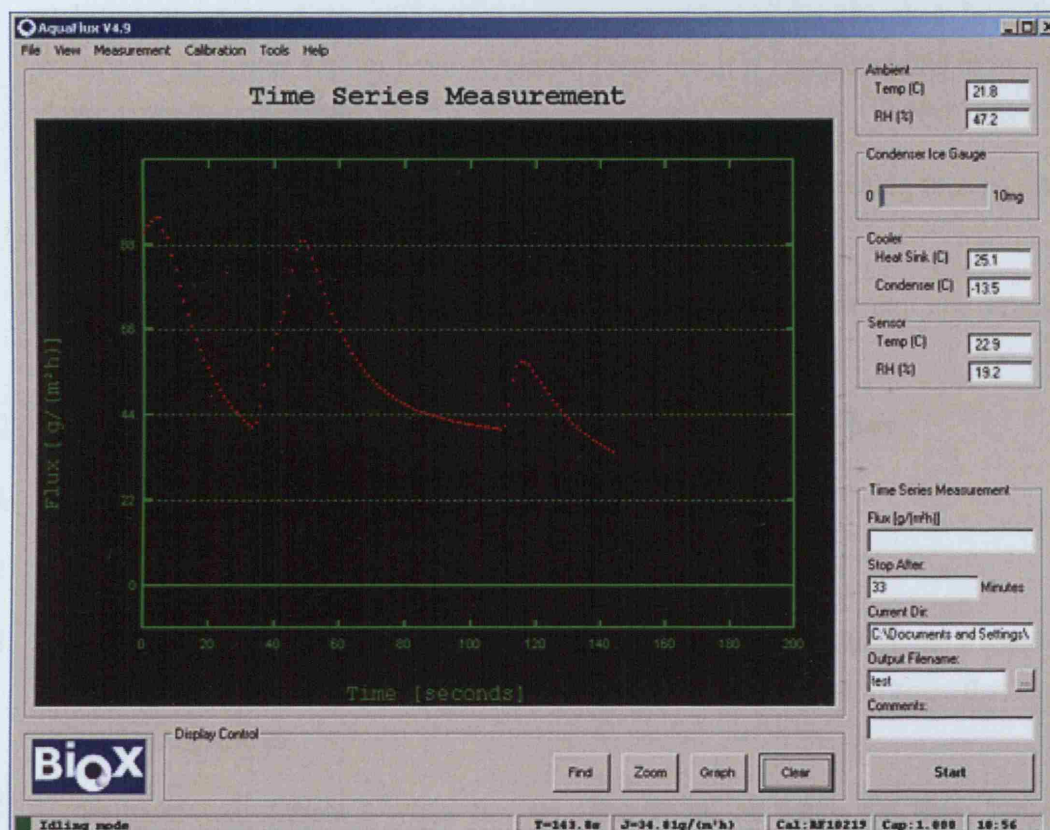
1.   Open the **AquaFlux** program, it will automatically detect the probe

2.   The probe should be in stand-by mode (showed by the orange colour LED on the base unit) with measurement cap fitted and the probe parked in the open position

3.   Switch on the probe by pressing the power button at the back of the base unit, you will then hear a fan noise coming from the probe, and the LED indicator will change from orange to blue

4.   Wait for about one minute while the condenser cools, before replacing the measurement cap with a calibration cap

5.   It should now be noted that the flux value on the curve on the program should decreases towards zero as the humidity sensor settles, the sorbed water in the

chamber walls desorbs and the materials in the vicinity of the condenser reach thermal equilibrium

6. Wait for another 30 minutes before priming the condenser by moving a clean dental stick over the surface of the condenser in a light scribing motion for 5-10 seconds, to convert super-cooled water to ice through mechanical disturbance, causing ice crystals to nucleate

7. After priming, wait until the baseline flux has stabilised again. The time it takes to stabilise depends on the amount of water vapour inside the chamber. In order to ensure all the water vapour have condensed into ice, it is recommended to leave the device running overnight

8. Once stable, perform a **Baseline Calibration** to set the flux reading to zero. Select **Calibration** and **Baseline Calibration**, then **Start**

9. The calibration cap can then be replaced by the measurement cap and ready for experiment.

10. Choose the desired path and filename on the **Output filename box**

11. Set the stopping time in minutes at the **Stop After** box

12. **Comments** can be added to the data before measurement starts

13. Measurement can then be commenced by pressing the **Start** button, the logged data will automatically be stored into your selected filename in the format that can be opened using Excel

14. Experiment will finished when the set time is up or when the **Stop** button is pressed

Appendix D

Results of the evaporimetry experiments

D1. Background TEWL results

The following graphs show background TEWL measurements on *different days* on Subject I:
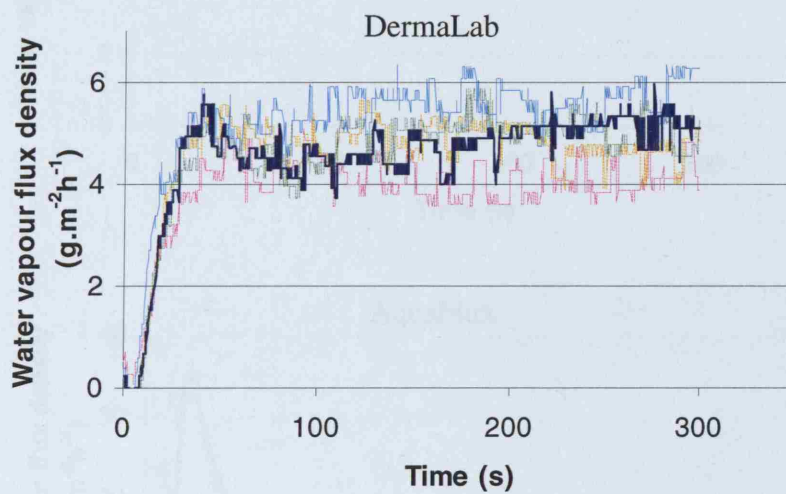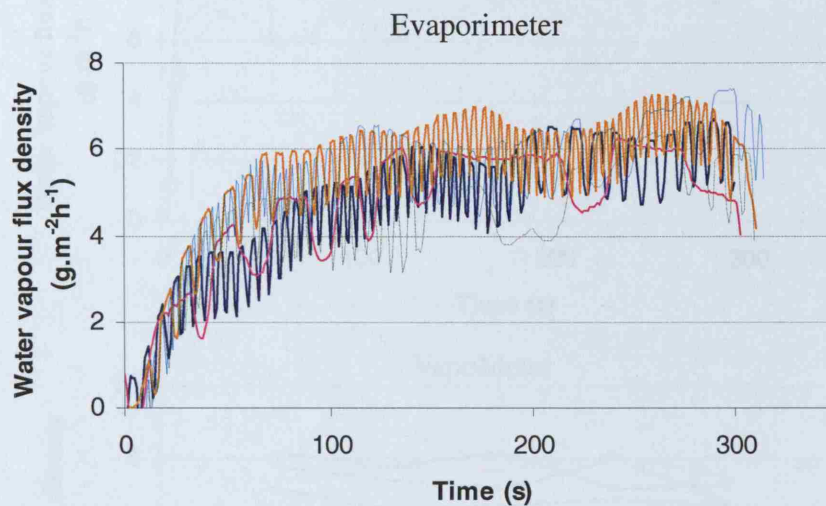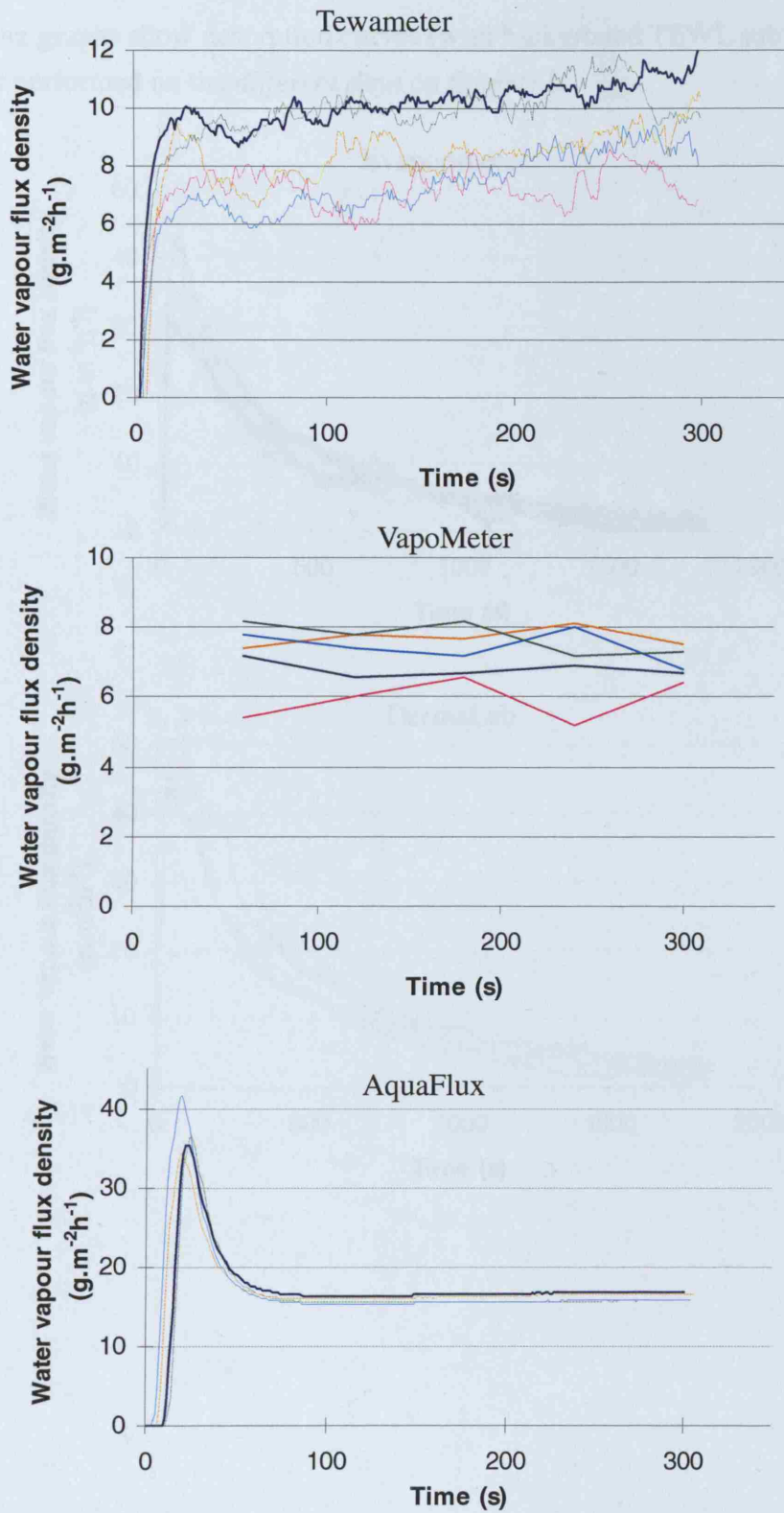
Fig D1 Results of background TEWL measured on *different days* on Subject I.

D2. SSWL results

The following graphs show desorption curves (with background TEWL subtracted) for experiments performed on the *different days* on Subject I:

Evaporimeter

DermaLab

Tewameter

VapoMeter

AquaFlux
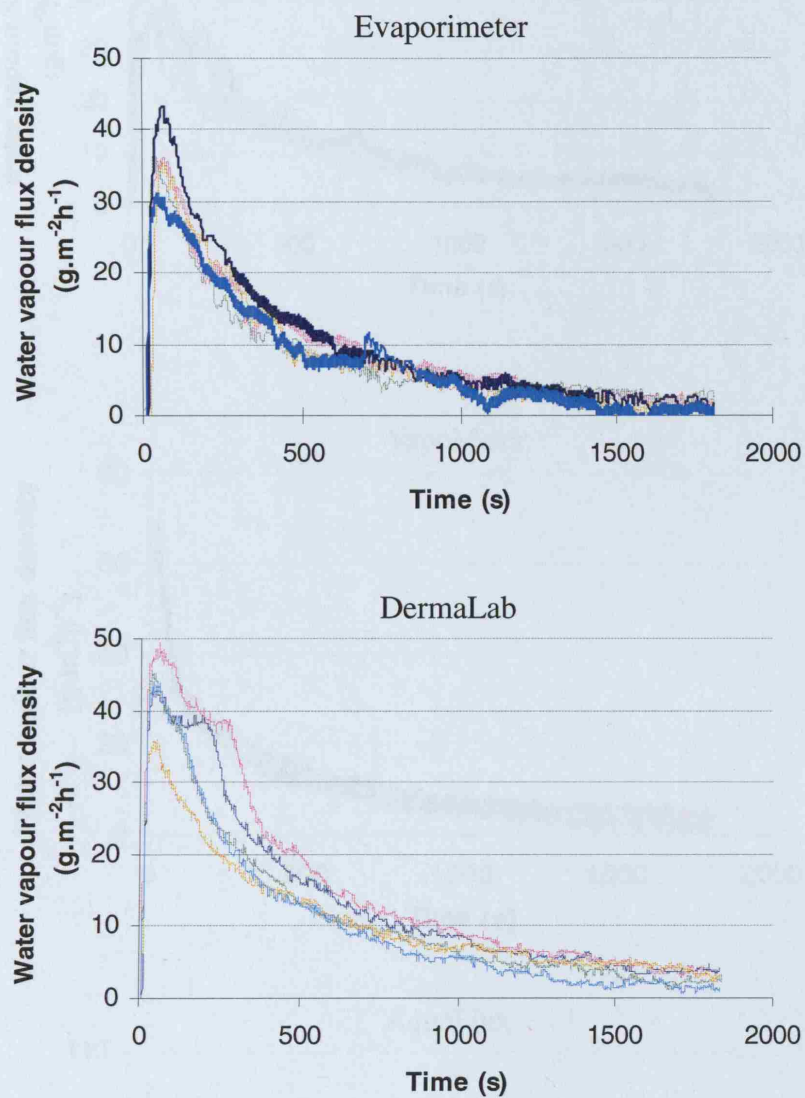
Fig D2 Results of SSWL measured on *different days* on Subject I.

Appendix E

Procedures and settings for the OTTER software

The following is the procedure for taking OTTER measurements using the OTTER software.
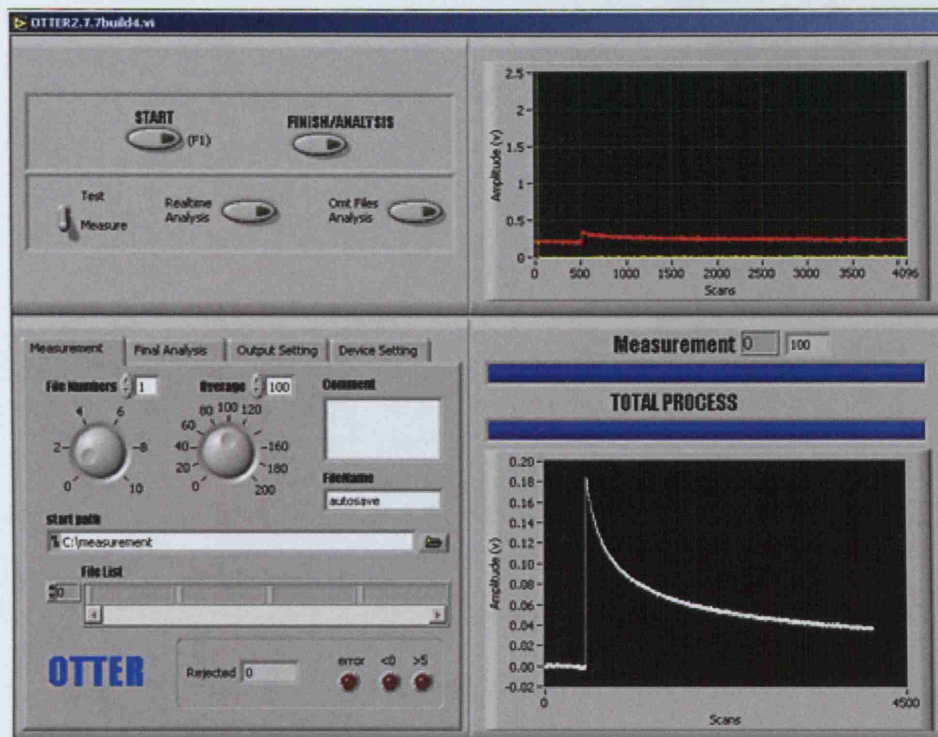
1. Open the **OTTER** program

2. Click on **Start Path** to set the path for saving the data

3. The filename of the saved data is changed on the **FileName** field prior to the experiment

4. Comments can be added to the data on the **Comment** box

5. **File Numbers** is the number of repeats for each measurement, and the **Average** is the number of laser pulse for each repeat, which will be averaged for analysis

6. The graph on top right shows the signal of each laser pulse, the graph on bottom right shows the average of the number of signals for each repeat

7. When the **Path**, **Filename**, **File Numbers** and **Average** is set, measurement is ready to commenced

8. Press the **START** button on the top or **F1** on the keyboard to start the measurement

9. When finished, press **Omt Files Analysis** button for analysis, a window will then pop up

10. Select Analysis, then choose the files and press Open. Analysis will then process and results are recorded into a Output.txt file.

Appendix F

Procedures and settings for the software for measuring friction

The following is the procedure for taking friction measurements using the software provided with the Dia-Stron Miniature Tensile Tester 170 (MTT170).

1.   In the MTT program, select **File**, then **New** (This provides a blank sheet).

2.   Select **Instrument**, **standard method** and then the **full option method** is open. Set the parameters shown below.

```
┌─ Full OptionsTest Method ──────────────────────────────────────── ✕ ┐
│                                                                      │
│  ┌─ Motion Options - Set Phase 1 & 3 Units ─┐  ┌─ Cycle Options ──────────────┐  │
│  │    ○ Units: %   ● Units: mm              │  │  Cycles:          [1    ]    │  │
│  │                                          │  │                              │  │
│  │  Sample Size (mm):       [3.  ]          │  │  ○ Start Each Cycle at Current Position │  │
│  │  Phase 1 Movement:       [0.  ]          │  │  ● Start Each Cycle at Origin Position  │  │
│  │  Phase 2 Static (sec):   [10. ]          │  └─ Gauge Force Options ─────────┐  │
│  │  Phase 3 Movement:       [30. ]          │     Gauge Force (gmf):   [0.  ]  │  │
│  │  Phase 4 Static (sec):   [0.  ]          │     ● Apply Gauging to First Cycle Only │
│  │  Rate (mm/min):          [150.]          │     ○ Apply Gauging to Each Cycle │  │
│  └──────────────────────────────────────────┘  └──────────────────────────────┘  │
│  ┌─ Force Range Options ────────────┐  ┌─ End of Method Options ───────────┐  │
│  │  Maximum Force (gmf):  [1000.]   │  │  ☐ Return Sample to Pick Up Position │  │
│  └──────────────────────────────────┘  └────────────────────────────────────┘  │
│  ┌─ Break Detection ────────────────┐  ┌─ Carousel Options ─────────────────┐  │
│  │  ● Disabled  [Edit Break Detection]│  │                                  │  │
│  │  ○ Enabled                        │  │                                  │  │
│  └──────────────────────────────────┘  └────────────────────────────────────┘  │
│                                                                      │
│     [ Cancel ]     [ Save ]     [ Run After Delay ]   [ Save & Run ]  │
└──────────────────────────────────────────────────────────────────────┘
```

3.   Select **Save and run**. The instrument will initialise and move to the 3mm start position. A dialogue box will have appeared saying *Load sample-continue with method?* Select **Yes** and the measurement will commence.

4.   When the first reading is finished, take subsequent readings by selecting **Instrument**, **standard method** and **save and run** and **yes** (i.e. follow the same procedure as for the first measurement).

5.   To save the file at the end of the measurement period, choose **save as** and save.

6.   To export into another program (e.g. MS Excel) select **Analysis, convert data points to ASCii tool** and choose **OK**. Click **Start**, you will then be prompted to save the file in your directory as a .txt file and click **OK**. You have successfully converted the files to .txt files so they can be opened in other programs.

Appendix G

Analysis of friction on convex prisms

Cottenden (2007) found a general solution for convex prisms for finding μ_s from F_1 and F_2 of the curved configuration (Fig 6.1b):

$$\mu_s = \frac{\ln(F_1/F_2)}{\tan^{-1}[R'(0)/R(0)] - \tan^{-1}[R'(\Theta)/R(\Theta)] + \Theta} \quad \ldots\ldots\ldots \text{Equation G1}$$

where the first contact of the fabric with the skin defines $\Theta = 0$, Θ is the angle over which the fabric contacts the skin; the radial function $R(\Theta)$ gives the distance from an arbitrary centre of the arm to the surface in terms of the angle Θ (Fig G1).

Fig G1. Illustration of the curved configuration, where $F_1 > F_2$.

If tangents are drawn to the curve of $R(\Theta)$ at 0 and Θ, perpendicular bisectors are constructed, and if the intersect is chosen as the co-ordinate centre, then $R(0)$ and $R(\Theta)$ from the Eq G1 above would become 0 and Eq G1 reduces to the same equation as Eq 6.1.

$$\mu_s = \frac{\ln(F_1/F_2)}{\Theta} \quad \ldots\ldots\ldots\ldots\ldots \text{Equation G2}$$

This mathematical model showed that Eq 6.1 can be used to extract the μ on any shape of arm as long as the surface of the arm is a convex prism.

Appendix H

Skevos Karavokiros' MSc project

(supervised by Wong and Cottenden)

The mathematical model introduced by Cottenden (2007) in Appendix G was investigated further in a Master of Science (MSc) project (Karavokiros, 2007) co-supervised by the author. The aim of the project was to investigate the model experimentally using a variety of surrogate arm shapes.

The surrogate arms were made by putting a steel studding rod into some plaster of Paris (moulded into different shapes), and wrapped by a piece of 1 mm thick Neoprene (Fig H1a). The project started with the simplest shape – a uniform circular cylinder, then a uniform ellipse in different orientations (vertical, 45° and horizontal), followed by cones of different angles (Fig H1b), and finally a replica of a real arm shape (Fig H2).

The real arm replica was made based on the laser scan of a real arm (Fig 6.10b). The scan was used to make a real arm replica on a rapid prototyping machine, smoothed by emery paper and plaster of Paris before wrapping it with the Neoprene (Fig H2).
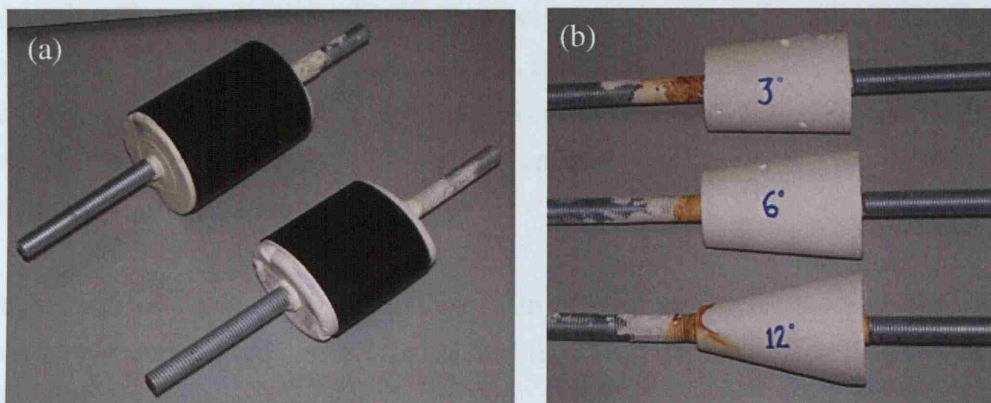
Fig H1. Surrogate arms made from plaster of Paris in (a) uniform circular cylinder and ellipse covered with Neoprene; (b) cones of different angles (3°, 6 ° and 12 °) before covering with Neoprene.
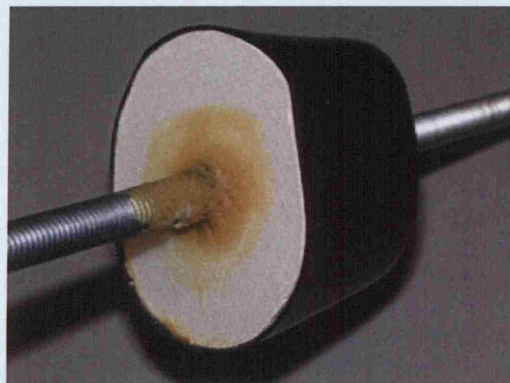
Fig H2 Replica of real arm for measurements.
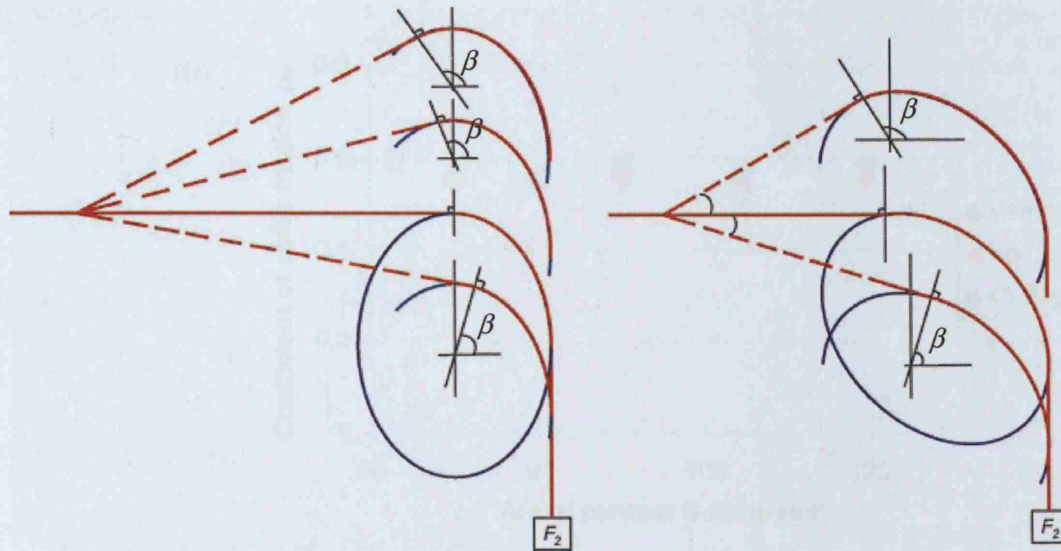
Fig H3. Illustration of uniform ellipse in vertical (left) and 45° (right) orientation for various arcs of contact by adjusting the height of the arm.

By changing F_2 and adjusting the vertical height of the surrogate arm, i.e. varying the arc of contact by the fabric β of Eq 6.1 (as illustrated on Fig H3), the coefficients of static friction μ_s, for the given arc of contacts could be found. If the mathematical model was valid, the μ_s measured for all the arc of contacts used on the surrogate arms would be expected to be the same.

The means of the coefficients of static friction of five repeats for the five different arcs of contact measured were plotted for each of the surrogate arms used (Fig H4, error bar is $\pm$ 1 standard deviation).

(a)
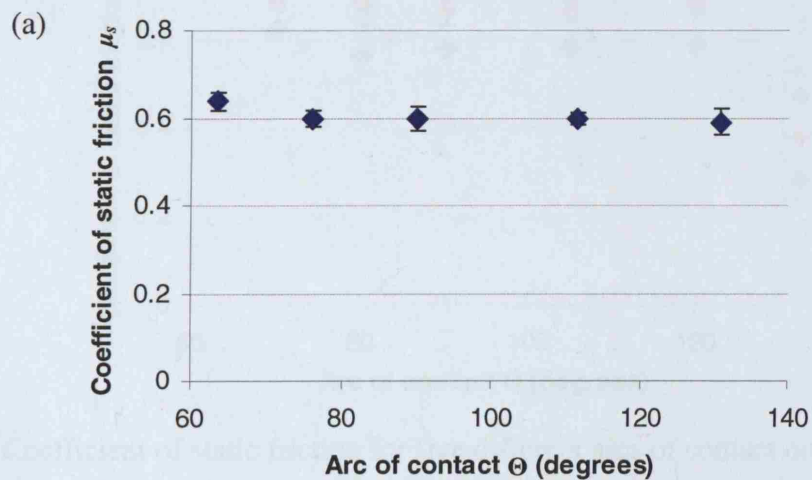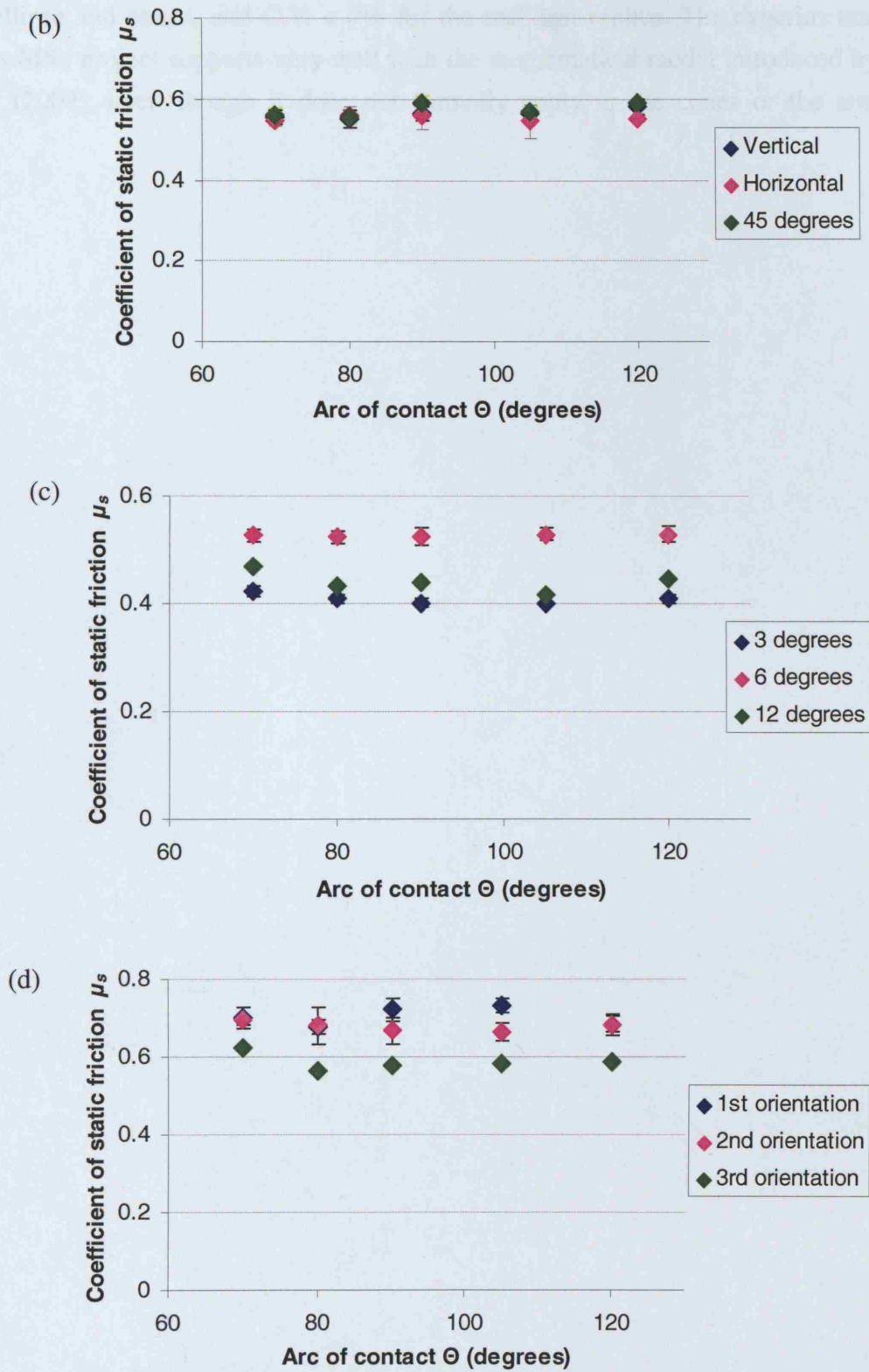
Fig H4. Coefficient of static friction for five different arcs of contact on (a) uniform circular cylinder; (b) uniform ellipse in different orientation (vertical, 45° and horizontal); (c) cones of different degrees and (d) replica of real arm shape.

The results showed a constant coefficient of static friction with C.V. < 5% for circular cylinder, ellipse and cones; and C.V. < 7% for the real arm replica. The experimental data in this MSc project supports very well with the mathematical model introduced by Cottenden (2007), even though it does not formally apply to the cones or the arm replica.

REFERENCES

(Abrams et al., 2002) **Abrams, P., Cardozo, L., Khoury, S., Wein, A. eds.** (2002) Incontinence. Report of the Second International Consultation, second ed. Health Publications Ltd.

(Abrams et al., 2005) **Abrams, P., Cardozo, L., Khoury, S., Wein, A. eds.** (2005) Incontinence: Volume 1 - Basics & Evaluation.

(Agner and Serup, 1993) **Agner, T. and Serup, J.** (1993) Time course of occlusive effects on skin evaluated by measurement of transepidermal water loss (TEWL). Including patch tests with sodium lauryl sulphate and water. *Contact Dermatitis.* **28**(1), 6-9.

(Akin et al., 1997) **Akin, F., Lemmen, J., Bozarth, D., Garofalo, M., Grove, G.** (1997) A refined method to evaluate diapers for effectiveness in reducing skin hydration using the adult forearm. *Skin Research and Technology*, **3**, 173-176.

(Alanen et al., 2003) **Alanen, E., Wiesemann, F., Nuutinen, J. and Lahtinen, T.** (2003) Measurement of skin hydration in the diapered area of infants with a closed chamber TEWL meter. *Skin Research and Technology.* **9**(2), 199.

(Aly et al., 1987) **Aly, R., Shirley, C., Cunico, B., Maibach, H.I.** (1978) Effect of prolonged occlusion on the microbial flora, pH, carbon dioxide and transepidermal water loss on human skin. *Journal of Investigative Dermatology.* **71**(6), 378-381.

(Amontons, 1706) **Amontons, G.** (1706) De la résistance causée dans les machines. Memoires de l'Academie Royale (1699), A. Chez, Gerard Kuyper, Amsterdam. 161.

(Anderson, 1997) **Anderson, C. H.** (1997) Analysis of contact stresses due to combined bending and sliding of high-performance fibers. *Mechanics of Composite Materials.* **33**(2), 101–106.

(Arimoto et al., 2005)	**Arimoto, H., Egawa, M. and Yamada, Y.** (2005) Depth profile of diffuse reflectance near-infrared spectroscopy for measurement of water content in skin. *Skin Research and Technology.* **11**, 27-35.
(Asserin et al., 2000)	**Asserin, J., Zahouani, H., Humbert, P., Couturaud, V. and Mougin, D.** (2000) Measurement of the friction coefficient of the human skin in vivo. Quantification of the cutaneous smoothness. *Colloid and Surfaces B: Biointerfaces,* **19**(1), 1-12.
(ASTM-E96, 1995)	**ASTM-E96 - 95.** (1995) Standard test methods for water vapour transmission of materials. *American Society for Testing and Materials.* E96 – 95.
(Attas et al., 2002)	**Attas, E.M., Sowa, M.G., Posthumus, T.B., Schattka, B., Mantsch, H.H. and Zhang, S.L.** (2002) Near-IR spectroscopic imaging for skin hydration: the long and the short of it. *Biopolymers.* **67**(2), 96-106
(Barel and Clarys, 1995a)	**Barel, A.O. and Clarys, P.** (1995) Measurement of Epidermal Capacitance. *In Serup J., Jemec G.B.E., eds. Handbook of Non-Invasive Methods and the Skin. Boca Raton: CRC Press.* 165-170.
(Barel and Clarys, 1995b)	**Barel, A.O. and Clarys, P.** (1995) Comparison of methods for measurement of transepidermal water loss. *In Serup J., Jemec G.B.E., eds. Handbook of Non-Invasive Methods and the Skin. Boca Raton: CRC Press.* 179-184.
(Bashir et al., 2001)	**Bashir, S.J., Chew, A.L., Anigbogu, A., Dreher, F., Maibach, H.I.** (2001) Physical and physiological effects of stratum corneum tape stripping. *Skin Research and Technology.* **7**(1), 40-48
(Behl et al., 1980)	**Behl, C.R., Flynn, G.L., Kurihara, T., Harper, N., Smith, W., Higuchi, W.I., Ho, N.F., Pierson, C.L.** (1980) Hydration and percutaneous absorption: I. Influence of hydration on alkanol permeation through hairless mouse skin. *Journal of Investigative Dermatology.* **75**(4), 346-52.
(Berardesca, 1997)	**Berardesca, E and the EEMCO Group.** (1997) EEMCO guidance for the assessment of stratum corneum hydration: electrical methods. *Skin Research and Technology.* **3**, 126-132.

(Berg et al., 1986)   **Berg, R.W., Buckingham, K.W., and Stewart, R.L.** (1986) Etiologic factors in diaper dermatitis: the role of urine. *Pediatric Dermatology.* 3(2), 102-106.

(Berg, 1987)   **Berg, R.W.** (1987) Etiologic factors in diaper dermatitis: a model for development of improved diapers. *Pediatrician.* 14(1), 27-33.

(Berg, 1988)   **Berg, R.W.** (1988) Etiology and pathophysiology of diaper dermatitis. *Advances in Dermatology.* 3, 75-98.

(Blank, 1953)   **Blank, I.H.** (1953) Further observations on factors which influence the water content of the strum corneum. *Journal of Investigative Dermatology.* 21, 259-269.

(Blank et al., 1984)   **Blank, I.H., Moloney, J. 3rd, Emslie, A.G., Simon, I., Apt, C.** (1984) The diffusion of water across the stratum corneum as a function of its water content. *Journal of Investigative Dermatology.* 82(2), 188-194.

(Blichmann and Serup, 1987)   **Blichmann, C.W. and Serup, J.** (1987) Reproducibility and variability of transepidermal water loss measurement. Studies on the Servo Med Evaporimeter. *Acta Dermato-Venereologica.* 67(3), 206-210.

(Bowden and Tabor, 1956)   **Bowden, F.P. and Tabor, D.** (1956) Friction and Lubrication. *Worsnop B.L. eds. Methuen & Co. LTD., London.*

(Bowden and Tabor, 1964)   **Bowden, F.P. and Tabor, D.** (1964) The friction and lubrication of solids Part II. *Oxford University Press, London.*

(Buckingham and Berg, 1986)   **Buckingham, K.W. and Berg, R.W.** (1986) Etiologic factors in diaper dermatitis: the role of feces. *Pediatric Dermatology.* 3(2), 107-112.

(Cameron et al., 1997)   **Cameron, B., Brown, D.M., Dallas, M.J. and Brandt, B.** (1997) Effect of natural and synthetic fibers and film moisture content on stratum corneum hydration in an occlusive system. *Textile Research Journal.* 67, 585-592.

(Campbell et al., 1977)   **Campbell, S.D., Kraing, K.K., Schibli, E.G. and Momii, S.T.** (1977) Hydration characteristics and electrical resistivity of stratum corneum using a non-invasive four-point electrode method. *Journal of Investigative Dermatology.* 69, 290-295.

(Campbell, 1987)

Campbell, R.L. (1987) Clinical tests with improved disposable diapers. *Pediatrician.* **14** Suppl 1, 34-38.

(Ciortea et al., 2002)

Ciortea, L., Fonseca, E., Sarramagnan, J. and Imhof, R.E. TEWL and stratum corneum hydration changes caused by prolonged contact with a TEWL measurement head. *In: Marks, R., Leveque, J.L., Voegeli, R,. eds. The essential stratum corneum.* London, Martin Dunitz Ltd: 255-257.

(Clar et al., 1975)

Clar, E.J. Her, C.P. and Sturelle, C.G. (1975) Skin impedance and moisturization. *Journal of the Society of Cosmetic Chemists.* **26**, 337-353.

(Comaish and Bottoms, 1971)

Comaish, S. and Bottoms, E. (1971) The skin and friction: deviations from Amonton's laws, and the effects of hydration and lubrication. *British Journal of Dermatology*, **84**(1), 37-43.

(Comaish et al., 1973)

Comaish, J.S., Harborow, P.R. and Hofman, D. (1973) A hand-held friction meter. *British Journal of Dermatology*, **89**(1), 33-35.

(Cottenden et al., 1998)

Cottenden, A.M., Dean, G.E., Brooks, R.J., Haines-Nutt, R.F., Rothwell, J.G., and Penfold, P.H. (1998) Disposable bedpads for incontinence: predicting their clinical leakage properties using laboratory tests. *Medical Engineering and Physics*, **20**, 347-359.

(Cottenden, 2007)

Cottenden, A.M., Cottenden, D.J., Karavokiros, S. and Wong, W.K.R. Development and experimental validation of a mathematical model for friction between fabrics and a volar forearm phantom. Submitted to *Journal of Engineering in Medicine.*

(Cowen et al., 2001)

Cowen, J.A., Imhof, R.E. and Xiao, P. (2001) Opto-thermal measurement of stratum corneum renewal time. *Analytical Sciences.* **17** Special Issue, s353-s356.

(Cua et al., 1990)

Cua, A.B., Wilhelm, K.P. and Maibach, H.I. (1990) Frictional properties of human skin: relation to age, sex and anatomical region, stratum corneum hydration and transepidermal water loss. *British Journal of Dermatology.* **123**(4), 473-479.

(Cua et al., 1995)

Cua, A.B., Wilhelm, K.P. and Maibach, H.I. (1995) Skin surface lipid and skin friction: relation to age, sex and anatomical region. *Skin Phamacology,* **8**(5), 246-251.

(Cui et al., 2005) **Cui, Y., Xiao, P. and Imhof, R.E.** (2005) Opto-thermal mathematical modeling and inverse depth profiling using genetic algorithm. *International Journal of Thermophysic.* **26**(1), 213-220.

(Dallas and Wilson, 1992) **Dallas, M.J. and Wilson, P.A.** (1992) Adult incontinence products: performance evaluation on healthy skin. *INDA Journal of Nonwovens Research.* **4**, 26-32.

(Davis et al., 1989) **Davis, J.A., Leyden, J.J., Grove, G.L., Raynor, W.J.** (1989) Comparison of disposable diapers with fluff absorbent and fluff plus absorbent polymers: effects on skin hydration, skin pH, and diaper dermatitis. *Pediatric dermatology.* **6**(2), 102-108.

(De Paepe et al., 2005) **De, Paepe K., Houben, E., Adam, R., Wieswmann, F. and Rogiers, V.** (2005) Validation of the VapoMeter, a closed unventilated chamber system to assess transepidermal water loss vs. the open-chamber Tewameter. *Skin Research and Technology.* **11**, 61-69.

(DOH, 2000) **Department of Health (DOH).** (2000) Good practice in Continence Services. *Department of Health,* London. 7-8.

(deRigal et al., 1993) **deRigal, J., Losch, M.J., Bazin, R., Camus, C., Sturelle, C., Descamps, V. And Leveque, J.L.** (1993) Near-infrared spectroscopy: A new approach to the characterization of dry skin. *Journal of the Society of Cosmetic Chemists.* **44**, 197-209.

(Doubal and Klemera, 1998) **Doubal, S. and Klemera, P.** (1998) Changes in mechanical properties of skin as a marker of biological age. *Sborník lékařský.* **99**(4), 423-428.

(Dowson, 1997) **Dowson, D.** (1997) Tribology and the Skin Surface. *In: Wilhelm K-P, Elsner P, Berardesca E and Maibach H, eds. Bioengineering of the skin: skin surface imaging and analysis. Boca Raton: CRC Press.* 159-179.

(du Vivier, 1992) **du Vivier, A.** (1992) Contact dermatitis. *In: Dermatology in practice. Gower Medical Publishing, London.*

(Ebling, 1992) **Ebling, F.J.G.** (1992) Functions of the skin. *In: Champion R.H., Burton J.L., Ebling F.J.G. eds. Textbook of dermatology. Blackwell Scientific Publications, Oxford.*

| (Egawa et al., 2002a) | **Egawa, M., Oguri, M., Hirao, T., Takahashi, M. and Miyakawa, M.** (2002) The evaluation of skin friction using a frictional feel analyzer. *Skin Research and Technology,* 8(1), 41-51. |

(Egawa et al., 2002b) **Egawa, M., Oguri, M., Kuwahara, T. and Takahashi, M.** (2002) Effect of exposure of human skin to a dry environment. *Skin Research and Technology,* 8(4), 212-218.

(El-Shimi, 1977) **El-Shimi, A.F.** (1977) In vivo skin friction measurements. *Journal of the Society of Cosmetic Chemists,* 28, 37-51

(Elias et al., 1981) **Elias, P.M., Cooper, E.R., Korc, A., Brown, B.E.** (1981) Percutaneous transport in relation to stratum corneum structure and lipid composition. *Journal of Investigative Dermatology.* 76(4), 297-301.

(Elkhyat et al., 2004) **Elkhyat, A., Courderot-Masuyer, C., Mac-Mary, S., Courau, S., Gharbi, T., Humbert, P.** (2004) Influence of the hydrophobic and hydrophilic characteristics of sliding and slider surfaces on friction coefficient: in vivo human skin friction comparison. *Skin Research and Technology.* 10, 215-221

(Elsner et al., 1990) **Elsner, P., Wilhelm, D. and Maibach, H.I.** (1990) Frictional properties of human forearm and vulvar skin: influence of age and correlation with transepidermal water loss and capacitance. *Dermatologica,* 181(2), 88-91.

(Ersser et al., 2005) **Ersser, S.J., Getliffe, K., Voegeli, D. and Regan, S.** (2005) A critical review of the inter-relationship between skin vulnerability and urinary incontinence and related nursing intervention. *International Journal of Nursing Studies,* 42, 823-835.

(Fader, 2005) **Fader, M.** Private communication.

(Fader et al., 2007) **Fader, M., Clarke-O'Neill, S., Wong, W.K.R., Runeman, B. and Cottenden, A.M.** Review and development of methods for quantifying excess water in over-hydrated skin using evaporimetry. Submitted to *Skin Research and Technology.*

(Fluhr et al., 1999)	**Fluhr, J.W., Lazzerini, S., Distante, F., Gloor, M., Berardesca, E.** (1999) Effects of prolonged occlusion on stratum corneum barrier function and water holding capacity. *Skin Pharmacology and Applied Skin Physiology*, **12**(4), 193-198.
(Fluhr et al., 2003)	**Fluhr, J.W., Bankova, L., Elias, P.M. and Feingold, K.R.** (2003) Assessment of permeability barrier function measuring transepidermal water loss: comparing 3 closed-loop systems and 4 open-loop systems in vivo and in vitro. *Skin Research and Technology.* **9**(2), 164.
(Gitis and Sivamani, 2004)	**Gitis, N. and Sivamani, R.** (2004) Tribometrology of skin. *Tribology Transactions,* **47**, 1-9.
(Gray, 2000)	**Gray, J.** (2000) The World Of Skin Care: A Scientific Companion. Milady Publishing.
(Grice, 1980)	**Grice, K.A.** (1980) Transepidermal water loss. *In: Jarrett A. eds. The Physiology and Pathophysiology of the Skin. London. Academic Press.* 2115-2146.
(Grove et al., 1998)	**Grove, G.L., Lemmen, J.T., Garafalo, M., Akin, F.J.** (1998) Assessment of skin hydration caused by diapers and incontinence articles. *Current Problems in Dermatology.* **26**, 183-195.
(Grove et al., 1999)	**Grove, G.L., Grove, M.J., Zerweck, C., Pierce, E.** (1999) Comparative metrology of the Evaporimeter and the DermaLab TEWL Probe. *Skin Research and Technology.* **5**(1), 1-8.
(Grubauer et al., 1989)	**Grubauer, G, Elias, P.M. and Feingold, K.R.** (1989) Transepidermal water loss: the signal for recovery of barrier structure and function. *Journal of Lipid Research.* **30**, 323-333.
(Guo et al., 2001a)	**Guo, X., Ciortea, L.I, Chilcott, R.P., Imhof, R.E., Xiao, P.** (2001) Opto-thermal measurements of barrier cream residence time on skin in-vivo. *Analytical Sciences.* **17**, s346-s348.
(Guo et al., 2001b)	**Guo, X., Imhof, R.E. and de Rigal, J.** (2001) Spectroscopic study of water-keratin interactions in stratum corneum. *Analytical Sciences.* **17**, s342-s345.

(Gwosdow et al., 1986)

Gwosdow, A.R., Stevens, J.C., Berglund, L.G., Stolwijk, J.A.J. (1986) Skin friction and fabric sensation in neutral and warm environments. *Textile Research Journal.* **56**, 574-580.

(Hammarlund and Sedin, 1979)

Hammarlund, K. and Sedin, G. (1979) Transepidermal water loss in newborn infants. III. Relation to gestational age. *Acta Paediatrica Scandinavica.* **68**, 795-801.

(Hatch et al., 1987)

Hatch, K.L., Wilson, D.R. and Maibach, H.I. (1987) Fabric-caused changes in human skin: in vivo stratum corneum water content and water evaporation. *Textile Research Journal.* **57**(10), 583-591.

(Hatch et al., 1992)

Hatch, K.L., Markee, N.L., Prato, H.H., Zeronian, S.H., Maibach, H.I., Kuehl, R.O. and Axelson, R.D. (1992) In vivo cutaneous and perceived comfort response to fabric. Part V: effect of fiber type and fabric moisture content on stratum corneum hydration. *Textile Research Journal.* **62**(11), 638-647.

(Hatch et al., 1997)

Hatch, K.L., Prato, H.H., Zeronian, S.H., and Maibach, H.I. (1997) *In vivo* cutaneous and preceived comfort response to fabric part VI: the effect of moist fabrics on stratum corneum hydration. *Textile Research Journal.* **67**(12), 926-931

(Highley et al., 1977)

Highley, D.R., Coomey, M., DenBeste, M., Wolfram, L.J. (1977) Frictional properties of skin. *Journal of Investigative Dermatology,* **69**, 303-305.

(Hills et al., 1994)

Hills, R.J., Unsworth, A. and Ive, F.A. (1994) A comparative study of the frictional properties of emollient bath additives using porcine skin. *British Journal of Dermatology,* **130**(1), 37-41.

(Holbrook, 1979)

Holbrook, K.A. (1979) Human epidermal embryogenesis. *International Journal of Dermatology.* **18**, 329-356.

(Hong et al., 2005)

Hong, K.H., Kim, S.C. and Kang, T.J. (2005) Effect of abrasion and absorbed water on the handle of nonwovens for disposable diapers. *Textile Research Journal,* **75**(7), 544-550.

(Imhof et al., 1984)

Imhof, R.E., Birch, D.J.S., Thornley, F.R., Gilchrist, J.R. and Strivens, T.A. (1984) Optothermal transient emission radiometry. *Journal of Physics E: Scentific Instruments.* **17**, 521-525.

(Imhof et al., 1990) **Imhof, R.E., Whitters, C.J. and Birch, D.J.S.** (1990) Opto-thermal *in vivo* monitoring of sunscreens on skin. *Physics in Medicine and Biology*, **35**, 95-102.

(Imhof et al., 1999) **Imhof, R.E., O'Driscoll, D., Xiao, P. and Berg, E.P.** (1999) New sensor for water vapour flux. In: *Sensors and their applications X*. Eds: Augousti A.T. and White N.M.: Institute of Physics, 173-177.

(Imhof, 2001) **Imhof, R.E.** (2001) Method and equipment for measuring water vapor flux from surfaces. US Patent 6439028.

(Imhof et al., 2002) **Imhof, R.E., Berg, E.P., Chilcott, R.P., Ciortea, L.I., Pascut, F.C., Xiao, P.** (2002) New instrument for measuring water vapour flux density from arbitrary surfaces. *IFSCC Magazine.* **5**(4), 297-301.

(Imhof et al., 2004) **Imhof, R.E., de Jesus, M.E.P, Xiao, P. and the TEWL Calibration Consortium.** (2004) Mathematical analysis of ASTM-96 based TEWL calibration method. ISBS Meeting, Orlando.

(Jacques, 1997) **Jacques, S.L.** (1997) A linear measurement of water content of the stratum corneum of human skin using a microwave probe. IEEE Engineering in Medicine and Biology Society. 1st Annual Conference, Denver, Colorado. 180.

(Johanson and Lafferty, 1996) **Johanson, J.F. and Lafferty, J.** (1996) Epidemiology of fecal incontinence: the silent affliction. *American Journal of Gastroenterology.* **91**, 33-36.

(Johnson et al., 1993) **Johnson, S.A., Gorman, D.M., Adams, M.J. and Briscoe B.J.** (1993) The friction and lubrication of human stratum corneum. *In: Dowson D, et al., eds. Thin Films in Trbology. Proceedings of the 19th Leeds-Lyon Symposium on Tribology.* Elsevier. 663-672.

(Karavokiros, 2007) **Karavokiros, S.** (2007) Skin friction: validating a mathematical model with a simple laboratory model. *MSc report, UCL.*

(Kenins, 1994) **Kenins, P.** (1994) Influence of fibre type and moisture on measured fabric-to-skin friction. *Textile Research Journal,* **64**(12), 722-728.

(Kondo, 2002a) **Kondo, S.** (2002) The frictional properties between fabrics and the human skin Part 1: Factors of human skin characteristics affecting the frictional properties between fabrics and the human skin. *Journal of the Japan Research Association for Textile End-Uses.* **43**(5), 264-275.

(Kondo,   **Kondo, S.** (2002) The frictional properties between fabrics and the
2002b)   human skin Part 2: Influences of stratum corneum water content,
               hardness of skin, friction pressure, and friction speed on the frictional
               properties. *Journal of the Japan Research Association for Textile
               End-Uses.* **43**(5), 305-321.

(Koudine et al., **Koudine, A.A., Barquins, M., Anthoine, P.H., Aubert, L. and**
2002)   **Leveque, J.L.** (2002) Frictional properties of skin: proposal of a new
               approach. *International Journal of Cosmetic Science,* **22,** 11-20.

(Kuss and   **Kuss, O. and Diepgen, T.L.** (1998) Proper statistical analysis of
Diepgen, 1998) transepidermal water loss (TEWL) measurements in bioengineering
               studies. *Contact Dermatitis.* **39**(2), 64-67.

(Lévêque and   **Lévêque, J.L. and de Rigal, J.** (1983) Impedance methods for
de Rigal, 1983) studying skin moisturization. *Journal of the Society of Cosmetic
               Chemists.* **34,** 419-428.

(Lévêque,   **Lévêque, J.L.** (2004) Water-keratin interactions. In: *Bioengineering
2004)   of the skin: Water and the stratum corneum.* Eds. Elsner P.,
               Berardesca E. & Maibach H.I.: CRC Press, Boca Raton, 13-22.

(Loden, et al., **Loden, M., Olsson, H., Axell, T. and Linde, Y.W.** (1992) Friction,
1992)   capacitance and transepidermal water loss (TEWL) in dry atopic and
               normal skin. *British Journal of Dermatology,*   **126**(2), 137-141.

(Manukiatti et **Manuskiatti, W., Schwindt, D.A., Maibach, H.I.** (1998) Influence
al., 1998)   of age, anatomic site and race on skin roughness and scaliness.
               Dermatology. **196**(4), 401-407.

(Markee et al., **Markee, N. L., Hatch, K. L., Prato, H. H., Zeronian, S. H., and**
1993)   **Maibach, H. I.** (1993) Effect of fiber type and fabric moisture content
               on the hydration state of human stratum corneum. *Journal of Thermal
               Biology.* **18**(5/6), 421-427.

(Martin, 1993) **Martin, K.A.** (!993) Direct measurement of moisture in skin by NIR
               spectroscopy. *Journal of the Society of Cosmetic Chemists.* **44,**
               249-261.

(Martin, 1998) **Martin, K.A.** (1998) In vivo measurements of water in skin by
               near-infrared reflectance. *Applied Spectroscopy.* **52**(7), 1001-1007.

(Mathias et al., 1981)   **Mathias, C.G.T., Wilson, D.M. and Maibach, H.I.** (1981) Transepidermal water loss as a function of skin temperature. *Journal of Investigative Dermatology.* 77, 219-220.

(Medical Devices Agency, 2003)   **Medical Devices Agency (UK)** (2003) A survey of continence products use in residential settings. *Disability Equipment Assessment Report No. IN.10.*

(Montagna, 1961)   **Montagna, W.** (1961) *The structure and function of skin. 2nd ed. Academic Press: New York,* 454.

(Montagna and Parakkal, 1974)   **Montagna, W. and Parakkal, P.F.** (1974) *Structure and function of skin. Academic Press: New York and London.*

(Monteiro-Riviere et al., 2001)   **Monteiro-Riviere, N.A., Inman, A.O., Mak, V., Wertz, P., Riviere, J.E.** (2001) Effect of selective lipid extraction from different body regions on epidermal barrier function. *Pharmaceutical Research,* **18,** 992-998.

(Nacht et al., 1981)   **Nacht, S., Close, J., Yeung D. and Gans E.H.** (1981) Skin friction coefficient: changes induced by skin hydration and emollient application and correlation with perceived skin feel. *Journal of the Society of Cosmetic Chemists,* 32, 55-65.

(Nakajima and Narasaka, 1993)   **Nakajima, K. and Narasaka, H.** (1993) Evaluation of skin surface associated with morphology and coefficient of friction. *Journal of the Society of Cosmetic Chemists,* 15, 135-151.

(Naylor, 1955)   **Naylor, P.F.** (1955) The skin surface and friction. *British Journal of Dermatology,* 67(7), 239-246.

(Newman, 2002)   **Newman, D.K.** (2002) Managing and Treating Urinary Incontinence. *Health Profession Press, Baltimore, MD.*

(Nilsson, 1977)   **Nilsson, G.E.** (1977) On the measurement of evaporative water loss: methods and clinical applications. *Linkoping University Dissertation, Linkoping.*

(Nuutinen et al., 2003)   **Nuutinen, J., Alanen, E., Autio, P., Lahtinen, M-R., Harvima, I. and Lahtinen, T.** (2003) A closed unventilated chamber for the measurement of transepidermal water loss. *Skin Research and Technology.* 9, 85-89.

(Orsmark et al., 1980) **Orsmark, K., Wilson, D., Maibacch, H.** (1980) In vivo transepidermal water loss and epidermal occlusive hydration in newborn infants: Anatomical region variation. *Acta Dermato-Venereologica (Stockholm).* **67,** 403-407.

(Panisset et al., 1992) **Panisset, F., Treffel, P., Faivre, B., Lecomte, P.B. and Agache, P.** (1992) Transepidermal water loss related to volar forearm sites in humans. *Acta Dermato-Venereologica.* **72**(1), 4-5.

(Pascut et al., 2001) **Pascut, F.C., Xiao, P., O'Driscoll, D.G., Katzir, A., Gannot, I., Croitoru, N., Notingher, I., Imhof, R.E.** (2001) Fibre-optic opto-thermal hand held probe for in-vivo measurement on human skin. *Analytical Sciences.* **17** Special Issue, s368-s370.

(Perlman, 1991) **Perlman, A.L.** (1991) Meeting the demand of the retail market: a look at critical issues for the incontinence products manufacturer. *Nonwoven Industry.* **22**(3), 38-41.

(Pinnagoda et al., 1989) **Pinnagoda, J., Tupker, R.A., Coenraads, P.J., and Nater, J.P.** (1989) Comparability and reproducibility of the results of water loss measurements: a study of 4 evaporimeters. *Contact Dermatitis.* **20**(4), 241-246

(Pinnagoda et al., 1990) **Pinnagoda, J., Tupker, R.A., Agner, T., Serup, J.** (1990) Guidelines for transepidermal water loss (TEWL) measurement. A report from the Standardization Group of the European Society of Contact Dermatitis. *Contact Dermatitis.* **22**(3), 164-178.

(Pinnagoda and Tupker, 1995) **Pinnagoda, J. and Tupker R.A.** (1995) Measurement of the Transepidermal Water Loss. In: *Handbook of Non-Invasive Methods and the Skin. Ed. Serup J and Jemec G.B.E.* Florida: CRC Press, 173-178.

(Potts, 1986) **Potts, R.O.** (1986) Stratum Corneum hydration: Experimental techniques and interpretations of results. *Journal of the Society of Cosmetic Chemists.* **37,** 9-33.

(Prall, 1973) **Prall, J.K.** (1973) Instrumental evaluation of the effects of cosmetic products on skin surfaces with particular reference to smoothness. *Journal of the Society of Cosmetic Chemists.* **24,** 693-707.

(Richey et al., 1988)   **Richey, M.L., Richey, H.K., Fenske, N.A.** (1988) Aging-related skin changes: development and clinical meaning. *Geriatrics*. **43**(4), 49-52, 57-59, 63-64.

(Rogiers, 2001)   **Rogiers, V. and the EEMCO Group.** (2001) EEMCO guidance for the assessment of transepidermal water loss in cosmetic sciences. *Skin Pharmacology and Applied Skin Physiology*. **14**, 117-128.

(Rodrigues and Pereira, 1998)   **Rodrigues, L. and Pereira, L.M.** (1998) Basal transepidermal water loss: right/left forearm difference and motoric dominance. Skin Research and Technology, **4**(3), 135-137.

(Royal College of Physicians, 1995)   **Royal College of Physicians** (1995) Incontinence. Causes, management and provision of services. *Journal of the Royal College of Physicians*. **29**, 272-274.

(Schafer et al., 2002)   **Schafer, P., Bewick-Sonntag, C., Capri, M.G., Berardesca, E.** (2002) Physiological changes in skin barrier function in relation to occlusion level, exposure time and climatic conditions. *Skin pharmacology and applied skin physiology*. **15**(1), 7-19.

(Scheuplein and Blank, 1971)   **Scheuplein, R.J. and Blank, I.H.** (1971) Permeability of the skin. *Physiological reviews*. **51**(4), 702-747.

(Shah et al., 2005)   **Shah, J.H., Zhai, H. and Maibach, H.I.** (2005) Comparative evaporimetry in man. *Skin Research and Technology*. **11**, 205-208.

(Shames, 1996)   **Shames, I.H.** (1996) Engineering Mechanics. Statics and Dynamics. *4th ed. Prentice-Hall, Englewood, Cliffs, NJ.*

(Shigley, 1956)   **Shigley, J.E.** (1956) Machine Design. McGraw-Hill, New York, pp.414.

(Sivamani et al., 2003a)   **Sivamani, R.K., Goodman, J., Gitis, N.V. and Maibach, H.I.** (2003a) Coefficient of friction: tribological studies in man - an overview. *Skin Research and Technology*, **9**(3), 227-234.

(Sivamani et al., 2003b)   **Sivamani, R.K., Goodman, J., Gitis, N.V. and Maibach, H.I.** (2003b) Friction coefficient of skin in real-time. *Skin Research and Technology*. **9**(3), 235-239.

References   258

(Sulzberger et   **Sulzberger, M.B., Cortese, T.A., Fishman, L., Wiley, H.S.** (1966)
al., 1966)   Studies on blisters produced by friction. I. Results of linear rubbing
                    and twisting technics. *The Journal of Investigative Dermatology,*
                    47(5), 456-465.

(Swarbrick et   **Swarbrick, J., Lee G., and Brom J.** (1982) Drug permeation through
al., 1982)   human skin: I. Effect of storage conditions of skin. *Journal of
                    Investigative Dermatology.* **78**(1), 63-66.

(Tagami, 1995)   **Tagami, H.** (1995) Measurement of electrical conductance and
                    impedance. *In Serup J., Jemec G.B.E., eds. Handbook of
                    Non-Invasive Methods and the Skin. Boca Raton: CRC Press.*
                    159-163.

(Tagami et al.,   **Tagami, H., Kobayashi, H., Kikuchi, K.** (2002) A portable device
2002)   using a closed chamber system for measuring transepidermal water
                    loss: comparison with the conventional method. *Skin Research and
                    Technology.* **8**(1), 7-12.

(CK electronic,   **CK electronic GmbH.** (2005) Information and Operating Instructions
2005)   for the Multi Probe Adapter MPA and its probes.

(Treffel et al.,   **Treffel, P., Panisset, F., Faivre, B. and Agache, P.** (1994) Hydration,
1994)   transepidermal water loss, pH and skin surface parameters:
                    correlations and variations between dominant and non-dominant
                    forearms. *British Journal of Dermatology.* **130**(3), 325-328.

(Tsai and   **Tsai, T.F., and Maibach, H.I..** (1999) How irritant is water? An
Maibach,   overview. *Contact Dermatitis.* **41**(6), 311-314.
1999)

(Van Sam et   **Van Sam, V., Passet, J., Maillols, H., Guillot, B. and Guilhou, J.J..**
al., 1994)   (1994) TEWL measurement standardization: kinetic and topographic
                    aspects. *Acta Dermato-Venereologica.* **74** (3), 168-170.

(Verdell and   **Verdell, L.L. and Bouda, J.M.** (1990) Help for Incontinent People
Bouda, 1990)   (HIP) resource guide of continence products and services, 4th ed.

(Wang and Wu,   **Wang, L. and Wu, H.** (2007) Biomedical optics, Principles and
2007)   imaging. Wiley Interscience, John Wiley and Sons, New Jersey.

(Wheldon and Monteith, 1980)

Wheldon, A.E. and Monteith, J.L. (1980) Performance of a skin Evaporimeter. *Medical and Biological Engineering and Computing,* **18**, 201-205.

(Xiao and Imhof, 1996)

Xiao, P. and Imhof, R.E. (1996) Opto-thermal skin water concentration gradient measurement. *SPIE Proc.* **2681**, 31-41.

(Xiao and Imhof, 1999)

Xiao, P. and Imhof, R.E. (1999) Water diffusion within the stratum corneum. *AIP Conference Proceedings.* 10th International Conference on Photoacoustic and Photothermal Phenomena, Rome, Italy. **463**, 573-575.

(Xiao et al., 2001)

Xiao, P., Cowen, J.A., Imhof, R.E. (2001) In-vivo transdermal drug diffusion depth profiling - a new approach to opto-thermal signal analysis. *Analytical Sciences.* **17**, s349-s352.

(Xiao et al., 2007)

Xiao, P., Packham, H., Zheng, X., Singh, H., Wlliott, C., Berg, E.P. and Imhof, R.E. (2007) Opto-thermal radiometry and condenser-chamber method for stratum corneum water concentration measurements. *Applied Physics B, Lasers and Optics.* 2007, **86**, 715-719.

(Yosipovitch et al., 1998)

Yosipovitch, G., Xiang, G.L., Haus, E., Sackett-Lundeen, L., Ashkenazi, I., Maibach, H.I. (1998) Time-dependent variations of the skin barrier function in humans: transepidermal water loss, stratum corneum hydration, skin surface pH, and skin temperature. *Journal of Investigative Dermatology.* **110**(1), 20–23.

(Zhang and Mak, 1999)

Zhang, M. and Mak, A.F. (1999) In vivo friction properties of human skin. *Prosthetics and Orthotics International,* **23**(2), 135-141.

(Zimmerer et al., 1986)

Zimmerer, R.E., Lawson, K.D. and Calvert, C.J. (1986) The effects of wearing diapers on skin. *Pediatric Dermatology,* **3**(2), 95-101.